Modern pharmacokinetic-pharmacodynamic techniques to study physiological mechanisms of pharmacokinetic drug-drug interactions and disposition of antibiotics and to assess clinical relevance

Dissertation zur Erlangung des

naturwissenschaftlichen Doktorgrades

der Bayerischen Julius-Maximilians-Universität Würzburg

vorgelegt von

Cornelia Landersdorfer

aus Eching bei Landshut

Würzburg 2006

Eingereicht am: …………………………………

Bei der Fakultät für Chemie und Pharmazie

1. Gutachter: ……………………………………

2. Gutachter: ……………………………………

der Dissertation

1. Prüfer: ………………………………………

2. Prüfer: ………………………………………

3. Prüfer: ………………………………………

des Öffentlichen Promotionskolloquiums

Tag des Öffentlichen Promotionskolloquiums: ……………………………

Doktorurkunde ausgehändigt am: ……………………………

Für meine Familie

Acknowledgement

The work for this thesis has been accomplished under the supervision of Professor Dr Fritz Sörgel, Institute for Biomedical and Pharmaceutical Research – IBMP in Nürnberg-Heroldsberg, and Professor Dr Ulrike Holzgrabe, Department of Pharmaceutical Chemistry, University of Würzburg.

First and foremost, I greatly thank Professor Dr Sörgel for the assignment of the scientific topic for this Ph.D. thesis, for his continuous support, advice and guidance during this thesis and for making it possible for me to work with the groups in Brisbane, Australia, and in Albany, NY, USA.

My warmest thank you goes to Professor Dr Holzgrabe for supporting this Ph.D. work, for her time, for her help in organizational issues, and for reading and constructive commenting on the text of this thesis.

I am very thankful to Dr Martina Kinzig-Schippers and the whole laboratory team of the IBMP who did the analysis of the samples and helped me with the analytical work of the moxifloxacin samples. I am very grateful to all clinical study teams and all people otherwise involved in those studies, without their work the data which were analyzed in this thesis would not exist.

My warmest thank you goes to Professor Dr George L Drusano, Ordway Research Institute, Albany, New York, USA, for valuable guidance on analysis and interpretation of the data and comments on draft manuscripts that were the basis for this thesis.

My warmest thank you also goes to Dr Carl Kirkpatrick, University of Queensland, Brisbane, Australia, for the opportunity of training at the University of Queensland, for his support in analysis and interpretation of the modeling results, for discussions on modeling questions and comments on draft manuscripts.

I thank Jürgen Bulitta for his support in data analytical questions and for proof reading this thesis. I am very happy to thank all my friends at the IBMP, in GoldLab and at the Ordway Research Institute who made the time of my Ph.D. work unforgettable.

Publications

Full papers:

1. Sörgel F, Weissenbacher R, Kinzig-Schippers M, Hofmann A, Illauer M, Skott A, Landersdorfer C: Acrylamide: increased concentrations in homemade food and first evidence of its variable absorption from food, variable metabolism and placental and breast milk transfer in humans. Chemotherapy 2002; 48:267-74.

2. Sörgel F, Landersdorfer C, Bulitta J: Zur Pharmakokinetik von Linezolid und Telithromycin: Zwei neue Antibiotika mit besonderen Eigenschaften. (Two new antibiotics with special qualities: the pharmacokinetics of linezolid and telithromycin.) Pharm Unserer Zeit 2004; 33:28-36.

3. Sörgel F, Landersdorfer C, Bulitta J, Keppler B: Vom Farbstoff zum Rezeptor: Paul Ehrlich und die Chemie. Nachrichten aus der Chemie 2004; 52:777-82.

4. Sörgel F, Landersdorfer C, Holzgrabe U: Welche Berufsbezeichnung wird Ehrlichs Wirken gerecht? Bemerkungen zu seinem 150. Geburtstag. Chemother J 2004; 13:157-65.

5. Krueger WA, Bulitta J, Kinzig-Schippers M, Landersdorfer C, Holzgrabe U, Naber KG, Drusano GL, Sorgel F. Evaluation by Monte Carlo Simulation of the Pharmacokinetics of Two Doses of Meropenem Administered Intermittently or as a Continuous Infusion in Healthy Volunteers. Antimicrob Agents Chemother 2005; 49:1881-9.

Congress presentations:

1. Landersdorfer C, Kinzig-Schippers M, Skott A, Gusinde J, Hennig FF, Sörgel F: Determination of moxifloxacin in bone by HPLC-FLUO. Poster P K10, Annual meeting of the German Pharmaceutical Society (Deutsche Pharmazeutische Gesellschaft, DPhG); Würzburg, Germany; October 8 - 11, 2003.

2. Sörgel F, Bulitta J, Kinzig-Schippers M, Landersdorfer C, Tomalik-Scharte D, Jetter A, Fuhr U, Cascorbi I: Dosing of antiinfectives – "One size fits all" vs. individualized therapy. Poster P K18, Annual meeting of the German Pharmaceutical Society (Deutsche Pharmazeutische Gesellschaft, DPhG); Würzburg, Germany; October 8 - 11, 2003.

3. Landersdorfer C, Skott A, Kinzig-Schippers M, Holzgrabe U, Sörgel F: Determination of Moxifloxacin in Bone by HPLC-FLUO. Abstract no. 288, World Conference on Magic Bullets; Nürnberg, Germany; September 9 - 11, 2004.

4. Landersdorfer C, Holzgrabe U, Kinzig-Schippers M, Gusinde J, Hennig FF, Rodamer M, Skott A, Sörgel F: Concept of Internal Standard Used to Standardize Tissue Level Measurements and Allow Valid Comparison Between Agents. 44th Interscience Conference on Antimicrobial Agents and Chemotherapy; Washington, DC, USA; October 30 - November 2, 2004.

5. Landersdorfer C, Kirkpatrick C. M. J., Kinzig-Schippers M., Bulitta J., Holzgrabe U., Sörgel F: New Insights into the Most Commonly Studied Drug Interaction with Antibiotics: Pharmacokinetic Interaction between Ciprofloxacin, Gemifloxacin and Probenecid at Renal and Non-renal Sites. Abstract 882, 15th Annual Meeting of the Population Approach Group in Europe (PAGE); Brugge, Belgium; June 14 - 16, 2006.

Table of contents

List of figures

List of tables

List of chemical structures

1   Introduction

1.1   Pharmacokinetics

1.1.1   Definition of pharmacokinetics

The origin of pharmacokinetics (PK) can be traced to two papers by Teorell, published in 1937 (301, 302). However, already in 1885 Paul Ehrlich (1854 - 1915) studied the distribution of dyes into different tissues of animals. He found that lipophilicity and acid/base characteristics have an influence on the distribution. Together with his coworker Goldman he was the first to describe the existence of the blood-brain barrier.

Pharmacokinetics has been defined as follows by Holford and Sheiner (147): "Pharmacokinetics encompasses the study of movement of drugs into, through and out of the body. It describes the processes and rates of drug movement from the site of absorption into the blood, distribution into the tissues and elimination by metabolism or excretion."

This definition addresses three key points:

a) Pharmacokinetics specifically aims at describing the time course of concentrations, not only the total drug exposure.

b) This refers to the plasma concentration and the concentration at the target site(s).

c) If metabolites are present, their concentration time course may also need to be considered.

1.1.2   Why are we studying pharmacokinetics?

Application of PK principles allows us to describe the relationship between dose and drug concentration. This is one important component of the relationship between dosage regimen and time course of effect (Figure 1.1-1). The existence of the second component, the concentration-effect relationship (pharmacodynamics, PD), is a fundamental hypothesis of pharmacology and

has been documented for many drugs (149). Therefore, by predicting the time course of drug concentrations we have made one important step towards predicting the time course of drug effect.

Figure 1.1-1   Dose – concentration – effect relationship

| Dose | **PK** → | Concentration | **PD** → | Effect |
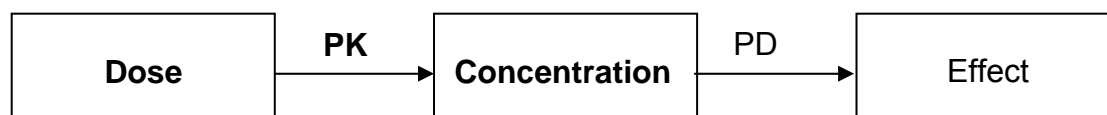
If the same dosage regimen of a drug is given to different patients, there is true between subject variability (BSV) in the observed drug concentrations. For cytotoxic drugs, the total exposure of two patients may differ by a factor of two to ten at the same dose (311). After oral administration of 50 mg etoposide to seven patients, the coefficient of variation for total drug exposure was 58% (136). Assuming a log-normal distribution of drug exposure, this corresponds to a ratio of about 10 for the 95th percentile of the distribution of exposures divided by the 5th percentile (chapter 2.8.1).

A reason for high BSV may be that patients differ in their ability to absorb or eliminate a drug. By including the variability of the PK parameters into a PK model, one can predict drug effect more precisely and optimize dosage regimens for the patient population. This provides a basis for choosing dosage regimens at initiation of therapy, i.e. when no PK information about the patient is available. In addition to the PK model, knowledge about the concentration-effect relationship (see below) is necessary to optimize dosage regimens. If the concentration-effect relationship is known, the PK model alone can be used to make predictions about drug effect (147).

1.2   Pharmacodynamics

Pharmacodynamics (PD) is "the study of the biochemical and physiological effects of drugs and the mechanisms of their actions" (89). It describes the relationship between concentration and drug effect. The

existence of a relationship between the drug concentration (ideally determined at the site of action) and drug effect has been shown for many drugs.

As a useful separation between PK and PD, PK can be thought of what the body does to the drug and PD as what the drug does to the body (147). Antimicrobial PD has been described as "the discipline that attempts to link measures of drug exposure to the microbiological or clinical effects that are observed once an anti-infective drug has been administered" (89). One difference between antimicrobials and other drug groups is that one can measure antibiotic activity against a pathogen outside the human body, for example by determination of the minimal inhibitory concentration (MIC) (89).

1.3   How is pharmacokinetics combined with pharmacodynamics?

1.3.1   Definition of pharmacokinetics-pharmacodynamics

Pharmacokinetics-pharmacodynamics (PKPD) is the combination of the dose-concentration relationship with the concentration-effect relationship. PK and PD are combined in order to describe the time course of drug effect for a chosen dosage regimen. Knowledge about the time course of drug effect allows one to compare and optimize dosage regimens. This is one important clinical application of PKPD models.

PKPD models can be classified into two groups: the first group of models characterizes the whole system at each time point. These models can predict the plasma (or target site) concentration, the drug effect (e.g. bacterial killing), and the cumulative effect (e.g. total number of bacteria) at any time point. To derive these models e.g. for antibiotics, measured data (observations) about the time course of drug concentrations and bacterial counts is necessary. These models are powerful and very informative. Thibonnier et al. (303) used such a model to investigate the relationship between unbound disopyramide concentrations and prolongation of the QT interval. For antibiotics these models have been established e.g. by the group of Drusano. They applied mathematical modeling to identify dosage regimens

that suppress emergence of resistance during antibiotic therapy with levofloxacin (166) or moxifloxacin (133).

The second group of models uses a surrogate target to predict the treatment outcome. An example for this type of models is a study by Drusano et al. (93) on rational dose selection for clinical trials with evernimicin. For antibiotics the outcome is often microbiological or clinical success. Surrogate targets for successful outcome of antibiotic treatment have been developed by Craig et al. (67) and others. Those simplified models assume that achieving a surrogate target is equivalent to microbiological or clinical success. Therefore, it is not necessary to investigate the full time course of drug effect. Those models can be implemented more easily and no data on the PD effect is required once a surrogate target has been established and validated and is applicable to the patient population of interest. By use of a surrogate target, prior knowledge about the drug or drug group is incorporated into the model.

1.3.2 Advantages of pharmacokinetic-pharmacodynamic models

PK models alone cannot predict the time course or magnitude of drug effect (148), since they do not account for the concentration-effect relationship (PD model). Combination of PK and PD models allows one to describe the full time course of the interaction between the drug and the body. For antibacterials, such a PKPD model can describe the growth and killing of bacteria over time dependent on the drug concentration-time course. Understanding the time course of drug effect is important to optimize the clinical benefit (148).

A PKPD model can be extremely helpful, if there is a delay between the dose and the observed response. Such a delay can be caused by PK, PD or by both. Once a PKPD model is established, the predicted time course of response can be compared to the observed response in a patient. Comparing the predicted and observed response may be very helpful to guide future decisions on the dosage regimen. Vinks et al. presented a clinical application of modeling the time course of bacterial growth and killing for aminoglycoside therapy in dialysis patients at the Interscience Conference on Antimicrobial

Agents and Chemotherapy (ICAAC) 2005. It was shown that understanding the time course of bacterial killing may greatly support selection of future dosage regimens.

1.3.3   Clinical applications

Application of PKPD models can be used to improve treatment success. Two different strategies to optimize drug-related response are therapeutic drug monitoring (TDM) and target concentration intervention (TCI). TDM aims at adjusting plasma drug concentrations of patients within a target range of plasma concentrations (therapeutic window). This range is usually derived from observation of therapeutic and adverse effects in small groups of patients (36). Different drug effects in patients that receive the same dose can arise from both PK and PD variability. TDM seeks to reduce the PK variability by adjusting drug concentrations to a target range.

TDM uses the same target range for each patient and assumes that all patients have the same therapeutic window. However, the concentration-effect relationship might not be the same for all patients and PD variability is not reduced by TDM. TDM has its greatest benefit, if there is only a small range between effective and toxic concentrations, and if there is large variability in drug concentrations between patients. If there is no readily available measure of drug effect, like for example blood pressure (36), the safe and effective use of a drug might require TDM. Gentamicin and theophylline are monitored by TDM, as both are drugs with a narrow therapeutic window and serious adverse effects (36, 323). In a meta-analysis of 52 studies, Kim et al. (174) applied Bayes theorem to investigate the incidence of aminoglycoside-associated nephrotoxicity related to once daily dosing, multiple daily dosing, and individualized PK monitoring. Individualized PK monitoring used patient specific PK parameters for designing dosage regimens that are likely to achieve the desired peak and trough concentrations. This approach resulted in lower probabilities for nephrotoxicity (incidence rate: 10 to 11%) than once daily (12 to 13%) and multiple daily dosing (13 to 14%) by use of nomograms.

The target serum concentration range for TDM of theophylline is 10 to 20 mg/L (36, 323). In a randomized double-blind study in patients on intravenous theophylline the target concentrations 10 and 20 mg/L were compared. There was no difference in treatment success between the two groups, but significantly more toxicity in the 20 mg/L group (144).

A target range introduces variability, as practitioners might aim for any concentration within this range and drug effect changes continuously throughout the concentration range. Therefore, a target concentration strategy has been proposed (146). TCI seeks to select the best dose to achieve the desired therapeutic effect. TCI aims at a drug effect in the individual patient and not at a concentration range that is the same for the whole population. Concentration measurements are used to determine the individual PK parameters in order to optimize future dosage regimens (146). Patient and disease specific factors like body weight or creatinine clearance can be included in the calculations to individualize PK parameters. That way, PK and PD concepts are combined with information about the individual patient and disease in TCI (146).

1.3.4   Applications for drug development

There are numerous applications of PKPD models in drug development. Some examples are:

1) Selection of optimal dosage regimens to be studied in future clinical trials,
2) decision about continuation or abandonment of clinical drug development,
3) optimal design of clinical trials, including the number of subjects and number of samples per subject, and
4) visualization and application of already available knowledge (data).

Selection of optimal dosage regimens for clinical studies is extremely important as, according to a report from the US Food and Drug Administration (FDA) from 2003, almost 50% of phase III trials do not succeed, often due to

poor dose selection. Therefore the FDA requests sponsors to present exposure-response analyses to support dose selection for further clinical trials (190). Pre-clinical data from e.g. *in vitro* or animal studies can be used in PKPD models to select optimal dosage regimens for clinical studies. Oritavancin is a new glycopeptide antibiotic and an example for the application of PKPD models during clinical development. Bhavnani et al. (33) studied the relationship between oritavancin exposure and microbiological and clinical outcome in 55 patients with *Staphylococcus aureus* bacteremia to select optimal dosage regimens for future clinical trials. It was established that the time that the free drug concentration remains above the minimum inhibitory concentration ($fT_{>MIC}$) correlated with microbiological as well as with clinical success (see also chapter 2.7.1). A percentage of the $fT_{>MIC}$ of 22% of the dosing interval resulted in a probability of 93% for microbiological and of 87% for clinical success. Rational dose selection by use of such a PKPD model allows one to optimize the information which will be gained from future clinical studies.

Another example for optimization of dosage regimens is a study by Gumbo et al. (133). They used an *in vitro* infection model, human PK data, and PKPD modeling to identify a moxifloxacin dose that is likely to achieve a successful microbiological outcome and suppress resistance of *Mycobacterium tuberculosis* against moxifloxacin. They intended to provide optimal dosage regimens for future clinical trials on the use of moxifloxacin against tuberculosis. A ratio of the area under the non-protein bound concentration vs. time curve to the MIC of the pathogen of 53 ($fAUC/MIC=53$) was associated with complete suppression of the drug resistant mutants. A dose of 800 mg per day is likely to achieve excellent microbial kill and supression of resistant mutants. Predictions about emergence of resistance, or about which PKPD target is associated with effectiveness or resistance could not have been made without PKPD modeling.

There may be situations where PKPD modeling suggests to stop further development of a drug. As the PD of antibiotics can be measured *in vitro*, phase I PK data and *in vitro* activity data can be combined to predict the probability of efficacious treatment for antibiotics in future clinical trials.

Drusano et al. (93) performed the first such analysis in the field of anti-infectives. They combined pre-clinical microbiological and animal model data with PK data from early phase I studies to identify efficacious dosage regimens for evernimicin. A low probability of successful treatment was predicted even for the optimized dosage regimens of evernimicin. For a dose of 9 mg/kg the probability of attaining 90% of the maximum effect was 98% for *Streptococcus pneumoniae*, but only 51% for *S. aureus* and 75% for *Enterococcus* ssp. Those predictions were confirmed by phase II/III clinical trials. In these trials no sufficient advantage of evernimicin over approved antibiotics could be shown for treatment of infections by vancomycin susceptible and resistant gram-positive bacteria. Subsequently, evernimicin did not reach the market. This is one example that shows, how PKPD modeling could save millions of dollars spent on phase II/III clinical trials.

Once the decision has been taken to continue clinical development, it is a formidable task to optimize the design of clinical trials. There is a tremendous amount of resources and time involved in the performance and analysis of phase II/III clinical trials. Therefore, it would be very valuable to increase the chance of success for those clinical trials. By optimization of the design with PKPD models, future clinical studies can be made considerably more cost-effective (95, 267).

A possible application of all PKPD models is their ability to visualize knowledge which has already been gained in past experiments. It is often difficult to visualize and interpret the results of clinical studies with a large number of dosage regimens, compliant and non-compliant patients, disease progression, and patients with unstable clinical conditions (e.g. changing renal function in ICU patients). In those situations PKPD models are probably the only possibility to visualize the results of the clinical trials and to use the past experience for designing new trials and dosage regimens.

1.4 Why are we studying antibiotics?

1.4.1 Drug development

Drug development is a complicated and cost-intensive process. As only a very small percentage of drugs that are investigated eventually reaches the market, drug development carries a high risk for the pharmaceutical industry. The average total costs for development of a new drug have been reported as 802 million US dollars (year 2000) (84). About 80% of all drugs entering phase I are not approved for marketing.

For treatment of infections with antibiotics usually only a relatively short duration of therapy is required. This reduces drug development costs for antibiotics. However, unlike other drug groups, e.g. cardiovascular drugs or antidiabetics, antibiotics are rarely given as chronic medication. Therefore, more patients need to be treated with an antibiotic in order to regain the high investments in drug development. Maybe due to some of these difficulties, currently relatively few new antibiotics seem to be developed.

As has been reported at the ICAAC in December 2005, there are at the moment three antibiotics against gram-negative pathogens in phase II or III of clinical development: ceftobiprole, a cephalosporin with activity against methicillin-resistant *S. aureus* (MRSA), doripenem, a new carbapenem, and garenoxacin, a Des-(F6)-quinolone (46). Tigecycline, a glycylcyline, is already marketed in the US and waiting for final approval in the European Union (46, 343). It has been difficult to find new antibiotics that work by a completely different mechanism of action and that have no cross-resistance (90). Therefore it is even more important to optimize therapy with the available antibiotics.

1.4.2   Clinical situation – drug resistance

While fewer new antibiotics are being developed, drug resistance among pathogens is increasing in the hospital setting as well as in the community (47). According to data from 300 microbiological laboratories throughout the United States, resistance rates of *S. aureus* have increased continuously since 1998. In March 2005, 50-60% of *S. aureus* isolates from inpatients and outpatients were methicillin-resistant (MRSA). About 60% of MRSA from inpatients and 40% from outpatients were resistant to more than three non-beta-lactam antibiotics (298). Methicillin resistance in *S. aureus* bacteremia results in significantly longer hospitalization times and higher hospital charges than methicillin-susceptible *S. aureus* bacteremia (65).

At the ECCMID in April 2006, data from the European Antimicrobial Resistance Surveillance System (EARSS), i.e. data from laboratories that serve more than 30% of the European population, have been presented (314). Fluoroquinolone resistance in *Escherichia coli* continues to increase in most European countries. Rates of MRSA are rising in Northern and Central Europe. Recently, in Germany, France and Ireland, the rate of vancomycin resistant *Enterococcus faecium* has increased significantly.

PKPD models are helpful for the choice of the most suitable drug, selection of optimal dosage regimens, reduction of toxicity and prevention of resistance, among other purposes. By application of PKPD modeling, the probability for successful microbiological or clinical outcome can be predicted for each drug and pathogen. The highest MIC for which a PKPD target is attained with a probability of at least 90% is often defined as the PKPD breakpoint. There is a high probability of successful treatment, if the individual MIC of the infecting pathogen is lower than the PKPD breakpoint. To prevent further emergence of resistance, antibiotics that are the treatment of choice against nosocomial infections or in intensive care units should not be used for less severe infections, if there is an alternative antibiotic with a sufficiently high PKPD breakpoint. In the case of severe infections by problematic pathogens like *Pseudomonas aeruginosa*, PKPD models for combinations of two or more drugs may guide therapy, as they can predict up to which MIC of

a pathogen the dosage regimen will be successful. Hope et al. (151) applied PKPD models to investigate and optimize antifungal combination therapy. Combination chemotherapy is sometimes applied to increase the chance of drug susceptibility in empiric therapy and to maximize effectiveness.

After choosing the most promising drug, optimal dosage regimens for the antibiotic should be selected to further increase the PKPD breakpoint. This applies to both, empirical treatment and individualized dosage regimens. Other treatment outcomes to be optimized by PKPD models are reduction of toxicity (261) and prevention of selection of resistant mutants (chapter 1.3.4).

1.5   Why are we studying healthy volunteers?

Our dose linearity and drug interaction studies were performed in healthy volunteers as the variability in healthy volunteers is usually much lower (e.g. 2-10 times lower variance) than in ill patients. Healthy volunteer studies have the advantage that e.g. food and fluid intake, clinical procedures, and drug administration are highly standardized and supervised or performed by professional investigators. Those standardized trial designs are difficult to perform in parallel to routine clinical practice. In a crossover study, subjects act as their own controls and therefore, BSV, a considerable component of the total variability, is removed from the comparison. However, it is not feasible to perform crossover studies in patients who need antibiotic treatment against an acute infection. Also, in healthy volunteer studies, there is no bias from an impaired renal function or from intake of co-medication, whereas both is often the case in hospitalized patients.

If frequent blood samples are collected, more information can be gained about the pathways of elimination and about the mechanisms of PK drug-drug interactions. This is especially true for complex PK models, to which population PK sometimes cannot be applied due to exhaustive computation time. It is not practical to obtain more than ten blood samples per day from a patient and the same total blood loss might be more critical for an ill patient than for a healthy volunteer.

For exploring mechanisms of PK interactions or elimination, as in the dose linearity and interaction studies described in this thesis, it is advantageous to study healthy volunteers. However, if dosage regimens are developed from a healthy volunteer study, it needs to be considered that ill patients might differ in their PK from healthy volunteers. We used PK data from healthy volunteers to calculate the probabilities of attaining a PKPD target (PTA) which is associated with successful clinical outcome (for details see chapter 2.7). Compared to healthy volunteers, patients often have lower clearances and larger volumes of distribution, which result in higher average plasma concentrations and longer elimination half-lives. Both these alterations for the PK in patients increase the PTA. Thus, our estimates for the PTA in healthy volunteers are conservative (i.e. low) estimates for the PTA in patients. Lodise et al. (194) compared data from healthy volunteers to hospitalized patients after administration of piperacillin / tazobactam, and report an approximately 27% lower total body clearance and a higher volume of distribution of piperacillin at steady-state for patients. Consequently they found lower PTAs for healthy volunteers than for patients.

We studied bone concentrations of antibiotics in patients undergoing hip replacement due to arthrosis. Knowledge about antibiotic concentrations in bone is useful for prophylaxis in orthopedic surgery and for treatment of osteomyelitis. Samples from volunteers undergoing joint replacement have the advantage that there are no pathological changes to the bone tissue. In patients suffering from bone infections the tissue is usually changed due to inflammation, existence of pus, or sequesters. Therefore the variability of bone concentrations in joint replacement patients is probably lower than in osteomyelitis patients. After the methodology of bone sample preparation and drug analysis has been optimized in joint replacement patients, further studies in osteomyelitis patients are required to investigate the influence of disease state on bone penetration of antibiotics. We chose hip replacement patients with arthrosis for our investigations on antibiotic bone penetration.

1.6   Contributions by the author of this thesis

The clinical and bio-analytical parts of the dose linearity and drug-drug interaction studies described in this thesis were conducted by the group of Professor Dr. Fritz Sörgel, head of the Institute for Biomedical and Pharmaceutical Research – IBMP, before the start of this Ph.D. work. The author contributed to the clinical and bio-analytical work related to the moxifloxacin bone penetration study. The PKPD data analyses, simulations and literature searches were conducted by the author. The reporting of the results including all PKPD data analyses, introductions and discussions, but not the details of the bio-analytical section of the respective projects, was done by the author of this thesis.

1.7   Aims and scopes

1.7.1   General aims and scopes

The overall aim of this thesis was to study the pharmacokinetic and pharmacodynamic aspects of saturable elimination, drug-drug interactions and bone penetration of antibiotics by applying population PKPD techniques. Our general aim was to optimize antibiotic dosage regimens by application of PKPD modeling and Monte Carlo simulation (MCS). We combined the known pharmacology of the respective group of antibiotics with the PK properties and the bacterial susceptibility data to predict the probability for successful therapy. Our population PKPD models specifically account for the true between subject variability. This carries great advantages compared to standard non-compartmental analysis (NCA) especially for MCS. If the variability and correlation of PK parameters is known for a patient population, the pharmacological response and probability for successful therapy can be predicted by a population PKPD model in a MCS. The objectives of our individual studies are described in chapters 1.7.2 to 1.7.4. The individual

studies and study drugs are described monographically in the respective chapters of this thesis. PKPD modeling was expected to be advantageous for our study objectives compared to solely performing NCA and it was expected that different modeling approaches and programs would be necessary to deal with different problems.

1.7.2   Dose linearity

We studied the effect of a possible saturable elimination on the choice of optimized dosage regimens for piperacillin and flucloxacillin. Our first objective was to compare the PK at two dose levels for both drugs. We studied the extent of a possible saturation in the renal and nonrenal elimination at therapeutic concentrations. Our second objective was to study dosage regimens with an optimized PKPD profile. Our third objective was to estimate the influence of saturable elimination on the PKPD profile. This allowed us to estimate the clinical relevance of the saturation of elimination at therapeutic doses.

Saturable elimination of piperacillin has been discussed in literature for more than two decades, but so far no final conclusion has been drawn. Controversial results have been reported about the existence of nonlinear piperacillin PK at therapeutic concentrations. As a few newer studies indicate that saturable elimination of piperacillin may exist, it was expected to find saturable elimination. For flucloxacillin there was no indication for nonlinearity of PK in literature, but no population PK analysis has been published yet.

1.7.3   Pharmacokinetic drug-drug interactions

We assessed the extent, site, time course and possible mechanisms of PK drug-drug interactions *in vivo* and studied the possible therapeutic benefit of inhibiting the clearance of one drug by an inhibitor. The first objective of our interaction studies was to investigate the extent of change in drug exposure that is caused by PK drug-drug interactions between two quinolones and probenecid, and between two beta-lactams. The second objective was to

describe the time course and plausible mechanisms for the interactions at possible sites of interaction by developing full mechanistic interaction models. We were especially interested in the influence of probenecid on the formation and elimination of ciprofloxacin's 2-aminoethylamino-metabolite (M1). Such full mechanistic interaction models have the power to predict the time course of a PK interaction for other dosage regimens of interest. This allows one to predict the potential clinical impact of such a PK drug-drug interaction. It was expected that drug-drug interactions exist between the two beta-lactams investigated and between the two quinolones and probenecid due to their common and saturable pathways of elimination.

1.7.4   Bone penetration

The extent and time course of antibiotic bone penetration is important to assure antibiotic effectiveness in prophylaxis and treatment of bone infections. However, advanced techniques of PK analysis have not yet been applied to bone penetration data for antibiotics. After a literature review on antibiotic bone penetration, we applied population PKPD models to describe the time course of bone and serum concentrations and to optimize antibiotic dosage regimens for treatment of bone infections.

The primary objective of our overview of bone penetration studies from literature was to compare the different methods that have been used to assess bone penetration. The need of standardized methods for drug analysis in bone, PK evaluation of bone penetration studies, and reporting of their results is discussed. A short overview of the results from bone penetration studies is given.

The first objective of the bone penetration studies was to determine antibiotic concentrations in cancellous and cortical bone in a controlled study in subjects undergoing hip replacement surgery. As our second objective, we intended to develop a PK model to describe the time course of antibiotic concentrations in bone as well as the exposure of these drugs in bone relative to serum. Our third objective was to assess the PKPD profile in serum, cortical, and cancellous bone. Reports from literature, that were evaluated for

the overview of antibiotic bone penetration, show that quinolone antibiotics often achieve higher bone penetration than beta-lactams. Therefore, a moderate to high extent of penetration of moxifloxacin into bone and a lower extent of penetration of amoxicillin and clavulanic acid were expected.

2   General methods, procedures and modeling

2.1   Study participants

Ten to twenty-four Caucasian subjects (females and males), participated in each PK study. Prior to entry into the study, all subjects were given a physical examination, electrocardiography and laboratory tests, including analysis of urine samples for various laboratory values (urinalysis), and screening for drugs of abuse. During the drug administration periods, the volunteers were encouraged to report any discomfort or adverse reactions, and were closely observed by physicians. Each day of the study the subjects were asked to complete a questionnaire on their health status. All studies were approved by the local ethics committees, and all subjects gave their written informed consent prior to entering the respective study.

2.2   Study design and drug administration

The interaction and dose linearity studies were randomized controlled crossover studies. Food and fluid intake were strictly standardized. Treatment periods were separated by a washout period of at least four to seven days, depending on the half-life of the study drugs. Subjects were requested to abstain from alcohol and caffeine containing products during the study periods. The bone penetration studies were not randomized as only one treatment was studied, and this treatment was the same for all subjects.

2.3   Sample collection

All blood samples were drawn from a forearm vein via an intravenous catheter contralateral to the one used for drug administration. In each of the dose linearity and interaction studies 13, 19 or 23 blood samples were drawn from each subject up to 24 or 48h after administration plus one sample immediately before administration. Urine was collected from the time of

administration until 24, 72 or 96h after administration, divided into nine, ten or eleven sampling intervals.

In the bone penetration studies, blood samples were collected pre-dose and at the time of femoral bone resection. Hip replacement involved resection of the femoral head, or both femoral head and femoral neck, prior to implantation of the prosthetic hip joint. Bone samples consisted of femoral head or femoral head and femoral neck. Blood and bone samples for drug analysis were collected 2 to 7h after oral administration of moxifloxacin and 0 to 1.1h after the end of the amoxicillin / clavulanic acid infusion. Bone samples were immediately frozen on dry ice and stored at -70°C until analysis.

2.4   Sample preparation

2.4.1   Serum and plasma samples

When serum was obtained, blood samples were allowed to clot before centrifugation. After centrifugation serum or plasma samples were immediately frozen and stored at -20°C (gemifloxacin and ciprofloxacin) or at -70°C (moxifloxacin and beta-lactams) until analysis. All quinolones and probenecid were protected from sunlight throughout sample preparation and analysis to prevent degradation of the study drugs from daylight exposure. Blood samples containing beta-lactams were cooled in an ice-water bath before centrifugation at 4°C to prevent degradation at room temperature. Spiked quality controls (SQC) in human plasma or serum were prepared for control of inter-assay variation. Defined volumes of the stock solution or of an SQC of higher concentration were added to defined volumes of tested drug-free plasma or serum samples.

2.4.2   Urine samples

Urine samples containing beta-lactams were stored at 4°C during the collection period. The amount and pH of the urine were measured. After

shaking the samples, aliquots were taken, immediately frozen and stored at -20°C (gemifloxacin and ciprofloxacin) or -70°C (moxifloxacin and beta-lactams) until analysis. SQCs in human urine were prepared by adding defined volumes of the stock solution or of an SQC of higher concentration to defined volumes of tested drug-free urine samples.

2.4.3   Bone samples

Bone specimens consisting of femoral head and femoral neck, were separated into femoral head and femoral neck. Then the samples were separated into cortical and cancellous tissue. Adhering blood was removed from the samples that were then pulverized under liquid nitrogen by a cryogenic mill (Freezer/Mill®). All moxifloxacin samples were protected from sunlight during sample handling and analysis. For analysis of bone samples, calibration standards and SQCs were prepared by adding appropriate amounts of standard solutions to bone tissue that was shown to be free of the study drug.

2.5   Determination of drug concentrations

The general principles of the methods used for drug determination are described here. Assay details are included in the respective methods sections of chapters 3 to 5.

2.5.1   HPLC with UV or fluorescence detection

High performance liquid chromatography (HPLC) is a frequently used method for bioanalytical determination of drug concentrations. The drug to be analyzed is chromatographically separated from the other components of the sample and then quantified. Chromatography is a physical method of separation. The components partition between a mobile and a stationary phase. In HPLC the sample to be analyzed is dissolved in a solvent and then transported with the mobile phase under high pressure over the stationary

phase. The solutes are separated due to differences in their affinity to the two phases. In normal phase HPLC, the stationary phase is more polar than the mobile phase, however reversed phase HPLC is more common in bioanalysis of antibiotics. In reversed phase HPLC the mobile phase is more polar than the stationary phase, and polar substances are eluted faster than nonpolar substances, as polar substances have less affinity to the stationary phase. Thus, reversed phase HPLC is most useful for nonpolar drugs or compounds with low polarity at the chosen pH.

The mobile phase is usually a mixture of different solvents. In isocratic elution the mixture is the same during the whole analysis. If the use of a single mobile phase composition does not result in adequate separation of all compounds, often gradient elution is advantageous. In gradient elution the composition of the mobile phase changes in a pre-defined way during the analysis of each sample to improve the resolution or shorten retention times. This change can be continuous or stepwise. In gradient elution the strength of the mobile phase to elute the analyte is increased during the analysis. In reversed phase HPLC this means that the mobile phase becomes less polar. Therefore the retention times of compounds with very high affinity to the stationary phase are shortened and sharper peaks for those compounds are obtained. In reversed phase HPLC the mobile phase is often a mixture containing water, buffers, methanol, acetonitrile or tetrahydrofuran.

The stationary phase consists of small particles, that produce a bed with a very high flow impedance. Consequently, very high pressures are necessary to force the mobile phase through the column. In reversed phase HPLC the stationary phase consists of silica gel with hydrocarbon chains that are bound to the surface. The polarity of the stationary phase depends on the length of the hydrocarbon chains. Common stationary phases contain C8 or C18 chains.

A HPLC system consists of one or more pumps, an injection system, a column, a detector, and a computer (Figure 2.5-1). The pump pushes the mobile phase through the system with a constant or changing flow rate. The injector transports the sample into the mobile phase. The column is a stainless steel tube that contains the stationary phase.

Figure 2.5-1   Block diagram of a HPLC system
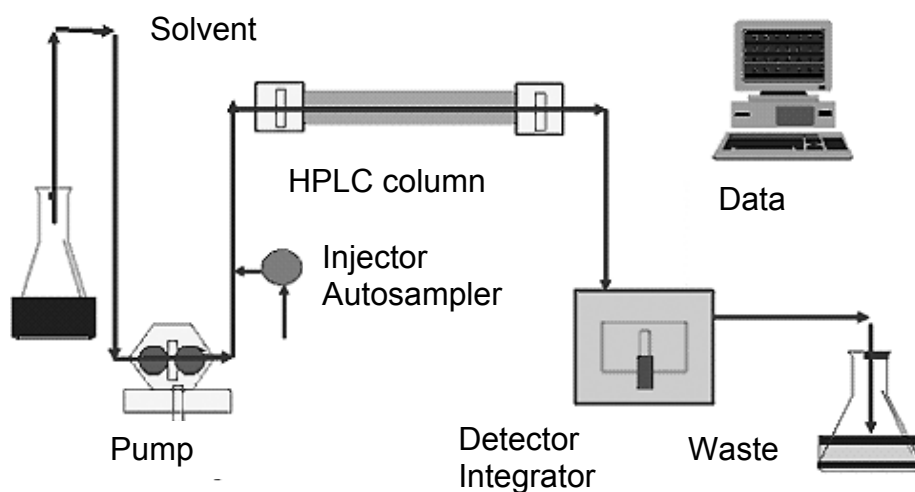
adapted from reference (326)

The detector detects the compounds as they elute from the column by measuring response changes between the mobile phase alone and the mobile phase containing the sample. The electrical response from the detector is recorded and sent to a data system. A peak on the chromatogram is observed.

The most appropriate method of detection depends on the properties of the drug to be quantified. Besides mass spectrometers, ultraviolet (UV) detectors and fluorescence detectors are two of the most common detectors. A UV detector measures the ability of a sample to absorb light at one or several wavelengths. As many compounds contain conjugated π-electron systems that can act as chromophores and absorb UV light, this detector is widely applied. The solvents that make up the mobile phase should not absorb UV light at the same wavelengths as the analyte. The Beer-Lambert law describes the relationship between the intensity of the transmitted light and the concentration of the analyte in the solution.

Fluorescence detectors measure the ability of a compound to absorb and then re-emit light at certain wavelengths. The excitation source passes through the flow-cell to a photodetector while a monochromator selects the emission wavelengths. The fluorescence detector is generally more sensitive than UV detectors, because the excitation as well as the emission wavelength

is specified. The emission light beam is detected in a 90° angle to the excitation beam that goes through the sample. Therefore diffused light from the excitation beam that might interfere with the detection is minimized. The selected emission wavelength strikes a photomultiplier that measures the intensity of the emission beam as a function of time. If the analyte exhibits fluorescence, a fluorescence detector is usually a good choice as this is both a specific and sensitive method.

For quantification of the analyte in the sample, the peaks in the chromatogram are evaluated by different methods. Two common methods are determination of the peak height or the peak area of the analytes. An internal standard is used to account for variations e.g. during sample preparation or due to inaccuracy in injection volume. The internal standard is added to each sample in a known concentration. The peak height or peak area of the analyte is then compared to the respective value of the internal standard. By this method the concentration ratio between the analyte and the internal standard, and finally the concentration of the analyte in the sample may be calculated.

2.5.2   LC-MS/MS

LC-MS is the combination of liquid chromatography (HPLC) with mass spectrometry (MS). A mass spectrometer separates ions in the gas phase according to their mass to charge ratio (m/z). The resulting mass spectrum is a plot of the relative intensity vs. m/z. In LC-MS/MS, HPLC is combined with two consecutive MS experiments by coupling multiple analyzers.

HPLC removes interferences that would influence ionization. Then an interface eliminates the solvent and generates gas phase ions that are transferred into the mass spectrometer. The two most common methods for ionization are electrospray ionization (ESI) and atmospheric pressure chemical ionization (APCI). With both techniques ionization takes place at atmospheric pressure.

The electrospray probe consists of a metallic capillary to which a voltage is applied. Due to the difference in potential a spray is generated at the tip of the capillary <1> (see number <1> in Figure 2.5-2). A heated

auxiliary gas, e.g. nitrogen, is used to facilitate ionization <2>. The surface of the droplets gets charged in the electrical field and due to solvent evaporation the size of the droplets is reduced. The density of charges at the droplet surface increases and the droplet explodes due to the repulsion between the charges (Coulombic explosion). Eventually, after repeated explosions analyte ions evaporate from the droplet. The so formed molecule ions <3> reach the analyzer (first quadrupole) <4> through a nitrogen flow (291).

Figure 2.5-2   Electrospray ionization
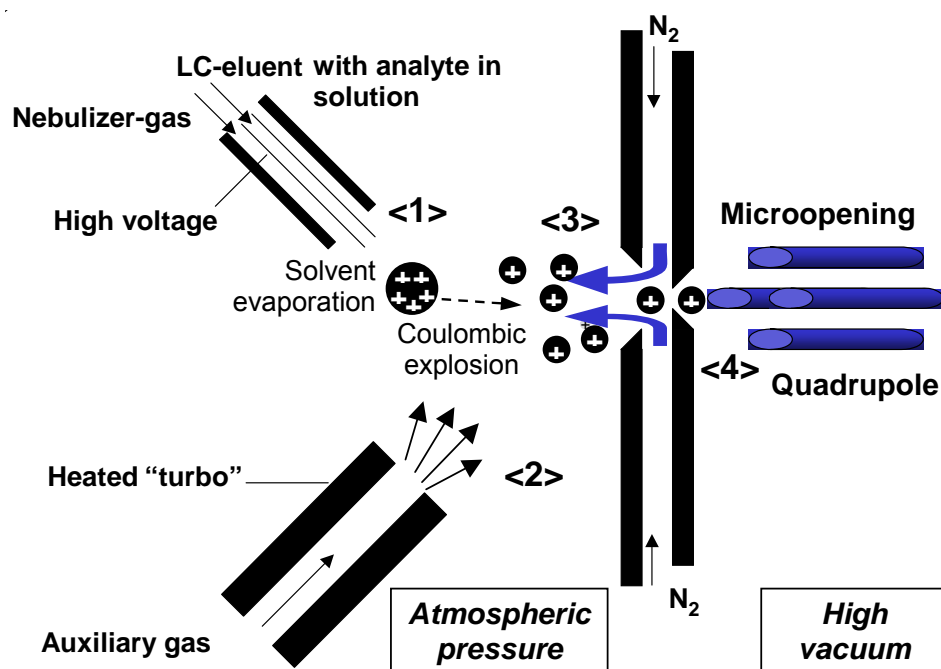
(modified from Steinhauer (291))

In APCI ionization occurs by chemical reactions in the gas phase. The APCI probe is surrounded by a nitrogen flow (nebulizer gas, Figure 2.5-3). The eluent from HPLC including the analyte is vaporized by a heating device and an additional gas flow (auxiliary gas) in or close to the APCI probe. Close to the probe, there is a metallic needle, which is at a potential of a few kilovolts. This leads to ionization and electrical breakdown of the vapor that is generated from the HPLC eluent, nitrogen, and the analyte molecules. The analyte molecules are ionized by chemical reaction with ionized solvent molecules (Figure 2.5-4). This process is called chemical ionization.

Figure 2.5-3   APCI ionization by a heated nebulizer source
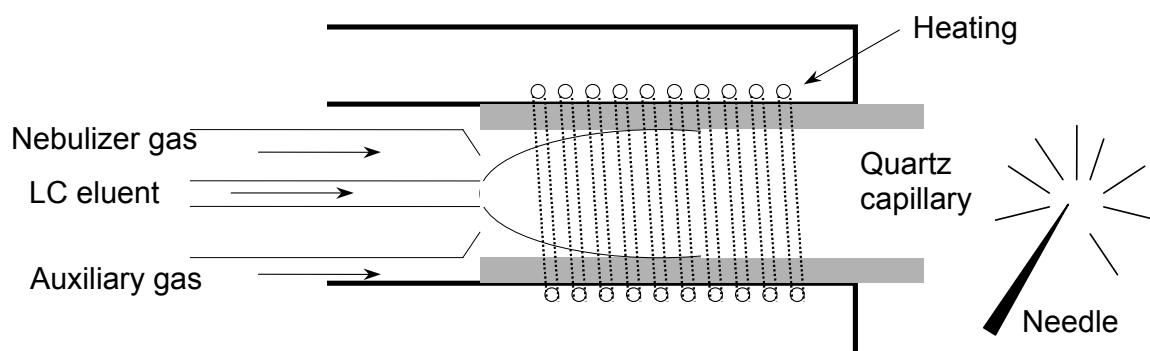
(modified from Steinhauer (291))

Figure 2.5-4   Chemical ionization reactions

$$NH_3 + e^- \longrightarrow NH_3^{+\bullet} + 2\,e^- \quad [1]$$

$$NH_3^{+\bullet} + NH_3 \longrightarrow NH_4^+ + NH_2^\bullet \quad [2]$$

$$NH_4^+ + A \longrightarrow AH^+ + NH_3 \quad [3]$$

$$NH_4^+ + A \longrightarrow ANH_4^+ \quad\quad [4]$$
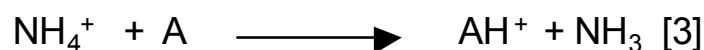
Production of a protonated molecular ion [3] and an ammonium adduct [4]. The primary reaction is ionization [1] of the reaction gas to form a radical cation. The radical cation reacts with a second ammonium molecule [2]. A denotes an analyte molecule. (modified from Steinhauer (291))

    The so produced gas phase ions are then separated in the analyzer. A common analyzer is the quadrupole. The quadrupole consists of two pairs of metallic rods. One pair of opposed rods is charged with a positive electrical potential, and the other with a negative potential. By this method, an electrical field is generated that allows only ions with specific m/z values to pass the quadrupole and be detected. Ions with other m/z values are deflected and do not reach the detector. As the separations are based on an electrical field, m/z is important and not mass alone. The quadrupole is operated under high vacuum to allow the ions to travel to the detector in a sufficient yield.

    In tandem mass spectrometry (MS/MS), the analyzer consists of two quadrupoles (Q1 and Q3) that are separated by a collision cell (Q2) (Figure 2.5-5). MS/MS was developed to improve the selectivity and sensitivity of a

single quadrupole. The ions may be focussed by a quadrupole Q0. A precursor ion is selected by the quadrupole Q1 according to the m/z of the precursor. The precursor ion is then fragmented in the collision cell (Q2) by acceleration in the presence of an inert collision gas, e.g. argon or helium. The collision cell might also consist of a quadrupole. The resulting fragments are then analyzed by the quadrupole Q3 based on the m/z of the fragment ion.

Figure 2.5-5   Tandem mass spectrometer
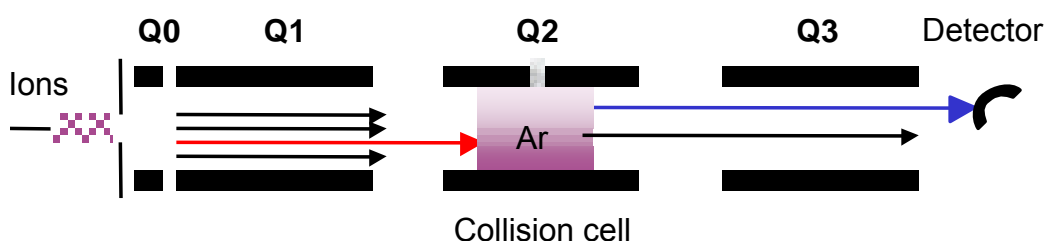
(modified from Steinhauer (291))

After separation of the ions in the analyzer they are detected by the detector. In quadrupole instruments electron multipliers are widely used as detectors. The negative or positive ions are converted into electrons by a conversion dynode. The resulting electrons are amplified by subsequent dynodes. The dynodes are acceleration electrodes that accelerate the electrons to speeds which allow them to generate more than one new electron when hitting the next dynode.

2.6   Pharmacokinetic calculations

2.6.1   Non-compartmental analysis

Non-compartmental analysis (NCA) is a standard technique of PK analysis. NCA is easier to apply and relies on fewer assumptions than compartmental modeling (chapter 2.6.2). Standard NCA assumes linear PK, i.e. all transport processes are assumed to follow first-order kinetics (113). NCA does not provide a mechanistic description e.g. of saturable elimination.

The PK parameters are calculated from the individual plasma concentration time curves.

In our NCA, we read the maximum plasma concentration (Cmax) and time to peak concentration (Tmax) for each subject directly from the plasma concentration time raw data. For determination of the terminal half-life ($T_{1/2}$), the slope ($-\lambda_Z$) of the terminal part of the time versus logarithmic plasma concentration curve was determined by linear regression (Figure 2.6-1). To determine the terminal slope, at least three or four observations should lie in this part of the curve (113). $T_{1/2}$ was then calculated as ln(2) divided by λ_Z.

Figure 2.6-1   Determination of terminal half-life by NCA
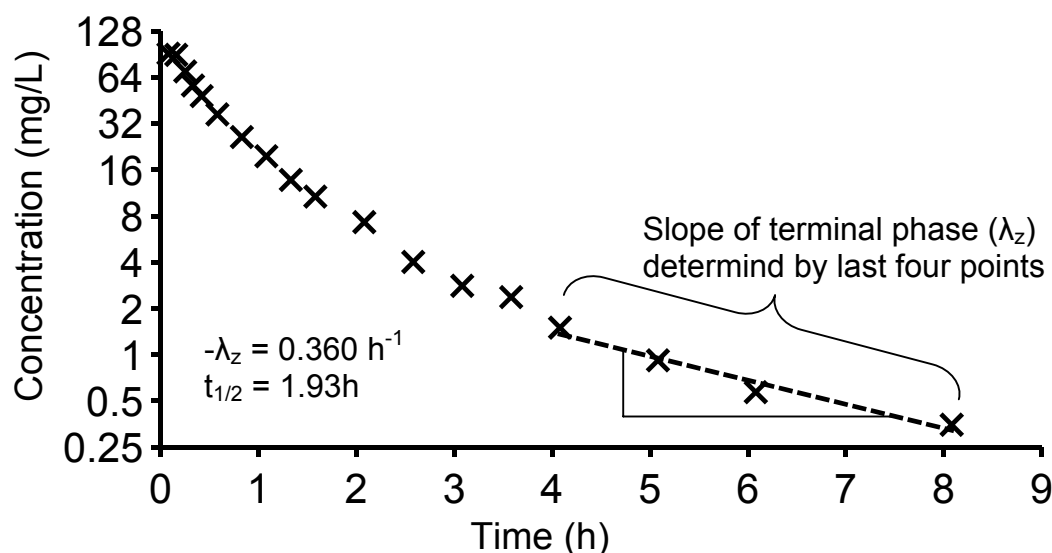
The area under the plasma (or serum) concentration time curve (AUC) was calculated by the trapezoidal method (Figure 2.6-2). We used the linear up log down trapezoidal method for calculation of the AUC. This means that linear interpolation is used for ascending parts of the curve and logarithmic interpolation is used for descending parts of the curve. Plasma concentrations are assumed to decline mono-exponentially between two measured concentrations for the descending part of the curve (113). We calculated the AUC from time of administration up to the last quantifiable concentration ($AUC_{0-\infty}$) for our PK dat after single dose. The last quantifiable concentration is the last sample with a concentration above the limit of quantification of the analytical method. The AUC from the last quantifiable concentration (C_{last}) to

time infinity was extrapolated based on the terminal half-life by the formula C_{last}/λ_Z. The AUC from time of administration up to time infinity was calculated as $AUC_{0-\infty} = AUC_{0-last} + C_{last}/\lambda_Z$.

Figure 2.6-2   Determination of AUC by linear interpolation between measured concentrations
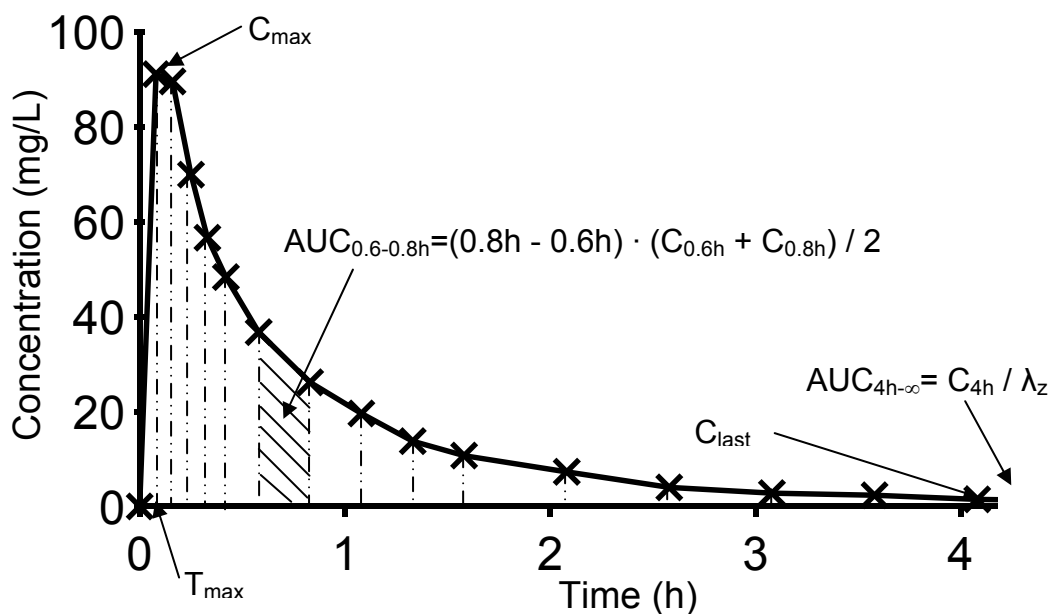
Total body clearance (CL_T) was determined by dividing the administered dose by the $AUC_{0-\infty}$ in plasma. For calculation of renal clearance (CL_R), cumulative renal excretion until the time of the last urine sample was divided by the AUC for the respective time interval in plasma. Nonrenal clearance (CL_{NR}) was calculated as the difference between CL_T and CL_R: $CL_{NR} = CL_T - CL_R$.

The area under the product of the concentration and time versus time curve is called the area under the first moment concentration time curve (AUMC). AUC is the area under the zero moment curve. Mean residence time (MRT) is the time that a drug molecule stays in the body, excluding the gastrointestinal tract. MRT is calculated as the ratio of AUMC divided by AUC (113). After intravenous dosing, volume of distribution at steady-state (Vss) was calculated as MRT · CL_T. The fraction excreted unchanged in urine (Ae) was calculated by dividing the cumulative amount excreted in urine by the

dose. We used WinNonlin^{TM} Professional (version 4.0.1, Pharsight Corp., Mountain View, CA, USA) for NCA.

2.6.2   Compartmental modeling by the standard-two-stage approach

The standard-two-stage approach (STS) is frequently used for data analysis from PK studies (Figure 2.6-3). In the first step the PK parameters are estimated by compartmental modeling for each subject individually. For a PK model with five structural PK parameters, STS requires at least six data points (observations) to estimate those five parameters. Therefore, STS is best applied for rich datasets i.e. studies with frequent observations from each subject. In the second step the distribution of the individual PK parameters is calculated by descriptive statistics (83). It is usually assumed that each subject contributes an equal amount of information, or equivalently that the respective PK parameter (e.g. clearance) is estimated with the same precision in each subject. As the number (and timing) of observations determines the precision, it is desirable that about the same number of samples is collected from each subject.

Figure 2.6-3   Standard-two-stage modeling of a plasma concentration time profile
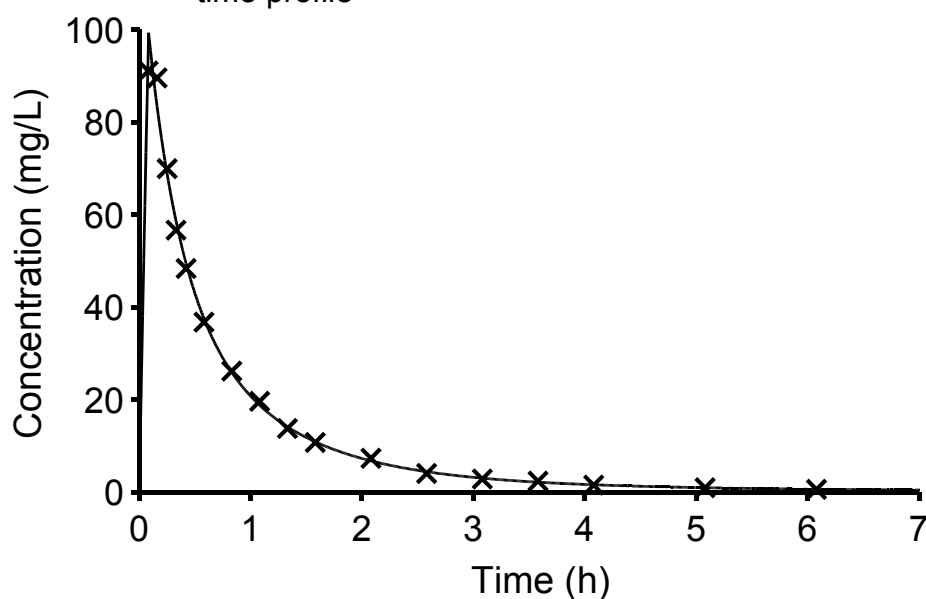
In compartmental models the body is represented as a system of compartments. It is assumed that the rate of change of drug concentration is the same within one compartment, i.e. distribution within one compartment is instantaneous. Therefore, a one compartment model assumes that, if drug concentration in plasma increases by 20% during a certain period of time, concentrations in all other tissues and fluids of the body also increase by 20% during this time period. However, after entering the systemic circulation most drugs require some time to distribute throughout the body. Highly perfused organs like the liver or kidneys are often in a rapid equilibrium with the blood. Generally, together with the blood, those readily accessible tissues are referred to as the central compartment (120).

In a two compartment model the second compartment is called the peripheral compartment which has a slower equilibrium with the blood. This compartment often represents less perfused tissues like muscle or fat. Besides the perfusion rate, the physico-chemical characteristics (e.g. the lipophilicity and pKa values) of the drug influence the time to reach equilibrium. Three compartment models (Figure 2.6-4) comprise a central, a shallow peripheral (fast equilibration) and a deep peripheral (slow equilibration) compartment.

Figure 2.6-4 Three compartment model with zero-order input of an intravenous infusion
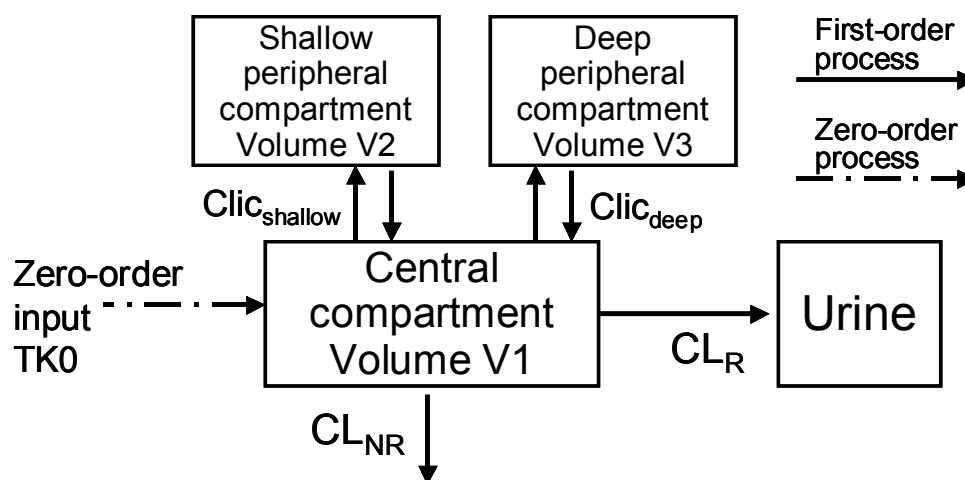
$CLic_{shallow}$: intercompartmental clearance between the central and the shallow peripheral compartment, $CLic_{deep}$: intercompartmental clearance between the central and the deep peripheral compartment, TK0: duration of zero order input.

The number of compartments required to describe a plasma concentration time curve depends on factors like the physico-chemical characteristics of the drug, the mode of administration and the number and timing of blood samples. If the logarithmically transformed plasma concentration time curve shows first a fast decline (drug is distributed from the blood into other fluids and tissues and an equilibrium has not yet been reached) and then a slower decline, two or three compartments are usually most appropriate to model the plasma concentration time curves.

In most "standard" compartment models, it is assumed that the rate of transfer between compartments and the rate of elimination from compartments follows first-order (linear) kinetics (120). A situation where this assumption does not apply is saturable elimination. Another common assumption is that elimination only occurs from the central compartment.

We used WinNonlin^{TM} Professional (version 4.0.1, Pharsight Corp., Mountain View, CA, USA) for compartmental analysis by the STS approach. The models were programmed in Fortran 90. Compaq Visual Fortran 6.6 (© 2000, Compaq Computer Corporation) was used as Fortran compiler. The compiled models were loaded into WinNonlin.

As plasma concentrations often span a wide range, it is useful to employ a weighting procedure for the raw data that allows one to fit low concentrations and high concentrations simultaneously. We used weighting by the reciprocal of the concentration or iterative reweighting by the reciprocal of the predicted concentration. The Nelder-Mead simplex algorithm, which is implemented in WinNonlin, was used as fitting algorithm (113). Figure 2.6-5 shows an example for a PK model with two parameters. In the first step the weighted residual sum of squares (WRSS) is computed at three equally spaced points from the initial estimates for the two parameters. This generates an equilateral triangle (simplex) with the vertices 1, 2, and 3 (Figure 2.6-5). The contours in the plot depict similar values of WRSS. As 1 is the vertex with the largest WRSS, the simplex is reflected about the line connecting 2 and 3. This produces a new vertex 4. In the triangle 2, 3, 4, the vertex 2 is associated with the largest WRSS, and now the triangle is reflected about the line connecting 3 and 4. This procedure is repeated until one of the

vertices remains unchanged and then the size of the triangle is reduced. When the size has been reduced by a pre-specified factor, convergence is assumed. For three parameters the simplex would be replaced by a regular tetrahedron (113).

Figure 2.6-5   Illustration of the simplex algorithm for two parameters
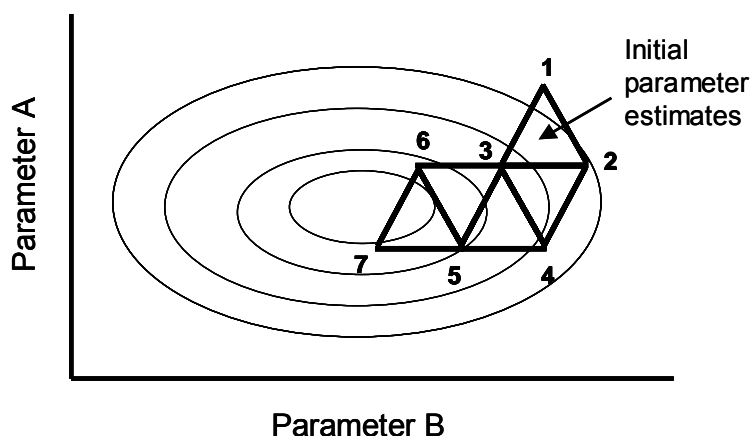
2.6.3   **Population pharmacokinetics – nonlinear mixed effects modeling**

Population PK, according to the definition of the FDA, is "the study of the sources and correlates of variability in drug concentrations among individuals who are the target patient population receiving clinically relevant doses of a drug of interest". Population PK modeling can be used to evaluate both rich and sparse datasets. In the extreme case, sparse datasets might only comprise one sample per subject. The data from all subjects are analyzed simultaneously, while the individuality of each subject is maintained. Therefore clinical data like the sparse datasets from our bone penetration studies can be evaluated by population PK models, whereas applying the STS approach would have severe limitations for analysis of these data.

NONMEM is the abbreviation of NONlinear Mixed Effects Modeling, as well as a popular program (NONMEM®) which uses this technique primarily for population PKPD analyses. We used NONMEM version V release 1.1 (NONMEM Project Group, University of California, San Francisco, CA, USA) (25) for all population PK modeling. There are three types of parameters to be

estimated for our population PK models: 1) structural PK parameters (= fixed effect), 2) parameters for the BSV model (= random effect), and 3) parameters for the residual error model (= random effect). As both fixed and random effects are simultaneously estimated, these models are called mixed effects models. NONMEM uses a maximum likelihood approach. Maximum likelihood estimation searches for the model parameters which optimize the probability (likelihood) of the model given the observed data (e.g. plasma concentrations). The estimation in NONMEM seeks to maximize the likelihood or equivalently to minimize NONMEM's objective function which is -2 times the log-likelihood. The model with the lowest objective function is regarded to give the best model fit. Technically, NONMEM approximates the likelihood to accelerate computation time. We used the FOCE approximation method with the INTERACTION option for all population PK modelling as implemented in NONMEM. NONMEM's optimization algorithm involves calculation of the gradient for each model parameter. During the optimization these gradients become smaller until convergence is reached. Importantly, we are not aware of any general method to assure that the minimum found by NONMEM is a global minimum and not a local minimum. However, it is possible to assure, whether the model yields an adequate model fit and useful predictions (see Figure 2.6-6).

Fixed effects comprise the population PK parameters, e.g. clearance, and the parameters which describe the influence of covariates (like weight or creatinine clearance) on the population PK parameters. The common characteristic of a fixed effect is that this part of the model does not contain a random component. Random effects comprise the random BSV in the PK parameters and the random residual error. The residual error includes within subject variability and measurement error.

Covariates are included into the model to decrease the unexplained BSV. The fraction of the BSV that is explained by a covariate is called the predictable component of the BSV. Usually more than 50 subjects are required to study the influence of covariates on PK parameters. As our studies had a small sample size and most studies were in healthy volunteers, we did not include covariates into our population PK models.

A population PK model directly estimates the variability in the PK parameters within the whole study population, while fitting the concentration time curves of all subjects simultaneously. The variability in the concentration time curves is described by variability in the PK parameters. Table 2.6-1 shows an example of a variance-covariance matrix from the study on dose linearity of flucloxacillin (see chapter 3.2) assuming a log-normal distribution.

Table 2.6-1   Variance-covariance matrix for flucloxacillin

	CL_R	CL_{NR}	V1	V2	V3
CL_R	0.0343				
CL_{NR}	0.0124	0.112			
V1	0.00488	0.00551	0.0282		
V2	0.0415	0.0641	0.00168	0.138	
V3	0.0172	0.00804	0.0175	0.0351	0.023

The diagonal elements denote the variance of the respective parameters (Var), i.e. 0.0343 for renal and 0.112 for nonrenal clearance. The square root of the variance is an approximation to the apparent coefficient of variation of a normal distribution on log-scale, i.e. 19% for renal and 33% for nonrenal clearance. We report BSV as apparent between subject coefficient of variation in the results of our population PK analyses. It is often advantageous to consider the pairwise variability (covariance) of PK parameters. The covariance (Cov) is described by the off-diagonal elements of the variance-covariance matrix. The covariance between renal and nonrenal clearance is 0.0124 in this example. The coefficient of correlation (r) between two parameters P1 and P2 may be calculated as follows:

$$r(P1,P2) = \frac{Cov(P1,P2)}{\sqrt{Var(P1) \cdot Var(P2)}}$$ Formula 2.6-1

In this example the coefficient of correlation between renal and nonrenal clearance is 0.20.

By considering both average PK parameters and their variability, a population PK model can predict the expected range of concentration time profiles for the study population. This is done by simulating a large number

(e.g. 1,000 to 10,000) of concentration time curves. The resulting large number of profiles can be used for PKPD calculations to predict microbiological or clinical success within the target population. This method assumes that the subjects from the original study are representative for the population of interest with regard to their PK.

2.6.4   Bayesian estimation

Sometimes the information contained in the observed concentrations from a new study is too sparse to estimate a full population PK model. In those situations Bayesian methods allow one to combine prior information with the information from the new study. In our case, prior information about PK parameters and their BSV was used to define a PK model. We assumed that the patients for whom those PK parameters (=prior information) were determined, were comparable to the patients of our new study.

The individual PK parameters of the patients from the new study are estimated by "balancing" the prior information and the information contained in the new dataset. The prior information becomes increasingly unimportant, the more new information becomes available. This process of estimating the individual PK parameters from the new study is called maximum *a posteriori* probability (MAP) Bayesian estimation. By combining the prior information with new data, this method yields the most likely ("maximum probability") individual PK parameters (*"posterior"* parameters) for the subjects of the new study.

The assumption that the patients used to derive the prior information and the patients from the new study come from the same population (or are at least comparable) may be critical. Although this assumption might not be perfectly valid, MAP-Bayesian estimation is a powerful tool to estimate the individual PK parameters in case of very sparse data. We used MAP-Bayesian estimation as implemented in ADAPT II (74), which is comparable to the STS approach, since the PK parameters are estimated for each subject individually. However, MAP-Bayesian estimation is applicable to sparse datasets, to which the STS method cannot be applied.

2.6.5   Model discrimination

Model discrimination aims at finding out which of the studied models has the "best" performance according to the following two criteria: 1) How well does the model fit the raw data? 2) how well do the simulated concentrations mirror the average and variability of the observed concentrations, if one simulates from the model? While the first criterion evaluates the model fit, the second criterion studies the predictive performance of the PK model. The second criterion is especially important for a model which is to be used in MCS.

For the STS approach, we used the following criteria for model discrimination: 1) visual inspection of the individual observed and predicted plasma and urine concentration time curves, 2) visual comparison of the patterns of residuals, 3) intra subject comparison of Akaike information criteria (AIC) between competing models, and 4) the number of subjects who had the best (i.e. lowest) AIC for each model. The AIC is a measure of goodness of fit and is calculated as follows:

$$AIC = N \cdot \log(WRSS) + 2P \qquad\qquad \text{Formula 2.6-2}$$

The AIC considers both the model fit (sum of squared residuals) and the number of parameters of the model. N is the number of observations. WRSS is the weighted residual sum of squares, an estimate of the variance of the residuals. P is the number of parameters in the model. When comparing several models for the same dataset, the model associated with the smallest AIC value is regarded as the "best" model. If model A has a 2 point lower AIC than model B, there is a 73% probability that model A is better and a 27% chance that model B is better. As two times the value of P is added for calculation of the AIC, from two models that fit the data equally well (same WSSR) the model with the lower number of parameters (i.e. the simpler model) is preferred. Because the weighted residuals are used for the AIC, only AIC values for models estimated by the same weighting scheme can be compared.

In our population PK analyses, we discriminated competing models by NONMEM's objective function and residual plots. As for the AIC, the absolute number of the objective function is not meaningful. Only the difference in NONMEM's objective function between two or more competing models is informative. The model with the smallest objective function for the smallest number of PK parameters is regarded to give the best fit to the data. If two models had an insignificant difference in the objective function, we selected the simpler model. In NONMEM, the objective function is -2 times the log of the likelihood (plus a constant).

In addition to the criteria described above which all assess the goodness of model fit, we evaluated the predictive performance of our models from STS and population PK analysis via visual predictive checks. We simulated the plasma, serum, urine, or bone concentration time profiles for 4,000 to 10,000 virtual subjects for each competing model. From those simulated concentration time curves we calculated the median and e.g. the nonparametric 80% prediction interval (10% to 90% percentile) of the predicted concentration time profiles. These prediction interval lines were then over-layed on the original raw data. If the model described the data correctly, then 20% of the observed data points should fall outside the 80% prediction interval at each time point (Figure 2.6-6).

Figure 2.6-6   Visual predictive check
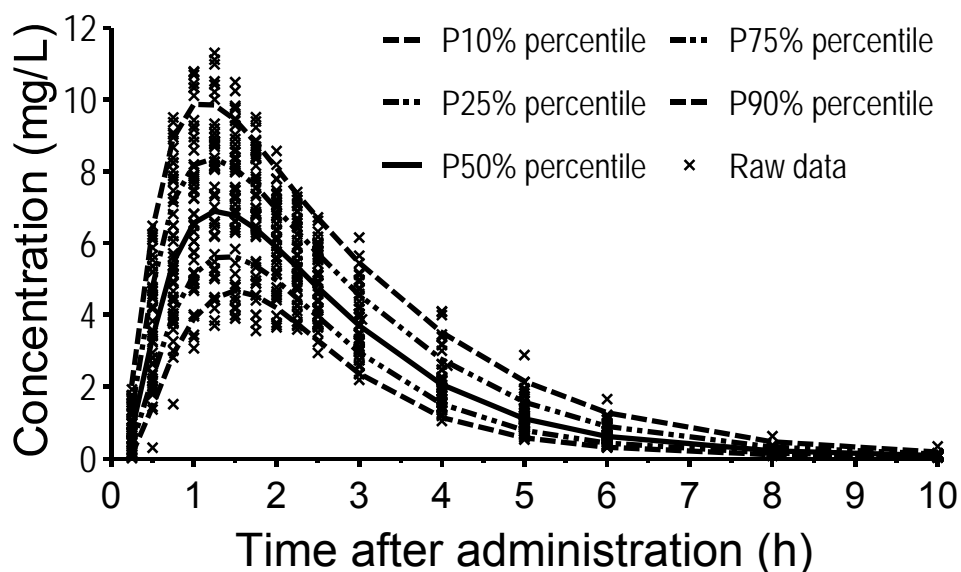
We compared the median predicted concentrations and the 80% prediction interval with the raw data and assessed visually, whether the median and the 80% prediction interval mirrored the central tendency and the variability of the raw data for the respective model adequately.

2.7   Pharmacodynamic simulations

2.7.1   Background

PD simulations are used to determine the probability of successful microbiological or clinical outcome for a specific antimicrobial dosage regimen. The microbiological outcome of antimicrobial treatment is related to the ability of an antibiotic to kill the pathogens causing the infection or to inhibit their growth. Besides the "right" choice of antibiotic, a sufficient exposure to the antimicrobial is necessary for successful microbiological outcome. As protein binding was shown to have an adverse impact on microbiological activity of antibiotics (35, 223), only free (non-protein bound) drug is considered microbiologically active (89).

In the late 1940s and 1950s Eagle et al. (98) first showed in a mouse thigh infection model that not only the total exposure but also the shape of the concentration time curve is important for successful outcome. Their work was continued and further substantiated by Craig and coworkers (319) in the 1980s and thereafter. They found that beta-lactams exhibit relatively concentration-independent rates of killing. The rate of killing for beta-lactams reaches its maximum very quickly as their concentration increases from 1 times the MIC to 4-6 times the MIC of the infecting pathogen. The time that the non-protein bound plasma concentration remains above the MIC for the pathogen ($fT_{>MIC}$) is established as the PKPD index (228) that best predicts microbiological outcome for beta-lactams. The time above MIC should be reported as the cumulative percentage of a 24h period that the drug concentration exceeds the MIC at steady-state conditions (228).

Craig et al. (67) found in a mouse infection model for penicillins that the concentration of free drug has to exceed the MIC for about 30% of the dosing interval to achieve bacteriostasis, and for about 50% of the dosing interval to achieve the near-maximal bactericidal effect (89). Therefore $fT_{>MIC} \geq 50\%$ is called the PKPD target for near-maximal bactericidal activity of penicillins. Attainment of the PKPD target is often used as a surrogate endpoint for successful clinical outcome. The choice of the PKPD target depends, among other factors, on the status of the patient's immune system and on the seriousness of the infection (67). Treatment of a minor infection might require only bacteriostatic activity of the antibiotic, as the infection can then be eliminated by the patient's immune system. For treatment of severe infections in immuno-compromised patients, near-maximal bacterial killing should be achieved (89). Slow-growing bacteria in infection sites that require the use of antibiotics with bactericidal activity for efficacious treatment, such as osteomyelitis or endocarditis, may need higher PKPD targets compared to acute respiratory infections (67). Figure 2.7-1 shows how $fT_{>MIC}$ is derived from a plasma concentration time profile.

Figure 2.7-1   Derivation of time above MIC
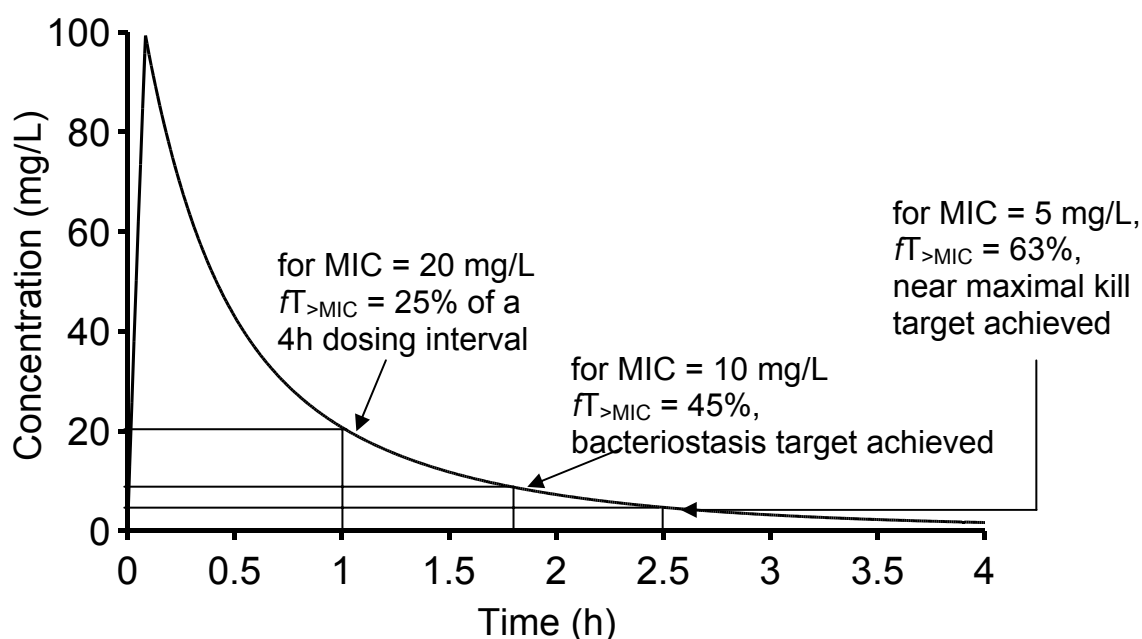
For quinolones the rates of killing are concentration-dependent over a wide range of concentrations. The ratio of the free area under the concentration-time curve over 24h to the MIC (*f*AUC/MIC) best predicts the microbiological effect of quinolones (89).

2.7.2   Monte Carlo simulation in the field of PKPD

Monte Carlo simulation (MCS) was originally called "statistical sampling". MCS is a stochastic simulation method that uses random numbers to simulate data. Therefore, the exact result of a single experiment cannot be predicted. This differentiates MCS from deterministic simulations. In deterministic simulations, one specific input will always give the same result and therefore the simulations are fully predictable. The name Monte Carlo simulation refers to the famous casino and was chosen because of the randomness and repetitions involved in the simulations. MCS has been used for very different purposes like studying the properties of the neutron in 1930, or the development of the hydrogen bomb in the 1950s. The first use of MCS for selection of antibiotic doses and setting susceptibility breakpoints was presented in 1998 by Drusano et al. (89). They showed that MCS is a valuable tool in rational dose selection for phase II/III clinical trials (93) (chapter 1.3.4).

Although MCS cannot predict the concentration time profile for a new subject, it can predict the expected range of concentration time profiles for a population of individuals for a chosen dosage regimen. Based on this expected range of profiles, the probability of attaining a PKPD target for a dosage regimen of interest can be predicted. This PTA depends on the antibiotic concentrations in the patient population and on the susceptibility of the infecting pathogen. There is variability in the concentration time profiles between patients and in the bacterial susceptibility to an antibiotic (described by the MIC).

To describe the distribution of expected antibiotic concentrations for a chosen dosage regimen, the concentration time profiles for a large number of virtual subjects (e.g. 10,000) are simulated. Simulating 10,000 subjects

provides a robust prediction for the PTA. Those simulations are based on a population PK model which must have adequate predictive performance to yield unbiased estimates for the PTA.

The PKPD targets for antibiotics are based on the MIC of the pathogens. Therefore, the PTA is predicted for a range of MICs. The PKPD indices (e.g. $fT_{>MIC}$ for beta-lactams or $fAUC/MIC$ for quinolones) are then calculated for the 10,000 subjects at each MIC within this range. The values of the PKPD indices are compared to the PKPD target (e.g. $fT_{>MIC}$ at least 50% of dosing interval) for all 10,000 simulated subjects at each MIC. The PTA at each MIC is then derived by calculating the fraction of subjects who attained the target at each MIC.

The highest MIC for which the target is attained by at least 90% of the simulated subjects is often defined as the PKPD breakpoint (Figure 2.7-2).

Figure 2.7-2   PTA vs. MIC profile and derivation of the PKPD breakpoint
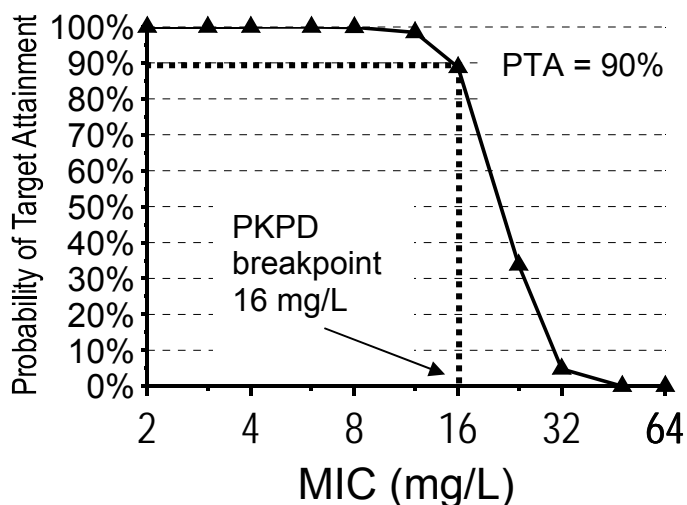
This definition is also used in this thesis. Therefore the PKPD breakpoint is the highest MIC, for which the probability of successful treatment with the chosen dosage regimen is ≥90%. If a patient is infected by pathogens with an MIC higher than the PKPD breakpoint, another dosage regimen should be chosen. Importantly, the PKPD breakpoint is determined in a different way compared to the susceptibility breakpoints which are set by national organizations like the DIN (Deutsches Institut für Normung), the CLSI (Clinical and Laboratory Standards Institute), and the BSAC (British Society

for Antimicrobial Chemotherapy). Consequently, the PKPD breakpoint and the susceptibility breakpoints set by those organizations may differ by more than a factor of 4.

To put the PTAs into clinical perspective, the PTA expectation value (also called cumulative fraction of response (228)) is calculated. The PTA expectation value is an estimate of the proportion of the population that will achieve the PKPD target, for a specific drug dose and a specific population of microorganisms. MIC distributions of pathogens of clinical interest can be obtained from published studies where large numbers of isolates were collected and their MICs determined. Alternatively the MIC distribution of a local hospital can be used. The PTA expectation value is calculated by multiplying the PTA at each MIC by the fraction of the population of microorganisms at each MIC (Figure 2.7-3). Ideally, a PK model which has been determined in the patient population of interest is combined with the MIC distribution typically observed in those patients at a local hospital. The PTA expectation value can then be used to predict the probability of microbiological or clinical success in this local hospital.

Figure 2.7-3   Calculation of the PTA expectation value based on the PTA vs. MIC profile and the expected MIC distribution
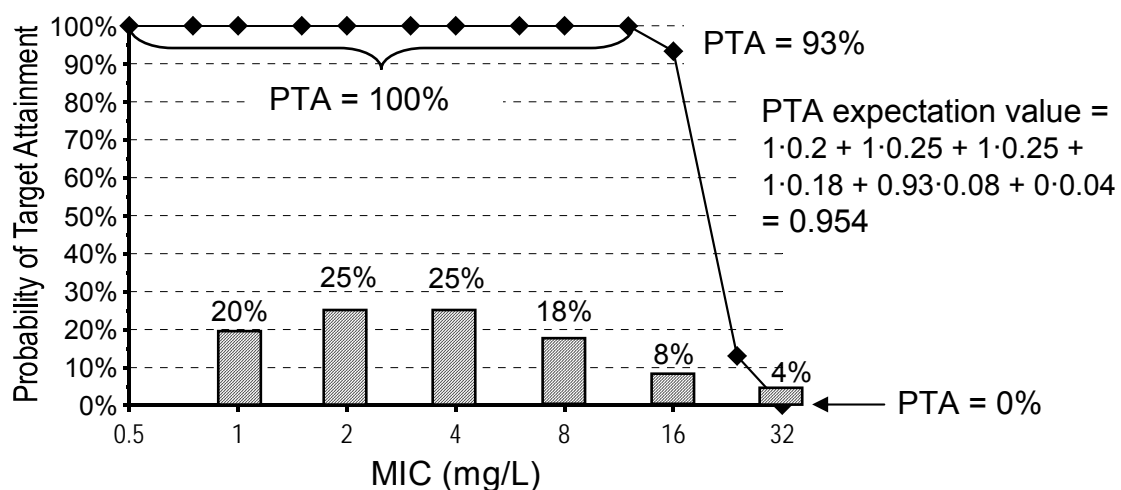
2.8   Statistical analysis

2.8.1   Descriptive statistics – parametric and non-parametric approach

The aim of descriptive statistics is to summarize the central tendency and variability for a set of data. If the distribution of values (roughly) follows a normal distribution, the data can be adequately described by the arithmetic mean and standard deviation (122). This approach is called parametric statistics, as it assumes that the data follow a normal distribution.

If the distribution of data deviates notably from a normal distribution, the arithmetic mean and standard deviation are not appropriate to describe the central tendency and variability. PK parameters like clearance, volume of distribution, and half-life often tend to follow a log-normal distribution, i.e. a normal distribution can be achieved by taking the logarithm of each value and calculating the average and standard deviation on log-scale. In case of a log-normal distribution, the geometric mean and the coefficient of variation (CV) are appropriate statistics to describe the central tendency and variability of the data (Figure 2.8-1, Figure 2.8-2).

If there is insufficient prior knowledge on the form of a distribution, the most reasonable way to describe a distribution is by the median and representative percentiles. Percentiles are calculated by sorting the list of values. The median is the 50% percentile. Half of the data fall below and half of the data fall above the median. Describing a distribution by the median and e.g. the 10% and 90% percentile (P10 and P90) is a non-parametric approach, as no specific distribution is assumed (Figure 2.8-1). The median is very insensitive towards outliers, whereas the arithmetic mean is sensitive to outliers with high values and the geometric mean is sensitive to outliers with low values. As it is difficult to identify an outlier for a small dataset of e.g. 20 samples, the non-parametric approach is a reasonable way to summarize the PK parameters for a study with a small sample size.

Figure 2.8-1   Log-normal distribution of clearances without and with interaction

	Without interaction	With interaction
Geometric mean	0.883	0.727
CV	48%	67%
P10	0.516	0.418
Median	0.872	0.669
P90	1.524	1.604
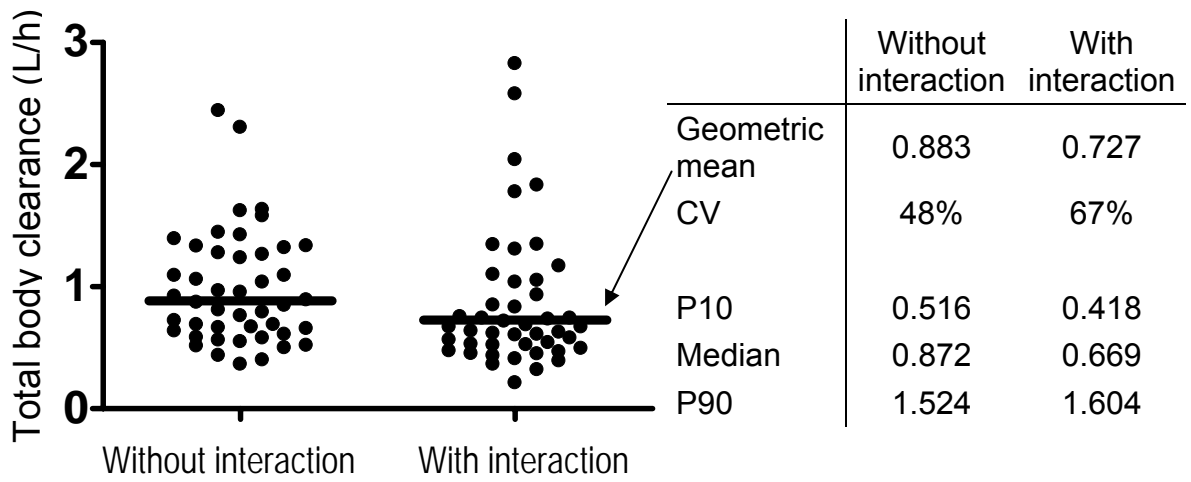
Figure 2.8-2   Histograms including estimated log-normal distributions
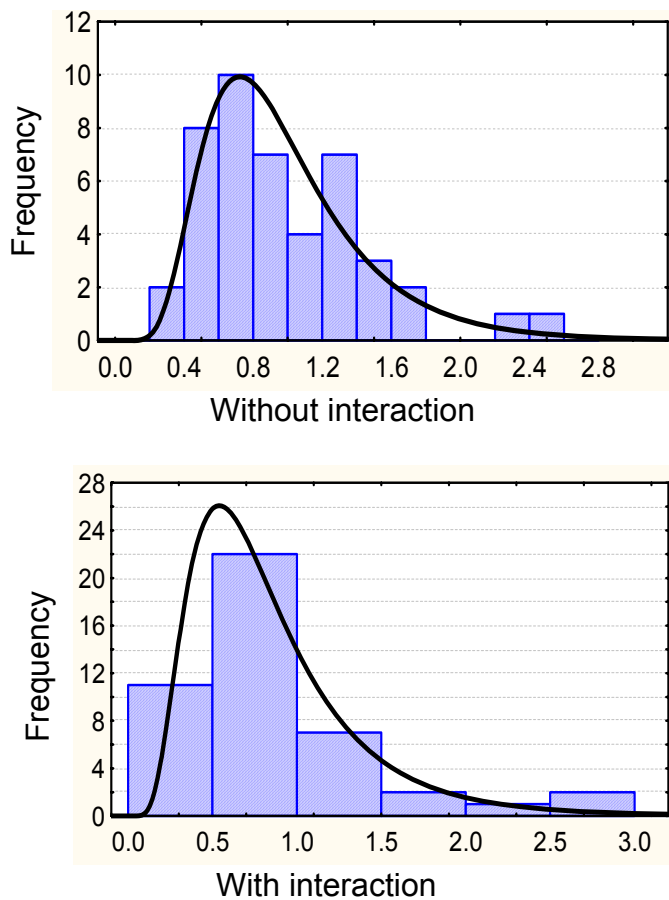
2.8.2   Analysis of variance (ANOVA)

ANOVA is a parametric method which allows one to test for significant differences between means of two (or more) groups of data. ANOVA is based on the average and standard deviation. It assumes that the samples are randomly drawn from normally distributed populations with the same standard deviations (homoscedasticity). The null hypothesis is that the differences between the means are simply due to random variability of data which all arise from the same population. If the differences between the means are larger than would be expected due to population variability, the null hypothesis is rejected. We used an α-level of significance of 0.05.

If the populations are normally distributed, parametric methods generally are more likely (i.e. have a higher power) to detect a real difference than non-parametric methods (122). PK parameters in a population are usually assumed to follow a log-normal distribution rather than a normal distribution. It has been recommended by Cawello (56) to use a log-normal distribution for AUC, clearance, peak concentration, terminal half-life, and volume of distribution. This assumption is often reasonable, however, there is no mathematical proof for this assumption. According to FDA guidelines AUC and Cmax in bioequivalence studies are assumed to follow a log-normal distribution and should be tested on log-scale (2).

We used ANOVA on log-scale to test for differences between treatments in our dose linearity and drug-drug interaction studies. We tested the non-compartmental parameter estimates for our study drugs for differences between treatments (e.g. low versus high dose for assessment of dose linearity, or with versus without concomitant administration of another drug for the interaction studies). We used WinNonlin^{TM} Professional for descriptive statistics, ANOVA, and equivalence statistics.

Figure 2.8-3 shows the scheme of an interaction study at two dose levels, like the study described in chapter 4.4 of this thesis. Two factors, dose level and presence or absence of an interacting agent, have to be taken into account in the ANOVA.

Figure 2.8-3   Scheme of an interaction study at two dose levels
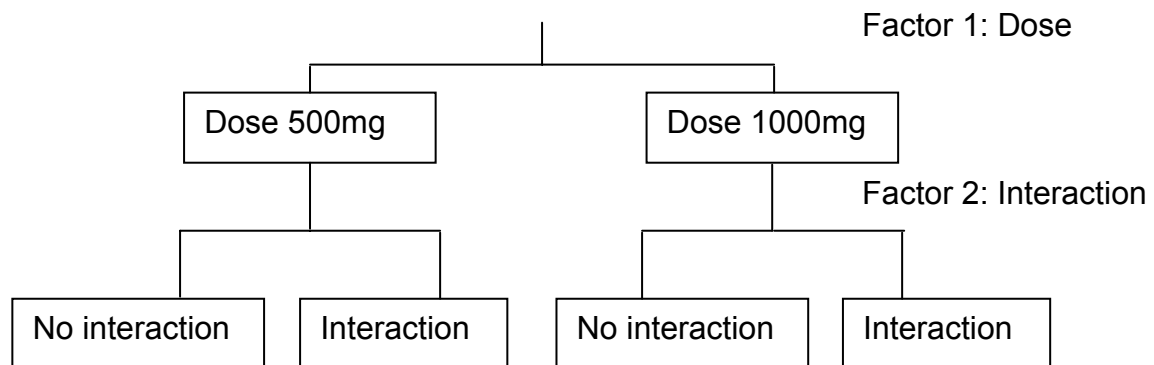
Figure 2.8-4 shows some individual clearances from the distributions of Figure 2.8-1 and Figure 2.8-2, and how the individual values change in the presence of an interacting agent.

Figure 2.8-4   Individual clearances with and without interaction
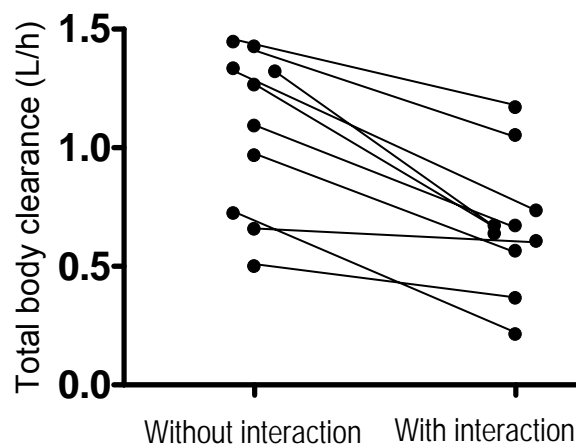
**3   Assessment of dose linearity, the extent of saturable drug
           elimination and its predicted clinical significance**

3.1   Background on dose linearity and saturable elimination

Plasma drug concentrations increase linearly with dose, if all transport processes follow first-order kinetics. This is called dose-independent or linear PK and is a reasonable assumption for many drugs within their therapeutic range. However some drugs exhibit nonlinear, i.e. time- or concentration-dependent PK. When the same dose of a drug results in different concentrations when given at different times, or concentrations after repeated dosing cannot be predicted from single dose data, time-dependent PK might be the reason. A drug that exhibits time-dependent PK is carbamazepine. Due to autoinduction of metabolizing enzymes, carbamazepine clearance increases with time on repetitive oral administration. Other reasons for time-dependent PK may be diurnal variations in urine pH, gastrointestinal physiology or cardiac output (262). For drugs with concentration-dependent PK, the PK parameters change with dose. Concentration dependence in PK parameters may arise from saturation of drug absorption or first-pass metabolism, which results in decreased or increased bioavailability, respectively. Saturation of active renal secretion or reabsorption causes a change in renal clearance, and capacity-limited biotransformation decreases nonrenal clearance with increasing dose (201, 262). Generally, processes are saturable when enzymes or transporters are involved. Concentration-dependent PK is often called dose-dependent PK. Dose-dependent PK might be the preferable term if the drug absorption is saturable. However, saturation of drug transport or metabolism depends on the drug concentration at the transporter or enzyme. Therefore we use the term concentration dependence.

Saturable elimination may be caused by capacity-limited drug transport like renal tubular secretion, or capacity-limited metabolism in the liver. These capacity-limited (saturable) processes can be described by the Michaelis Menten equation:

$$v = \frac{Vmax \cdot [C]}{K_m + [C]}$$ Formula 3.1-1

where v is the rate of drug elimination, Vmax is the maximum rate of elimination, [C] the drug concentration and K_m the drug concentration associated with a half maximal rate ($Vmax_R/2$) of elimination. Most commonly [C] denotes the drug concentration in plasma (or serum).

As the rate of elimination (v) is given by CL · [C], clearance as a function of [C] is calculated as follows:

$$CL = \frac{Vmax}{K_m + [C]}$$ Formula 3.1-2

If drug concentrations are much lower than the value of K_m, clearance is approximately:

$$CL \cong \frac{Vmax}{K_m}$$ Formula 3.1-3

and the elimination can be described by first-order kinetics, because Vmax and K_m are constants. This situation is often called pseudo-linear or pseudo-first-order kinetics.

Saturation of elimination becomes apparent when drug concentrations are close to or higher than the value of K_m. Clearance decreases as drug concentration increases. At very high concentrations relative to K_m the rate of elimination approaches Vmax. Once Vmax is reached, elimination resembles zero-order kinetics, i.e. a constant amount of drug is eliminated per time unit. In contrast, first-order kinetics means that clearance remains constant and a constant proportion of drug is eliminated per time unit.

If a drug is only eliminated by a saturable process and if the dose rate exceeds the maximal rate of elimination (Vmax), this drug could accumulate indefinitely. However, virtually all drugs are likely to have a parallel first-order (linear) pathway and are not eliminated by saturable pathways alone (201). Ethanol and phenytoin are extreme examples for saturable elimination as they

are almost exclusively eliminated by saturable pathways (262), whereas theophylline and salicylate are examples for parallel saturable and linear elimination (201). By a first-order pathway, a constant proportion of drug is eliminated per time unit, independent of the concentration. The amount of drug eliminated by this pathway increases linearly with concentration (dose). The amount of drug eliminated by a saturable pathway cannot increase once essentially complete saturation is reached. Therefore, if a drug is eliminated in parallel by a first-order and a saturable pathway, the contribution of the first-order pathway relative to the saturable pathway increases with drug concentration. At very high drug concentrations most of the drug elimination occurs via the first-order pathway, even if this pathway is only responsible for a small percentage of the clearance that is seen at low concentrations (201).

Capacity-limited metabolism is a possible reason for saturable elimination. Enzymatic reactions are generally capacity-limited as there is only a finite number of enzymes present in the body. However, only very few drugs reach high enough concentrations in the body to exceed the capacity of the metabolizing enzymes. One example is ethanol that is metabolized by two isoenzymes of alcohol dehydrogenase and a microsomal ethanol-oxidizing system. Those enzymes have different K_m values. A "pooled" K_m has been derived. The concentrations achieved after one or more alcoholic beverages are well above this pooled K_m value for ethanol (about 0.08 g/L) (201). This means that the elimination of ethanol is saturated and the rate of elimination approaches Vmax already at those concentrations. Therefore, zero-order kinetics are often applied to describe ethanol elimination. However, Holford (145) points out the limitations of applying a zero-order model to ethanol elimination and concludes that elimination of ethanol can be described by a model with capacity-limited elimination.

Another example for saturable metabolism is phenytoin. The therapeutic range of phenytoin is usually given as 10 to 20 mg/L, but due to saturable elimination the difference between doses that result in a subtherapeutic effect and doses that cause toxicity is very small (262). An additional difficulty is the high variability in K_m between patients (201).

Therefore, therapeutic drug monitoring is used for phenytoin (323) (chapter 1.3.3).

Saturable elimination may also be due to saturation of renal elimination. Renal clearance is the sum of glomerular filtration, tubular secretion and tubular reabsorption. Filtration is a passive process, reabsorption can be passive or active, and tubular secretion is an active saturable process. Saturation of active tubular reabsorption might result in concentration-dependent renal elimination. Saturation in reabsorption causes an increase in renal clearance of ascorbic acid at very high doses. Therefore, and because of saturable absorption, plasma concentrations of ascorbic acid do not change greatly even if the dose is much increased (262). A different mechanism causes nonlinear elimination of salicylate. Salicylate decreases urinary pH and shows pH-dependent tubular reabsorption, therefore renal clearance decreases at higher doses. However, because of the small contribution of renal clearance to total salicylate clearance this mechanism has little influence on plasma concentrations (201).

Active secretion of anions and cations is mediated by a wide variety of transporters located in the renal tubules. However active renal secretion does not occur as the only pathway by which a drug is eliminated, as glomerular filtration is always present if a drug is excreted by the kidneys. Therefore, saturation of active renal secretion is not likely to result in accumulation of a drug to an extent as it might happen with ethanol or phenytoin. Nonlinear kinetics due to saturation of renal secretion has been reported for several acylureido-penicillins (azlocillin (27), mezlocillin (29, 106, 212), piperacillin (304, 317)) and dicloxacillin (234, 262).

There are contradictory reports about the existence of saturable elimination of piperacillin at therapeutic concentrations. We are not aware of a study using population PK to explore dose linearity of flucloxacillin, which is also eliminated by active renal secretion. Therefore we investigated if saturation of elimination becomes apparent at therapeutic concentrations. We intended to compare various dosage regimens via MCS, and for this knowledge about a possibly existing saturable elimination of the study drugs is important.

3.2 Population pharmacokinetics at two dose levels and pharmacodynamic profiling of flucloxacillin

3.2.1 Chemical structure of flucloxacillin

$(C_{19}H_{16}ClFN_3NaO_5S,$ Mol. Wt.: 475.85$)$
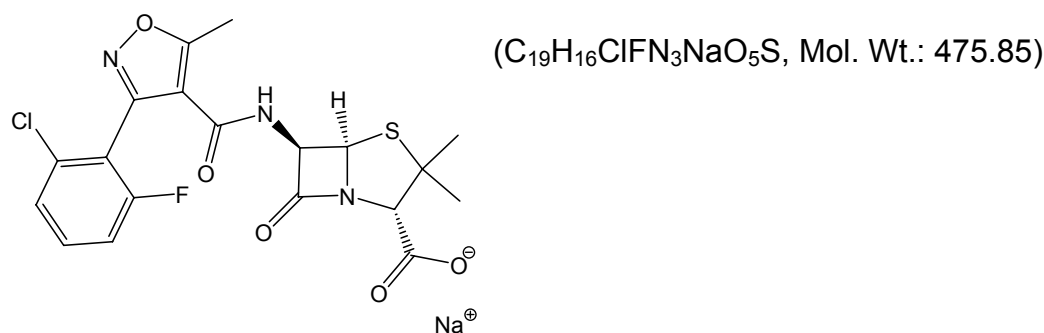
Chemical structure 3.2-1 Flucloxacillin

3.2.2 Indications and dosing of flucloxacillin

Flucloxacillin is an isoxazolyl penicillin and is active against many gram positive bacteria, including penicillinase producing staphylococci and streptococci, but not against MRSA (123). In the United Kingdom flucloxacillin remains the predominantly prescribed anti-staphylococcal oral antibiotic (263). It is typically used for skin, soft tissue, and respiratory tract infections. For serious infections like endocarditis or osteomyelitis caused by MSSA it is administered intravenously as slow injection, short-term infusion, or continuous infusion. In a randomized comparison trial with flucloxacillin at a dose of 1g every 6h (1g q6h) and teicoplanin (6mg/kg q12h for three doses, then the same dose given once daily) in the treatment of burn wound infections due to gram positive pathogens, no significant differences in clinical and microbiological success rates between flucloxacillin and teicoplanin were found (289). Resistance against glycopeptides is increasing and restricting glycopeptide use has been reported to be helpful in controlling vancomycin-resistant enterococci (40, 125). Therefore it might be preferable to use alternatives like flucloxacillin against MSSA, if the alternative grants a sufficient probability for successful clinical outcome. In addition, flucloxacillin

has been suggested to show more rapid killing of MSSA than vancomycin *in vitro* and *in vivo*, and usually flucloxacillin levels do not need to be monitored (185).

Attainment of the PKPD targets $fT_{>MIC} \geq 50\%$ is often used as a surrogate endpoint for successful clinical outcome (67, 89) (chapter 2.7.1). For drugs with short half-lives like beta-lactams, prolonged and continuous infusion have been shown to achieve longer $fT_{>MIC}$ than short-term infusions at the same daily dose (69). Consequently, Drusano (90) proposed prolonged infusions for carbapenems to optimize their PTA. Prolonged or continuous infusions may require lower daily doses compared to intermittent treatment, while achieving the same PTA as high dose intermittent treatment.

Conditions like endocarditis and osteomyelitis usually require prolonged high dose treatment. Continuous infusion treatment can be managed at patients' homes better than frequent intermittent infusions (q6h or q4h) and has been reported to be efficacious for completion of treatment against serious staphylococcal infections as home-based treatment (153, 185). However the optimal doses for continuous and prolonged infusion of flucloxacillin have not yet been determined by population PK and MCS. In absence of these data, some authors report that they administered the same daily doses via continuous infusion as for intermittent treatment (153, 185).

We used population PK and MCS to investigate differences in the PTA between intermittent and continuous infusions. For this task it is important to know, whether clearance changes with plasma concentration at therapeutic concentrations. Therefore, our second objective was to compare the PK of flucloxacillin at two different dose levels.

3.2.3 Methods

Study design and drug administration: Ten healthy subjects (five males and five females) participated in the study. In each of the two study periods each subject received a single dose of 500 mg or 1000 mg flucloxacillin as a 5min intravenous infusion.

Sampling Schedule: Blood samples were drawn immediately before start of infusion, at the end of infusion as well as at 5, 10, 15, 20, 25, 45, 60, 75, 90 minutes and 2, 2.5, 3, 3.5, 4, 5, 6, 8, and 24h after the end of the infusion. Urine samples were collected immediately before start of the infusion, from start of the infusion until 1h after end of infusion and in the following time intervals: 1 to 2, 2 to 3, 3 to 4, 4 to 5, 5 to 6, 6 to 8, 8 to 12, 12 to 24h after the end of the infusion.

Determination of Plasma and Urine Concentrations: For determination of flucloxacillin in plasma 100µL of the sample were deproteinized with 200µL acetonitrile containing the internal standard. After mixing and centrifugation at 15,000 rounds/min 40µL were injected onto the HPLC-system. For determination of flucloxacillin in urine 20µL of the sample were diluted with 180µL water. After mixing 40µL were injected onto the HPLC-system. Flucloxacillin was determined using a reversed phase column, potassium dihydrogen phosphate (pH 6.2) / acetonitrile mobile phase with a flow of 2 mL/min. Flucloxacillin and the internal standard were detected at 220nm. The plasma and urine samples were measured against a plasma or urine calibration row. The calibration row in plasma (urine) was prepared by a 10:1 dilution of a tested drug-free plasma (urine) with a stock solution to obtain the highest calibration level. The other calibration levels were obtained by 1:1 dilution of the highest calibration level or a level of higher concentration with drug-free plasma (urine).

No interferences were observed in plasma or urine for flucloxacillin or the internal standard. Calibration was performed by linear regression. The linearity of flucloxacillin calibration curves in plasma and urine was shown between 0.500 - 250 mg/L and 5.00 - 400 mg/L, respectively. The quantification limits were identical with the lowest calibration levels. The inter-day precision and the analytical recovery of the spiked quality control standards of flucloxacillin in human plasma (urine) ranged from 4.1 to 7.7% (3.3 to 5.1%) and from 84.9 to 106.0% (100.0 to 103.0%), respectively.

Pharmacokinetics

Non-compartmental analysis: NCA was performed for both dose levels according to the methods described above.

Population PK analysis: We tested two and three compartment disposition models. The drug input was modeled as a zero order process with a fixed duration of 5 min.

Individual PK model: We estimated the BSV for all parameters except duration of zero order input and intercompartmental clearances. We assumed a log-normal distribution for the PK parameters and used a full variance-covariance matrix to describe the variability of the PK parameters as well as their pairwise correlations. BSV was estimated as variance but we report the square root of the estimate. We have expressed these values as a percentage because this quantity is an apparent coefficient of variation of a log-normal distribution (chapter 2.6.3).

Observation model: We described the residual unidentified variability by a combined additive and proportional error model for plasma concentrations and amounts excreted in urine.

Monte Carlo simulation: We used a non-protein bound plasma concentration above the MIC ($fT_{>MIC}$) for at least 30% or 50% of the dosing interval as PKPD targets for flucloxacillin. We calculated the PTA within the MIC range from 0.0625 to 2 mg/L and used a protein binding of 96% for flucloxacillin (28, 30). Three dosage regimens at a daily dose of 6g were compared: 1) continuous infusion, 2) prolonged (4h) infusion of 2g q8h and 3) short-term (0.5h) infusion of 1.5g q6h. We simulated 10,000 virtual subjects for each of these three dosage regimens at steady-state in absence of residual error. We derived the PTA, the PKPD breakpoint, and the PTA expectation value for each of the two targets.

3.2.4   Results

Demographics: All 10 subjects completed the study. The median [range] weight was 71 [52-83] kg, height was 178 [165-190] cm and age was 25 [23-34] years.

Non-compartmental analysis: Plasma concentrations and amounts in urine of flucloxacillin after infusion of 500 mg and 1000 mg are shown in Figure 3.2-1.

Figure 3.2-1   Average ± SD profiles of flucloxacillin in healthy volunteers
after a 5min infusion of 500 mg or 1000 mg flucloxacillin

Plasma concentrations

Cumulative amounts excreted
unchanged in urine
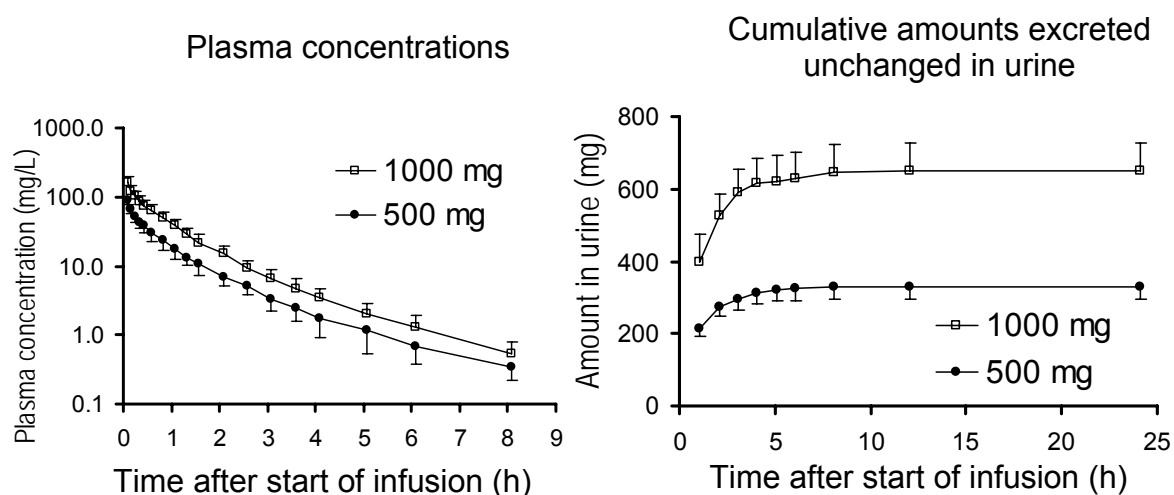
Table 3.2-1 shows the results of the NCA. Peak concentrations and
AUCs were dose linear. All other PK parameters were very similar at both
dose levels.

Table 3.2-1   PK parameters for 500 and 1000 mg flucloxacillin from
non-compartmental analysis

	Geometric mean (%coefficient of variation)		Point estimate (90% confidence interval)	p-value from ANOVA
	500 mg	1000 mg	1000 mg / 500 mg	
Total body clearance (L/h)	8.16 (21%)	8.18 (20%)	100 [94-107]	0.94
Renal clearance (L/h)	5.37 (22%)	5.29 (22%)	99 [90-108]	0.77
Nonrenal clearance (L/h)	2.72 (30%)	2.79 (33%)	103 [88-119]	0.77
Fraction excreted unchanged in urine	0.66 (10%)	0.65 (12%)	98 [93-104]	0.62
Volume of distribution at steady-state (L)	9.63 (15%)	9.97 (17%)	104 [96-112]	0.44
Peak plasma concentration (mg/L)	86.8 (13%)	167 (16%)	192 [175-211]	< 0.01
Terminal half-life (h)	1.40 (26%)	1.62 (25%)	116 [87-153]	0.36
Mean residence time (h)	1.18 (19%)	1.22 (14%)	103 [97-110]	0.36

Population Pharmacokinetics: The three compartment model had a 200 points better objective function and a better predictive performance than the two compartment model. Therefore, we selected the three compartment model. The parameter estimates for this model are shown in Table 3.2-2 and the variance covariance matrix is shown in Table 3.2-3.

Table 3.2-2 Population parameter estimates: Values are geometric means (between subject coefficients of variation)

Parameter	Unit	Estimate
$CL_T°$	$L\ h^{-1}$	8.10
CL_R	$L\ h^{-1}$	5.37 (19%)
CL_{NR}	$L\ h^{-1}$	2.73 (33%)
$Vss°$	L	9.57
V1	L	4.79 (17%)
V2	L	2.61 (37%)
V3	L	2.17 (15%)
$CLic_{shallow}$ *	$L\ h^{-1}$	15.3
$CLic_{deep}$ *	$L\ h^{-1}$	1.23
TK0 (fixed)	min	5
CV_C	-	9.4%
SD_C	$mg\ L^{-1}$	0.155
CV_{AU}	-	20.9%
SD_{AU}	mg	1.04

*: No BSV included for distributional clearance

°: Derived from parameter estimates (not estimated).

CL_T: total clearance; CL_R: renal clearance (non-saturable), CL_{NR}: nonrenal clearance (non-saturable), Vss: volume of distribution at steady-state, V1: volume of distribution for the central compartment, V2: volume of distribution for the shallow peripheral compartment, V3: volume of distribution for the deep peripheral compartment, $CLic_{shallow}$: intercompartmental clearance between the central and the shallow peripheral compartment, $CLic_{deep}$: intercompartmental clearance between the central and the deep peripheral compartment, TK0: duration of zero order input (not estimated), CV_C is the proportional and SD_C is the additive residual error component for the plasma concentrations. CV_{AU} is the proportional and SD_{AU} is the additive residual error component for the amounts excreted in urine.

Table 3.2-3   Variance-covariance matrix for flucloxacillin assuming
                     normal distributions of the PK parameters on log-scale

	CL_R	CL_{NR}	V1	V2	V3
CL_R	0.0343				
CL_{NR}	0.0124	0.112			
V1	0.00488	0.00551	0.0282		
V2	0.0415	0.0641	0.00168	0.138	
V3	0.0172	0.00804	0.0175	0.0351	0.023

See Table 3.2-2 for parameter explanation and chapters 3.2.3 and 2.6.3 for details.

Figure 3.2-2 shows the visual predictive checks for this model. There was no indication that clearance decreased with the increase in dose from 500 mg to 1000 mg. The distribution of subjects with lower/higher individual estimates for the 500 mg dose than for the 1000 mg dose was 5/5 for total clearance, 5/5 for renal clearance, and 5/5 for nonrenal clearance. Thus, there was no trend of any saturation of clearance at these dose levels.

Figure 3.2-2   Visual predictive check for plasma concentrations and amounts excreted unchanged in urine

Dose: 500 mg

Plasma concentrations (0-8h)

Plasma concentrations (0-1.75h)

Amounts excreted unchanged in urine

Dose: 1000 mg

Plasma concentrations (0-8h)

Plasma concentrations (0-1.75h)

Amounts excreted unchanged in urine
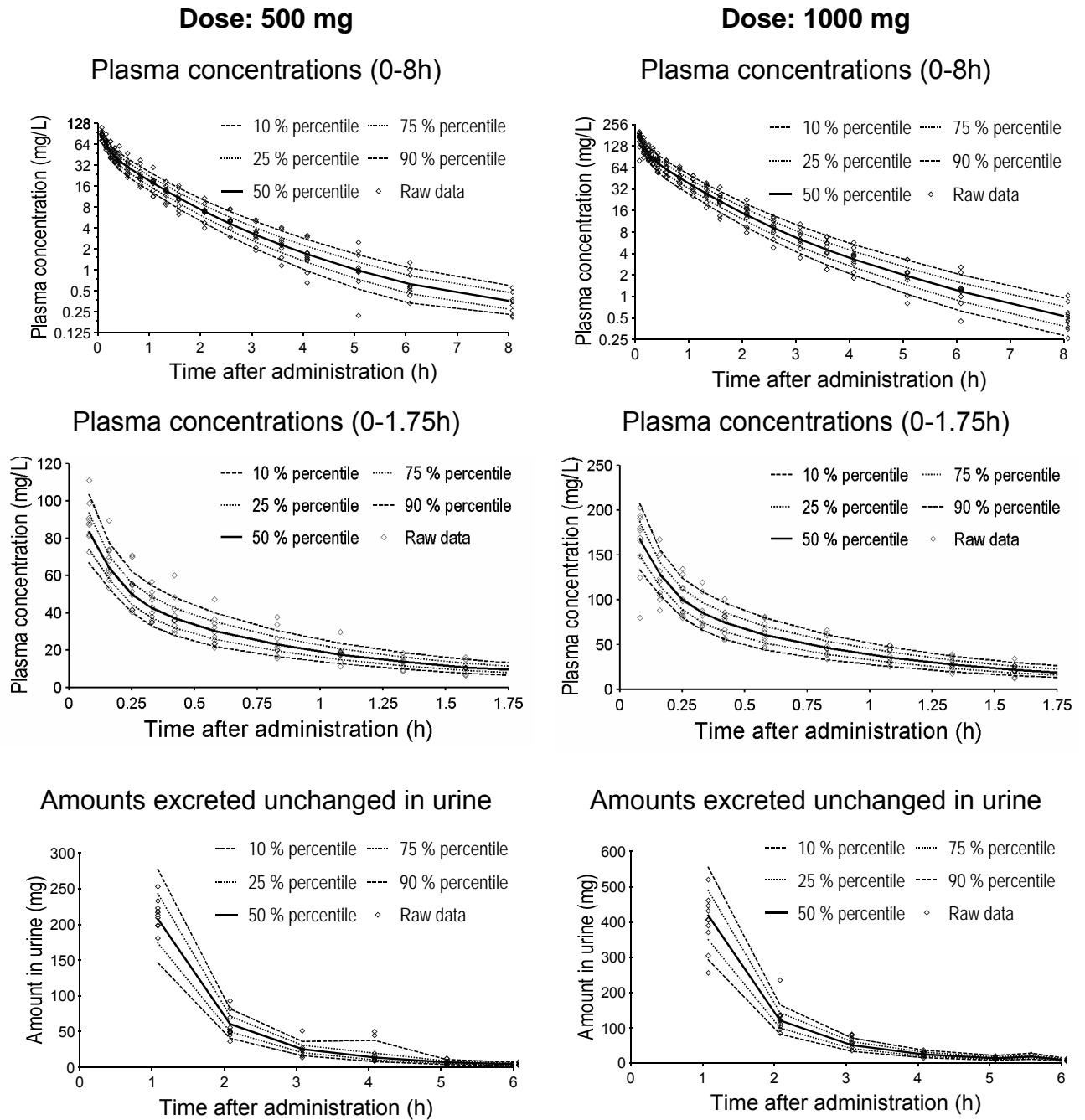
The plots show the raw data, the 80% prediction interval [10 - 90% percentile] and the interquartile range [25 - 75% percentile]. Ideally, 50% of the raw data points should fall inside the interquartile range at each time point and 80% of the raw data should fall inside the 80% prediction interval.

Monte Carlo simulations: We compared the PTA vs. MIC profiles for three dosage regimens with a daily dose of 6g at two PKPD targets (Figure 3.2-3). For the target of $fT_{>MIC} \geq 50\%$ for near-maximal bactericidal activity of penicillins, continuous infusion and prolonged infusion (4h) showed virtually identical PTAs and short-term infusion (0.5h) had lower PTAs. The PKPD breakpoint for near-maximal bactericidal activity was 0.75 to 1 mg/L (PTA 86% at 1 mg/L) for continuous infusion as well as prolonged infusion, and 0.25 to 0.375 mg/L (PTA 79% at 0.375 mg/L) for short-term infusion.

At the target for bacteriostasis ($fT_{>MIC} \geq 30\%$), prolonged infusion reached the highest PTAs. Continuous infusion and short-term infusion had very similar PTAs (Figure 3.2-3). The breakpoints were 1.5 to 2 mg/L for prolonged infusion, 0.75 to 1 mg/L (PTA 86% at 1 mg/L) for continuous infusion, and 0.75 to 1 mg/L (PTA 83% at 1 mg/L) for short-term infusion.

Figure 3.2-3   Probabilities of target attainment for different dosage regimens and PKPD targets of flucloxacillin at a daily dose of 6g flucloxacillin

-▲- continuous infusion of 6g / day

-▱- 2g q8h as 4h infusions

-◇- 1.5g q6h as 0.5h infusions

Target: $fT_{>MIC} \geq 30\%$

Target: $fT_{>MIC} \geq 50\%$

Dose linearity of flucloxacillin
Dose linearity & saturable
elimination
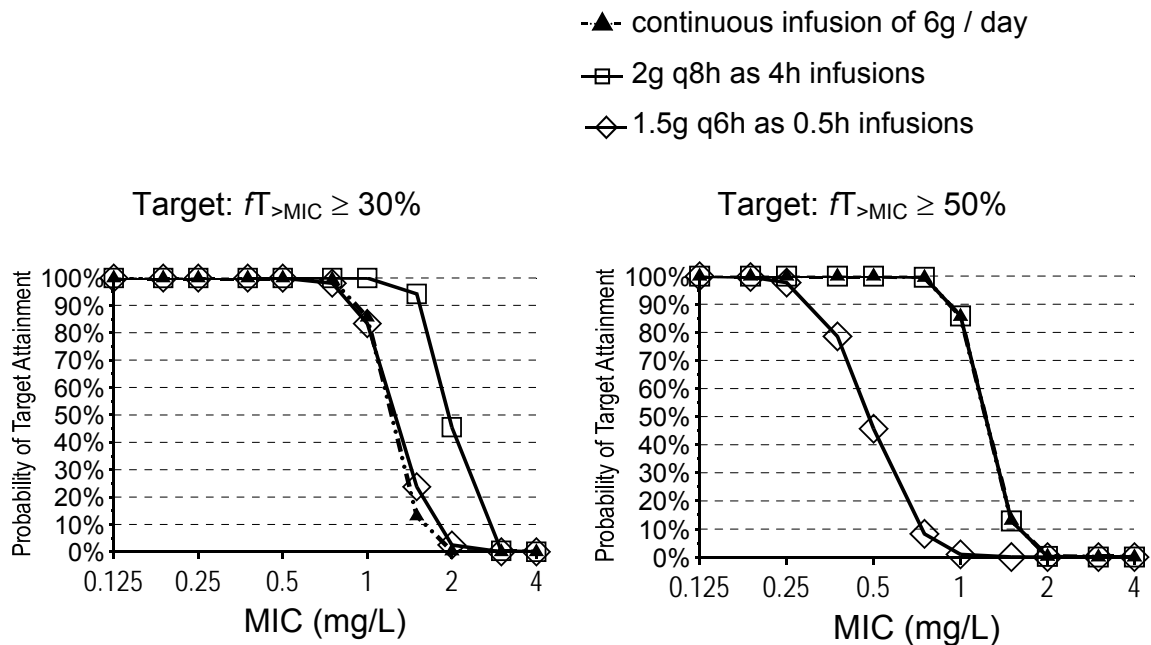
3.2.5   Discussion

We compared the PK of flucloxacillin at two dose levels in a crossover study with healthy volunteers. For studying dosage regimens via MCS at various doses, other modes of administration, or both, it is important to know, whether the clearance changes with plasma concentration at therapeutic concentrations. Different dose levels often help to estimate the concentration dependence of clearance. Frequent plasma and urine samples were collected and highly specific, precise and sensitive bioanalytical methods were applied. We used population PK to fit plasma and urine data simultaneously.

Our NCA showed no differences in clearance and volume of distribution between the low and the high dose (Table 3.2-1). A three compartment population PK model with linear renal and nonrenal elimination had excellent predictive performance and there was no indication for a decrease in total, renal, or nonrenal clearance with the increase in dose from 500 mg to 1000 mg. Therefore, we used this model estimated from plasma and urine data at both dose levels for MCS to compare the PTA vs. MIC profiles for the three dosage regimens (Figure 3.2-3). The target in our MCS was based on non-protein bound plasma concentrations. A range of 94.6 to 96.2% for the plasma protein binding of flucloxacillin has been reported (28, 32, 258). This corresponds to a rather wide range for the non-protein bound fraction of 3.8 to 5.4%, which is a difference of 42% (5.4 vs. 3.8%) for the non-protein bound concentrations. To account for this situation, we chose a relatively high protein binding of 96%, which has also been reported by Bergan (28), as this choice results in conservative (i.e. low) non-protein bound plasma concentrations.

Our MCS with the bacteriostasis target ($fT_{>MIC} \geq 30\%$) showed that prolonged infusion had higher PTAs than continuous infusion and short-term infusion. The PKPD breakpoints were 1.5 mg/L for prolonged infusion and 0.75 mg/L for continuous infusion and short-term infusion. For the target near-maximal killing ($fT_{>MIC} \geq 50\%$), prolonged infusion and continuous infusion both had a 3 times higher PKPD breakpoint than short-term infusion at the

same daily dose of 6g. The PKPD breakpoints were 0.75 mg/L for prolonged infusion and continuous infusion, and 0.25 mg/L for short-term infusion. Thus, prolonged infusion achieved PTAs that were higher than or similar to the PTAs of the other two dosage regimens for both targets.

The different ranking of the three dosage regimens for the two targets can be explained as follows: The breakpoint for continuous infusion at steady-state is independent of the chosen target, as for any one patient $fT_{>MIC}$ can only be 0% or 100%. The profile for short-term infusions shows a rather pronounced peak without a plateau and the profile for prolonged infusion shows a flat peak with a rather broad plateau. Subsequently, short-term infusions reach very high concentrations for a short period of time and prolonged infusions reach only moderately high concentrations, but these for a longer period of time. We determined for flucloxacillin that short-term (0.5h) infusions had the highest PTAs for targets up to $fT_{>MIC} \geq 20\%$, prolonged (4h) infusions performed best for targets between 20% and 50%, and continuous infusion had the highest PTAs for longer targets (55% and above). Continuous infusion was superior to short-term infusions for targets of 30% and above.

To put these results into clinical perspective, the PKPD breakpoints need to be compared to the MICs encountered in clinical practice. MIC_{90} values of MSSA for flucloxacillin are usually reported to be ≤ 0.5 mg/L (153, 224, 229, 289). For an MIC of 0.5 mg/L, continuous infusion and prolonged infusion of 6g / day have a PTA of more than 99%, whereas short-term infusion of 6g / day reaches a PTA of only 46% based on the target for near-maximal killing. As flucloxacillin is also available for oral treatment, intravenous dosing is more relevant for patients with serious infections, where attainment of the target for near-maximal bactericidal activity of the antibiotic might be required (89) (chapter 2.7.1).

We could show that the PK of flucloxacillin was linear within our studied dose range. Therefore, doubling the dose means that also the breakpoint will double. As the PKPD breakpoint of the short-term infusion q6h of 6g / day was 0.25 mg/L, about 12g / day would be required to reach a breakpoint of 0.5 mg/L for near-maximal killing for short-term infusions. However, 4g / day

as continuous or prolonged infusion would be sufficient to reach a breakpoint of 0.5 mg/L.

The MIC_{90} of flucloxacillin is typically ≤ 0.5 mg/L for MSSA. Even without data on an MIC distribution for flucloxacillin against MSSA, it is still possible to calculate the PTA expectation value for an MIC_{90} of 0.5 mg/L. The PTA vs. MIC profile for continuous or prolonged infusion of 4g / day with a PKPD breakpoint of 0.5 mg/L for near-maximal killing can be roughly simplified to assuming a PTA of 100% for all MICs ≤ 0.5 mg/L and a PTA of 0% for all MICs above 0.5 mg/L. For an MIC_{90} of 0.5 mg/L, 90% of the patients (PTA=100% for MICs ≤ 0.5 mg/L) will achieve the target (corresponding to the 90th percentile of the MIC distribution) and 10% of the patients (PTA=0% for MICs > 0.5 mg/L) will not achieve the target. Therefore, the PTA expectation value will be at least 90% for prolonged or continuous infusion of 4g / day and an MIC_{90} of 0.5 mg/L. As described above, a dose of 12g / day given as short-term infusions would be required to reach a PKPD breakpoint of 0.5 mg/L and a PTA expectation value of about 90% for an MIC_{90} of 0.5 mg/L. This means that a 66% lower daily dose (4g vs. 12g) is sufficient for continuous or prolonged infusion compared to short-term infusion in order to reach the same PTA expectation value for successful clinical outcome.

Besides a cost reduction for drug acquisition secondary to the dose reduction for prolonged or continuous infusion, a lower risk for adverse events of flucloxacillin is probably a major advantage of prolonged and continuous infusion. Cholestatic jaundice and hepatitis rarely occur in relation with flucloxacillin intake, risk factors being patients' age, preexisting hepatic impairment, and long term use (> 14 days, (1)). In a population based case control study, de Abajo et al. (76) identified a dose dependency for these adverse effects. It remains to be determined whether high peak concentrations, total exposure, or trough concentrations contribute to the frequency of adverse events for flucloxacillin. However, prolonged and continuous infusion allow a significant dose reduction and avoid high peak concentrations while achieving the same PTAs as short-term infusion.

Whether prolonged or continuous infusion would be preferred depends on the clinical situation of the patient. Continuous infusion of flucloxacillin may be used for home treatment of MSSA infections that require high dose intravenous treatment over prolonged time periods. This procedure has been shown safe, convenient and effective for the follow up treatment of serious staphylococcal infections (e.g. sepsis, endocarditis, osteomyelitis) and cellulitis. Sufficient stability of flucloxacillin solutions at room temperature has also been reported (203). However in the hospital setting and with patients receiving multiple intravenous drugs, one of the major drawbacks of continuous infusion is the need for an additional infusion line to prevent incompatibilities with other drugs, and the resulting increase of the risk for line infections (195).

In conclusion, we found that the PK of flucloxacillin is linear for the doses of 500 and 1000 mg administered as 5min intravenous infusions. For near-maximal killing (target: $fT_{>MIC} \geq 50\%$) flucloxacillin showed robust ($\geq 90\%$) PTAs up to MICs of 0.75 to 1 mg/L (PTA 86% at 1 mg/L) for prolonged infusions or continuous infusion of 6g / day. Short-term infusions of 6g / day had a lower breakpoint of 0.25 to 0.375 mg/L (PTA 79% at 0.375 mg/L). For MIC_{90}'s of 0.5 mg/L which are typically found for flucloxacillin against MSSA, prolonged and continuous infusion at a dose of 4g / day had a PTA expectation value of at least 90%. To achieve the same PTA expectation value, a dose of 12g / day would be required as short-term infusions. This dose reduction from 12g / day for short-term infusion to 4g / day for prolonged infusion and continuous infusion might be a considerable advantage in terms of the risk for adverse events and drug acquisition costs. Future comparative clinical trials are warranted to show whether prolonged and continuous infusion of flucloxacillin at lower dose levels achieve similar or better clinical success rates than short-term infusion.

3.3 Saturable elimination of piperacillin and its impact on the pharmacodynamic profile

3.3.1 Chemical structure of piperacillin

$(C_{23}H_{26}N_5NaO_7S$, Mol. Wt.: 539.54)
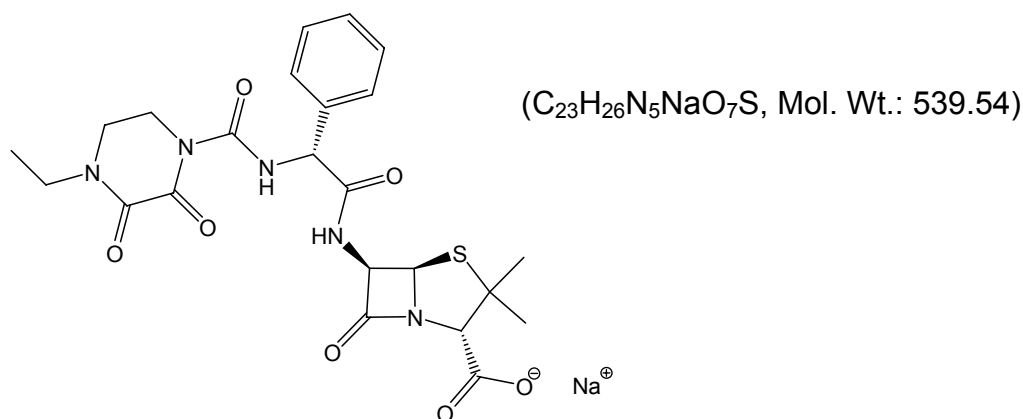
Chemical structure 3.3-1 Piperacillin

3.3.2 Background on dose linearity of piperacillin

Piperacillin in combination with the betalactamase inhibitor tazobactam is one of the most frequently used intravenous antibiotic choices. It has good bactericidal activity against gram-positive microorganisms and *P. aeruginosa* (308) and is frequently used in the empirical treatment of hospital acquired infections. It has sufficient stability at room temperature which makes it attractive for prolonged or continuous infusion.

During piperacillin's use for more than two decades there have been many attempts to determine the extent of saturation for the elimination of piperacillin. Tjandramaga et al. (304) and Bergan and Williams (31) reported a decrease in clearance with increasing doses of piperacillin. These results are supported by two recent studies that used population PK analysis and found that a model with saturable elimination fits the data better than a model with only first order elimination (194, 317). However there is no final agreement on the extent of saturation of piperacillin elimination. The existence of a clinically significant saturable elimination pathway may have consequences for the choice of the optimal dosage regimen. This becomes especially important

when different doses and schedules or other modes of administration are studied by MCS and when short-term versus continuous infusions are compared (317).

Additionally there is conflicting data about whether the saturation arises from the renal or the nonrenal elimination or both. Piperacillin is excreted by the kidneys in parallel by glomerular filtration (a first order non-saturable process) and active tubular secretion (a capacity-limited process). Batra et al. (23) find a decreased renal clearance at higher doses. Tjandramaga et al. (304) observe a decrease in renal clearance and an even more marked decrease in nonrenal clearance at higher doses, whereas Bergan and Williams (31) report a decreased nonrenal clearance and no changes in renal clearance at higher doses. As both of the latter two studies find increasing fractions excreted unchanged in urine at higher doses, nonrenal clearance decreased more than renal clearance with increasing doses. A higher fraction excreted unchanged in urine at steady-state than after single dose has also been reported (284). Additionally probenecid, a well known inhibitor of various active transport processes in the body, has been shown to decrease not only the renal but also the nonrenal elimination of piperacillin (304). These findings suggest a saturation in both renal and nonrenal elimination of piperacillin, with the nonrenal pathway perhaps even more saturable than the renal one.

Our primary objective was to explore the PK of piperacillin based on data from a crossover study at two dose levels in healthy volunteers. We applied population PK to study the extent of saturation in the renal and nonrenal elimination of piperacillin at therapeutic concentrations. Our secondary objective was to study the influence of saturable elimination on the PKPD characteristics of piperacillin via MCS and to estimate the clinical relevance of the saturation of piperacillin elimination at therapeutic doses.

3.3.3   Methods

Study design and drug administration: Ten healthy subjects (five males and five females) participated in the study. In each of the two study

periods each subject received a single dose of 1500 mg or 3000 mg piperacillin as a 5min intravenous infusion.

Sampling Schedule: Blood samples were drawn immediately before start of infusion, at the end of infusion as well as at 5, 10, 15, 20, 25, 45, 60, 75, 90min and 2, 2.5, 3, 3.5, 4, 5, 6, 8, and 24h after the end of the infusion. Urine samples were collected immediately before start of the infusion, from start of the infusion until 1h after end of infusion and in the following time intervals: 1 to 2, 2 to 3, 3 to 4, 4 to 5, 5 to 6, 6 to 8, 8 to 12, 12 to 24h after the end of the infusion.

Determination of Plasma and Urine Concentrations: Piperacillin concentrations in plasma and urine were determined by HPLC. For determination of piperacillin in plasma 100µL of the sample were deproteinized with 200µL acetonitrile containing the internal standard. After mixing and centrifugation at 15,000 rpm 40µL were injected onto the HPLC system. For determination of piperacillin in urine 20µL of the sample were diluted with 180µL water. After mixing 40µL were injected onto the HPLC system. Piperacillin was determined using a reversed phase column, potassium dihydrogen phosphate (pH 6.2) / acetonitrile mobile phase at a flow of 2 mL/min. Piperacillin and the internal standard were detected at 220nm.

The calibration rows in plasma and urine were prepared as described in chapter 3.2.3 for flucloxacillin. No interferences were observed in plasma and urine for piperacillin or the internal standard. Calibration was performed by linear regression. The linearity of piperacillin calibration curves in plasma and urine was demonstrated between 0.200 - 150 mg/L and 1.00 - 1000 mg/L, respectively. The quantification limits were identical with the lowest calibration levels. The inter-day precision and the analytical recovery of the spiked quality control standards of piperacillin in human plasma (urine) ranged from 3.5 to 9.2% (3.0 to 5.5%) and from 95.0 to 106.9% (92.0 to 97.9%), respectively.

Pharmacokinetics

Non-compartmental analysis: NCA was performed for the data at both dose levels according to the methods described above.

Population PK analysis: We tested one, two, and three compartment disposition models. The drug input was modeled as a zero order process with a fixed duration of 5min.

Clearance: We assumed a nonrenal (CL_{NR}) and a renal (CL_R) component of clearance. We estimated the renal clearance based on the amount of piperacillin excreted unchanged into urine. According to prior population PK models and data on piperacillin (31, 194, 304, 317), we studied four different elimination models for piperacillin, as shown below. The respective formulas for total clearance (CL_T) are:

$$\text{Model 1: } CL_T = CL_R + CL_{NR} \qquad\qquad \text{Formula 3.3-1}$$

$$\text{Model 2: } CL_T = \frac{Vmax_R}{K_{mR} + C} + CL_{NR} \qquad\qquad \text{Formula 3.3-2}$$

$$\text{Model 3: } CL_T = CL_R + \frac{Vmax_R}{K_{mR} + C} + CL_{NR} \qquad\qquad \text{Formula 3.3-3}$$

$$\text{Model 4: } CL_T = CL_R + \frac{Vmax_R}{K_{mR} + C} + \frac{Vmax_{NR}}{K_{mNR} + C} \qquad\qquad \text{Formula 3.3-4}$$

In these formulas, C is the concentration of piperacillin in the central compartment, $Vmax_R$ and $Vmax_{NR}$ are the maximum rates of elimination for the mixed order renal and nonrenal elimination, and K_{mR} and K_{mNR} are the Michaelis Menten constants for the mixed order renal and nonrenal elimination, respectively. Model 1 assumes that renal and nonrenal clearance are non-saturable. Model 2 assumes that renal clearance is saturable and nonrenal clearance is non-saturable. Model 3 assumes that renal clearance has a saturable and a non-saturable component and nonrenal clearance is non-saturable. Model 4 assumes that renal clearance has a saturable and a non-saturable component and nonrenal clearance is saturable.

Between subject variability model: We estimated the BSV for all parameters except duration of zero order input and intercompartmental

clearances. An exponential parameter variability model and a full variance-covariance matrix was used.

Observation model: We described the residual unidentified variability by a combined additive and proportional error model for plasma concentrations and amounts excreted in urine.

Monte Carlo simulation: We used $fT_{>MIC} \geq 50\%$ as PKPD target for near-maximal bactericidal activity of piperacillin (67, 89). We calculated the PTA within the MIC range from 2 to 64 mg/L and used a protein binding of 30% for piperacillin (16, 283). Five dosage regimens were simulated: 1) continuous infusion of 6g / day, 2) prolonged (4h) infusion of 3g q8h (daily dose 9g), 3) continuous infusion of 18g / day, 4) short-term (30min) infusion of 6g q8h (daily dose 18g), and 5) short-term (30min) infusion of 3g q4h (daily dose 18g). We simulated each of those five dosage regimens for all four population PK models at steady-state in absence of residual error and used 2,000 subjects for each combination of population PK model and dosage regimen. We calculated the PTA and the PKPD breakpoint.

In order to estimate the clinical relevance of the differences between the four elimination models of piperacillin, we calculated the PTA expectation value. We calculated the cumulative fraction of response (93, 228) of the five dosage regimens against *Klebsiella pneumoniae*, *E. coli*, and *P. aeruginosa* based on published MIC distributions (10, 182). Kuti et al. (182) determined the MICs for 557 *P. aeruginosa* isolates by E-test[®] for piperacillin/tazobactam at the Hartford Hospital. The E-test is a plastic strip with reference MIC dilutions of an antibiotic, that is placed onto an inoculated agar plate. An antibiotic gradient is formed beneath the strip and where the inhibition ellipse intersects with the scale, the MIC can be read (14). Ambrose et al. (10) had 105 ESBL phenotype (NCCLS criteria) strains of *E. coli* and *K. pneumoniae* from bloodstream isolates recovered during 2000 in the United States and Canada (SENTRY Antimicrobial Surveillance Program, 2000).

3.3.4   Results

All 10 subjects completed the study. The average ± SD weight was
69.6 ± 9.7 kg, height was 177.5 ± 8.0 cm and age 25.7 ± 3.1 years. Plasma
concentrations and amounts in urine of piperacillin after infusion of 1500 mg
and 3000 mg are shown in Figure 3.3-1.

Figure 3.3-1   Average ± SD profiles of piperacillin in healthy volunteers
after 5min infusions of 1500 mg or 3000 mg piperacillin

Panel A: Plasma concentrations
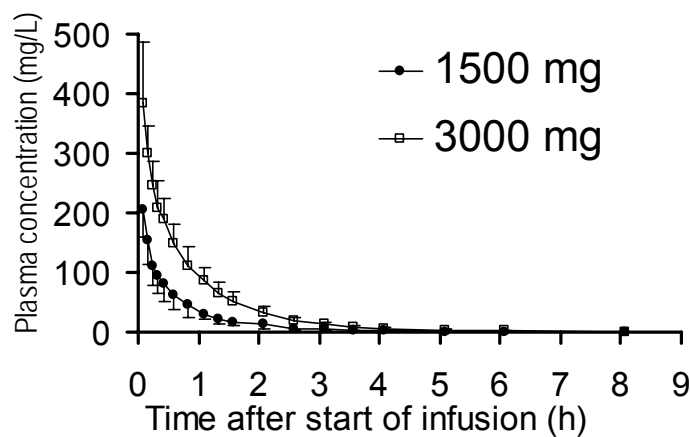
Panel B: Cumulative amounts excreted unchanged in urine
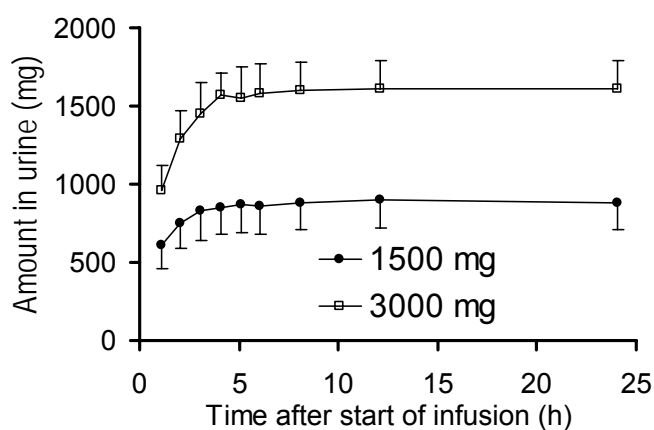
Non-compartmental analysis: The results of the NCA are shown in
Table 3.3-1.

Table 3.3-1   PK parameters for 1500 mg and 3000 mg piperacillin from
                         non-compartmental analysis

	Geometric mean (%confidence interval)		Point estimate (90% confidence interval)	p-value from
	1500 mg	3000 mg	3000 mg / 1500 mg	ANOVA
Total body clearance (L/h)	13.5 (24%)	11.0 (23%)	82% [76 - 89%]	< 0.01
Renal clearance (L/h)	7.77 (34%)	5.88 (27%)	76% [63 - 91%]	0.02
Nonrenal clearance (L/h)	5.34 (31%)	5.08 (23%)	95% [80 - 114%]	0.62
Fraction excreted unchanged in urine	0.58 (20%)	0.53 (11%)	92% [81 - 106%]	0.31
Volume of distribution at steady-state (L)	12.1 (22%)	10.8 (17%)	89% [79 - 101%]	0.13
Peak plasma concentration (mg/L)	201 (22%)	377 (25%)	187% [155 - 226%]	< 0.01
Terminal half-life (h)	1.18 (77%)	1.05 (26%)	89% [60 - 132%]	0.60
Mean residence time (h)	0.90 (27%)	0.98 (10%)	109% [98 - 121%]	0.17

Doubling the dose of piperacillin reduced the renal clearance by 24% (p
= 0.02), whereas nonrenal clearance was not affected significantly. Figure
3.3-2 shows the box-plots for renal and nonrenal clearance at the two dose
levels. Total body clearance was decreased by 18% (p < 0.01) for the 3000
mg dose. Volume of distribution at steady-state, terminal half-life and mean
residence time were not affected significantly by the higher dose of piperacillin
(Table 3.3-1).

Figure 3.3-2   Renal and nonrenal clearance from non-compartmental analysis after administration of 1500 mg or 3000 mg piperacillin to healthy volunteers

The markers represent the median, the boxes the 25% and 75% percentiles and the whiskers minimum and maximum
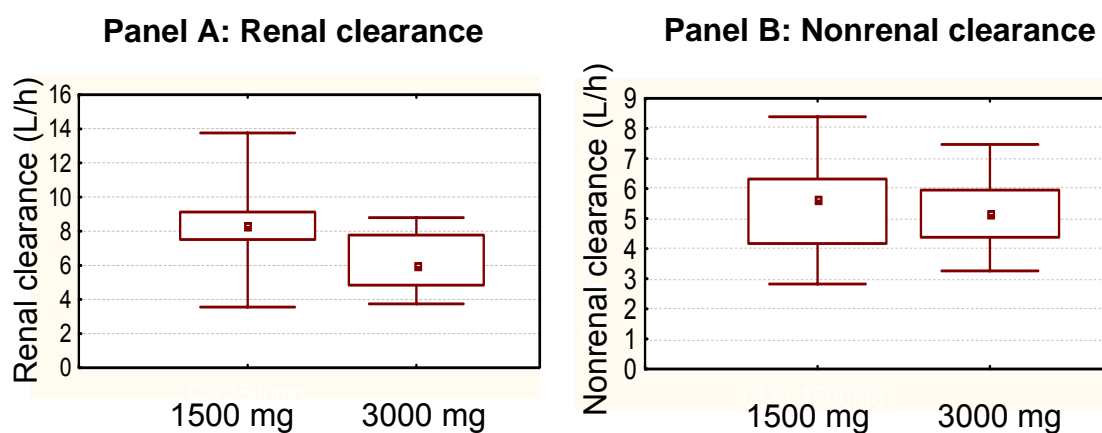
Population Pharmacokinetics: Three compartment models had an approximately 130 points better objective function than two compartment models, whereas the one compartment model had insufficient predictive performance. Therefore, we selected models with three disposition compartments. The parameter estimates for the four different elimination models are shown in Table 3.3-2.

Table 3.3-2   PK parameter estimates of different elimination models:
Values for structural PK parameters are geometric means
(coefficients of variation for the BSV)

Parameter	Unit	Model 1	Model 2	Model 3	Model 4
Renal elimination		First order	Mixed order	Parallel first order & mixed order	Parallel first order & mixed order
Nonrenal elimination		First order	First order	First order	Mixed order
Delta objective function		90.8	27.8	12.1	0
CL_R	L h^{-1}	8.46 (39%)	-	4.11 (38%)	4.94 (42%)
$Vmax_R$	mg h^{-1}	-	1990 (33%)	303 (33%)	138 (71%)
K_{mR}	mg L^{-1}	-	200 (66%)	46.8 (90%)	24.4 (111%)
CL_{NR}	L h^{-1}	3.40 (30%)	5.48 (18%)	5.52 (18%)	-
$Vmax_{NR}$	mg h^{-1}	-	-	-	3100 (137%)
K_{mNR}	mg L^{-1}	-	-	-	419 (117%)
Vss	L	12.0	12.8	12.7	13.4
V1	L	6.42 (18%)	6.20 (18%)	6.30 (17%)	6.32 (21%)
V2	L	3.63 (40%)	4.02 (48%)	3.64 (49%)	3.52 (44%)
V3	L	1.92 (31%)	2.60 (16%)	2.73 (15%)	3.60 (7%)
$CLic_{shallow}$	L h^{-1}	14.0	18.3	15.7	16.3
$CLic_{deep}$	L h^{-1}	0.621	1.65	1.72	2.58
TK0 (fixed)	min	5	5	5	5
CV_C	-	13.1%	12.8%	12.8%	12.4%
SD_C	mg L^{-1}	0.31	0.27	0.26	0.28
CV_{AU}	-	39.1%	25.6%	24.3%	22.4%
SD_{AU}	mg	1.42	4.20	4.25	4.30

See Table 3.2-2 and chapter 3.3.3 for parameter explanation.

The objective function was 63 points better for the model with mixed
order renal elimination and first order nonrenal elimination (model 2) than for
the model with first order elimination for both pathways (model 1). K_m for the
mixed order renal elimination (K_{mR}) for model 2 was estimated to be 200 mg/L

which is relatively high compared to the plasma concentrations observed after
a dose of 1500 mg or 3000 mg (Figure 3.3-1).

Inclusion of a first order renal clearance in parallel to the mixed order
renal clearance (model 3) improved the objective function by 15.7 points. The
estimate for the first order renal clearance (CL_R) was 4.11 L/h which is similar
to the glomerular filtration rate multiplied by the unbound fraction (70%) of
piperacillin in plasma. K_{mR} was 46.8 mg/L which is about 4 times lower than
K_{mR} for model 2. When we simulated the median plasma concentration at
steady-state for the models with saturable elimination shown in Table 3.3-2, a
continuous infusion of 6g daily achieved an average plasma concentration at
steady-state of 16-17 mg/L (median) and a continuous infusion of 18g daily
reached 58-61 mg/L. As K_{mR} for model 3 was 46.8 mg/L, the mixed order
renal elimination in model 3 is much more saturated at therapeutic
concentrations of piperacillin than in model 2. Figure 3.3-3 shows the
decrease in total and renal clearance with increasing concentrations for
model 3.

Figure 3.3-3   Renal, nonrenal, and total body clearance at various
plasma concentrations of piperacillin for model 3 (see
Table 3.3-2)
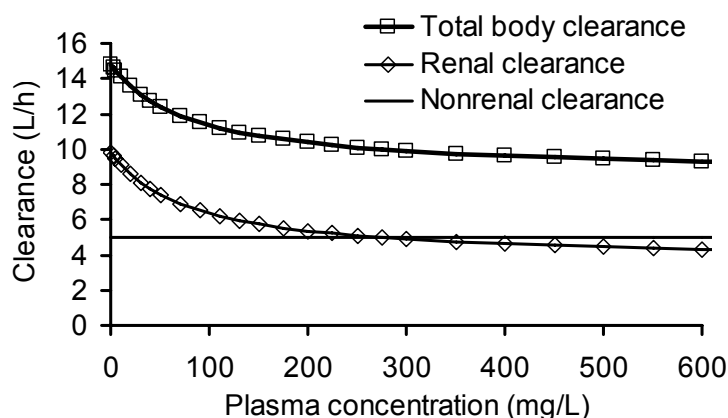
When we modeled the nonrenal elimination as a mixed order process,
we observed an improvement in the objective function by 12.1 points and got
an estimate of 419 mg/L (117% coefficient of variation) for the Michaelis
Menten constant of the nonrenal elimination (K_{mNR}). This estimate suggests
that only some subjects showed saturation for the nonrenal elimination. When
we studied the individual estimates for nonrenal clearance from the population

PK analysis after 1500 mg and 3000 mg for model 3, we observed a nominal value of 18% higher nonrenal clearances for the 1500 mg dose in six of the ten subjects. Only one subject had a lower nonrenal clearance for the 1500 mg dose. The p-value for this comparison was 0.01 (paired two-sided t-test).

Figure 3.3-4 Visual predictive check for plasma concentrations and amounts excreted unchanged in urine for model 3 (see Table 3.3-2)
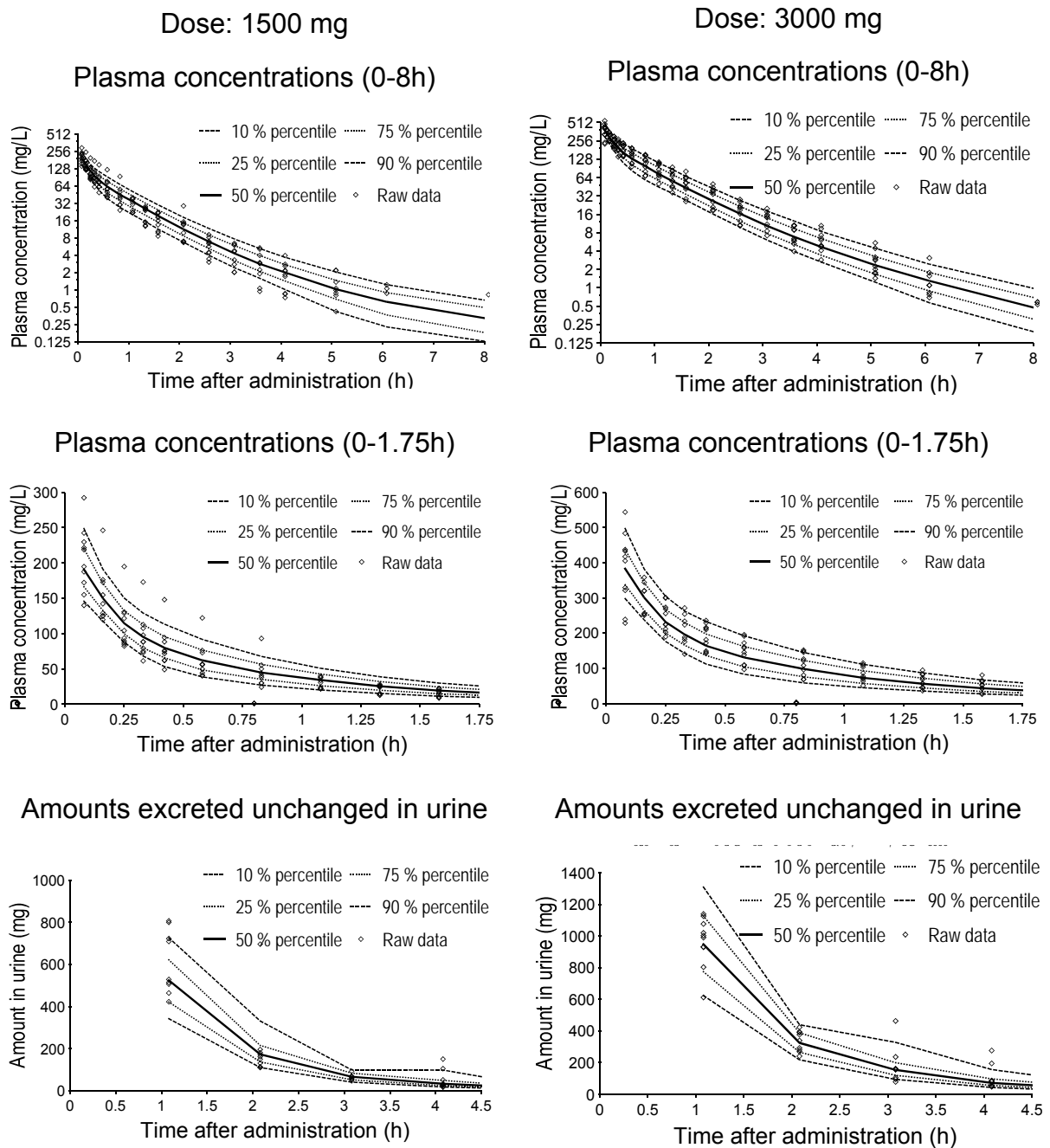
See chapter 2.6.5 and Figure 3.2-2 for explanation of the plots.

The visual predictive checks for model 3 are shown in Figure 3.3-4. The predictive performance of models 2 and 4 was very similar to model 3 and was excellent for all three models. Model 1 (only first order elimination) predicted a median amount in urine one hour after end of infusion which was 24% higher than the highest observed amount. Besides this considerable over-prediction in urine, model 1 showed a small over-prediction for the plasma concentrations of the 1500 mg dose and a small under-prediction for the plasma concentrations of the 3000 mg dose.

Monte Carlo simulations: We compared the PTA vs. MIC profiles for the four elimination models (Figure 3.3-5) and observed very similar PTA vs. MIC profiles with all models for the 4h infusion of 3g piperacillin q8h, the 30min infusion of 3g q4h, and the continuous infusion of 18g / day. For a continuous infusion of 6g / day we observed slightly higher PTAs for model 1 than for the other models. For a dosage regimen with pronounced peaks (30min infusion of 6g q8h) model 1 predicted lower PTAs and had an about 1.5 fold lower PKPD breakpoint than models 2 to 4. For the three models with saturable elimination (models 2 to 4) we determined a PKPD breakpoint of 8 mg/L for the continuous infusion of 6g / day and a breakpoint of 24-32 mg/L for the continuous infusion of 18g / day. Models 2 to 4 yielded a PKPD breakpoint of 12 mg/L for prolonged infusions of 3g q8h, about 6 mg/L for 30min infusions of 6g q8h, and about 16 mg/L for 30min infusions of 3g q4h.

In order to put the PTAs and PKPD breakpoints into clinical perspective, we derived the PTA expectation value against the MIC distributions of three different pathogens. The results are shown in Table 3.3-3. As expected, the continuous infusion of 18g / day had the highest PTA expectation values and the high dose short-term infusions of 6g q8h had the lowest PTA expectation values. Continuous infusion at 18g / day had the most pronounced advantages over the other dosage regimens for *K. pneumoniae* and *P. aeruginosa* whereas the advantages were slightly less pronounced against *E. coli*.

Figure 3.3-5 Probabilities of target attainment for the four different population PK models and different dosage regimens of piperacillin (PKPD target: $fT_{>MIC} \geq 50\%$)

-▲- First order renal & first order nonrenal elimination (model 1)

-□- Mixed order renal & first order nonrenal elimination (model 2)

-◇- Parallel first and mixed order renal & first order nonrenal elimination (model 3)

-○- Parallel first and mixed order renal & mixed order nonrenal elimination (model 4)
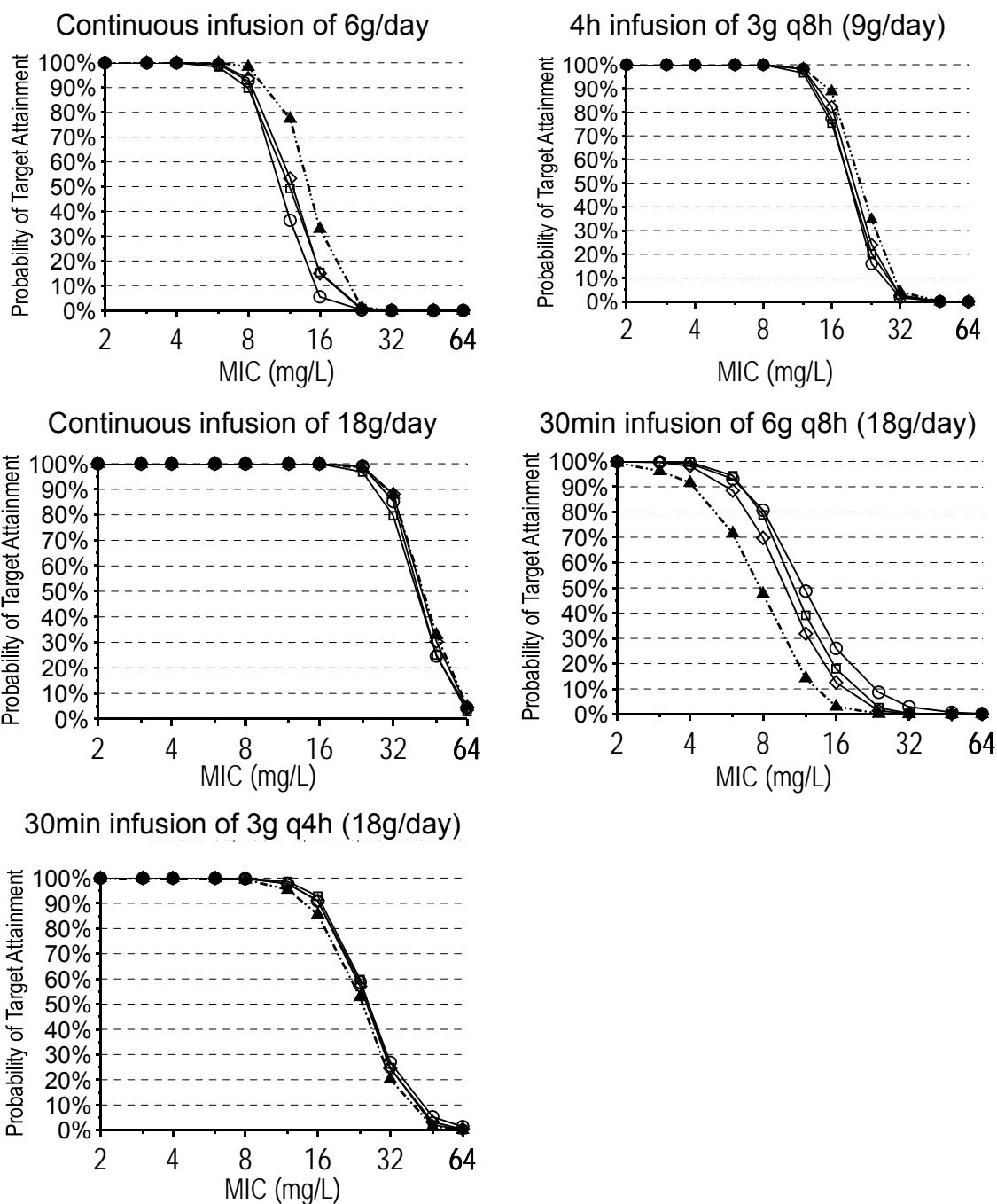
Table 3.3-3   Comparison of the PTA expectation value against *E. coli*, *K. pneumoniae*, and *P. aeruginosa* (10, 182) for piperacillin based on the PKPD target $fT_{>MIC} \geq 50\%$ for near-maximal killing

Dosage regimen	Elimination Model*	PTA expectation value		
		E. coli (n=65)	*K. pneumoniae* (n=40)	*P. aeruginosa* (n=557 isolates)
Daily dose: 6g	1	**83.6%**	**52.2%**	**89.4%**
piperacillin	2	80.6%	48.5%	86.0%
as continuous	3	81.3%	49.0%	86.7%
infusion	4	80.3%	47.4%	85.1%
Daily dose: 9g	1	88.2%	61.2%	93.4%
piperacillin	2	87.2%	59.1%	92.5%
3g q8h as	3	87.7%	60.1%	92.9%
4h infusions	4	87.3%	59.3%	92.6%
Daily dose: 18g	1	89.2%	71.7%	97.4%
piperacillin as	2	89.2%	70.7%	97.0%
continuous	3	89.2%	71.6%	97.4%
infusion	4	89.2%	71.4%	97.2%
Daily dose: 18g	1	**68.6%**	**39.5%**	**74.2%**
piperacillin	2	78.6%	47.5%	84.0%
6g q8h as	3	75.9%	45.2%	81.5%
0.5h infusions	4	79.4%	49.1%	84.9%
Daily dose: 18g	1	87.9%	62.3%	93.7%
piperacillin	2	88.5%	63.9%	94.5%
3g q4h as	3	88.4%	63.6%	94.3%
0.5h infusions	4	88.4%	63.9%	94.4%

*: See method section and Table 3.3-2 for details on the elimination models.

Short-term infusions of 3g q4h (18g/day) had only slightly higher PTA expectation values than prolonged (4h) infusions q8h at a daily dose of 9g piperacillin. The latter regimen had higher PTA expectation values than the continuous infusion at 6g / day. However, these results may differ, if the MIC distributions of a specific clinic are used for calculation of the PTA expectation value.

Comparing the results for the different elimination models, there were very small differences between models 2 to 4 (see also Figure 3.3-5). Model 1 predicted 2-5% higher PTA expectation values for the 6g / day continuous infusion and 6-11% lower PTA expectation values for the high dose intermittent short-term infusions relative to models 2 to 4. For these two dosage regimens the PTA expection values from model 1 are shown in bold in Table 3.3-3. These differences may be smaller or larger depending on the respective MIC distribution used for calculation of the PTA expectation value. However, these deviations provide an estimate of what might be expected in clinical practice.

3.3.5   Discussion

The most direct way to study the extent of saturation in the renal and nonrenal elimination at therapeutic concentrations is to collect plasma and urine samples in a well controlled healthy volunteer crossover study at different dose levels (see also chapter 1.5). Different dose levels result in different average plasma concentrations which often help to estimate the saturable component of elimination. Studying both sides of the renal elimination (i.e. plasma concentrations and amounts excreted in urine) further supports the estimation of the parameters for renal elimination. Through a highly standardized study design and bioanalysis, additional process noise is minimized.

We had data from a well controlled crossover study with two different dose levels that was performed in ten healthy volunteers. Frequent plasma and urine samples were collected, and highly specific, precise and sensitive bioanalytical methods were applied. We used population PK to fit plasma and urine data at the two different dose levels simultaneously, and to estimate the extent of saturation in the renal and nonrenal elimination of piperacillin at therapeutic concentrations. Then we estimated the influence of saturable elimination on the PKPD characteristics of piperacillin via MCS. We compared the PTAs for different PK models with saturable and non-saturable elimination and for various dosage regimens. From these PTAs, we derived the PKPD

breakpoints and the PTA expectation values against *E. coli*, *K. pneumoniae*, and *P. aeruginosa*. This allowed us to estimate the clinical relevance of the saturation of piperacillin elimination at therapeutic doses.

In clinical practice, piperacillin is given in combination with tazobactam to prevent degradation of piperacillin by betalactamases, whereas in our study piperacillin was given alone. It has been shown that the PK of piperacillin is not affected by concomitant administration of tazobactam at dose ratios of 4:1 or 8:1 (283). However, if concomitant administration of tazobactam had an effect on piperacillin elimination, this would result in a higher extent of saturation of piperacillin elimination, as both drugs are secreted by the renal tubules. Therefore, our PTAs are conservative estimates for the treatment situation with piperacillin and tazobactam in combination.

We studied four elimination models for piperacillin (Table 3.3-2). Our model with first order renal and first order nonrenal clearance (model 1) over-predicted the amounts excreted in urine during the first sampling interval of the high dose treatment considerably and showed a small bias in the predicted plasma concentrations at both dose levels. This over-prediction and bias were removed by adding a mixed order renal elimination term (model 3). Model 3 is the physiologically most reasonable model for the renal elimination, as it includes parallel first order and mixed order renal elimination. Model 3 had an excellent predictive performance (Figure 3.3-4) and its Michaelis Menten constant (K_{mR}) of the renal mixed order elimination was estimated to be 46.8 mg/L. This is well in the range of plasma concentrations which are reached after therapeutic doses of piperacillin. Together with the significant decrease in renal clearance at the higher dose shown by NCA, this is considerable evidence for the presence of a partly saturable renal elimination.

NCA did not show a significantly lower nonrenal clearance at the higher dose level. Our population PK model with mixed order nonrenal elimination had a slightly better objective function than the model with linear nonrenal elimination, but there was no visible difference in predictive performance between the two models. The geometric mean of the Michaelis Menten constant for the nonrenal pathway (K_{mNR}) was estimated to be 419 mg/L (117% CV). For the majority of patients, the concentrations after continuous

infusion of therapeutic doses are far below this K_{mNR}. Thus, the saturation of nonrenal elimination is probably of less clinical relevance than the saturation of the renal elimination. However, it should be noted that for four of the 20 profiles (two for each subject) K_{mNR} was between 50 and 100 mg/L, and for a further four profiles between 100 and 210 mg/L. Therefore, at clinically relevant plasma concentrations the renal elimination showed a considerable extent of saturation, but for the nonrenal pathway this extent is much smaller and saturation becomes only apparent at higher concentrations and not for all subjects.

Models 3 and 4 are the physiologically most reasonable models for the elimination of piperacillin. Our data only showed a saturation of nonrenal elimination for at most half of the subjects. The estimates for the first order component of renal elimination were physiologically reasonable for models 3 and 4. More importantly, models 3 and 4 showed no clinically relevant differences in the PKPD simulations. We selected model 3 as our final model, because it had excellent predictive performance and is less complex than model 4.

Overall, the saturation of piperacillin elimination at therapeutic concentrations seems to be lower than has been reported e.g. for azlocillin (27). This might be one reason why a saturation in piperacillin PK has not been reported in some other studies that did not use different dose levels, urinary excretion data, or a standardized crossover design in a homogenous population. We tried to estimate the saturation of piperacillin elimination by models 1 to 3 with 1) only plasma data from both dose levels, 2) urine and plasma data from one dose level, or 3) only plasma data (no urine) from one dose level. For cases 1) and 2) the estimated elimination parameters of piperacillin were in agreement with the parameter estimates from the full dataset. In case 3) the parameter estimates for the mixed-order elimination ranged from underestimation by a factor of 22 to overestimation by a factor of 3.7 for K_m, and from underestimation by a factor of 2.3 to overestimation by a factor of 2.8 for Vmax, compared to the estimates based on plasma data at both dose levels. Therefore, plasma data at two dose levels or plasma and

urine data at one dose level seem to be necessary to estimate Vmax and K_m of the mixed-order (renal) elimination of piperacillin.

A known saturation in elimination, as for mezlocillin (29, 106, 212), is not always seen in real patients. Mangione et al. (212) performed a crossover study in volunteers with various degrees of renal impairment at single doses of 1g and 5g mezlocillin and found a significant saturation. In a crossover study with acutely infected, traumatized patients with renal dysfunction, a fixed daily dose of mezlocillin was given as large doses with long intervals or as small frequent doses (91). The authors observed a similar net saturation and similar clearances after both regimens at steady-state, probably due to continuous saturation of the saturable elimination component of mezlocillin. Thus the PK appeared pseudo-linear for this study design.

To put the saturation of elimination into clinical perspective we compared the predicted PTA between the four different models by MCS. As shown in Figure 3.3-5, the predicted PTA vs. MIC profiles did not differ much between models which included mixed order elimination (models 2 to 4). Model 1 predicted lower PTAs for the 30min infusion of 6g q8h relative to models 2 to 4. This result was expected as saturation of the elimination was not included in the linear model and becomes most apparent for dosage regimens with (temporarily) high plasma concentrations. When compared to models 2 to 4, model 1 predicted lower PTAs for MICs between 4 and 12 mg/L, and 6-11% lower PTA expectation values for the 30min infusions of 6g q8h. On the contrary, model 1 predicted 2-5% higher PTA expectation values for the 6g / day continuous infusion compared to models 2 to 4. At permanently low concentrations relative to K_m, the saturable models predict higher clearances than the non-saturable model. Consequently the saturable models predict lower plasma concentrations (and lower PTAs) for low dose continuous infusion relative to the non-saturable model. If PK data on continuous infusion of piperacillin at different dose levels become available, these model predictions should be substantiated. The population PTAs of the four studied models were very similar (± 2%) for the other three dosage regimens (Table 3.3-3).

In conclusion, we found a saturable renal elimination of piperacillin and a smaller degree of saturation for the nonrenal elimination. Our population PK model with parallel mixed order and first order renal elimination and first order nonrenal elimination had excellent predictive performance. At therapeutic concentrations the renal elimination was significantly saturated, whereas the degree of saturation for the nonrenal pathway was smaller and was only observed in at most 50% of the subjects. A population PK model without saturable elimination under-predicted the PTA expectation values for high dose (6g piperacillin q8h) short-term infusions by 6-11% and over-predicted the PTA expectation values for low dose continuous infusions (6g piperacillin per day) by 2-5% compared to models with saturable elimination. As these results depend on the choice of the MIC distribution, the differences may become smaller or larger, if the MIC distributions from a local hospital are used. However, probably more accurate estimates for the PTA expectation value can be obtained by MCS with population PK models which include a saturable elimination component for piperacillin.

3.4   Saturable versus non-saturable elimination

3.4.1   Advantages of population pharmacokinetics for this type of analysis

Population PK modeling is advantageous for detection of saturable drug elimination. Jonsson et al. (163) showed that population PK modeling can detect saturable elimination at an at least 4-fold lower dose level than modeling by the STS approach. By the STS approach each subject's data are modeled individually (chapter 2.6.2) and a single subject's data may not contain enough information to find the most appropriate model. Different models may be preferred for different subjects. Population PK modeling fits all subjects' data simultaneously and therefore the largest amount of information can be drawn from the data (163) (chapter 2.6.3). Jonsson et al. (163) simulated two PK studies with saturable elimination, each with only one dose level. The difference between population PK and STS in the ability to detect a saturable elimination might not be so pronounced, if two dose levels are studied as in our piperacillin and flucloxacillin study. Our crossover design with two dose levels in combination with a population PK analysis was a powerful method to detect a saturable elimination and to quantify the extent and sites of saturation. We could show for piperacillin that plasma data at two dose levels or plasma and urine data at one dose level were necessary to obtain reasonable estimates for Vmax and K_m of the mixed-order elimination of piperacillin. This might be due to the lesser extent of saturation of piperacillin elimination at therapeutic doses compared to some other drugs (chapter 3.1).

Besides studying saturable elimination, our objective was to compare the probability for successful treatment between different dosage regimens by MCS. The expected range of concentration time profiles in the population was predicted in our MCS. For this, knowledge about the variability of the PK parameters in the subject population is needed. Contrary to the STS approach, population PK directly estimates this variability. Estimates for BSV

from the STS approach tend to be imprecise and biased towards higher values (268), whereas the estimates from population PK have been shown to be less biased and more precise.

3.4.2   Assessment of pharmacodynamic profiles via Monte Carlo simulation

The expected range of concentration time profiles for a population of individuals can be predicted by MCS. Those simulations are based on a population PK model and on a specific dosage regimen. Then the PTA at each MIC is calculated. This allows one to calculate the PKPD breakpoint for the specific drug and dosage regimen. The PKPD breakpoint is a valuable information, as for MICs at or below the PKPD breakpoint the dosage regimen is likely to result in successful outcome for the patient. MCS combines the variability in PK and the expected variability in PD to predict the probability of successful treatment.

For obtaining reliable conclusions by this method, ideally several prerequisites should be met. The subjects in the PK study which is used to build the population PK model should have similar PK to the patient population for which the outcome is predicted. The MIC distributions used for calculation of the PTA expectation value should reflect the susceptibility situation at the local hospital.

The PKPD target should ideally have been established for the disease and patients of interest. For instance for quinolones different targets for the *f*AUC/MIC have been validated for different infections and depending on the seriousness of the infection. The PKPD target should be chosen with regard to the clinical situation of the patient population of interest. It needs to be considered, how the applied PKPD target has been determined. Craig et al. (67) first determined the PKPD indices and targets in animal models of infection. During the last decade, several clinical studies have been performed to study PKPD targets in ill patients in the clinic, e.g. for beta-lactams and quinolones (11, 109, 251, 299). In clinical trials with patients with otitis media

and various beta-lactams, generally a $fT_{>MIC} > 40\%$ was needed to achieve an 85% to 100% bacteriological cure rate (67, 68).

The population PK model used in a MCS must have adequate predictive performance. However, even if this is the case, the population PK model is only as good as the raw data that were used to derive the model. If the PK in the subjects from the original PK study is not representative of the patients for whom the probability of successful treatment should be predicted, these predictions might be biased. Simulating a population from a very small number of subjects might result in biased estimates for the BSV. Also, possible inaccuracies in the performance of the clinical part of the PK study, drug analysis, data analysis or determination of the MICs are reflected in the quality of the predictions from the MCS.

However, if possible limitations are taken into account and the predictions are interpreted conservatively, MCS is a valuable tool to predict the probability of microbiological or clinical success in patients. It also provides helpful guidance for investigators about which dosage regimens have a high probability to show clinical success and should therefore be investigated in a clinical study.

3.4.3   When is saturable elimination important?

Saturable elimination is clinically important, if it is apparent within the range of therapeutic drug concentrations in plasma. By a huge increase in the dose, nonlinear PK could probably be detected for many drugs. However, for most drugs saturation of elimination is not seen at the usually administered doses. For some drugs it could become important in an overdose (262).

Saturable elimination at therapeutic concentrations should be included in a model that is used for predicting plasma concentrations or used in a MCS. If plasma concentrations of a drug with saturable elimination are much lower than the value of K_m, first-order kinetics might be sufficient. If the concentrations exceed K_m, a mixed-order process better predicts the plasma concentrations. A high BSV in K_m might cause that the STS approach cannot

detect a saturable elimination for all subjects. Population PK is more powerful than STS in this situation (chapter 3.4.1).

Knowledge about an existing saturable elimination pathway is important, when concentration time profiles are predicted for doses outside the range of doses that were investigated in the PK study. A linear model might be able to describe the elimination within a certain range of concentrations. However, if this model is then used to predict the PK over a wider range of concentrations, (e.g. for much higher or much lower doses), the predictions may be biased. For example at higher doses, saturable elimination becomes more important, and concentrations increase to a higher extent than would be predicted by a linear (non-saturable) model. Inclusion of a saturable elimination component may also be important, if different modes of administration are compared (e.g. continuous and short-term infusion).

In dose escalation studies with drugs in clinical development, it is an advantage if the data are evaluated by population PK modeling at each dose level simultaneously. If nonlinear PK is present, the investigators can be more cautious in increasing the dose and inappropriately high doses possibly carrying an increased risk for toxicity can be avoided (163).

For dosage adjustment in patients it needs to be considered that the time to reach steady-state increases with decreasing clearance (and therefore increasing half-life). This is important e.g. for phenytoin, that is monitored by TDM and where the time to reach steady-state can increase from several days to two to three weeks at high dose rates. Higher than expected plasma concentrations due to saturable elimination are clinically important, if concentration-dependent side effects are likely to occur. Also, if other drugs that share the same saturable elimination pathway are given in combination, drug concentrations might increase more than expected.

4   Pharmacokinetic drug-drug interactions of antibiotics and their pharmacodynamic impact

4.1   Background on pharmacokinetic drug-drug interactions involving transporters

4.1.1   Drug transport and mechanisms of interaction at transporters

Drug transport through membranes happens mostly by passive diffusion, active transport or both. Passive diffusion occurs because of a concentration gradient between both sides of the membrane and continues until an equilibrium is reached. At equilibrium molecules still traverse the membrane, but concentrations stay the same at both sides of the membrane. No metabolic energy is needed for passive diffusion.

Active transport occurs through carrier proteins located in the membranes. Transport proteins have been identified to be involved in numerous processes in the body, e.g. renal tubular secretion, biliary secretion, transport across the blood-brain barrier, gastro-intestinal absorption and secretion. Contrary to passive diffusion, active transport can move drug molecules against a concentration gradient, has a maximum rate of drug transport, and can be inhibited by other substances or by metabolic inhibitors. Active transport is a saturable (capacity-limited) process, and can be described by the Michaelis Menten equation (see chapter 3.1 and Figure 4.1-1). The rate of transport increases less than linearly at concentrations approaching or exceeding K_m and at very high concentrations a maximum rate of drug transport (Vmax) is reached asymptotically.

Figure 4.1-1   Michaelis Menten reaction scheme without inhibition

$$[S] + [T] \underset{k_{-1}}{\overset{k_1}{\rightleftharpoons}} [TS] \xrightarrow{k_2} [T] + [S]$$

Michaelis Menten condition: $k_2 \ll k_{-1}$

$$v = \frac{V_{max} \cdot [S]}{K_m + [S]}$$

$$V_{max} = k_2 \cdot T_0$$

$$K_m = k_{-1} / k_1$$

T	transporter
S	substrate
TS	transporter-substrate complex
k_1, k_2, k_{-1}	rate constants
v	rate of transport
Vmax	maximum rate of transport
K_m	Michaelis Menten constant
T0	concentration of the transporter
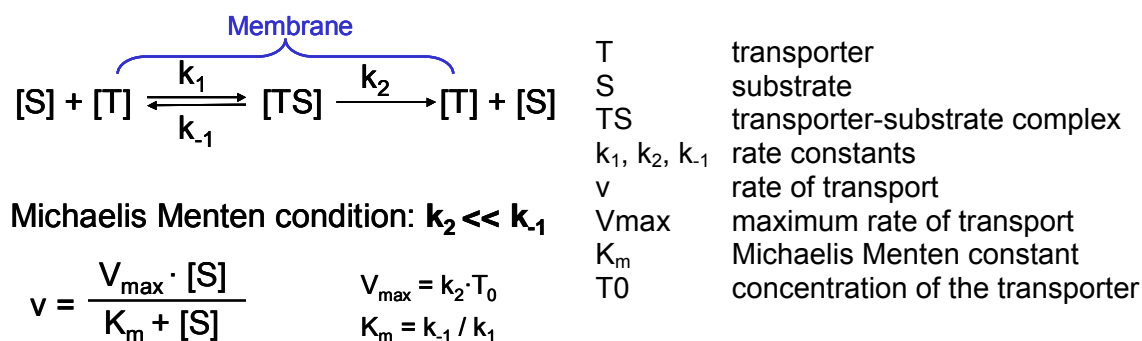
Drug-drug interactions at transporters occur, when the transport of a drug is inhibited by another drug. There are various mechanisms of inhibition. It can be distinguished between reversible and irreversible inhibition. Irreversible inhibition is characterized by a very strong interaction between an enzyme or transporter and the inhibitor, often by formation of covalent bonds. The inhibitor is not released from the enzyme or transporter again and the activity of this enzyme or transporter molecule cannot be recovered. The inhibition cannot be reversed by decreasing the concentration of the inhibitor. Examples for irreversible inhibition are inhibition of the proton pump by omeprazole, inhibition of cyclo-oxygenase by acetyl-salicylic acid and inhibition of transpeptidase by penicillins.

In the case of a reversible inhibition the inhibitor binds non-covalently to the transporter. If the inhibitor is removed or dissociates, the transporter regains its activity. Several mechanisms of reversible inhibition can be distinguished: competitive, uncompetitive, mixed and noncompetitive inhibition. Figure 4.1-2 to Figure 4.1-5 show how the different interaction models are parameterized. As K_m, Vmax or both are influenced by the inhibition, they are called apparent K_m and apparent Vmax in the presence of an inhibitor. Additionally, in Figure 4.1-2 to Figure 4.1-5 the reaction schemes of the different types of interaction are described and it is shown how the rate of transport changes with substrate concentration.

Competitive inhibition describes the situation where both substrate and inhibitor compete for the same binding site at a transporter (Figure 4.1-2). By increasing the substrate concentration, the inhibitor can eventually be

displaced and Vmax can be reached at high substrate concentrations. Therefore the extent of interaction decreases at high substrate concentrations, i.e. above K_m the difference in rate between the curves with and without interaction decreases with increasing substrate concentrations. In competitive inhibition the apparent K_m is increased compared to the situation without an inhibition, while Vmax is not changed. The competitive inhibition constant (Kic) describes the affinity of the inhibitor to the transporter. A low Kic stands for a high affinity of the inhibitor. The relative affinity of the substrate to the transporter compared to the affinity of the inhibitor to the transporter is calculated by the ratio of Kic / K_m. A ratio greater than 1 means that the affinity of the substrate is higher than that of the inhibitor. An example is ethanol, that competitively inhibits the alcohol dehydrogenase and prevents production of toxic metabolites after ethylene glycole poisoning. Sulfonamide antibiotics compete with *p*-aminobenzoic acid and therefore inhibit production of tetrahydrofolic acid in bacteria and multiplication of bacteria.

Figure 4.1-2   Competitive inhibition

$$[T] + [S] \underset{k_{-1}}{\overset{k_1}{\rightleftharpoons}} [TS] \overset{k_2}{\longrightarrow} [T] + [S]$$

$$v = \frac{V_{max} \cdot [S]}{K_m + [S]}$$

Rate of drug transport for a constant inhibitor concentration [I]

Vmax / 2 (no inhibition)

Km no inhibition (30 mg/L)

Km competitive (62 mg/L)

Apparent K_m Apparent Vmax

$$K_m \cdot \left(1 + \frac{[I]}{Kic}\right)$$ Vmax

I   inhibitor
TI   transporter-inhibitor complex
Kic   competitive inhibition constant
        competitive inhibition
        no inhibition
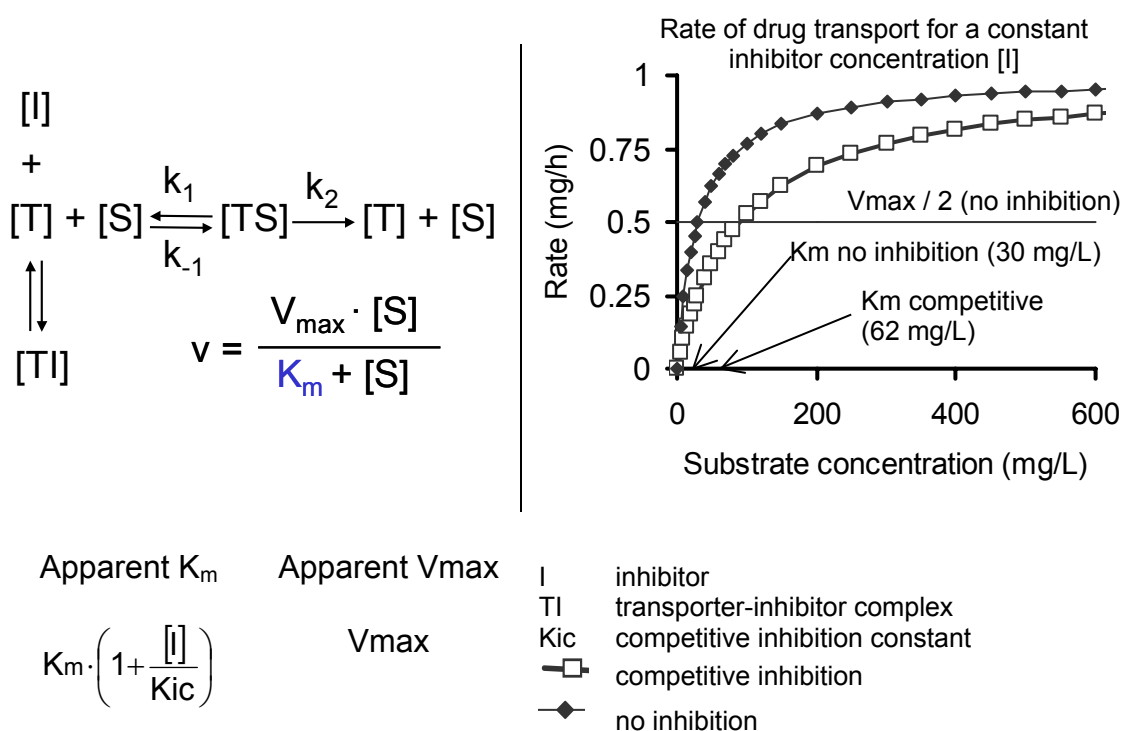
Uncompetitive inhibition means that the inhibitor only binds to the transporter-substrate complex, i.e. after the substrate has bound to the transporter (Figure 4.1-3). The uncompetitive inhibition constant (Kiu) describes the affinity of the inhibitor to the transporter-substrate complex. Both apparent K_m and apparent Vmax are decreased by this inhibition. Contrary to competitive inhibition, in uncompetitive inhibition the value of Vmax without inhibition cannot be reached, even by greatly increasing the substrate concentration. The extent of interaction is highest at high substrate concentrations, i.e. the difference in rate between the curves with and without interaction increases with increasing substrate concentrations (Figure 4.1-3). The therapeutic effect of lithium in manic-depressive psychosis is caused by uncompetitive inhibition of inositolmonophosphatase in the brain (200). Memantine, an uncompetitive antagonist of the N-methyl-D-aspartate (NMDA) receptor, is used for treatment of Alzheimer's disease (102, 316). Despite similar names, uncompetitive and noncompetitive inhibition (Figure 4.1-5) are two different mechanisms of inhibition.

Figure 4.1-3   Uncompetitive inhibition

Rate of drug transport for a constant inhibitor concentration [I]

$$[T] + [S] \underset{k_{-1}}{\overset{k_1}{\rightleftharpoons}} [TS] \xrightarrow{k_2} [T] + [S]$$

$$v = \frac{V_{max} \cdot [S]}{K_m + [S]}$$

Apparent K_m

$$\frac{K_m}{1+\dfrac{[I]}{Kiu}}$$

Apparent Vmax

$$\frac{Vmax}{1+\dfrac{[I]}{Kiu}}$$

TSI   transporter-substrate-inhibitor complex
Kiu   uncompetitive inhibition constant
⊡   uncompetitive inhibition
◆   no inhibition
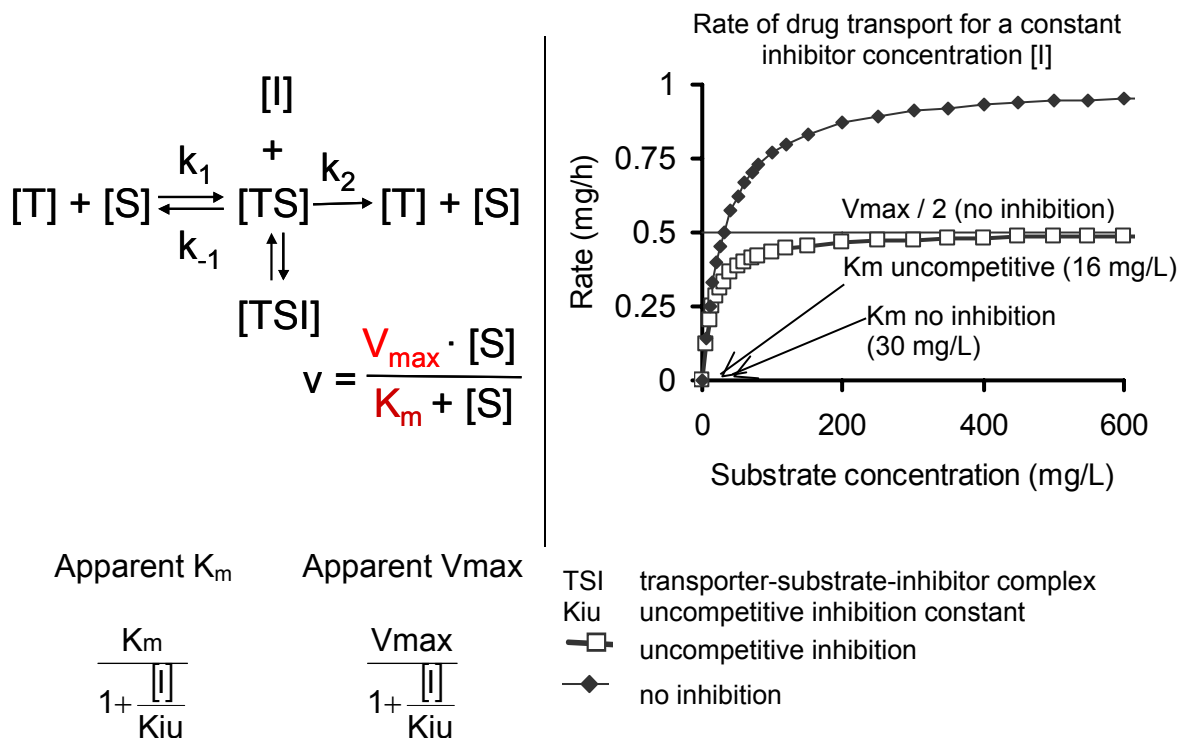
In mixed inhibition, the inhibitor binds to both the free transporter and the transporter-substrate complex. Therefore it can be described as a "mixture" of competitive and uncompetitive inhibition. The apparent Vmax is decreased by the inhibition (Figure 4.1-4). If Kic is higher than Kiu, this means that the inhibition is predominantly uncompetitive and therefore the apparent K_m is decreased as in uncompetitive inhibition. Then, the shape of the curve resembles the one for uncompetitive inhibition (Figure 4.1-3 and left side of Figure 4.1-4), as the extent of interaction is highest at high substrate concentrations. If Kiu is higher than Kic (predominantly competitive inhibition), the shape of the curve (but not Vmax) resembles more the one for competitive inhibition (Figure 4.1-2 and right side of Figure 4.1-4). Loperamide has been shown to exhibit mixed inhibition of the intestinal Na^+-dependent D-glucose transporter (177).

Figure 4.1-4   Mixed inhibition

Rate of drug transport for a constant inhibitor concentration [I]
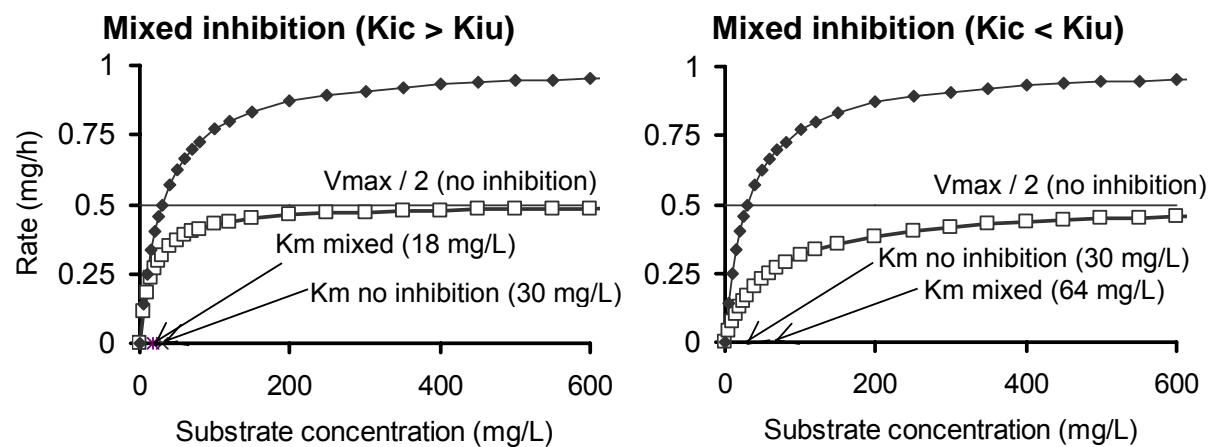
Apparent K_m

$$\frac{K_m \cdot \left(1 + \dfrac{[I]}{Kic}\right)}{1 + \dfrac{[I]}{Kiu}}$$

Apparent Vmax

$$\frac{Vmax}{1 + \dfrac{[I]}{Kiu}}$$

$$[T] + [S] \underset{k_{-1}}{\overset{k_1}{\rightleftharpoons}} [TS] \xrightarrow{k_2} [T] + [S]$$

$$v = \frac{V_{max} \cdot [S]}{K_m + [S]}$$
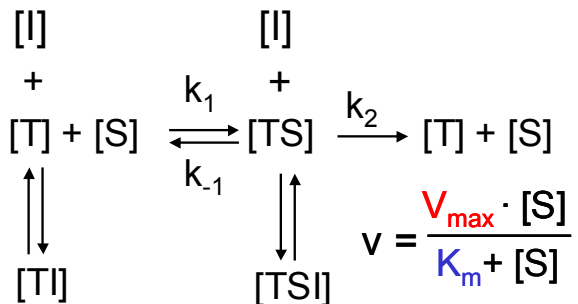
Kic   competitive inhibition constant
Kiu   uncompetitive inhibition constant
TI   transporter-inhibitor complex
TSI   transporter-inhibitor-substrate complex

Noncompetitive inhibition is a special case of mixed inhibition, where the affinity of the inhibitor to the free transporter is identical to the affinity of the inhibitor to the transporter-substrate complex. In noncompetitive inhibition the inhibitor binds to both the free transporter and the transporter-substrate complex (Figure 4.1-5), whereas in uncompetitive inhibition the inhibitor binds only to the transporter-substrate complex. In noncompetitive inhibition the apparent Vmax is decreased, but the apparent K_m is not changed by the inhibition, whereas in uncompetitive inhibition both apparent K_m and apparent Vmax are decreased. In noncompetitive inhibition Ki = Kiu = Kic, which means that the competitive and the uncompetitive part of the interaction have an equal influence. Therefore Km is not changed and the shape of the curve is in between the ones for competitive and uncompetitive inhibition (Figure 4.1-2, Figure 4.1-3 and Figure 4.1-5). Noncompetitive inhibition may be observed in allosteric enzymes.

Figure 4.1-5   Noncompetitive inhibition

$$v = \frac{V_{max} \cdot [S]}{K_m + [S]}$$

Apparent K_m

$$K_m$$

Apparent Vmax

$$\frac{Vmax}{1+\dfrac{[I]}{Ki}}$$

Ki   noncompetitive inhibition constant (Ki = Kic = Kiu)

noncompetitive inhibition

no inhibition
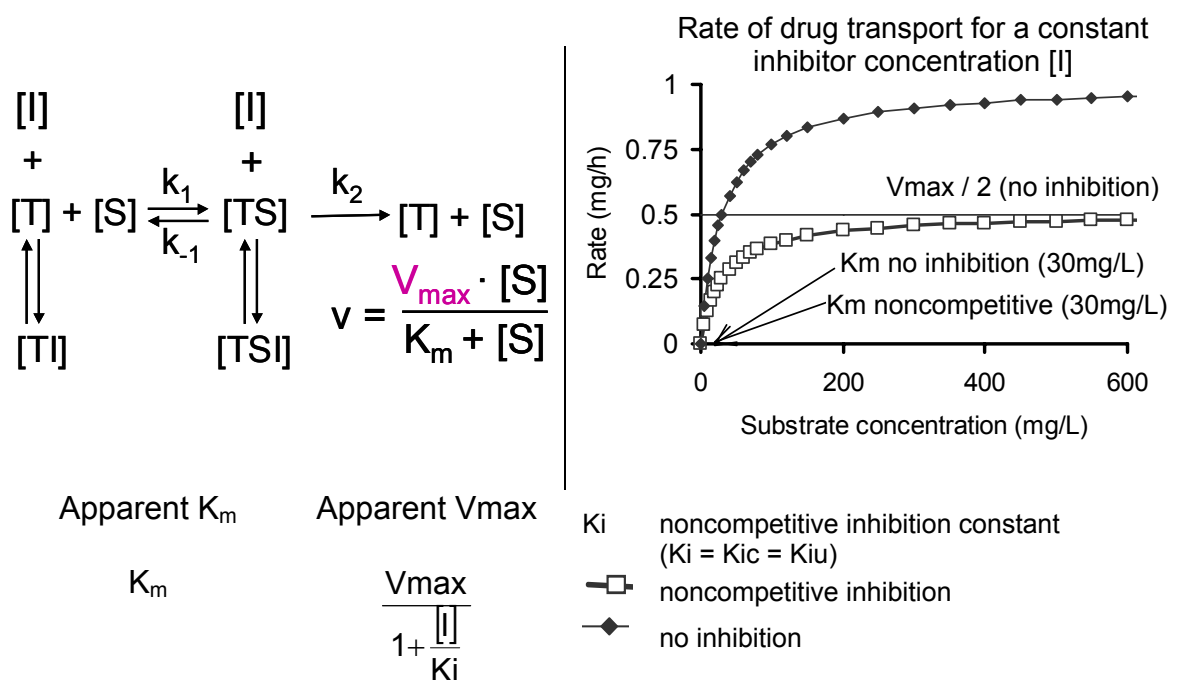
4.1.2   Literature data on interactions with probenecid

A commonly studied drug-drug interaction with antibiotics is the interaction with probenecid. This interaction has been studied for a long time and for many quinolones and beta-lactams (123, 186, 304). Probenecid interacts with both organic anion and organic cation transporters that are involved in the active renal secretion of drug molecules. The extent of interaction with probenecid may reach clinical significance for drugs which display active tubular secretion (116, 233, 318). Probenecid is well documented to decrease the renal secretion of many quinolones, e.g. gatifloxacin (233), levofloxacin (105, 114), norfloxacin (271), fleroxacin (269), and enoxacin (330), whereas moxifloxacin and sparfloxacin are not affected by probenecid (270, 288).

In the vast majority of studies, the interaction with probenecid is studied for the renal site. Less is known about the interaction of probenecid with drugs at other sites in the body. Organic anion and organic cation transporters are not only involved in the active renal secretion of drug molecules (121), but have been found also at various other sites in the body (219, 272). Recently probenecid was shown to affect active transport processes at the blood brain barrier (61). The importance of drug transporters in hepatocytes has been highlighted by Cummins et al. (71). Through an influence of probenecid on drug transporters in the hepatocytes or enterocytes, changes in the nonrenal elimination and metabolism of drugs seem likely. In humans, probenecid decreases the renal excretion of paracetamol glucuronide by 79% (168) and also increases the biotransformation of carbamazepine (173).

Recently it has been discussed that the shortage of oseltamivir might be eased by concomitant administration of probenecid (53). By inhibition of renal secretion, probenecid has been shown to increase the AUC of oseltamivir's active metabolite 2.5fold (140). However, to date no clinical trials have been performed to investigate the effectiveness of lower oseltamivir doses in combination with probenecid.

4.2 Competitive inhibition of renal tubular secretion of gemifloxacin by probenecid

4.2.1 Chemical structure of gemifloxacin

$(C_{18}H_{20}FN_5O_4$, Mol. Wt.: 389.38)
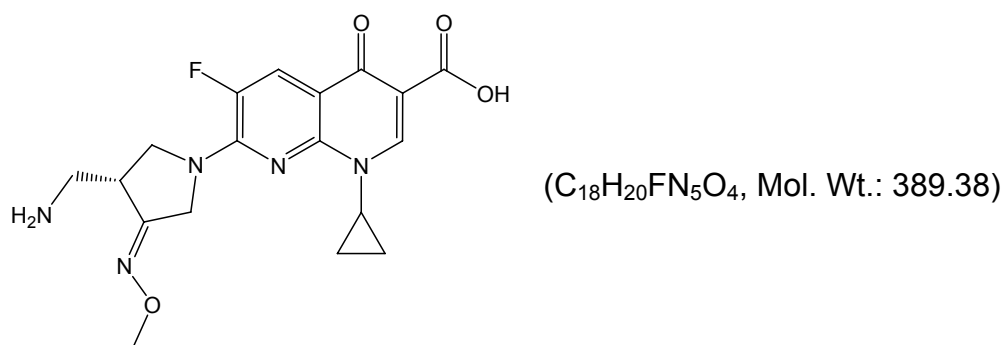
Chemical structure 4.2-1   Gemifloxacin

4.2.2 Specific background on gemifloxacin

Gemifloxacin is a fluoronaphthyridone antimicrobial with an enhanced activity against gram-positive pathogens (64). Renal clearance of gemifloxacin exceeds the glomerular filtration rate which indicates net tubular secretion (8). As gemifloxacin exists primarily as a zwitterion at physiological pH values (pKa_1=6.5, pKa_2=8.9), it is likely to interact with organic anion as well as organic cation transporters in the renal tubular cells (282, 310). The renal elimination of unchanged gemifloxacin accounts for 20-40% of the dose. Most of the dose is eliminated via other routes, which offers various possibilities for an interaction with probenecid at the nonrenal site(s). Cimetidine, an inhibitor of the renal organic cation transport, decreases the renal clearance of gemifloxacin by 28% (7).

Probenecid inhibits active transport processes of anionic and cationic drug molecules at several sites in the body (121, 168, 169) and decreases the renal secretion of many quinolones. However there are no reports on the interaction between probenecid and gemifloxacin.

Our primary objective was to investigate the extent of interaction between gemifloxacin and probenecid by modeling data from a study with

administration of multiple doses of probenecid. Our secondary objective was to describe the time course and plausible mechanisms for the interaction between gemifloxacin and probenecid at the renal and nonrenal sites by compartmental modeling techniques.

4.2.3   Methods

Study design and drug administration: Seventeen healthy subjects (nine males and eight females) participated in the study. Subjects fasted from 12h before until 3h after administration of gemifloxacin. In each of the two study periods each subject received a single oral dose of 320 mg gemifloxacin (Factive® 320 mg tablets) either alone or with 4.5g of probenecid (Probenecid Weimer® 500 mg tablets) divided in eight oral doses. It was intended to study the maximum extent of interaction between probenecid and gemifloxacin. Therefore, relatively high doses of probenecid were administered throughout the whole gemifloxacin plasma concentration time profile. Probenecid was administered as follows: 1000 mg at 10h and 2h before gemifloxacin, followed by 250 mg at 6h and 14h after, and 500 mg at 24h, 36h, 48h and 60h after the dose of gemifloxacin.

Sampling Schedule: Blood samples were collected immediately before the gemifloxacin dose and at 0.5, 1, 1.5, 2, 3, 4, 6, 8, 12, 16, 24, 36, and 48h post-dose. Urine samples were collected before gemifloxacin administration and in the following time intervals: 0 to 4, 4 to 8, 8 to 12, 12 to 16, 16 to 24, 24 to 30, 30 to 36, 36 to 48, 48 to 60 and 60 to 72h after gemifloxacin dose.

Determination of Plasma and Urine Concentrations: For determination of gemifloxacin concentrations, 50µL of each human plasma sample were precipitated with 250µL acetonitrile containing the internal standard. After thorough mixing, the samples were left to stand at room temperature for approximately 10min, and were then centrifuged for approximately 15min at 11,000 g. Of each human urine sample 50µL were diluted by 400µL of mobile phase containing the internal standard. Of each so prepared plasma and urine sample 10µL were chromatographed on a

reversed phase column by isocratic elution. The samples were analyzed by LC-MS/MS with a selected reaction monitoring (SRM) method as follows: Precursor $\rightarrow$ product ion for gemifloxacin m/z 390 $\rightarrow$ m/z 313 and internal standard m/z 394 $\rightarrow$ m/z 313. Both analyses were in positive mode. Under these conditions gemifloxacin and the internal standard were eluted after approximately 1.1 minutes. Calibration was performed by weighted $(1/y^2)$ linear regression.

For determination of probenecid concentrations, 100µL of each human plasma sample were precipitated with 300µL acetonitrile containing the internal standard. After thorough mixing the samples were centrifuged for approximately 5 minutes at 3280 g. Of each sample 15µL were injected onto the HPLC-MS/MS system. The samples were chromatographed on a reversed phase column, eluted with an isocratic solvent and monitored by LC-MS/MS with a SRM method as follows: Precursor $\rightarrow$ product ion for probenecid m/z 284 $\rightarrow$ m/z 240 and internal standard m/z 329 $\rightarrow$ m/z 205. Both analyses were in negative mode. Under these conditions probenecid and the internal standard were eluted after approximately 1.4 and 0.8 minutes, respectively. Calibration was performed by weighted $(1/x^2)$ linear regression. The MacQuan software (version 1.6, PE Sciex, Thornhill, Ontario, Canada, 1991 - 1998) was used for evaluation of chromatograms.

Calibration standards in plasma and urine were prepared by adding the appropriate volume of standard solution of gemifloxacin or probenecid or of the higher concentrated calibration standard to drug-free human plasma or urine. No interferences were observed in plasma and urine for gemifloxacin, probenecid, or the internal standard. The linearity of the gemifloxacin calibration curves in plasma and urine was determined between 0.0100 and 5.00 mg/L. The linearity of the probenecid calibration curves in plasma was shown between 2.45 and 97.6 mg/L. The quantification limits were identical with the lowest calibration levels. The inter-day precision and the analytical recovery of the SQCs of gemifloxacin in human plasma (urine) ranged from 3.7 to 7.2% (5.7 to 7.7%) and from 100.9 to 101.4% (98.1 to 103.3%), respectively. The inter-day precision and the analytical recovery of the SQCs

of probenecid in human plasma ranged from 5.1 to 5.8% and from 90.3 to 102.6%, respectively.

Pharmacokinetic Calculations: We applied NCA and compartmental modeling methods to analyze the concentration-time data of gemifloxacin in plasma and urine and of probenecid in plasma. We used NONMEM for visual predictive checks (25).

Compartmental modeling:

Absorption and disposition of gemifloxacin: We tested one, two and three compartment disposition models for gemifloxacin with first order absorption and with or without lag-time for oral absorption. Identification of the renal and nonrenal components of clearance was possible, because we had both plasma and urine data. We used the following equation to describe the renal clearance of gemifloxacin:

$$CL_R = fu \cdot GFR + \frac{Vmax_R}{K_{mR} + [G]}$$ Formula 4.2-1

The first part ($f_u \cdot GFR$) describes the filtration clearance and the second part of the equation describes the net tubular secretion. f_u is the non-protein bound fraction of gemifloxacin in plasma, GFR is the glomerular filtration rate, $Vmax_R$ is the maximum rate of the mixed order renal elimination, K_{mR} is the gemifloxacin concentration associated with a half maximal rate ($Vmax_R/2$) for the mixed order renal elimination of gemifloxacin, and [G] is the plasma concentration of gemifloxacin. The range of f_u is between 0.3 and 0.4, as a protein binding of 60 to 70% has been reported for gemifloxacin (15). All subjects had normal renal function. Therefore, the renal filtration clearance of gemifloxacin, $f_u \cdot GFR$, is about 2 L/h and accounts only for about 6% of the total body clearance. Hence, we fixed the first order component of renal clearance to 2 L/h in our models.

We described the nonrenal elimination of gemifloxacin as a first-order process for the treatment with gemifloxacin alone. For models with a static interaction for nonrenal clearance of gemifloxacin, we estimated first order nonrenal clearance of gemifloxacin with ($CL_{NR,with\ P}$) and without ($CL_{NR,without\ P}$)

probenecid. For models with a mechanistic interaction at the nonrenal site, we described the nonrenal clearance of gemifloxacin as mixed order process:

$$CL_{NR} = \frac{Vmax_{NR}}{K_{mNR} + [G]}$$ Formula 4.2-2

$Vmax_{NR}$ is the maximum rate of the nonrenal elimination, K_{mNR} is the gemifloxacin concentration associated with a half maximal rate ($Vmax_{NR}/2$) for the mixed order nonrenal elimination of gemifloxacin.

Absorption and disposition of probenecid: For probenecid we tested one and two compartment disposition models with parallel first order and mixed order elimination pathways, since saturable elimination of probenecid has been reported previously (100, 321). We described the oral absorption of probenecid as first order process with or without a lag-time.

Interaction models: We assumed that the first order renal elimination (glomerular filtration) of gemifloxacin was not influenced by probenecid. We expected that probenecid interacts with the tubular secretion, the nonrenal elimination, or with both, and described these interactions by one of the following mechanisms for each interaction site: Competitive, uncompetitive, and noncompetitive inhibition. Besides those three mechanisms, we studied static interactions which were expressed either as two different nonrenal clearances for gemifloxacin with ($CL_{NR,with\ P}$) and without ($CL_{NR,without\ P}$) probenecid or as two different intercompartmental clearances.

We studied interaction models which comprised either a single interaction mechanism or a combination of interaction mechanisms for different interaction sites. The models with different combinations of interactions at the renal and nonrenal site are shown in Table 4.2-1. For the competitive interactions, we calculated the relative affinity (= ratio Kic / K_m) of gemifloxacin and probenecid to the transporter (see chapter 4.1.1).

Table 4.2-1   Interaction models – combinations of mechanisms of interaction at different interaction sites

Model	1	2	3	4	5	6
Inhibition of renal tubular secretion	C	NC	UC	C	NC	C
Inhibition of nonrenal clearance	S	S	S	C	NC	S
Inhibition of distributional clearance	None	None	None	None	None	S
Number of subjects for whom the model had the best AIC	8	2	1	-	5	1

C: Competitive inhibition (see Figure 4.1-2)
NC: Noncompetitive inhibition (see Figure 4.1-5)
UC: Uncompetitive inhibition (see Figure 4.1-3)
S: Static inhibition (two different parameters for treatment with and without probenecid)

4.2.4   Results

All 17 subjects completed the study. The average $\pm$ SD weight was 69.1 $\pm$ 13 kg and height was 173 $\pm$ 10 cm. Plasma and urine concentrations of gemifloxacin with and without probenecid and probenecid concentrations in plasma are shown in Figure 4.2-1. Gemifloxacin concentrations in plasma were slightly higher for the treatment with probenecid (Panel A). The amount of gemifloxacin excreted in urine was reduced by probenecid (Panel B).

Figure 4.2-1   Gemifloxacin and probenecid plasma concentrations and amounts in urine (average ± standard deviation)

Panel A: Gemifloxacin concentrations in plasma with and without probenecid
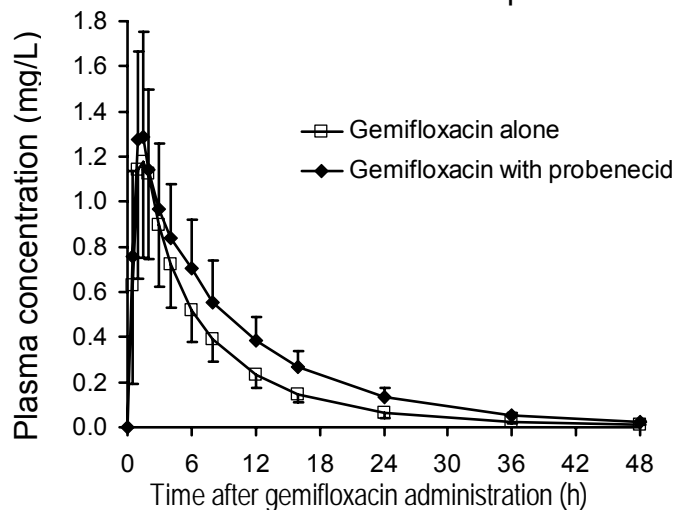
Panel B: Gemifloxacin amounts excreted in urine with and without probenecid
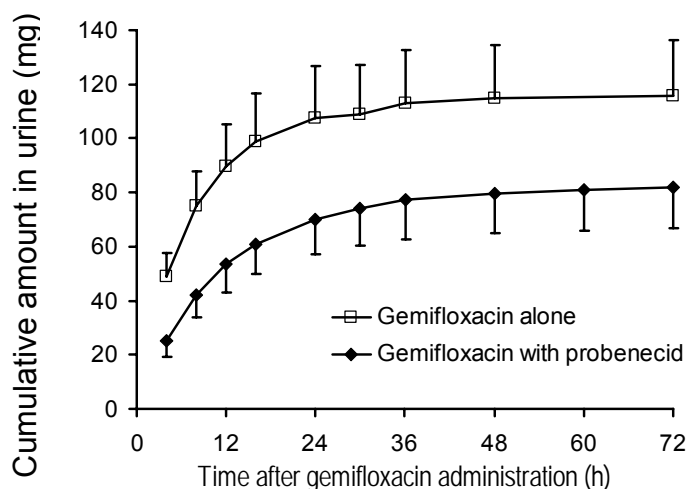
Panel C: Probenecid concentrations in plasma
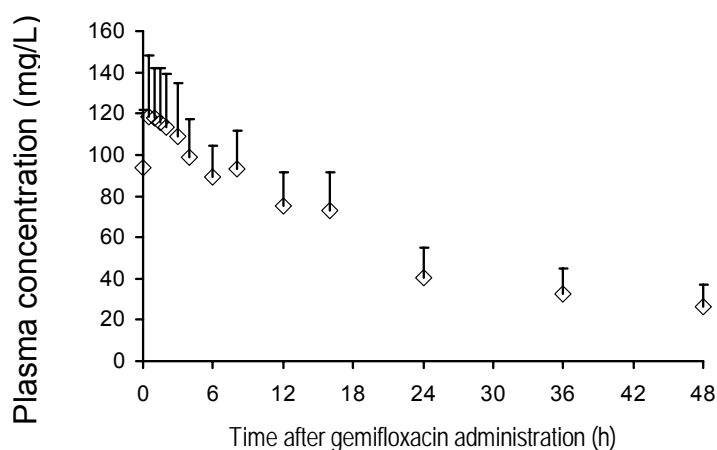
Non-compartmental analysis: The results of the NCA are shown in Table 4.2-2. Addition of probenecid to gemifloxacin reduced the median renal clearance by 51% (p<0.01) and the median nonrenal clearance by 19% (p<0.01). Therefore, total body clearance was decreased by 31% (p<0.01). Although NCA indicated that the median volume of distribution at steady-state (Vss) decreased from 367 to 315 L (p=0.06, Table 4.2-2), this is probably an artifact from NCA and not a true decrease of Vss. We simulated the plasma concentrations of gemifloxacin with and without probenecid with identical PK parameters (including volume of distribution) for both profiles. We derived Vss from both simulated profiles by NCA and observed an about 10% lower Vss for the interaction profiles compared to when gemifloxacin was simulated alone, although the true volume was identical in the simulation.

Table 4.2-2   PK parameters of gemifloxacin given alone or with probenecid derived from NCA (median [25% percentile – 75% percentile], ratio of geometric means (90% confidence interval), and p-value from ANOVA)

	GEM with PRO	GEM alone	Ratio of geometric means: with PRO vs alone	p-value
Total clearance (L/h)	26.0 [20.1 - 29.7]	35.2 [30.7 - 43.8]	0.69 (0.65 - 0.73)	< 0.01
Renal clearance (L/h)	6.49 [4.92 - 8.15]	13.1 [9.91 - 16.2]	0.49 (0.47 - 0.51)	< 0.01
Non-renal clearance (L/h)	19.0 [15.4 - 22.3]	24.2 [19.0 - 26.4]	0.81 (0.74 - 0.88)	< 0.01
Volume of distribution at steady-state (L)	315 [251 - 366]	367 [278 - 389]	0.93 (0.87 - 0.99)	0.06
Fraction excreted unchanged in urine (%)	24.2 [22.9 - 29.0]	35.4 [31.1 - 42.2]	0.71 (0.66 - 0.76)	< 0.01
Peak concentration in plasma (mg/L)	1.30 [1.14 - 1.73]	1.29 [1.08 - 1.48]	1.07 (0.95 - 1.21)	0.32
Time of peak concentration in plasma (h)	1.02 [1.00 - 1.50]	1.05 [1.00 - 1.76]	1.01 (0.85 - 1.20)	0.94
Terminal half-life in plasma (h)	9.49 [8.89 - 9.98]	8.09 [6.92 - 8.90]	1.22 (1.15 - 1.30)	< 0.01

The median terminal half-life of gemifloxacin in plasma was increased from 8.09 to 9.49h (+22%, p<0.01) with probenecid, which is predominantly caused by a decreased clearance. Maximum concentration in plasma and time of peak concentration were not affected significantly by the addition of probenecid suggesting that probenecid did not alter the gut wall transporters which may have contributed to the rate and extent of gemifloxacin absorption.

Compartmental modeling: Based on the plasma and urine concentration time data of gemifloxacin given alone, we chose the two compartment disposition model with a lag-time. This decision was based on the AIC (see chapter 2.6.5) and visual inspection of the observed and predicted plasma and urine profiles. For probenecid, we selected a one compartment model with a lag-time as the final structural model.

Figure 4.2-2   Visual predictive check for plasma concentrations of gemifloxacin with or without probenecid for model 1 (see Table 4.2-1)

See chapter 2.6.5 and Figure 3.2-2 for explanation of the plots.

Gemifloxacin without probenecid (logarithmic scale)

Gemifloxacin with probenecid (logarithmic scale)

Gemifloxacin without probenecid (linear scale)

Gemifloxacin with probenecid (linear scale)
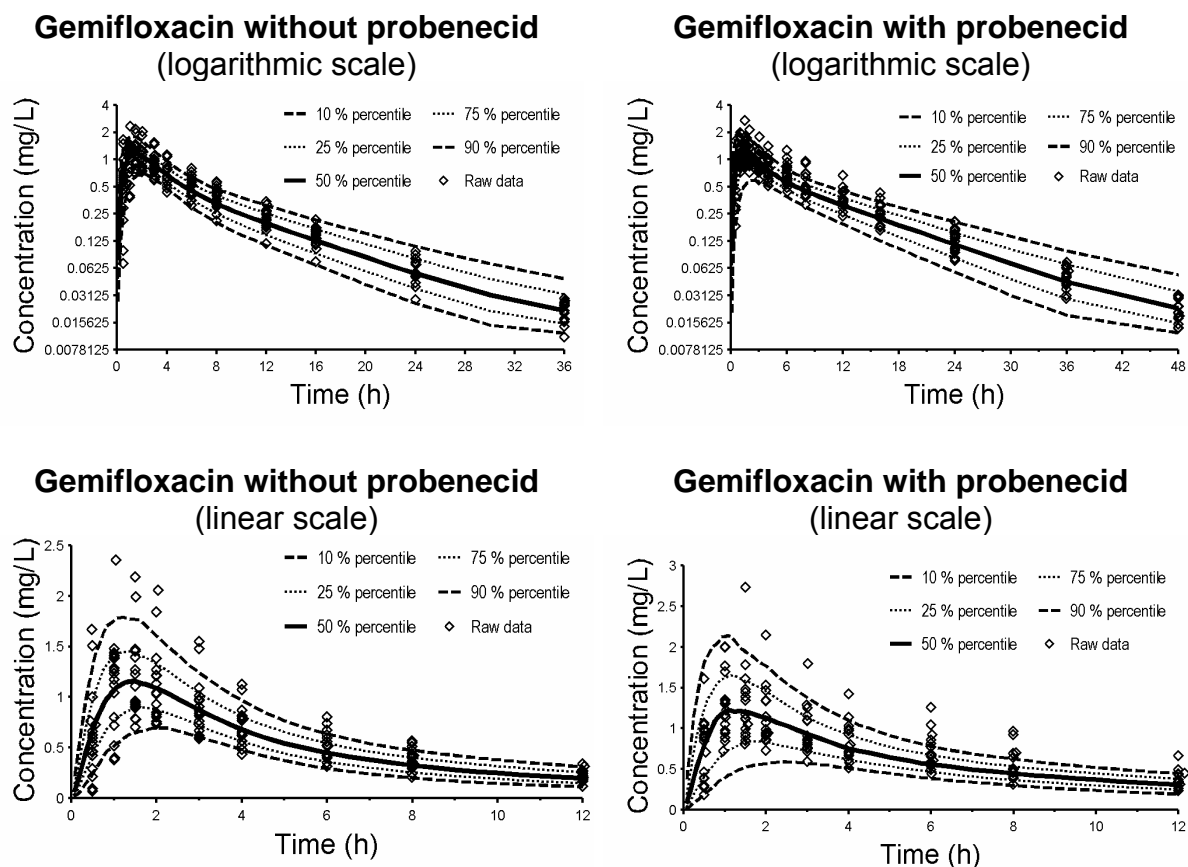
The AIC and the visual predictive checks showed that model 1 had the best predictive performance between the tested interaction models (Table 4.2-1 and Figure 4.2-2). This suggested a competitive inhibition of the renal tubular secretion of gemifloxacin by probenecid as the most likely mechanism. Table 4.2-3 lists the average PK parameters of gemifloxacin for model 1. The average nonrenal clearance of gemifloxacin was significantly reduced from 25.2 to 21.0 L/h (reduction by 17%, p<0.01) with probenecid. Absorption lag-time and absorption rate constant Ka were not affected by probenecid.

The affinity of gemifloxacin to the renal tubular transporter was 7.2 [5.8-8.6] times (median [P25-P75]) higher than the affinity of probenecid. As shown in Figure 4.2-1, probenecid reached about 150 times higher average plasma

concentrations than gemifloxacin and therefore inhibited the secretion of gemifloxacin at the renal transporter to the extent shown in Table 4.2-2.

Table 4.2-3   PK parameter estimates and BSV of gemifloxacin for model 1 (see Table 4.2-1)

Parameter	Unit	Average (%coefficient of variation) for gemifloxacin	
		with probenecid	without probenecid
Ka	h^{-1}	0.897 (104%)	0.839 (62%)
Tlag	h	0.129 (104%)	0.223 (104%)
CL_{NR}	$L\,h^{-1}$	21.0 (23%)°	25.2 (26%)°
K_{mR}	$mg\,L^{-1}$	9.16 (20%)	
$Vmax_R$	$mg\,h^{-1}$	113 (21%)	
$CL_{R,Lin}$	$L\,h^{-1}$	$2^{\#}$	
Kic	$mg\,L^{-1}$	69.3 (26%)	
V1	L	89.5 (62%)	
V2	L	160 (31%)	
CL_{IC}	$L\,h^{-1}$	39.8 (58%)	

°: Significantly different (paired t-test: $p<0.01$).

#: Fixed, not estimated.

Ka: Absorption rate constant, Tlag: Absorption lag-time, CL_{NR}: Apparent nonrenal clearance, K_{mR}: Michaelis Menten constant of the mixed order renal elimination, $Vmax_R$: Apparent maximum rate of the mixed order renal elimination, $CL_{R,Lin}$: First order renal clearance, Kic: Competitive inhibition constant, V1: Apparent volume of distribution of central compartment, V2: Apparent volume of distribution of peripheral compartment, CL_{IC}: Apparent intercompartmental clearance.

4.2.5   Discussion

We are not aware of any reports on the interaction between gemifloxacin and probenecid. Therefore, our primary aim was to study the extent of this interaction. Our secondary aim was to explore the time course, mechanism, and site(s) of interaction. Frequent plasma and urine samples were collected after administration of gemifloxacin alone and together with probenecid, and gemifloxacin and probenecid were quantified. Our NCA

results for gemifloxacin alone were within the range of other studies (8, 117, 199). Probenecid significantly (p<0.01) decreased the median renal clearance of gemifloxacin by 51%, the median nonrenal clearance by 19%, and the median total clearance by 31% as determined by NCA. The peak concentration was not significantly affected by probenecid. These findings show that probenecid inhibited primarily the renal elimination of gemifloxacin. However, also the nonrenal elimination was decreased.

The results from NCA provided an estimate for the maximum extent of interaction between probenecid and gemifloxacin, since the probenecid doses were rather high. We modeled the mechanistic interaction between probenecid and gemifloxacin to further investigate the time course and mechanism of the interaction between probenecid and gemifloxacin. We fitted the plasma and urine profiles of gemifloxacin (with and without probenecid) and of probenecid simultaneously, in order to derive the maximum amount of information from the data. This method uses all data of an individual simultaneously to derive the PK parameters of both drugs and to estimate the time course of interaction.

Our compartmental modeling showed that model 1 (competitive interaction at the renal site and static interaction at the nonrenal site) had the best predictive performance of the tested models. It was the model with the lowest AIC value in 8 of the 17 subjects, whereas the next best model (model 5) had the lowest AIC in 5 subjects (see Table 4.2-1 for performance of the other models). The visual predictive check (Figure 4.2-2) showed that model 1 also had the best predictive performance and was able to capture both the central tendency and the variability of the raw data. The highly sufficient predictive performance further supported our estimates for the PK parameters and their variability for the mechanistic interpretation.

We also found an interaction between gemifloxacin and probenecid for the nonrenal elimination of gemifloxacin. However we could not identify a specific mechanism for the nonrenal interaction, probably because the extent of inhibition at the nonrenal site was much smaller than at the renal site. The estimates for the intercompartmental clearance of gemifloxacin were very similar with and without probenecid. Consequently, model 6 (Table 4.2-1) was

only preferred for one subject. Therefore our final model (model 1 in Table 4.2-1) had a competitive interaction at the renal site and a static interaction at the nonrenal site. From the physiological point of view a competitive mechanism seems the most reasonable as it describes the situation that gemifloxacin and probenecid compete for the same active site of the renal tubular transporter.

This interaction has not been studied before and we are not aware of any reports where a mechanistic model for the interaction of quinolones and probenecid in humans or animals has been developed. As most quinolones are eliminated via tubular secretion, the competitive inhibition of renal tubular secretion that we found for gemifloxacin with probenecid could also apply to other quinolones.

In conclusion, we found that probenecid significantly decreased the renal clearance of gemifloxacin from 13.1 to 6.49 L/h (medians) and the nonrenal clearance from 24.2 to 19.0 L/h. Consequently, the total gemifloxacin clearance was decreased by 31% (p<0.01). The absorption parameters, volume of distribution and peak concentration of gemifloxacin were unaffected by the interaction. Our data suggested a competitive inhibition of the renal tubular secretion of gemifloxacin by probenecid. The median affinity to the renal transporter was 7.2 times higher for gemifloxacin than for probenecid, but probenecid inhibited the secretion of gemifloxacin because probenecid reached about 150 times higher average plasma concentrations than gemifloxacin. Future mechanistic studies for other quinolones are required to further explore this mechanism of interaction.

4.3   Competitive inhibition of renal tubular secretion of ciprofloxacin and its metabolite by probenecid

4.3.1   Chemical structure of ciprofloxacin

$(C_{17}H_{18}FN_3O_3$, Mol. Wt.: 331.34)
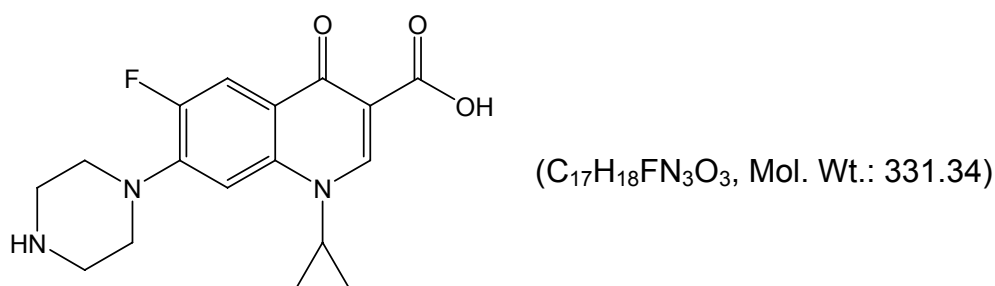
Chemical structure 4.3-1   Ciprofloxacin

4.3.2   Specific background on ciprofloxacin

Ciprofloxacin is a quinolone antimicrobial with a broad range of activity against a variety of gram-positive and gram-negative pathogens (99). Ciprofloxacin is eliminated by the kidneys by glomerular filtration and tubular secretion and shows only a negligible extent of tubular reabsorption (282). Unbound renal clearance of ciprofloxacin is much higher than creatinine clearance which also implies net tubular secretion. Like gemifloxacin, ciprofloxacin is a zwitterion at physiological pH values (pKa_1=6.1, pKa_2=8.7) and therefore might also be able to interact with both organic anion and cation transporters (282, 310). Cimetidine, an inhibitor of organic cation transporters, has been shown (7, 290) to decrease the renal clearance of several quinolones, e.g. gemifloxacin, enoxacin, temafloxacin and ofloxacin.

Jaehde et al. (158) studied the extent of interaction between probenecid, ciprofloxacin and its 2-aminoethylamino-metabolite ("desethylene-ciprofloxacin", M1) previously. As in most reports about quinolone-probenecid interactions, NCA was used then and the full time course of the interaction between ciprofloxacin, M1, and probenecid was not modeled at that time. By NCA in combination with ANOVA the concentration of probenecid is not included in the analysis. Although estimation of the PK and drug-drug

interaction parameters is computationally intensive, modern computation speeds and sophisticated software allow one to analyze those complex systems.

Our first objective was to develop a model that adequately describes the plasma concentrations and amounts in urine of ciprofloxacin and its metabolite M1, including the formation of M1. As our second objective we explored the possible influence of probenecid on renal clearance, nonrenal clearance and distribution of both ciprofloxacin and M1, as well as on the formation of M1. We intended to propose a possible mechanism for the interaction between ciprofloxacin, M1 and probenecid at each site of interaction. This full mechanistic interaction model can predict the time course of a PK interaction for other dosage regimens of interest.

4.3.3   Methods

Study design and drug administration: Twelve healthy subjects (six males and six females) participated in the study. The study was a randomized, controlled, three-way crossover. The third treatment which is not reported here was ciprofloxacin given together with charcoal. Subjects fasted from 12h before until 6h after administration of ciprofloxacin. In each of the two study periods reported here, each subject received a single dose of 200 mg ciprofloxacin (Ciprobay®) as 30min intravenous infusion either alone or with 3g of probenecid (Benemid®) divided in five oral doses. Probenecid was administered as follows: 500 mg at 10h and 1000 mg at 2h before the end of the ciprofloxacin infusion, and 500 mg at 4h, 10h and 16h after the end of the ciprofloxacin infusion.

Sampling schedule: Blood samples were taken before the start of the ciprofloxacin infusion, 10 and 20min after the start of infusion, at the end of infusion, and 5, 10, 20, 30, 45, 60, and 90min and 2, 3, 4, 5, 6, 8, 10, 12, 16, 24, 30, 36, and 48h after the end of infusion. Urine samples were collected before ciprofloxacin administration and from start of the infusion to 2h after end of infusion, as well as 2 to 4, 4 to 6, 6 to 8, 8 to 12, 12 to 16, 16 to 24, 24

to 36, 36 to 48, 48 to 72, and 72 to 96h after the end of the ciprofloxacin infusion.

Determination of plasma and urine concentrations: Ciprofloxacin and M1 concentrations in plasma and urine were determined by reversed phase HPLC as previously described (158). The assay was linear between 0.020 and 10 mg/L, with coefficients of correlation greater than 0.999. The between-day precision of the assay evaluated by pooled biologically derived plasma samples was found to be 2.6% (coefficient of variation) for ciprofloxacin and 3.5% for M1 (average values of three different concentrations). Probenecid concentrations in plasma were determined by LC-MS/MS as described in chapter 4.2.3.

Pharmacokinetic calculations: We applied NCA and compartmental modeling methods to analyze the concentration-time data of ciprofloxacin and M1 in plasma and urine, and of probenecid in plasma.

Compartmental modeling:

Initially we developed the compartment models for ciprofloxacin alone, ciprofloxacin plus M1, and probenecid separately. Then we combined the individual models to explore the interactions in the full model. We did not fix any of the model parameters (except duration of infusion) while estimating the full model. We modeled the plasma and urine profiles for ciprofloxacin with and without probenecid, plasma and urine profiles for M1 with and without probenecid, and plasma profiles for probenecid simultaneously.

Disposition of ciprofloxacin and M1: We tested two and three compartment disposition models for ciprofloxacin. The input of ciprofloxacin was modeled as a zero order process with a fixed duration of 30min. To describe the disposition of M1 we tested one and two compartment models.

For ciprofloxacin, identification of the renal and nonrenal components of clearance is possible, because both plasma concentrations and amounts in urine were available. For M1 also plasma and urine data were available which allows estimation of renal clearance for the metabolite. However the total amount of the metabolite formed is unknown. If no further assumptions are made, volume of distribution and nonrenal clearance of the metabolite are therefore not mathematically identifiable simultaneously.

In order to retain identifiability of all model parameters, e.g. one of the following assumptions has to be made: 1) the metabolite is only eliminated renally, 2) the volume of distribution for the metabolite is set to a pre-specified value, e.g. to the estimated volume of distribution of ciprofloxacin, or 3) the nonrenal clearance of the metabolite is set to a pre-specified value, e.g. to the estimated nonrenal clearance of ciprofloxacin. More specifically, to "set" a parameter to a pre-specified value meant in our analysis that the same parameter was used for ciprofloxacin and M1 and that this one parameter was optimized during the estimation process. We observed in the NCA that the renal clearances of ciprofloxacin and M1 were very similar. Due to this and other observations during model development we chose option 3) and assumed that the nonrenal clearance of M1 was identical to the nonrenal clearance of ciprofloxacin for each treatment.

We used the following equation to describe the renal clearance of ciprofloxacin:

$$CL_{R,CIP} = CL_{R,lin} + \frac{Vmax_R}{K_{mR,CIP} + [C]}$$
Formula 4.3-1

$CL_{R,lin}$ is the first-order renal clearance (filtration clearance), and the second part of the equation describes the net tubular secretion. $Vmax_R$ is the maximum rate of the mixed-order renal elimination, $K_{mR,CIP}$ is the ciprofloxacin concentration associated with a half maximal rate ($Vmax_R/2$) for the mixed-order renal elimination, and $[C]$ is the plasma concentration of ciprofloxacin.

Since the NCA showed a significant reduction of renal clearance of M1 by probenecid, we assumed a parallel first-order and mixed-order renal clearance for M1. This is the physiologically most reasonable way to describe the renal elimination of M1. The M1 concentrations were about 1/10th to 1/200th the ciprofloxacin concentrations and, therefore, most likely far below the K_{mR} for the mixed-order renal elimination. Therefore, we used the same parameter for the filtration clearance ($CL_{R,lin}$) and $Vmax_R$ for the metabolite as for ciprofloxacin and estimated $K_{mR,M1}$ for the metabolite. This yields the following equation for renal clearance of M1:

$$CL_{R,M1} = CL_{R,lin} + \frac{Vmax_R}{K_{mR,M1} + [M1]}$$ Formula 4.3-2

$K_{mR,M1}$ is the M1 concentration associated with a half maximal rate ($Vmax_R/2$) for the mixed-order renal elimination, and [M1] is the plasma concentration of M1.

Formation of M1: We studied the formation of M1 as a first-order or mixed-order process. For models with first-order formation of M1, we described the formation of M1 by a first-order formation clearance $CL_{F,M1}$. For mixed-order formation of M1, we used the following equation:

$$CL_{F,M1} = \frac{Vmax_{F,M1}}{K_{mF,M1} + [C]}$$ Formula 4.3-3

where $Vmax_{F,M1}$ is the maximum rate of the mixed-order formation of M1, $K_{mF,M1}$ is the ciprofloxacin concentration associated with a half maximal rate ($Vmax_R$) for the mixed-order formation of M1, and [C] is the plasma concentration of ciprofloxacin.

Absorption and disposition of probenecid: We tested one and two compartment disposition models with parallel first-order and mixed-order elimination pathways for probenecid, since saturable elimination of probenecid has been reported previously (100, 321). We described the oral absorption of probenecid as first-order process with or without a lag-time.

Interaction models: We assumed that the first-order renal elimination (glomerular filtration) of ciprofloxacin and M1 was not influenced by probenecid. We studied the effect of probenecid on the renal tubular secretion of ciprofloxacin, on the renal tubular secretion of M1, and on the formation of M1, and modeled the following mechanisms: Competitive (Figure 4.1-2), uncompetitive (Figure 4.1-3), and noncompetitive inhibition (Figure 4.1-5). Besides those three mechanisms, we also studied static interactions which were expressed either as two different nonrenal clearances for ciprofloxacin and M1 with ($CL_{NR,with\ P}$) and without ($CL_{NR,without\ P}$) probenecid, two different intercompartmental clearances for ciprofloxacin, two different volumes of

distribution for M1, two different first-order formation clearances of M1, or different $Vmax_{F,M1}$ and $K_{mF,M1}$ for the formation of M1.

We studied interaction models which comprised either a single interaction mechanism or a combination of interaction mechanisms for different interaction sites. Table 4.3-1 shows the tested interaction models for the disposition of ciprofloxacin. For the competitive interactions, we calculated the relative affinity (= ratio K_{ic} / K_m) of ciprofloxacin, M1 and probenecid to the transporter (chapter 4.1.1).

Table 4.3-1   Interaction models for ciprofloxacin

Model	1	2	3	4
Interaction in renal elimination	C	NC	UC	C
Interaction in nonrenal elimination	S	S	S	S
Interaction in distributional clearance	None	None	None	S
Number of subjects for whom the model had the best AIC values	6	3	2	1

C: Competitive inhibition (see Figure 4.1-2)
NC: Noncompetitive inhibition (see Figure 4.1-5)
UC: Uncompetitive inhibition (see Figure 4.1-3)
S: Static inhibition (two different parameters for treatment with and without probenecid).

4.3.4   Results

All 12 subjects completed the study. The average $\pm$ SD weight was 67.1 $\pm$ 12 kg, height was 175 $\pm$ 11 cm, and age was 28.5 $\pm$ 5.2 years. Plasma and urine profiles of ciprofloxacin and M1 with and without probenecid and probenecid concentrations in plasma are shown in Figure 4.3-1. Ciprofloxacin had about 10 to 200 times higher concentrations than the metabolite.

Plasma concentrations of both ciprofloxacin and M1 were higher for the treatment with probenecid. The amount of ciprofloxacin excreted in urine was reduced by probenecid, whereas the amount of M1 excreted in urine was increased by probenecid.

Figure 4.3-1   Ciprofloxacin, its metabolite M1 and probenecid plasma concentrations and amounts in urine (average ± standard deviation)

CIP plasma concentrations – *log-scale*   **M1 plasma concentrations** – *linear-scale*

CIP amounts in urine (0-96.5h)   **M1 amounts in urine** (0-96.5h)

Probenecid plasma concentrations
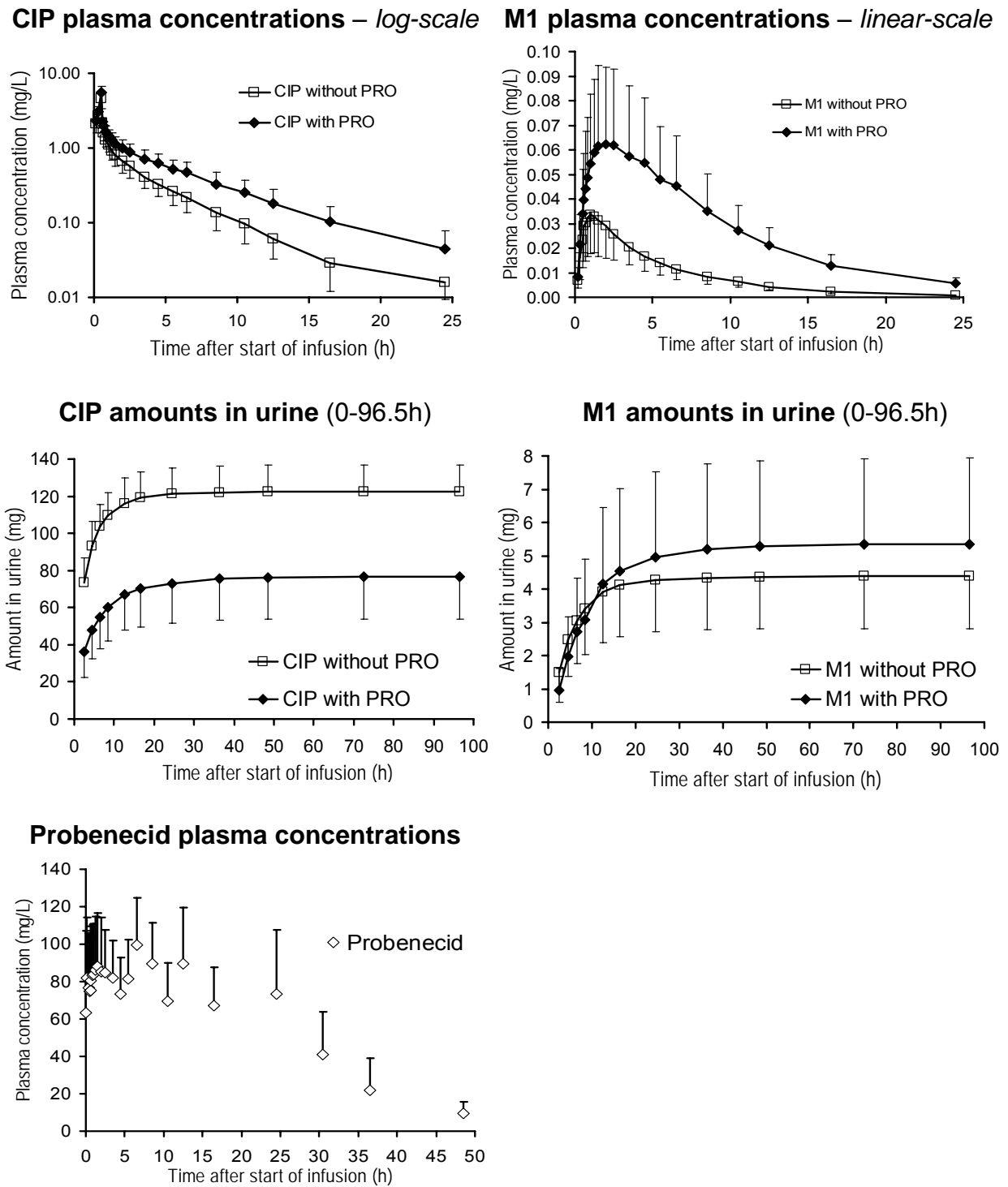
Non-compartmental analysis: The results of the NCA are shown in Table 4.3-2.

Table 4.3-2   PK parameters from NCA of ciprofloxacin and M1 after ciprofloxacin given alone or with probenecid (median [25% percentile - 75% percentile], ratio of geometric means (90% confidence interval) and p-value from ANOVA)

	Ciprofloxacin			Ciprofloxacin's metabolite (M1)			
	Median [P25%-P75%]		Point estimate (90% CI)	p-value	Median [P25%-P75%]		Point estimate (90% CI)	p-value
	With PRO	Without PRO	with PRO / without PRO		With PRO	Without PRO	with PRO / without PRO	
CL_T (L h^{-1})	21.4 [16.4-25.6]	37.4 [30.3-44.3]	58% (55-61)	<0.001	-	-	-	-
CL_R (L h^{-1})	8.25 [6.87-9.85]	23.8 [18.6-25.4]	35% (29-41)	<0.001	8.26 [4.90-9.88]	20.5 [18.7-24.6]	36% (31-42)	<0.001
CL_{NR} (L h^{-1})	14.1 [8.82-18.9]	13.5 [10.7-18.4]	92% (84-102)	0.192	-	-	-	-
$AUC_{0-\infty}$ (mg L h^{-1})	9.35 [7.8-12.23]	5.34 [4.51-6.61]	172% (163-181)	<0.001	0.72 [0.55-0.9]	0.22 [0.15-0.27]	329% (292-372)	<0.001
Ae (%)	39.0 [32.6-42.2]	59.7 [56.5-65.9]	60% (51-70)	<0.001	2.37 [1.65-3.21]	2.03 [1.51-3.01]	118% (99-141)	0.118
Vss (L)	120 [104-142]	129 [113-139]	94% (87-101)	0.169	-	-	-	-
Cmax (mg L^{-1})	5.95 [4.31-6.23]	4.70 [3.57-5.89]	120% (104-140)	0.047	0.065 [0.041-0.095]	0.033 [0.024-0.047]	187% (164-213)	<0.001
$T_{1/2}$ (h)	5.80 [5.24-6.49]	4.95 [3.26-5.78]	135% (119-153)	0.001	5.91 [5.38-7.61]	5.63 [4.28-6.62]	115% (90-147)	0.334
MRT (h)	5.49 [4.55-7.45]	3.54 [2.77-4.67]	162% (154-171)	<0.001	9.18 [8.14-11.8]	6.30 [5.56-8.25]	143% (133-155)	<0.001

CL_T: total body clearance, CL_R: renal clearance, CL_{NR}: nonrenal clearance, $AUC_{0-\infty}$: Area under the curve extrapolated to infinity, Ae: fraction excreted unchanged in urine, Vss: Volume of distribution at steady-state, Cmax: maximal plasma concentration, $T_{1/2}$: Terminal half-life in plasma, MRT: Mean residence time for ciprofloxacin and mean body residence time for M1.

Addition of probenecid reduced the median renal clearance by 65% (p<0.001) for ciprofloxacin, and by 64% (p<0.001) for M1 (Figure 4.3-2, Table 4.3-2). Therefore total body clearance of ciprofloxacin was decreased by 42% (p<0.001) with probenecid. Nonrenal clearance and volume of distribution at steady-state of ciprofloxacin were not affected significantly by probenecid. Peak concentrations in plasma were slightly higher for ciprofloxacin and

significantly higher for M1, when given with probenecid compared to baseline. Mean residence time was significantly prolonged (p<0.001) for both ciprofloxacin (from 3.54 to 5.49h) and M1 (from 6.30 to 9.18h), whereas half-life in plasma was significantly prolonged only for ciprofloxacin (from 4.95 to 5.80h) but less affected for M1.

Figure 4.3-2   Renal clearances of ciprofloxacin (CIP) and M1 with or without probenecid (PRO) determined via NCA
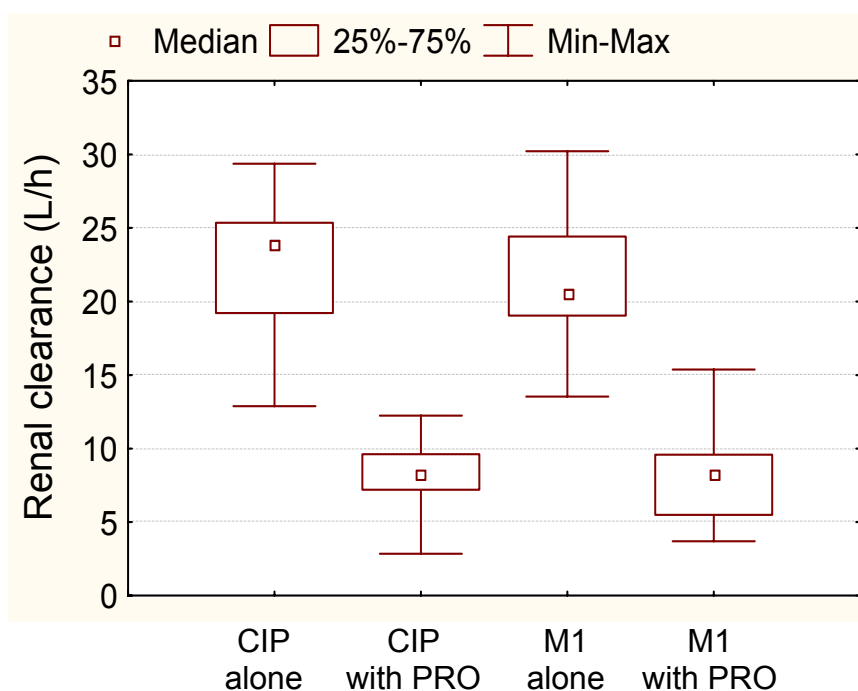
Compartmental modeling:

Disposition of ciprofloxacin and probenecid: For the plasma and urine profiles of ciprofloxacin we chose a three compartment model based on the AIC and residuals analysis. We selected a one compartment model with a lag-time as our final model for probenecid (Figure 4.3-3).

Figure 4.3-3   Compartmental model for CIP, M1, and PRO

Panel A: Treatment without probenecid

Panel B: Treatment with probenecid
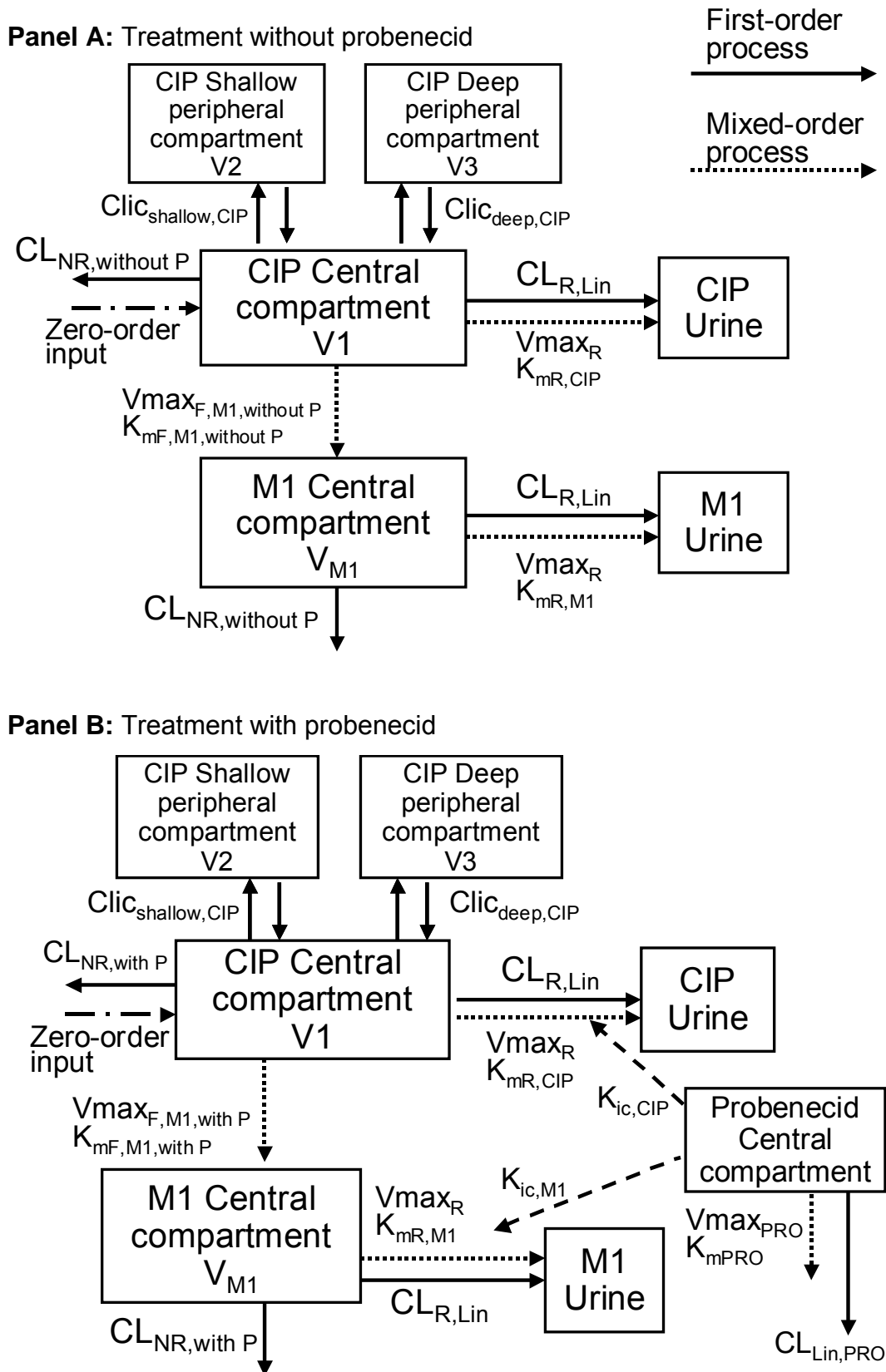
Interaction of ciprofloxacin and probenecid: Our models for ciprofloxacin and probenecid (without M1 data) suggested a competitive inhibition of renal tubular secretion of ciprofloxacin by probenecid as the most likely mechanism. We selected this mechanism for the interaction at the renal site. The estimates for nonrenal clearance of ciprofloxacin were only slightly lower for the treatment with probenecid (Table 4.3-3). Therefore we did not study a mechanistic model for an effect of probenecid on the nonrenal clearance of ciprofloxacin. We included two different parameters for the nonrenal clearance to account for the small reduction and for the variability in nonrenal clearance between both study periods.

Table 4.3-3   PK parameter estimates for ciprofloxacin and M1 (median [25% percentile - 75% percentile])

(see also Figure 4.3-3)

Ciprofloxacin			Ciprofloxacin's metabolite (M1)		
Parameter	Unit	Median [P25-P75]	Parameter	Unit	Median [P25-P75]
Renal elimination			*Renal elimination*		
$CL_{R,Lin}$[#]	L h^{-1}	5.04 [4.40-5.37]	$CL_{R,Lin}$[#]	L h^{-1}	5.04 [4.40-5.37]
$K_{mR,CIP}$	mg L^{-1}	4.66 [2.74-7.58]	$K_{mR,M1}$	mg L^{-1}	5.83 [3.98-9.82]
$Vmax_R$[#]	mg h^{-1}	106 [65.0-183]	$Vmax_R$[#]	mg h^{-1}	106 [65.0-183]
$K_{ic,CIP}$	mg L^{-1}	12.3 [5.76-22.6]	$K_{ic,M1}$	mg L^{-1}	18.5 [9.23-31.0]
$K_{ic,CIP}/K_{mR,CIP}$[*]	-	3.77 [1.71-6.18]	$K_{ic,M1}/K_{mR,M1}$[*]	-	3.20 [2.10-4.58]
Nonrenal elimination			*Nonrenal elimination*		
$CL_{NR,without P}$[#]	L h^{-1}	12.6 [9.69-15.9]	$CL_{NR,without P}$[#]	L h^{-1}	12.6 [9.69-15.9]
$CL_{NR,with P}$[#]	L h^{-1}	11.9 [8.48-13.0]	$CL_{NR,with P}$[#]	L h^{-1}	11.9 [8.48-13.0]
Volume of distribution			*Volume of distribution*		
$V1_{CIP}$	L	11.1 [4.17-15.4]	V_{M1}	L	15.8 [12.3-28.5]
$V2_{CIP}$	L	38.2 [28.5-59.9]			
$V3_{CIP}$	L	57.6 [44.1-67.7]	**Mixed order formation of M1**		
			$K_{mF,M1,without P}$	mg L^{-1}	0.608 [0.327-0.826]
Intercompartmental clearance			$K_{mF,M1,with P}$	mg L^{-1}	0.481 [0.422-1.41]
$CLic_{shallow,CIP}$	L h^{-1}	97.0 [65.6-151]	$Vmax_{F,M1,without P}$	mg h^{-1}	1.94 [1.29-2.70]
$CLic_{deep,CIP}$	L h^{-1}	16.2 [8.10-20.5]	$Vmax_{F,M1,with P}$	mg h^{-1}	1.89 [1.34-3.45]

[#]: Parameter assumed to be the same for ciprofloxacin and M1. Parameter was simultaneously estimated for ciprofloxacin and M1.

*: Derived from estimated parameters (not estimated).

$CL_{R,Lin}$: First-order renal clearance, $K_{mR,CIP}$: Michaelis Menten constant of the mixed-order renal elimination of ciprofloxacin, $Vmax_R$: Maximum rate of the mixed-order renal elimination, $K_{ic,CIP}$: Competitive inhibition constant of the mixed-order renal elimination of ciprofloxacin, $CL_{NR,without\ P}$: First-order nonrenal clearance without probenecid, $CL_{NR,with\ P}$: First-order nonrenal clearance with probenecid, $V1_{CIP}$: Volume of distribution of central compartment, $V2_{CIP}$: Volume of distribution of shallow peripheral compartment, $V3_{CIP}$: Volume of distribution of deep peripheral compartment, $CLic_{shallow,CIP}$: Intercompartmental clearance between the central and the shallow peripheral compartment, $CLic_{deep,CIP}$: Intercompartmental clearance between the central and the deep peripheral compartment, $K_{ic,CIP}$ / $K_{mR,CIP}$: Affinity of ciprofloxacin to the transporter divided by affinity of probenecid to the transporter, $K_{mR,M1}$: Michaelis Menten constant of the mixed-order renal elimination of M1, $K_{ic,M1}$: Competitive inhibition constant of the mixed-order renal elimination of M1, V_{M1}: Volume of distribution of M1, $K_{mF,M1,without\ P}$: Michaelis Menten constant of the mixed-order formation of M1 without probenecid, $K_{mF,M1,with\ P}$: Michaelis Menten constant of the mixed-order formation of M1 with probenecid, $Vmax_{F,M1,without\ P}$: Maximum rate of the mixed-order formation of M1 without probenecid, $Vmax_{F,M1,with\ P}$: Maximum rate of the mixed-order formation of M1 with probenecid, $K_{ic,M1}$ / $K_{mR,M1}$: Affinity of M1 to the transporter divided by affinity of probenecid to the transporter.

Disposition of M1: We observed in the NCA that ciprofloxacin and M1 had very similar terminal half-lives. The geometric mean of the ratio for terminal half-life(M1) / terminal half-life(ciprofloxacin) was 1.18 (34% coefficient of variation). In absence of data on the terminal half-life of M1 after iv dosing, we assumed that the formation of the metabolite determined its terminal half-life. The flip-flop situation for M1 seems reasonable due to the very similar terminal half-lives of parent and metabolite. The plasma concentration time curves of the metabolite showed no two-compartment behavior which was in agreement with the formation of the metabolite being the rate limiting step. Therefore, we selected a one-compartment model for M1 (Figure 4.3-3).

Formation of M1: Based on the ciprofloxacin and M1 data for the treatment without probenecid, a mixed-order process described the formation of the metabolite better than or equally well as a first-order formation process.

More importantly, the Michaelis Menten constant for the formation of the metabolite was about 0.6 mg/L which was well within the range of the ciprofloxacin plasma concentrations. Therefore, we selected a mixed-order process for the formation of the metabolite which is also the physiologically most reasonable choice. Our models showed that probenecid did not affect the formation parameters of M1, since the parameters for the mixed-order formation of M1, $Vmax_{F,M1}$ and $K_{mF,M1}$ (Table 4.3-3), were not significantly affected by the addition of probenecid.

Interaction of M1 and probenecid: We tested various models to describe the interaction between M1 and probenecid at the renal site. The AIC and residuals analysis suggested a competitive inhibition of renal tubular secretion as the most likely interaction mechanism between M1 and probenecid at the renal site.

As described in the methods section, we assumed that M1 had the same nonrenal clearance as ciprofloxacin (option 3), and the nonrenal clearance of ciprofloxacin and the metabolite was estimated simultaneously. When we made this assumption, the volume of distribution of the metabolite was very similar for the treatment with and without probenecid. Therefore, we used the same volume of distribution for M1 for both treatments in our final model. When we assumed that the metabolite was only eliminated renally (option 1), the volume of distribution of M1 was about 45% lower for the treatment with probenecid relative to the treatment without probenecid, and Vmax for the formation of M1 was reduced by about 40% under the influence of probenecid. Especially the reduction of volume of distribution would be a very unreasonable result, because the volume of distribution of ciprofloxacin was unaffected by probenecid. Therefore, this was a strong indication that assuming the same nonrenal clearance for ciprofloxacin and M1 (option 3) was a more reasonable choice than assuming that nonrenal clearance is zero for M1 (option 1).

Final model: Figure 4.3-3 shows the compartment structure of our final model and Table 4.3-3 lists the estimates for the PK parameters of ciprofloxacin and M1. Our final model included a competitive inhibition of the renal elimination of both ciprofloxacin and M1 by probenecid and described

the formation of the metabolite as a mixed-order process. For the competitive interaction at the renal site the affinity of ciprofloxacin for the renal transporter was 3.8 times (median) higher than the affinity of probenecid and the affinity of M1 was 3.2 times higher than the affinity of probenecid (Table 4.3-3). As shown in Figure 4.3-1, probenecid reached about 100 times higher average plasma concentrations than ciprofloxacin and about 1600-2100 times higher average plasma concentrations than M1. Therefore probenecid inhibited the renal tubular secretion of ciprofloxacin and M1 at the renal transporter to the extent shown in Table 4.3-2, although ciprofloxacin and M1 had higher affinities to the transporter than probenecid.

4.3.5   Discussion

The interaction with probenecid has been studied for several quinolones. However, little is known about the mechanism of interaction, site(s) of interaction, and the relative affinity of probenecid and quinolones to the involved transporter(s). To the best of our knowledge, no mechanistic model for the interaction of quinolones and probenecid in humans or animals has been published. We determined the PK parameters of ciprofloxacin and M1 via NCA to support model development and modeled the plasma and urine profiles of ciprofloxacin, M1, and probenecid simultaneously in order to derive the maximum amount of information from our data.

We explored several mechanisms of interaction between ciprofloxacin and probenecid (Table 4.3-1). We found that a competitive inhibition of the renal tubular secretion of ciprofloxacin by probenecid had the best AIC values for 6 of the 12 subjects (see model 1, Table 4.3-1), good AIC values in the other 6 subjects, and gave the best fit to our data. The other mechanisms of inhibition of renal tubular secretion were ranked less likely. Our models showed that there was no effect of probenecid on drug distribution. Neither the ciprofloxacin intercompartmental clearance nor the volume of distribution were affected by probenecid. In the treatment with probenecid the nonrenal clearance of ciprofloxacin was reduced only by 8% (Table 4.3-2) which would

appear to indicate that there was only a small (if any) inhibition of probenecid on the nonrenal clearance of ciprofloxacin.

As for ciprofloxacin, the time course of the renal interaction of M1 with probenecid was adequately described by a competitive inhibition of the renal tubular secretion by probenecid. Also from the physiological point of view, a competitive interaction seems the most reasonable one, as it describes the situation that ciprofloxacin and probenecid compete for the same active site of a renal transporter and that M1 and probenecid compete for the same active site of a renal transporter. Therefore, we chose a competitive renal interaction between ciprofloxacin and probenecid, and between M1 and probenecid.

Our models suggested that the affinity of ciprofloxacin for the renal transporter was 3.8 times (median) higher than the affinity of probenecid and the affinity of M1 was 3.2 times (median) higher than of probenecid (Table 4.3-3). The ratios of the relative affinity of ciprofloxacin to the transporter and of M1 to the transporter within the individual subjects were close to 1 (median 0.99). This suggests that ciprofloxacin and M1 are probably secreted by the same renal tubular transporter(s). The knowledge about transport proteins and their substrate specificity has increased considerably during the last decade(s) (216). OAT1, an organic ion transporter, has been suggested as possible candidate for the renal interaction between ciprofloxacin and probenecid, as OAT1 is inhibited by probenecid (226). Cinoxacin inhibited the uptake of p-aminohippuric acid by OAT1, whereas ofloxacin and norfloxacin showed no interaction (159). Further studies are required to identify the transporter(s) involved in the interaction between quinolones and probenecid.

We attempted to describe the formation of M1 by a first-order or a mixed-order process. The Michaelis Menten constant for the formation of M1 ($K_{mF,M1,without\ P}$, $K_{mF,M1,with\ P}$ Table 4.3-3) was estimated to be about 0.5-0.6 mg/L and was about $1/10^{th}$ the peak concentrations of ciprofloxacin. The ciprofloxacin concentrations were above 0.5 mg/L for about 3h when ciprofloxacin was given alone and for about 6h for ciprofloxacin plus probenecid. The plasma concentration profiles of M1 showed broad, plateau like peaks for the interaction treatment which were probably caused by a partial saturation of the formation of M1 at high ciprofloxacin concentrations.

The model with first-order formation does not account for a saturation of metabolism. Consequently, the model with first-order formation over-predicted the peak concentrations of the metabolite, whereas the model with mixed-order formation of M1 described the plasma and urine data of M1 for both treatments very well.

In our final model, we allowed the parameters for the mixed-order formation of M1 to vary between both treatments to account for variability between both study periods. The estimates for $K_{mF,M1,without\,P}$ and $K_{mF,M1,with\,P}$ as well as for $Vmax_{F,M1,without\,P}$ and $Vmax_{F,M1,with\,P}$ were similar (p>0.05) for both treatments (Table 4.3-3). The ratio of $Vmax/K_m$ which represents the formation clearance of M1 at low ciprofloxacin concentrations was 3.0 [0.72-13.9] L/h for ciprofloxacin alone and 3.1 [0.75-9.0] L/h for ciprofloxacin with probenecid (median [range]). Consequently, it was not surprising that models with a competitive or noncompetitive inhibition of the formation of M1 by probenecid were not supported by the data. Therefore, our models indicated that probenecid did not influence the formation of M1.

Compartmental modeling explicitly studies the full time course of the metabolite formation as well as the time course of the effect of probenecid on the disposition of ciprofloxacin and M1. We combined all features of the PK model in our final model which included the competitive inhibition of renal tubular secretion of ciprofloxacin and M1 by probenecid as well as the saturable formation of M1.

Our models showed that probenecid did not affect the intercompartmental clearance of ciprofloxacin. Consequently, probenecid did not alter the distribution of ciprofloxacin. Besides the ability of compartmental modeling to draw those mechanistic conclusions on the interaction of ciprofloxacin, M1, and probenecid, the most valuable advantage of compartmental analysis over NCA is probably the ability of our final compartmental model to predict the extent and time course of the interaction for other dosage regimens.

In conclusion, our compartmental analysis showed that the profiles of ciprofloxacin, M1 and probenecid in plasma and urine could be well described by a competitive inhibition of the renal tubular secretion of ciprofloxacin and

M1 by probenecid. The affinities to the renal transporter were similar for the parent drug and metabolite, and were 3 to 4 times higher for ciprofloxacin and M1 than for probenecid. Probenecid inhibited the secretion of ciprofloxacin and M1, because plasma concentrations of probenecid were about 100 times higher than for ciprofloxacin and about 1600 to 2100 times higher than for M1. The formation of M1 was best described by a mixed-order process. The formation of M1, nonrenal clearance and volume of distribution of ciprofloxacin and M1, as well as the intercompartmental clearance of ciprofloxacin were not affected by probenecid. Simultaneous modeling of plasma and urine data of ciprofloxacin, M1, and probenecid was a powerful method to study the interaction of ciprofloxacin and M1 with probenecid at various possible interaction sites. Future studies for other quinolones are required to further explore the mechanism of interaction for probenecid *in vivo*.

4.4   Competitive inhibition of flucloxacillin renal tubular secretion by piperacillin

4.4.1   Specific background on flucloxacillin, piperacillin and their use in combination

In serious hospital related infections, multiple pathogens may be involved and empirical treatment needs to be implemented as soon as possible. In order to widen the spectrum of pathogenic organisms covered, combination antibiotic treatment is frequently used. Betalactams are often given together with an aminoglycoside because of their synergistic activity. Combinations of betalactams are also frequently used, especially when there is concern about nephrotoxicity with aminoglycosides (1, 115, 335). The combination of piperacillin and moxalactam (latamoxef), a cephamycin antibiotic, was as effective as moxalactam together with amikacin in the treatment of febrile granulocytopenic cancer patients, while piperacillin and moxalactam was associated with significantly less frequent nephrotoxicity (77). However moxalactam, as other antibiotics containing a methyl-thiotetrazole group, is associated with an increased risk of bleeding and therefore not used therapeutically any more. Indeed a synergistic effect of betalactam combinations against some *P. aeruginosa* isolates *in vitro* has been shown recently (57).

The use of piperacillin / tazobactam and flucloxacillin in combination is recommended by the British National Formulary for the treatment of community or hospital acquired septicemia, if the presence of (flucloxacillin susceptible) staphylococci is suspected (1). The combination of piperacillin and flucloxacillin together with an aminoglycoside has been used successfully for the treatment of infections in children with cancer (162, 206).

Like most betalactams, piperacillin and flucloxacillin are predominantly eliminated renally (123, 342) by glomerular filtration and tubular secretion. As tubular secretion is an active saturable process, interactions may occur if two drugs using this elimination pathway are given concomitantly. This has been

frequently shown with betalactams and probenecid, a well known inhibitor of tubular secretion (123, 186, 304). Renal interactions have also been reported when two betalactams were given together (19, 139, 170, 259). Therefore, PK drug-drug interactions may occur when two or more betalactams are given in combination.

We used piperacillin and flucloxacillin as model drugs that are co-administered in certain clinical situations to explore their PK interactions at therapeutic doses. Frequent plasma and urine samples were collected in a well controlled healthy volunteer crossover study at different dose levels. In a crossover study BSV is removed from the treatment comparison and different dose levels often help to explore the mechanism of interaction and to estimate a saturable component of elimination.

The aim of our study was to describe the extent of interaction between flucloxacillin and piperacillin at different dose levels in healthy volunteers. Our secondary objective was to explore the time course, site(s) and possible mechanisms of the interaction between the two betalactams by compartmental modeling techniques.

4.4.2   Methods

Study design and drug administration: Ten healthy subjects (five males and five females) participated in the study. The study was a randomized, controlled, six-way crossover. Each subject received all of the following treatments: A) 1.5g piperacillin, B) 0.5g flucloxacillin, C) 1.5g piperacillin + 0.5g flucloxacillin, D) 3g piperacillin, E) 1g flucloxacillin, and F) 3g piperacillin + 1g flucloxacillin. The doses were administered as 5min intravenous infusions.

Sampling Schedule: Blood samples were drawn immediately before start of infusion, at the end of infusion as well as at 5, 10, 15, 20, 25, 45, 60, 75, 90min and 2, 2.5, 3, 3.5, 4, 5, 6, 8, and 24h after the end of the infusion. Urine samples were collected immediately before start of the infusion, from start of the infusion until 1h after end of infusion and in the following time

intervals: 1 to 2, 2 to 3, 3 to 4, 4 to 5, 5 to 6, 6 to 8, 8 to 12, 12 to 24h after the end of the infusion.

Determination of Plasma and Urine Concentrations: Plasma and urine concentrations were determined as described above for flucloxacillin (chapter 3.2.3) and piperacillin (chapter 3.3.3).

Pharmacokinetics

Models: We modeled the profiles from the six different treatments simultaneously. We tested one, two and three compartment disposition models for both piperacillin and flucloxacillin. The drug input was modeled as a zero order process with a duration of 5min. We could separate between renal and nonrenal elimination, because the amounts of piperacillin and flucloxacillin excreted in urine had been determined. We described renal clearance as a parallel linear and mixed-order elimination process and used the following equation for the renal clearances of piperacillin and flucloxacillin:

$$CL_R = CL_{R,linear} + \frac{Vmax_R}{K_{mR} + [C]} \qquad \text{Formula 4.4-1}$$

$CL_{R,linear}$ is the first order renal clearance, $Vmax_R$ is the maximum rate of the mixed order renal elimination, K_{mR} is the piperacillin or flucloxacillin concentration associated with a half maximal rate ($Vmax_R/2$) for the mixed order renal elimination of the respective drug, and [C] is the plasma concentration of piperacillin or flucloxacillin. As all subjects had normal renal function and the non-protein bound fraction in plasma (f_u) is reported as 6% (28, 30) for flucloxacillin, the renal filtration clearance of flucloxacillin ($f_u \cdot$ GFR) is about 0.432 L/h, which only accounts for approximately 5% of total body clearance. Therefore we fixed $CL_{R,linear}$ to 0.432 L/h for flucloxacillin.

For models without a mechanistic interaction for nonrenal clearance of flucloxacillin, we described the nonrenal elimination as a first order process with a nonrenal clearance ($CL_{NR,FLU}$). For models with a mechanistic interaction for nonrenal elimination we described the nonrenal clearance of flucloxacillin as a mixed-order process:

$$CL_{NR} = \frac{Vmax_{NR,FLU}}{K_{mNR,FLU} + [F]}$$ Formula 4.4-2

$Vmax_{NR,FLU}$ is the maximum rate of the nonrenal elimination, $K_{mNR,FLU}$ is the flucloxacillin concentration associated with a half maximal rate ($Vmax_{NR,FLU}$/2) for the mixed order nonrenal elimination of flucloxacillin and [F] is the plasma concentration of flucloxacillin.

Interaction models: We assumed that the first order renal elimination (glomerular filtration) of flucloxacillin was not influenced by piperacillin. We tested the following four mechanistic interactions for the mixed order renal elimination process: Competitive, uncompetitive, mixed and noncompetitive inhibition. Besides those mechanistic interactions we also studied static interactions. The static interactions were expressed as two different nonrenal clearances for flucloxacillin with ($CL_{NR,FLU\ with\ P}$) and without ($CL_{NR,FLU\ without\ P}$) piperacillin. The models with different combinations of interactions at the renal and nonrenal sites are shown in Table 4.4-1. For the competitive interactions we calculated the relative affinity (= ratio $K_{m,FLU}$ / Kic) of piperacillin and flucloxacillin to the transporter for each subject (see chapter 4.1.1).

Table 4.4-1   Interaction models studied for the influence of piperacillin on flucloxacillin

Model	1	2	3	4	5
Interaction in renal elimination	C	UC	M	NC	C
Interaction in nonrenal elimination	S	S	S	S	C

M: Mixed inhibition (see Figure 4.1-4)
See Table 4.2-1 for explanation of the other abbreviations.

4.4.3   Results

All ten subjects (5 males and 5 females) completed the study. The average ± SD weight was 75.6 ± 7.3kg for males and 63.6 ± 8.3kg for females, height was 183.2 ± 5.0cm for males and 171.8 ± 6.1cm for females, and age 26.8 ± 4.2 years for males and 24.6 ± 0.55 years for females. Plasma

concentrations of flucloxacillin after infusion of 0.5g and 1g were considerably higher with piperacillin compared to flucloxacillin given alone (Figure 4.4-1). Flucloxacillin amounts excreted in urine during the first 2h after administration were much lower with the interaction treatments compared to baseline.

Figure 4.4-1   Median [P25%-P75%] profiles of flucloxacillin in healthy volunteers after a 5min infusion of 0.5g and 1g flucloxacillin with or without piperacillin

 ━━ Flucloxacillin alone

 ▬ ▬ Flucloxacillin 0.5g with piperacillin 1.5g or
    Flucloxacillin 1g with piperacillin 3g
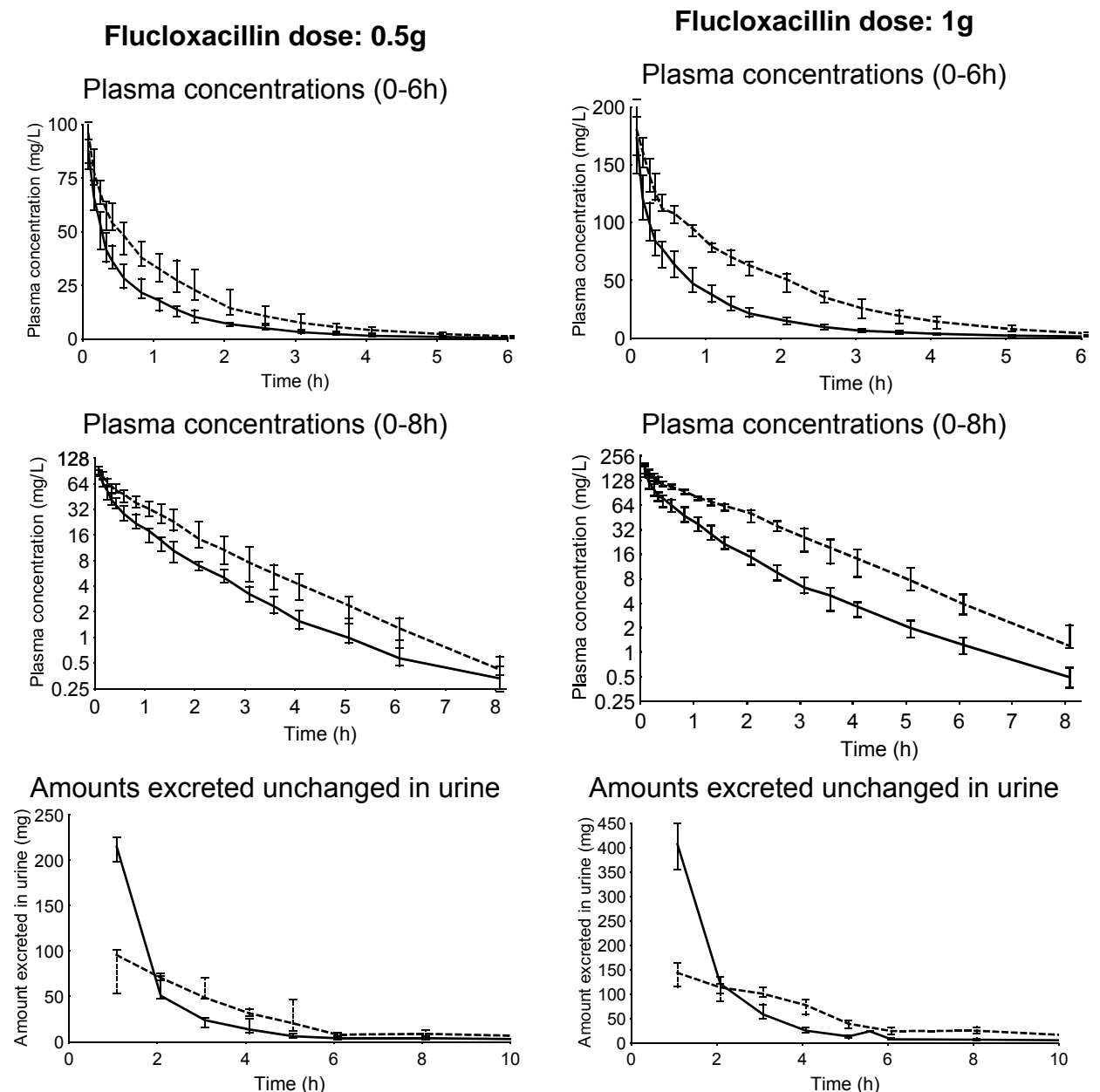
Non-compartmental analysis: The results of the NCA are shown in Table 4.4-2.

Table 4.4-2   PK parameters for 0.5g and 1g flucloxacillin with or without piperacillin from non-compartmental analysis

	Median (P25%-P75%)		Point estimate (90% CI)	* p-value	Median (P25%-P75%)		Point estimate (90% CI)	* p-value
Flucloxacillin	0.5g	0.5g	with PIP / without PIP		1g	1g	with PIP / without PIP	
Piperacillin	1.5g	-			3g	-		
CL_T (L/h)	5.04 [3.80-6.07]	7.82 [7.37-9.36]	59% (54-65%)	< 0.01	3.79 [3.53-4.21]	7.96 [6.81-9.57]	47% (44-50%)	< 0.01
CL_R (L/h)	2.90 [2.20-3.46]	5.44 [4.63-6.27]	54% (46-64%)	< 0.01	2.06 [1.88-2.35]	5.47 [4.52-6.07]	37% (34-41%)	< 0.01
CL_{NR} (L/h)	1.77 [1.53-2.60]	2.66 [2.18-3.44]	67% (56-80%)	< 0.01	1.80 [1.64-1.99]	2.79 [2.17-3.48]	65% (55-76%)	< 0.01
Ae (%)	56.7 [53.9-72.0]	68.6 [61.2-70.6]	92% (82-102%)	0.18	51.8 [50.8-58.5]	64.0 [59.7-74.6]	80% (73-87%)	< 0.01
Vss (L)	7.14 [6.23-7.77]	9.52 [8.38-11.1]	72% (64-80%)	< 0.01	6.56 [5.99-6.93]	10.4 [8.89-11.6]	64% (59-70%)	< 0.01
Cmax (mg/L)	95.8 [82.0-101]	87.7 [79.1-93.0]	106% (94-120%)	0.40	183 [164-209]	173 [144-192]	109% (99-120%)	0.13
$T_{1/2}$ (h)	1.35 [1.18-1.45]	1.44 [1.31-1.75]	95% (74-121%)	0.70	1.24 [1.13-1.39]	1.59 [1.32-1.84]	77% (70-85%)	< 0.01
MRT (h)	1.44 [1.33-1.56]	1.17 [1.06-1.41]	122% (115-130%)	< 0.01	1.64 [1.47-1.79]	1.18 [1.13-1.34]	136% (129-144%)	< 0.01

* p-value from ANOVA
MRT: Mean residence time. For explanation of other parameters see Table 4.3-2.

Addition of the 3 times (on a mg basis) higher dose of piperacillin reduced the renal clearance of flucloxacillin by 46% (from 5.44 to 2.90 L/h) for the low dose and by 63% (from 5.47 to 2.06 L/h) for the high dose (p< 0.01). Nonrenal clearance was reduced by 33% (from 2.66 to 1.77 L/h) for the low and by 35% (from 2.79 to 1.80 L/h) for the high dose (p< 0.01). Figure 4.4-2 shows box-plots for renal and nonrenal clearance of flucloxacillin with and without piperacillin.

Figure 4.4-2   Renal and nonrenal clearance of flucloxacillin with or without piperacillin

Panel A: Renal clearance   **Panel B: Nonrenal clearance**
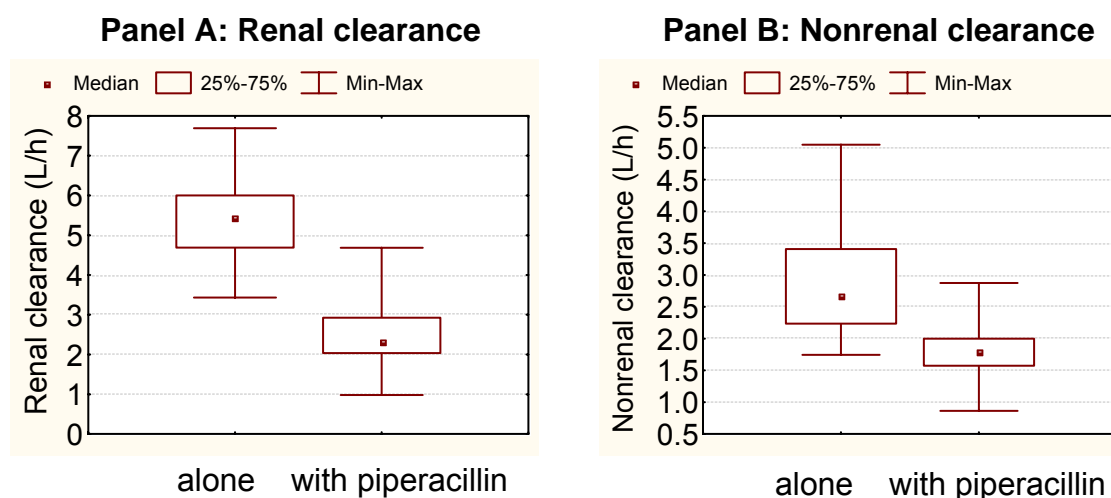
The time (and concentration) dependence of the observed interaction is shown in Figure 4.4-3. Median renal clearance of flucloxacillin in the presence of piperacillin increased from 1.2 L/h at 1h after the infusion to 5.2 L/h at 8h. The inhibition was more pronounced for the high dose regimen than for the low dose. Towards the end of the observation period renal clearances were similar for the interaction treatments and flucloxacillin given alone.

Figure 4.4-3   Median renal clearances of piperacillin and flucloxacillin from non-compartmental analysis

Median renal clearance was calculated for each urine collection interval (see chapter 4.4.2).

Panel A: Flucloxacillin
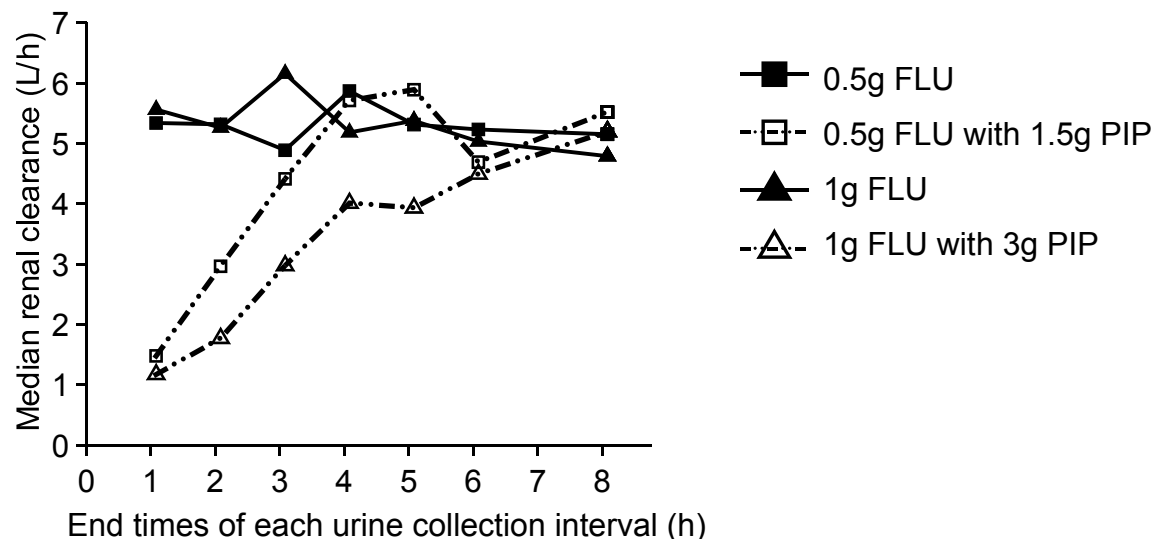
Panel B: Piperacillin
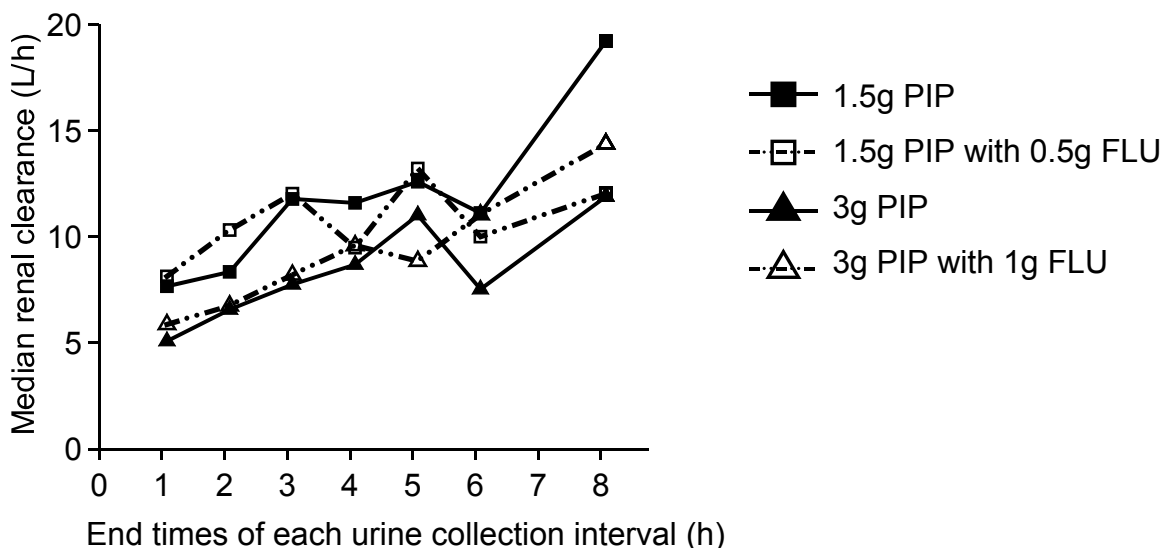
According to NCA, volume of distribution at steady-state and mean residence time were significantly changed by both interaction treatments compared to baseline. Terminal half-life in plasma and fraction excreted unchanged in urine were only significantly affected with the high dose interaction treatment (Table 4.4-2). A more pronounced effect of the

interaction was seen for all PK parameters at the higher dose level compared to the lower dose. Maximum concentrations in plasma were not affected significantly by the interaction.

PK parameters of piperacillin were very similar after the treatments with and without flucloxacillin. No significant differences were seen, except for a decrease in nonrenal clearance from 5.2 to 4.3 L/h (-23%, $p < 0.01$) and an increase from 0.53 to 0.60 (+15%, $p = 0.02$) in the fraction excreted unchanged in urine, when 3g piperacillin was given together with 1g flucloxacillin.

Models: For the plasma and urine concentration time data of both piperacillin and flucloxacillin we chose a three compartment model based on the AIC and visual inspection of the observed and predicted plasma and urine concentration time curves.

The results from the AIC and the visual predictive checks showed that models 1 and 4 (see Table 4.4-1) both had a highly sufficient predictive performance. The visual predictive checks gave virtually identical results for those two models. Model 3 achieved AIC values similar to models 1 and 4 but was probably over-parameterized, and models 2 and 5 were ranked less likely (median AIC at least 30 points higher, see also chapter 2.6.5). The visual predictive checks of model 1 are shown in Figure 4.4-4 for the interaction treatments. The visual predictive checks for the profiles of piperacillin and flucloxacillin alone showed also a highly sufficient predictive performance for model 1.

Figure 4.4-4   Visual predictive check for plasma concentrations and amounts excreted unchanged in urine of flucloxacillin for model 1 (see Table 4.4-1)
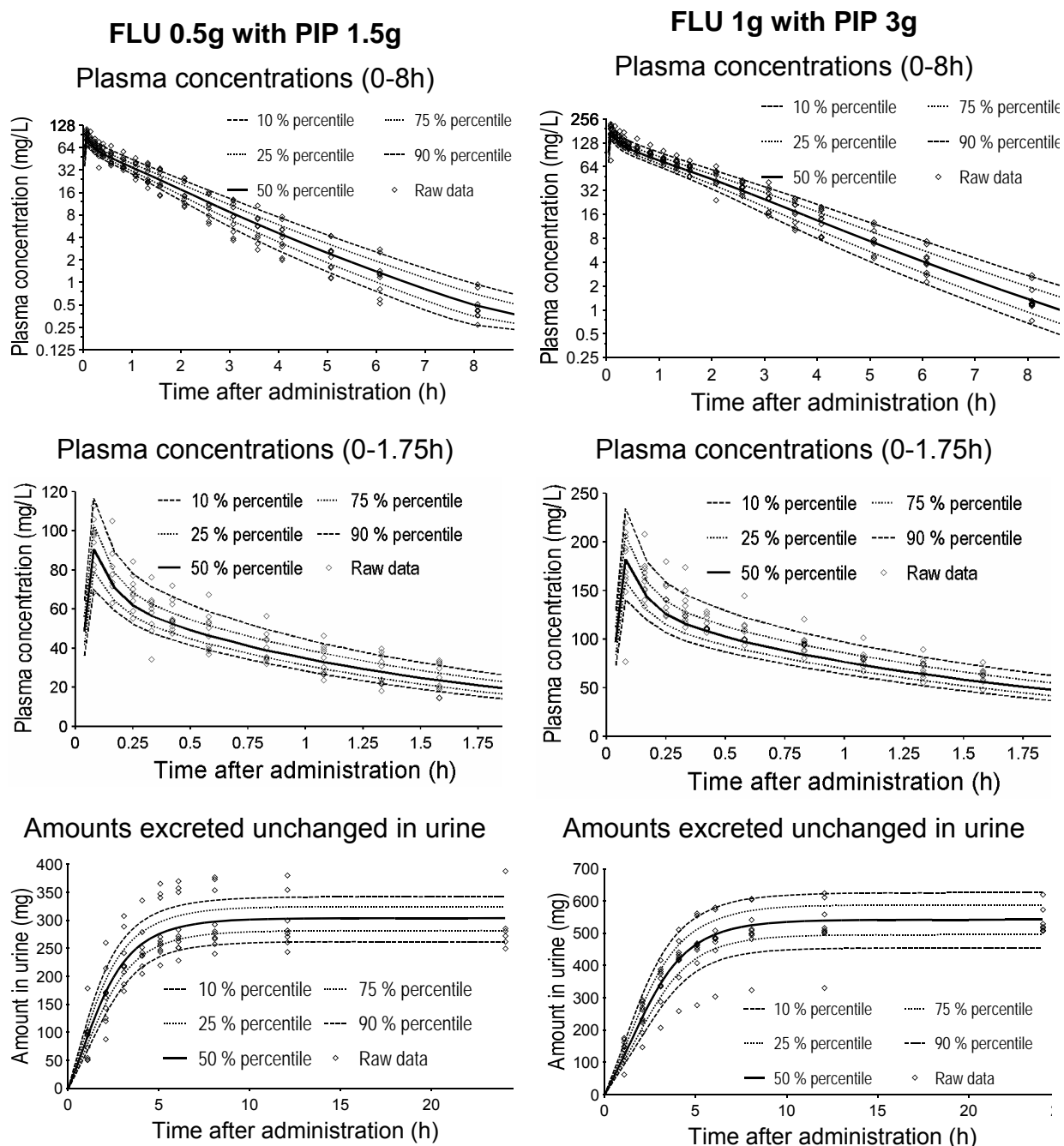
See chapter 2.6.5 and Figure 3.2-2 for explanation of the plots.

Table 4.4-3 lists the median PK parameter estimates of flucloxacillin for model 1. Piperacillin reduced the nonrenal clearance of flucloxacillin

significantly (p < 0.01) by 33% (23%-42%), point estimate (90% confidence interval).

The affinity of piperacillin for the renal transporter was 13.3 times (median) higher than the affinity of flucloxacillin, based on the competitive interaction model. As piperacillin had a higher affinity and similar (about 10% higher) average plasma concentrations than flucloxacillin, piperacillin inhibited the renal elimination of flucloxacillin whereas the effect of flucloxacillin on piperacillin was very small.

Table 4.4-3   PK parameter estimates for flucloxacillin from model 1 (see Table 4.4-1)

Parameter	Unit	Median [range]
$CL_{R,Lin}$[#]	$L\ h^{-1}$	0.432
$K_{mR,FLU}$	$mg\ L^{-1}$	334 [46.1-1406]
$Vmax_{R,FLU}$	$mg\ h^{-1}$	1786 [337-7194]
Kic	$mg\ L^{-1}$	21.7 [8.95-28.3]
$CL_{NR,\ FLU\ without\ P}$	$L\ h^{-1}$	2.86 [1.74-4.66]
$CL_{NR,\ FLU\ with\ P}$	$L\ h^{-1}$	1.76 [1.36-2.52]
$V1_{FLU}$	L	4.45 [3.61-7.41]
$V2_{FLU}$	L	1.99 [0.86-3.51]
$V3_{FLU}$	L	2.30 [1.60-2.92]
$CLic_{shallow,FLU}$	$L\ h^{-1}$	16.3 [2.65-22.5]
$CLic_{deep,FLU}$	$L\ h^{-1}$	1.49 [0.876-2.91]

[#]: Fixed, not estimated.

$CL_{R,Lin}$: First order renal clearance, $K_{mR,FLU}$: Michaelis Menten constant of the mixed order renal elimination, $Vmax_{R,FLU}$: Apparent maximum rate of the mixed order renal elimination, Kic: Competitive inhibition constant, $CL_{NR,FLU}$: Linear nonrenal clearance, $V1_{FLU}$: Volume of distribution of central compartment, $V2_{FLU}$: Volume of distribution of shallow peripheral compartment, $V3_{FLU}$: Volume of distribution of deep peripheral compartment, $CLic_{shallow,FLU}$: Intercompartmental clearance between the central and the shallow peripheral compartment, $CLic_{deep,FLU}$: Intercompartmental clearance between the central and the deep peripheral compartment

4.4.4   Discussion

Concomitant administration of multiple drugs carries the potential for PK drug-drug interactions. This is especially true, when these drugs share the same primary elimination pathway (216). Betalactams are organic anions and excreted by the kidneys by glomerular filtration and active tubular secretion (22, 27). Tubular secretion is a capacity-limited process. As betalactams are similar to some extent in their chemical structure and physicochemical properties, they may compete for the renal tubular secretion when given concomitantly. PK interactions between betalactams, often involving acylureidopenicillins like piperacillin, have been reported. Both azlocillin (170) and mezlocillin (259) reduce the renal and nonrenal clearance of cefotaxime, and mezlocillin also reduces the clearance of oxacillin (19). Piperacillin inhibits the renal clearance of cefazolin and renal and nonrenal clearance of cefoperazone in rabbits (139), as well as the total clearance of moxalactam (latamoxef) (19). In addition to the interactions with other betalactams, azlocillin reduces the renal and nonrenal clearance of ciprofloxacin (20).

These findings show that acylureidopenicillins have a high potential to inhibit the elimination of other betalactams given concomitantly. We used compartmental analysis to study the time course of the PK interaction between piperacillin and flucloxacillin as model drugs at two dose levels and tested various interaction models to explore possible mechanisms and site(s) of the interaction. We had data from ten healthy volunteers in a six-way crossover study. Although this is a small sample size, the design has distinct advantages: In healthy volunteers the between occasion variability (BOV), i.e. the variability in one subject between different study periods, of piperacillin for clearance and volume of distribution at steady-state is small (<15%) (50) and the subjects serve as their own controls (see also chapter 1.5). In our study piperacillin was given without tazobactam. However, as tazobactam has been reported not to affect the PK of piperacillin (283), a possible effect of tazobactam on piperacillin PK is likely to be small.

Our NCA showed, that overall concomitant administration of piperacillin significantly decreased the renal clearance of flucloxacillin from 5.44 to 2.29

L/h (p<0.01) and the nonrenal clearance of flucloxacillin from 2.67 to 1.80 L/h (p<0.01). Renal clearance of flucloxacillin became more similar between the treatments with and without piperacillin towards the end of the observation period when the piperacillin plasma concentrations were low (Figure 4.4-3). For all PK parameters the extent of interaction was larger with the high dose combination of piperacillin and flucloxacillin (Table 4.4-2). Although NCA indicated a significant decrease of volume of distribution at steady-state for flucloxacillin under the influence of piperacillin, we have shown by subsequent simulations that this is probably an artifact from NCA. We simulated two plasma concentration time profiles for flucloxacillin with and without piperacillin as competitive inhibitor of renal tubular secretion. All flucloxacillin PK parameters including volume of distribution were identical between both treatments. However, as for the gemifloxacin study, NCA of the simulated concentrations falsely indicated a decreased volume of distribution at steady-state and during the terminal phase for the interaction treatment. Jungbluth and Jusko showed that a decreased volume of distribution with increasing doses of mezlocillin in rats was an artifact from NCA due to saturable elimination of mezlocillin, as NCA assumes linear disposition (167).

Piperacillin PK parameters were not affected significantly by the low dose interaction treatment (1.5g piperacillin + 0.5g flucloxacillin). For the high dose interaction treatment (3g piperacillin + 1g flucloxacillin) nonrenal clearance of piperacillin was reduced from 5.2 to 4.3 L/h (-23%, p<0.01), and the fraction excreted unchanged in urine increased from 0.53 to 0.60 (+15%, p=0.02), compared to 3g piperacillin alone. As nonrenal clearance only accounted for about 40% of piperacillin elimination, the small decrease in nonrenal clearance did not result in a significant decrease in total body clearance. The increase in piperacillin renal clearance with decreasing plasma concentrations (Figure 4.4-3), was independent of flucloxacillin and may be attributed to saturable elimination of piperacillin (23, 31, 304). Therefore we used a saturable elimination model for piperacillin and did not include an influence of flucloxacillin on piperacillin PK.

We used compartmental modeling and tested several mechanistic models (Table 4.4-1). Models 1, 3 and 4 showed similar values for the AIC,

whereas models 2 and 5 were ranked less likely. Model 5 included a competitive interaction at the nonrenal site and therefore had two more parameters to describe the nonrenal interaction than models with static nonrenal interaction. Probably because of the relatively small extent of the nonrenal interaction, the data did not support this more complicated model with a mechanistic interaction at the renal and nonrenal site. Thus a specific mechanism for the nonrenal interaction could not be identified. Model 3 (mixed interaction) was probably over-parameterized and failed to indicate a significant noncompetitive interaction in addition to its competitive interaction component for 8 of 10 subjects. Therefore, we further considered the competitive (model 1) and the noncompetitive model (model 4) and evaluated their predictive performance. Models 1 and 4 both had excellent predictive performance and virtually identical visual predictive checks. From the physiological and biological point of view a competitive interaction seems the most reasonable one, as it describes the situation that flucloxacillin and piperacillin compete for the same active site of the renal transporter. Therefore, we chose model 1 with competitive renal and static nonrenal interaction as our final model.

Model 1 suggested that the affinity of piperacillin for the renal transporter was 13.3 times (median) higher than the affinity of flucloxacillin. The average plasma concentration of piperacillin from 0-8h was about 10% higher than for flucloxacillin when both were co-administered. Because of the higher affinity to the renal transporter, there was a marked effect of piperacillin on flucloxacillin but not vice versa. The extent of interaction can be quantified by the ratio of flucloxacillin clearance under the influence of piperacillin divided by the flucloxacillin clearance when given alone. A competitive interaction model predicts that this ratio is lower, when both substrates are given at higher doses, i.e. 1g flucloxacillin and 3g piperacillin, compared to lower doses, i.e. 0.5g flucloxacillin and 1.5g piperacillin, although the dose ratio stays constant at 1:3. This and the overall estimates from the compartmental model were in good agreement with the results from NCA.

We observed that concomitant administration of piperacillin decreased renal clearance and to a lesser extent also nonrenal clearance of flucloxacillin.

Betalactams have been reported to be secreted by and also to inhibit various members of the family of organic anion transporters (OAT) in the proximal renal tubules (51, 159, 186). More specifically, Jariyawat et al. (159) tested 25 different antibiotics, among those 17 betalactams including piperacillin and cloxacillin, which is structurally very similar to flucloxacillin. All of the tested betalactams showed competitive inhibition of *p*-aminohippuric acid transport by OAT 1 (159). These findings suggest that the site of the renal interaction of piperacillin and flucloxacillin could be an OAT in the proximal renal tubules. As OATs have been found in various organs of the body, including the liver (219, 272), a competitive interaction process could also be the reason for the decreased nonrenal clearance of flucloxacillin when given with piperacillin. Further studies would be needed to identify exactly which transporter(s) are involved in this interaction.

In conclusion, compartmental modeling identified a competitive inhibition of tubular secretion by piperacillin as the most likely mechanism of the renal interaction. Piperacillin had a 13.3 times higher (median) affinity to the renal transporter than flucloxacillin. The average plasma concentration of piperacillin from 0-8h was about 10% higher than for flucloxacillin when both were co-administered. Therefore piperacillin considerably inhibited the active tubular secretion of flucloxacillin. Overall, piperacillin significantly decreased the renal clearance of flucloxacillin from 5.44 to 2.29 L/h (p<0.01) and the nonrenal clearance of flucloxacillin from 2.67 to 1.80 L/h (p<0.01). The extent of the interaction was larger for the higher doses. The interaction reached clinical significance, since the total clearance decreased from 7.96 to 4.00 L/h (p<0.01) for flucloxacillin. Piperacillin PK was not affected by concomitant flucloxacillin, except for a decrease in the nonrenal clearance from 5.2 to 4.3 L/h (p<0.01) with the high dose interaction treatment compared to piperacillin alone. The inhibition of flucloxacillin clearance leads to a prolonged time of non-protein bound concentrations above the MIC, which may be used to improve effectiveness. As piperacillin has a higher affinity to the renal transporter than flucloxacillin, it is the more likely drug to be used as inhibitor in further studies which are required to show the clinical relevance of this or other PK interactions between betalactams.

4.5   Resume on pharmacokinetic drug-drug interactions and their possible clinical benefits

4.5.1   New insight into the mechanisms of interaction

Although the extent of interaction with probenecid is known for several quinolones, little is known about the mechanism of interaction, site(s) of interaction, and the relative affinity of probenecid and quinolones. We are not aware of any reports where a mechanistic model for the interaction of quinolones and probenecid in humans or animals has been developed.

Competitive inhibition of a saturable renal elimination pathway was the most likely mechanism for the interaction of gemifloxacin, ciprofloxacin and M1 with probenecid, as well as for the interaction between flucloxacillin and piperacillin. This is also physiologically reasonable as all those drugs are actively secreted by the renal tubular cells. As most quinolones are eliminated via tubular secretion, the competitive inhibition of renal tubular secretion by probenecid could also apply to other quinolones. If a mechanism and site of an interaction is identified, predictions can be made about possible interactions with other drugs that share the same elimination pathway.

The affinity of probenecid to the renal transporter was lower than the affinity of gemifloxacin, ciprofloxacin, and ciprofloxacin's metabolite M1. Probenecid reduced the renal clearance of those quinolones because of its much higher concentrations. Therefore concentrations of drug and inhibitor are important for the extent of interaction and by use of a mechanistic model the extent and time course of an interaction can be predicted for all different concentrations. The affinity of piperacillin for the renal transporter was 13 times higher than the affinity of flucloxacillin, therefore piperacillin is more likely to inhibit renal secretion of other drugs that are secreted by the same transporter than flucloxacillin.

Inhibition of nonrenal clearance was seen in all three studies in parallel to the inhibition of renal clearance. However, the extent of interaction at the nonrenal site was smaller than at the renal site. Our models could not identify

a mechanism for the interaction at the nonrenal site. Probably a higher extent of interaction is needed to be able to identify a mechanism for the interaction at the nonrenal site.

The interactions involve inhibition of transporters, but it is not possible to identify these transporter(s) by PK studies in humans alone. Additional data on the transporter itself are required. It might be possible that multiple transporters are involved in this interaction, therefore the estimated values for K_m and Kic might represent pooled values and not apply to one specific transporter. Findings from *in vitro* studies suggest that the site of the studied renal interactions could be organic anion or organic cation transporters. These transporters are located in the proximal renal tubules, but also in the liver (219, 272) and in other parts of the body. Therefore, a competitive interaction process like that at the renal site could also cause the decreased nonrenal clearances. Despite the increasing knowledge on transport proteins, it would be necessary to conduct further studies for an exact identification of the transporter(s) involved in our studied interactions.

4.5.2 Critical importance of modeling the full time course of drug-drug interactions

NCA in combination with ANOVA statistics treats the presence or absence of an inhibitor as a categorical variable, but the concentration of the inhibitor is not included in the analysis. Therefore, NCA does not directly account for the time and concentration dependence of an interaction. Although NCA is an adequate method to explore the extent of the interaction for the dose level used in the study, it cannot predict the extent of interaction for other dosage regimens which might be relevant for clinical practice. It would be very difficult – if at all possible – to draw a conclusion about the influence of an inhibitor on the formation of a metabolite by use of NCA. Furthermore, NCA is also not an adequate method to study a possible influence of an interaction on the volume of distribution of a drug.

As has been seen e.g. with probenecid, the concentration, and not only presence or absence, of an inhibitor is important for the extent and time

course of an interaction. The concentration of an inhibitor changes over time. In our interaction models the concentrations of drug and inhibitor are included to describe the interaction at each time point. The full time course of drug, inhibitor, and metabolite (in the case of ciprofloxacin) in plasma and urine is modeled simultaneously in order to derive the maximum amount of information from the data.

Therefore, compartmental modeling is more powerful than NCA to identify the site(s) of interaction, to propose a mechanism of interaction for each site, to calculate relative affinities of the drugs to the transporter, and to predict the time course of interaction for other dosage regimens via simulations. Probably the most important advantage of a mechanistic interaction model over NCA is the ability of an interaction model to predict the extent and time course of interaction for other dosage regimens. This ability of a mechanistic interaction model can be used in PD simulations to predict the effect of an inhibitor on the probability of successful antiinfective treatment. For PD simulations, generally a full population PK analysis would be preferred to the STS approach. We used the STS approach to construct a population PK model. We could show by visual predictive checks that our constructed population PK models had highly sufficient predictive performance (see Figure 4.2-2 and Figure 4.4-4). Direct estimation of a population PK model e.g. with NONMEM is superior to our STS approach. However investigating the mechanisms of interaction by population PK modeling would not have been feasible because of the tremendously long computation times of those complex interaction models in NONMEM. As computation speed is increasing this disadvantage of population PK modeling might become less important in the future.

4.5.3 Pharmacokinetic interaction and improved pharmacodynamic profile versus increased toxicity

A mechanistic interaction model allows one to predict the extent and time course of an interaction for other dosage regimens. Therefore we used MCS with therapeutic doses of probenecid at steady-state in order to estimate

the increase in the PKPD breakpoint which can be achieved by coadministration of probenecid with gemifloxacin.

For the ratio of the unbound area under the plasma concentration time curve over the MIC, we assumed a PKPD target of fAUC/MIC $\geq$ 30 for near-maximal bactericidal activity. This target was determined for gemifloxacin against *S. pneumoniae* (346). We assumed a protein binding of 65% for gemifloxacin.

The median predicted unbound plasma concentrations as well as the 80% prediction interval are shown in Figure 4.5-1 for gemifloxacin. Figure 4.5-2 shows the simulated unbound peak concentrations and unbound AUCs for gemifloxacin with or without therapeutic doses of probenecid (500 mg twice daily). The probability of target attainment for a variety of MICs is shown in Figure 4.5-3.

Figure 4.5-1   Predicted unbound plasma concentration time curves after an oral dose of 320 mg gemifloxacin once daily at steady-state with or without 500 mg probenecid twice daily

Gemifloxacin without probenecid **Gemifloxacin with probenecid**
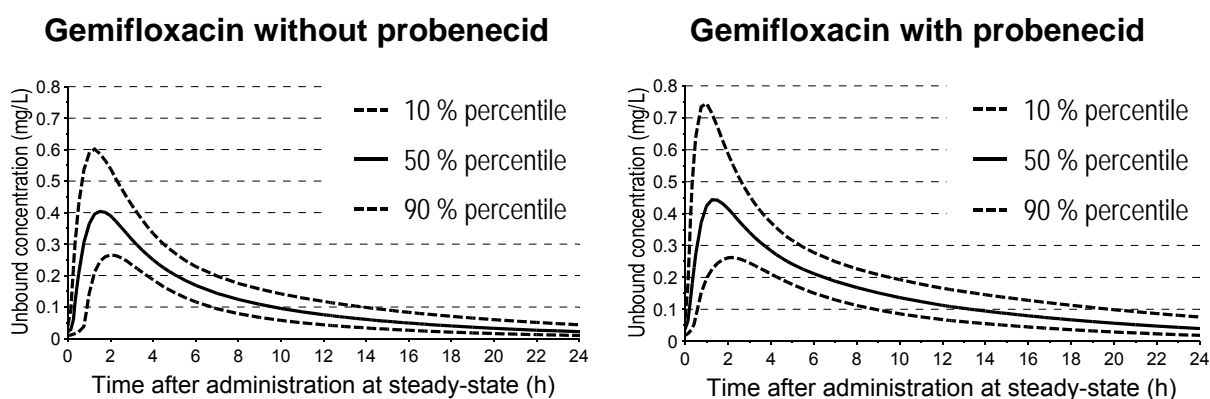
Figure 4.5-2   Unbound AUCs and peak concentrations after an oral dose of 320 mg gemifloxacin (GEM) once daily at steady-state with or without 500 mg probenecid (PRO) twice daily
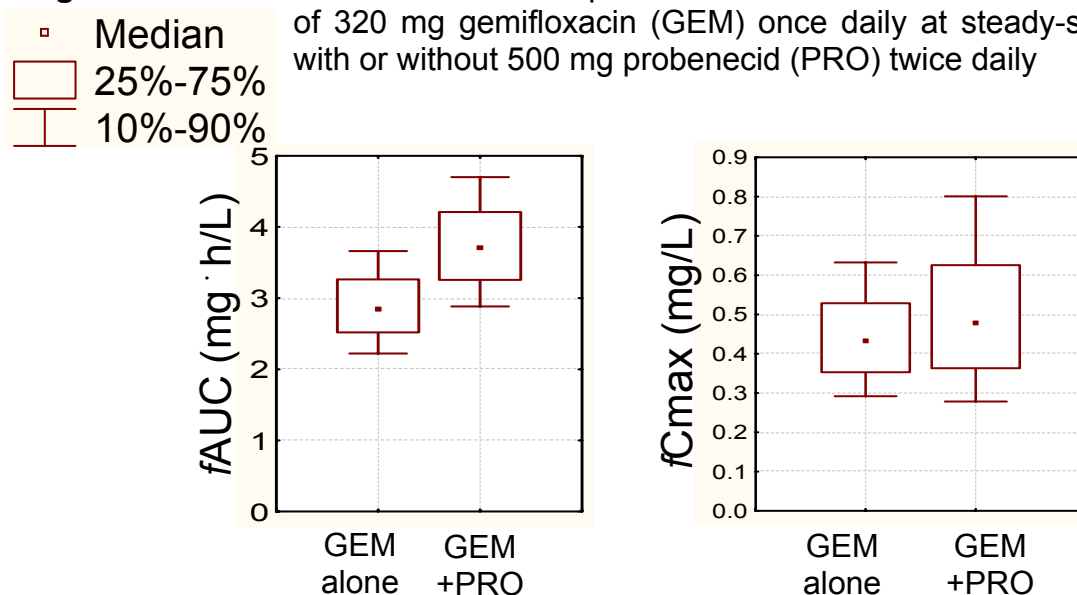
We found that the PKPD breakpoint for the PKPD target $f\text{AUC/MIC} \geq 30$ was increased by 29% from 0.0738 mg/L to 0.0953 mg/L (Figure 4.5-3), when 320 mg oral gemifloxacin once daily were co-administered with 500 mg oral probenecid twice daily as compared to gemifloxacin alone. This increase in the PKPD breakpoint was associated with a 10% increase in median peak concentrations.

Figure 4.5-3   Probability of target attainment for a 10,000 subject MCS for the PKPD target $f\text{AUC/MIC} \geq 30$ after an oral dose of 320 mg gemifloxacin once daily at steady-state with or without 500 mg probenecid twice daily
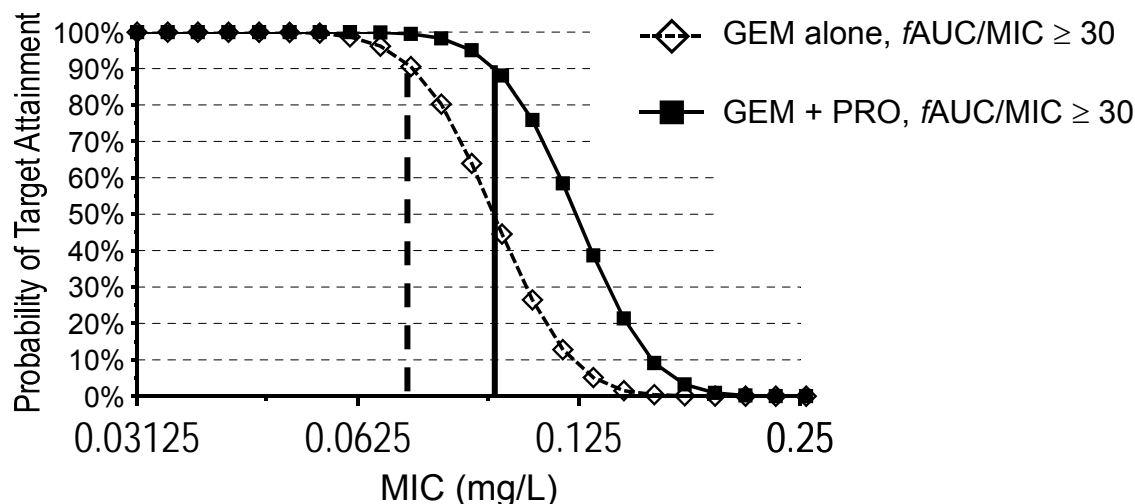
Considering only these results, the interaction with probenecid seems to offer an appealing feature for optimization of the PD profile of gemifloxacin. Coadministration of probenecid allows one to increase the extent of drug exposure (AUC) with a negligible increase in peak concentrations. Peak concentrations of sparfloxacin were shown to correlate well with cardiac repolarization (QT_c interval), whereas there was no correlation with AUC (227).

However, this small increase in the PKPD breakpoint needs to be viewed as opposed to the increased potential for side effects, when both drugs are co-administered. The most common adverse effect of both gemifloxacin and probenecid is rash. Thus, giving both drugs together would probably increase the risk for this side effect. Furthermore, if probenecid needs to be administered twice daily, one looses the advantage of once daily dosing for gemifloxacin. Therefore, the relatively small extent of interaction at clinical doses of probenecid does not counterbalance the increased risk for side effects and the less convenient dosing schedule.

In conclusion, probenecid can be an option to improve the PKPD profile of an antibiotic, as has been practiced with penicillin (323). PKPD modeling is a good method to investigate these interactions and their potential clinical benefit. However other factors, e.g. side effects, that might outweigh the improvements in PD, need to be considered. The increased risk for side effects with gemifloxacin and probenecid overrides the potential clinical benefit in the PKPD breakpoint for this drug combination.

5   Penetration of antibiotics into bone

5.1   Overview of bone penetration studies from literature

5.1.1   Introduction

Despite great advances in antimicrobial chemotherapy, bone infections remain difficult to diagnose and to treat. Chronic osteomyelitis requires prolonged antibiotic treatment in addition to surgical debridement and has a high recurrence rate even many years after the surgery (191). More importantly, treatment failure may cause irreversible damage of the affected bones. Since identification of the causative agent is often difficult, selection of an adequate antimicrobial agent at the beginning of therapy is critical. The overall number of infections has been predicted to increase because of the large increase in reconstructive orthopedic procedures with prosthetic materials. More than 1 million hip replacements are performed each year. It is unlikely that any preventive measure will reduce the rate of infections below 0.5% (192). Also diabetes and vascular insufficiency as predisposing factors for osteomyelitis are becoming more frequent. Consequently, appropriate surgical prophylaxis and antimicrobial therapy are very important.

Rate and extent of penetration of an antimicrobial into bone determine the therapeutic success, as does a high antibacterial activity of the chosen drug against pathogens encountered in bone infections. As bone, excluding bone marrow, is a less vascularised tissue compared e.g. to the lungs or skin, it is particularly important to investigate the penetration of an antimicrobial before starting a clinical trial on the effectiveness of antibacterial treatment in osteomyelitis patients (94, 313). The composition of bone is very different from other tissues, and it is difficult to predict whether agents showing good penetration into other tissues will also achieve high concentrations in bone.

The two macroscopically different types of bone tissue are cortical and cancellous bone. Cortical bone is a compact tissue composed of many Haversian systems (osteons) that consist of concentrically arranged lamellae

(Figure 5.1-1). Cancellous bone consists of trabeculae that form the inner part of the long bones. In general, bone tissue consists of an organic (30 - 35% of total bone mass) and an inorganic (65 - 70%) fraction (66, 134, 232). Organic matter consists mainly of collagen fibrils (ca. 90%), glycoproteins, proteoglycans and extracellular fluid (134), and is arranged in lamellae in cortical bone (Figure 5.1-1). The extracellular fluid in bone is believed to be of similar composition as the interstitial fluid of other tissues (329) and water has been reported to constitute 10% of total bone mass (232). Bone cells (osteoblasts, osteocytes, and osteoclasts) represent only 1-2% of total bone mass and are trapped within the organic matrix (66). The inorganic matrix consists mainly of calcium phosphate as hydroxyapatite crystals that are deposited inside the organic matrix. The inorganic and the organic matrix can only be separated by chemical methods e.g. by destroying organic matter via incubation of bone in peroxide solution (340) or by removing inorganic matter with acids. These methods may be used to determine the fractions of organic and inorganic matrix in a bone specimen.

Figure 5.1-1   Composition of cortical bone
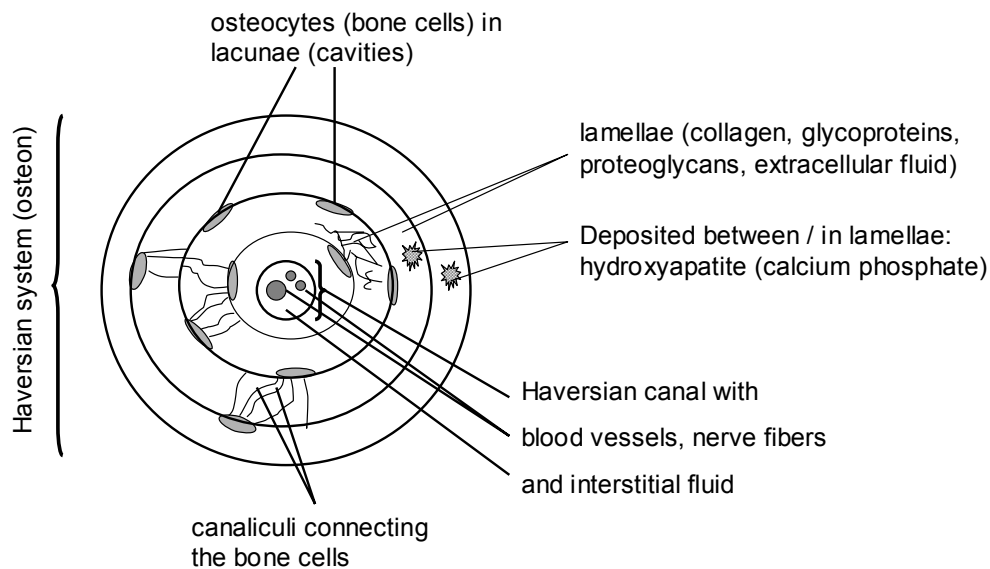
However it does not seem possible to separate a bone sample into e.g. extracellular fluid, collagen fibrils, bone cells, and hydroxyapatite, and to determine drug concentrations in each of those components separately. Therefore, the whole bone specimens are commonly homogenized for drug

analysis with chromatographic methods. Subsequently, total concentrations in bone homogenate are obtained.

Blood vessels are located in Haversian and Volkmann canals that vertically and horizontally traverse the bone matrix. In osteomyelitis, bacteria are believed to spread through these canals and distribute in the interstitial fluid (135). However *S. aureus*, the most frequently encountered pathogen in osteomyelitis, additionally forms biofilms and adheres to bone matrix and implants (192). *S. aureus* has been shown in *in vitro* studies to penetrate into and survive in bone cells i.e. in osteoblasts (154, 161) which may be a reason for relapses in chronic osteomyelitis (192).

Numerous studies have been conducted to determine antibiotic concentrations in bone tissues. However a large variety of methods for sample preparation, drug analysis, data analysis, and reporting of the results has been employed. Therefore, the reported bone concentrations often differ as much between studies with the same agent as between different drugs. To determine bone concentrations reliably and to compare these concentrations between antibiotics, standardization of methods is vital and an accurate and precise determination of total concentrations in bone is the first prerequisite to establish the PKPD profile of antibiotics in bone.

Boselli and Allaouchiche (42) reviewed the results from bone penetration studies published between 1978 and 1998. Therefore the present work summarizes the bone penetration studies before 1998 in brief and addresses the studies between 1998 and end of 2005. This work focuses on the methods of PK studies to assess bone penetration and on the standardization of the drug analysis in bone, PK evaluation, and reporting of the results.

5.1.2   Methods for sample preparation and drug determination

A large variety of techniques has been applied for sample preparation and drug analysis in bone. The collection and preparation of the bone sample at the clinical site and the drug extraction, analysis, and bioanalytical

validation in the laboratory are the most critical procedures of a bone penetration study.

After resection of the bone sample, adhering blood, bone marrow or soft tissues are often removed from the specimen by swabbing, scraping or rinsing it. Bone samples often contain a high amount of blood in excess of the intravascular portion due to intraoperative soaking of the sample with blood. This can result in artificially high bone concentrations due to high antibiotic concentrations in blood, if the excess blood is not removed (340). Separation of cortical and cancellous bone is often reported. As cancellous bone contains a higher proportion of extravascular fluid (135) and a lower percentage of inorganic matter than cortical bone (328), drug disposition may differ between the two types of bone tissue (292). Therefore it is important to specify whether the analyzed specimens consist of cancellous or cortical bone or both.

For drug extraction sometimes the whole specimen (243, 322) or smaller slices (187) are immersed in the extraction solution, or put onto the agar surface for microbiological assay without homogenization (54). In most studies one of various methods of homogenizing the bone specimens is used. Bone samples are sliced into small pieces, or ground to a powder using a mortar and pestle (80, 86, 129, 260, 333). Some authors use sand or aluminum oxide (81, 208, 209) to facilitate the grinding process. Others use liquid nitrogen (45, 181, 183, 306) to freeze the samples. Other devices being used include various mills or mixers (3, 45, 78, 107, 108, 112, 176, 221, 324, 327, 331, 332), hammers (171), hydraulic presses (129) and metal plates (171). Adsorption of the drug to the grinding devices or to sand and aluminum oxide needs to be prospectively validated.

Recently, cryogenic laboratory mills which chill samples in liquid nitrogen (-196°C) and pulverize the bone sample with a magnetically driven impactor have been used for processing of bone samples (26, 111, 213, 218, 244, 254). Chilling in liquid nitrogen embrittles the tissue, so it can be pulverized to a very fine powder. This can be used also for drugs prone to thermal degradation, e.g. some beta-lactams, as considerable heat develops due to the grinding if this process is not cooled. Petitjean et al. (246) compared three grinding procedures for the extraction of rokitamycin from rat

bone. Pulverization of bone samples by a magnetic stirring bar in liquid nitrogen gave a finer powder and a higher recovery during extraction than slicing the bone tissue into small pieces or crushing it with pestle and mortar (246). This would be expected, as creating a larger surface of the bone powder facilitates extraction.

For drug extraction, usually the resulting pieces or powder are immersed in buffer and left to stand (188) or put into a shaker, the latter being more efficient for extraction. It is rarely reported if extraction equilibrium has been reached (3), which could be tested e.g. by analyzing eluate from the same samples after different extraction times. Sufficient drug stability under the chosen extraction conditions is another requirement. The drug must be stable until the extraction equilibrium has been reached. Otherwise drug instability might result in artificially low bone concentrations. Some authors discuss incomplete extraction as a possible reason for low concentrations found in bone. Wittmann et al. (340) report that after 48h of shaking 72 to 75% of the maximum extractable amount of ofloxacin was reached and therefore they repeated the procedure 3 to 5 times with new buffer. Meissner et al. (220) performed 3 elutions over 20h each to obtain a "complete" extraction. In summary, the extraction of drug from bone powder is probably the most critical part of a bone penetration study. Sufficient recovery during extraction, drug instability, and adhesion of drug to bone powder and grinding devices all need to be considered during assay development and prior to starting the clinical study.

Calibration standards and quality control samples are most often prepared in serum, plasma or buffer. Some more recent studies used blank bone samples for preparation of calibration standards (26, 86, 107, 108, 111, 208, 209, 218, 253, 254). Among these studies that used blank bone powder for preparation of calibration and quality control standards, only Djabarouti et al. (86) report the use of an internal standard which they added to the powdered bone sample before drug extraction.

Other studies used an internal standard which was added at various stages of the extraction procedure, but did not report whether the calibration standards were prepared in blank bone samples or reported that they used

serum or buffer for calibration standards. The internal standard has been added to the bone samples either before homogenization (45, 320), or after homogenization but before drug extraction (176, 327), or after drug extraction (156, 171, 215, 331, 332).

Adherence of antibiotics to bone powder has been reported, e.g. by Fong et al. (107, 108), who compared the solution phase concentrations of ciprofloxacin and enoxacin in standards made up only with buffer to those prepared with blank bone powder. Addition of the internal standard to the ground bone powder before addition of the extraction solution would allow to determine an upper limit for the recovery of drug during extraction from bone powder. If the recovery of the internal standard in this experiment is low, the drug concentrations in bone are likely to be biased towards lower concentrations. Raymakers et al. (253, 254) prepared ceftazidime calibration standards in presence or absence of bone powder as external standards. They find a 10% bias toward lower concentrations in the reported concentration secondary to the interaction of ceftazidime with bone powder.

Many of the more recent studies (45, 79, 86, 156, 171, 176, 215, 244, 320, 327, 331, 332) used an internal standard to improve the precision of the measured bone concentrations, whereas many older studies lack an internal standard. Using an internal standard can improve the accuracy and precision of the steps after the extraction procedure. If the extraction procedure has a low precision, uncertainty due to sample preparation and analysis could be decreased by repeating the extraction and sample preparation procedure several times for each bone sample. A low precision of the bone assay can increase the BSV of the individual bone/serum concentration ratios. This will especially be important, if there is only one bone sample per patient.

For determination of concentrations in the extraction fluid, microbiological methods have been frequently used (3-5, 26, 44, 54, 78-81, 88, 111, 112, 126, 127, 132, 179, 188, 207-209, 221, 237, 249, 255, 260, 275, 281, 322, 324, 328, 331-333, 339, 344), especially in the older studies. Gas chromatography with mass spectrometry has been applied for determination of sulbactam (79, 324, 331, 332), fluorescence polarization immunoassay for vancomycin (129, 213, 218, 322), and tobramycin has also been determined

by an immunofluorescence method (333). Recent studies most often used HPLC with UV (86, 108, 156, 171, 176, 183, 196-198, 214, 215, 252-254, 257, 264) or fluorescence (107, 181, 217, 220, 244, 306, 320, 327, 340) detection. Bottcher et al. (45) compared HPLC with fluorescence detection to a microbiological assay for the determination of levofloxacin in several tissues, including bone. They conclude that HPLC was superior to a microbiological assay, although under optimized conditions the microbiological assay might yield comparable results. Most recently, our group used LC-MS/MS for analysis of antibiotics in bone (chapter 5.3.3).

Irrespective of the method chosen, the extraction procedures, the method how and in which step the internal standard was added, and the quality control data recovery, bias, and precision should be reported in detail for bone penetration studies.

5.1.3 Pharmacokinetic / pharmacodynamic methods

In the vast majority of bone penetration studies, PK analysis is done by calculating the concentration ratios between bone and serum. The nature of bone penetration studies (e.g. in joint replacement surgery) often permits only one bone sample per subject. However the concentration ratios between tissue and serum change over time, unless an equilibrium has been reached between the compartments. This phenomenon is known as system hysteresis, and renders interpretation of the concentration ratios based on concentrations from a single time point difficult, because this ratio depends on the sampling time.

More recently, some authors used the naïve averaging approach and NCA (181, 217) to derive AUC ratios between bone and serum. In these studies, patients were divided into several groups and the bone concentrations were averaged at about 5 different time points after dosing. Other authors used naïve pooling and least square estimation to fit the concentration time curves in bone (244, 328, 331, 340). However, both naïve averaging and naïve pooling have been shown to be flawed (138, 157), because these approaches ignore the BSV and are not recommended (268).

As both naïve approaches provide no measures for the BSV, they cannot be used to predict the probability of successful treatment.

Bailer's method has been developed (18, 235, 245, 247, 309) to obtain confidence intervals for the AUC, if only sparse data are available. However, this method does not provide estimates for the BSV. Subsequently, Bailer's method was extended to estimate variances (236), and non-parametric bootstrap resampling techniques (39, 204, 205) have been developed to obtain both confidence intervals and estimates for the BSV based on NCA. Although those bootstrap techniques exist, they are rarely applied, possibly due to a lack of available software as PK modeling tool.

Population PK models for analysis of sparse datasets have been evaluated (41, 341) and applied in toxicokinetic (143) and tissue penetration studies (94). Population PK considers the full time course of penetration and allows one to calculate the extent of penetration by the ratio of AUCs in tissue and serum and its BSV. Population PK is superior to NCA of tissue penetration studies, because population PK can estimate the plasma and the tissue concentration time course simultaneously. Even if only one tissue (bone) sample per patient can be obtained, several blood samples from this patient can help to improve the estimated rate and extent of tissue penetration. It is a strength of the population PK approach that the full time course of serum and bone concentrations is modeled simultaneously. Drusano et al. (94) used stochastic optimal design theory to select sampling times for modeling the penetration of levofloxacin into the prostate by population PK. Such techniques are very valuable in sparse data situations.

For PD analysis, most authors (42) compare the concentrations in bone and the MIC of commonly encountered pathogens in bone infections. However, this approach ignores the time course of bone penetration as well as its BSV. Jehl et al. (160) calculated the time above MIC for amoxicillin, probably by the naïve averaging or naïve pooling approach. They extrapolated the average bone concentration time curve by assuming a short half-life of 1h for amoxicillin. Unlike the naïve averaging and naïve pooling approach, population PK and MCS considers both the average antibiotic penetration to the site of infection as well as its BSV.

MCS can be used to predict the PTA for a specific PKPD target, e.g. $fT_{>MIC} \geq 50\%$ for near-maximal bactericidal activity of penicillins (67, 89) (see also chapter 2.7.1). It is important to note that this target has been determined for plasma concentrations, but has not yet been evaluated for bone concentrations. Furthermore, there is no easily available measure for the binding of antibiotics to proteins and other components in bone. It is likely that the binding of drugs in bone will differ between drugs. Therefore, a PKPD target in bone which is based on total bone concentrations will probably be specific to each drug.

5.1.4   Reporting

Different methods have been used to express bone concentrations. The numerical value for the concentration in bone will differ substantially, if the amount of drug found in bone is related to total bone mass, to organic bone mass, or to interstitial fluid in bone. It is therefore very important to describe in detail, how the reported concentrations have been calculated.

Concentrations in bone are mostly reported as mg/kg total bone mass. Some authors use an average bone density, e.g. 1.9 kg/L for both cortical and cancellous bone (220), or 1.4 kg/L for cancellous and 1.9 kg/L for cortical bone, and report bone concentrations as mg/L (43, 48). Djabarouti et al. (86) report that 1g of bone (cortical or cancellous not specified) displaces 0.66 mL of water, which would be equal to a bone density of 1.5 L/kg. If one assumes a homogenous distribution of drug in bone and if the bone density is higher than 1 kg/L, it is reasonable to compare the converted bone concentrations in mg/L to serum concentrations. However, if bone concentrations are reported in mg/L, the formula how the concentrations were calculated should be described in detail, and the concentrations should be reported additionally in mg/kg total bone mass, as has been done by Boselli et al. (43) and Breilh et al. (48). With a bone density of more than 1 kg/L, concentration ratios (bone / serum) based on mg/L are always higher than those based on mg/kg total bone mass and the numerical values cannot be compared directly.

Some authors determined the organic fraction of bone by using peroxide solution to dissolve it (3, 328, 340) (method not described in detail (339)) and reported the total amount of drug they found in total bone divided by the organic bone mass. The reason given is that the inorganic salts represent no nutrient for bacteria and therefore would not need to be considered in calculating antibiotic concentrations (340).

Furthermore, some authors dried bone samples (e.g. 1 cm³ of bone) over silica gel before weighing. Subsequently, the reported concentrations (in mg/kg) are probably related to dried and not to total bone mass (188). Other authors determined the amount of interstitial fluid as the difference in bone mass before and after freeze drying of the bone sample (221). Subsequently, the amount of drug in total bone was related to the amount of interstitial fluid. The resulting interstitial fluid concentrations in bone were on average about 5 times (range: 2 to 21 times) higher than the concentrations in total bone, because the interstitial fluid comprised only about 20% (median) of total bone mass on average.

The affinity of the antimicrobial towards hydroxyapatite as the main constituent of the inorganic matter needs to be considered at least for some drugs. No adsorption onto hydroxyapatite has been found for ticarcillin, clavulanic acid (3) and other betalactams (339). Those drugs are assumed to distribute only in the interstitial fluid in bone. The quinolones ofloxacin, ciprofloxacin and pefloxacin have also been reported to bind to hydroxyapatite and to be biologically active when re-extracted (340). The divalent cations (e.g. calcium or magnesium) of the inorganic matrix are possible centers for chelate complexes with quinolones. Fosfomycin has been shown to bind to hydroxyapatite and antibacterial activity was still shown by hydroxyapatite incubated in fosfomycin solution after 3 to 6 times of washing with normal saline for 5min each time. The released fosfomycin has been shown to have antimicrobial activity afterwards (24).

If one assumes that only unbound drug is microbiologically active (89), relating the total concentration of antibiotics that bind to hydroxyapatite (e.g. quinolones, fosfomycin or imipenem) to the organic bone mass or to the

amount of interstitial fluid (221) might overestimate the unbound bone concentrations.

Some authors measure the hemoglobin concentration in the eluate from the bone sample to quantify the total amount of blood in the bone sample. The methods applied comprise HPLC (253), colorimetric assays (188, 255, 264), spectrophotometry (86, 107), a benzidine-superoxide method (260), or determination of methemoglobin after oxidation (78). Irrespective of the method used, the assay should be reported in detail. The formula for the amount of drug in bone arising from contamination with an excess of blood should be reported, e.g. if a red blood cell / plasma partition coefficient has been used as reported by On et al. (244).

A so-called dextran method has also been used and is reported to yield relatively comparable results to measuring hemoglobin for cortical, but not for cancellous bone (249). As high molecular weight dextran does not leave the blood vessels into the tissues, blood content of tissues has been determined by quantification of dextran in tissue samples (249). The blood content of the bone samples and plasma concentration of the drug is then used to calculate the amount of drug in the blood of this bone sample and this amount is subtracted from the amount determined in the bone sample. The rationale for this correction procedure is that an excessive amount of blood might be present in the bone sample after the surgery due to intra-operative soaking (340). Contamination of bone samples with blood probably has the greatest impact on the results for bone concentrations of drugs whose concentrations in bone are much lower than in serum, e.g. many betalactams.

We propose that the concentrations in total bone (unit: mg/kg total bone mass) should always be reported at least in parallel, since this helps to compare the results from different authors and between different drug groups. If concentrations e.g. in the organic bone mass or in the interstitial bone fluid are calculated additionally, the method how these concentrations were calculated should be described in detail.

5.1.5   Patient groups and study design

Most studies are conducted in patients undergoing joint replacement surgery and antibiotic concentrations are determined in non-infected bone. The majority of these studies are in hip replacement patients and some in patients undergoing knee replacement. In knee replacement, a tourniquet is applied to the leg to be operated on. The tourniquet decreases blood circulation to the site of surgery (78, 184, 252) and therefore may affect the rate of bone penetration and maybe also its extent. Usually the antibiotic is administered about 1 to 2.5h before inflation of the tourniquet (78, 184, 252).

A small number of studies investigated antibiotic penetration in osteomyelitis patients or patients (225, 253, 254) with impaired peripheral circulation. In osteomyelitis, blood flow into bone may be increased because of reactive hyperemia in the infected area. However presence of pus and ischemic regions (sequester) may decrease blood circulation (155). Bacteria that persist in sequesters are not easily accessible by antibiotics and are probably the source of relapses in chronic osteomyelitis. Few studies have been conducted in patients with osteomyelitis (172, 183, 221) or in parallel in both patients with and without osteomyelitis (108, 129, 260). There is no clear trend in literature, if concentrations in infected bone are higher, lower or comparable to those in non-infected bone, since the data are sparse.

Fong et al. (107) conducted a study in both patients with or without osteomyelitis, and found 30-100% higher ciprofloxacin concentrations in infected bone samples than in non-infected bone samples, but the difference was not statistically significant because of the small number of patients. Wilson and Mader (334) found about 1.8 times higher vancomycin concentrations in bone from rats with osteomyelitis than in non-infected rats. Studies using samples from intact bone e.g. in hip replacement patients allow one to better compare the obtained concentrations between studies and between agents, whereas concentrations in osteomyelitic bone might depend on the presence of e.g. hyperemia or sequesters (155). Still one has to note that the distribution of drugs may differ between infected and non-infected

bone tissue and the penetration into infected bone needs to be studied in more detail.

The timing of the tissue and blood sample is very important in tissue penetration studies which allow only one tissue sample per patient. Since the introduction of optimal design to PK studies (72, 73), great advances have been made and this method has been extended to derive stochastic optimal designs for estimation of population PK models (94-97, 128, 130, 238, 256, 300, 305, 325). An optimal design which accounts also for the BSV in PK parameters allows one to estimate the population PK parameters (e.g. of a bone penetration model) more precisely and permits to study a lower number of patients. Therefore, stochastic optimal design techniques are very appealing for bone penetration studies and are warranted also for ethical reasons (see also chapters 5.4.3 and 5.4.4).

5.1.6   Limitations

When analyzing concentrations from bone specimens, one needs to consider that the resulting concentrations are homogenate concentrations that would be the unbound concentration in bone, if the antibiotic distributed uniformly throughout the bone tissue and if the antibiotic was not bound to any bone component. However, only free drug is microbiologically active (89) and there is no easily available measure of free concentrations in bone. Also the unbound fraction of a drug in bone could be different from the one in plasma. As bone consists of many different materials, most notably inorganic matter and organic tissue, neither antibiotics nor pathogens are expected to distribute uniformly into these different compartments. This should be noted if the total concentrations are compared to MICs. While antibiotics most likely do not distribute into inorganic crystals in the bone, they may be bound on the surface of the inorganic matrix. Exclusion from the volume of the inorganic bone material increases the unbound antibiotic concentration, whereas adsorption on the surface decreases the unbound antibiotic concentration. It is currently unknown which of those two effects is more important for antibiotics. Quinolones (340) and fosfomycin (24) have been shown to adsorb onto

hydroxyapatite, whereas it has been suggested for beta-lactams (3, 339) that they distribute in extracellular fluid spaces and are not bound to the inorganic matter in bone. Lunke et al. (202) report that the volume of distribution of cefamandole was similar to the sum of the volumes of plasma space and interstitial fluid in canine bone.

The site of the pathogens in bone is also not well known. Many studies have been conducted which show that *S. aureus* is able to enter and survive in bone cells (osteoblasts) (154, 161). *S. aureus* can also adhere to bone matrix by expressing receptors for components of the bone matrix, e.g. collagen (6). However, if total concentrations in bone homogenate are reliably determined, they might be more predictive of therapeutic success than serum concentrations. This will have to be evaluated in future clinical studies. Development of analytical techniques to bring more insight into unbound drug concentrations in bone is warranted.

5.1.7   PKPD for bone penetration studies & future perspectives

Although PK studies on bone penetration can provide valuable information on the rate and extent of bone penetration, they cannot replace large clinical effectiveness trials. However, it is important to investigate bone penetration of an antimicrobial before starting a clinical trial, as in bone infections relapses frequently occur and follow-up periods of at least one year are needed to determine the clinical outcome.

If the time course of the bone concentration profile has been determined and the treatment outcome e.g. for osteomyelitis patients has been evaluated, the most appropriate PKPD target in bone for the studied drug can be derived. This PKPD target links the drug exposure in bone to the microbiological or clinical outcome of the patients. After identification of the most appropriate measure of drug exposure (e.g. area under the curve in bone, peak concentration in bone, or time of total bone concentration above the MIC) and its associated target, optimal dosage regimens for treatment of patients with bone infections can be derived. Clinical evaluation of those

optimal dosage regimens would be the ultimate goal to optimize the treatment of patients with bone infections for a given drug.

5.1.8   New analytical techniques

Studies using microdialysis have been conducted for several tissues (164, 347). Stolle et al. studied gentamicin concentrations in cortical (294) and cancellous (293) bone of pigs, both by microdialysis and analysis of bone specimens. They find similar AUCs in bone by use of microdialysis compared to conventional analysis of resected bone specimens. However, they did not homogenize their bone samples and used a microbiological assay for drug determination. Recently, Stolle et al. (295) also used microdialysis for determination of unbound linezolid bone concentrations in pigs. Microdialysis seems to be an appealing technique to determine unbound drug concentrations in interstitial fluid of bone.

Radiolabeled drug molecules have been used to investigate concentrations of antibiotics in humans and in animal models of infection. Fischman et al. studied the PK of [^{18}F] trovafloxacin (103) and [^{18}F] fleroxacin (104) in bone of healthy volunteers by positron emission tomography (103). This method yields total concentrations of drug per bone mass and does not differentiate between intra- and extracellular drug. It allows multiple measurements in the same subjects at different time points and may therefore provide valuable information on the time course of total bone concentrations. Cremieux et al. (70) investigated autoradiographic diffusion patterns of [^{14}C] sparfloxacin in experimental *S. aureus* joint prosthesis infection in rabbits.

5.1.9   Antibiotic concentrations in bone

If not indicated otherwise, the bone concentrations in the following sections refer to concentrations in total bone homogenate (unit: mg/kg total bone mass). If no value of bone density is given for bone concentrations reported in mg/L, the authors of the respective studies did not specify a value for bone density. Possibly they assumed a density of 1 kg/L for bone, and

then their results could be directly compared to other studies with values given in mg/kg total bone mass. Times of sample collection are times after the start of the infusion, if this could be derived from the publications. The doses were given intravenously if not indicated otherwise. Concentration ratios in Figure 5.1-2 and Table 5.1-1 to Table 5.1-5 have been calculated as concentration in bone (mg/kg) / concentration in serum or plasma (mg/L). A bone density of 1 kg/L was assumed, if not otherwise reported by the authors of the respective publications. Each concentration ratio reported in Table 5.1-2 to Table 5.1-5 was based on at least 5 samples. Bone/serum or bone/plasma concentration ratios from literature for the different groups of antibiotics are shown in Figure 5.1-1.

Figure 5.1-2   Bone / serum or bone / plasma concentration ratios for the different groups of antibiotics
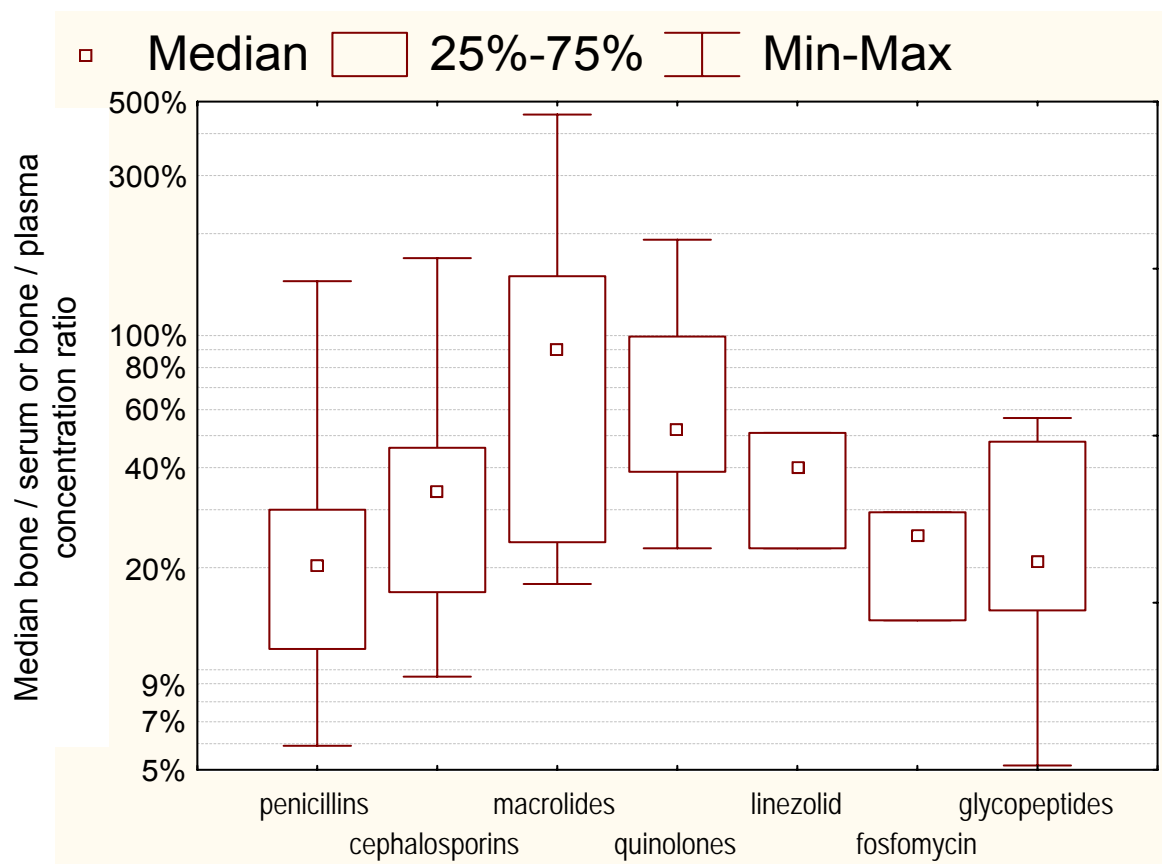
5.1.9.1   Quinolones

Fluoroquinolones are established in the treatment of osteomyelitis (193). In addition to their high concentrations in bone, their ability to penetrate into cells may be advantageous in bone infections, as *S. aureus* has been shown in *in vitro* studies to penetrate into and survive in bone cells (154, 161). Binding to calcium in the inorganic bone matrix might be a reason for the high total bone concentrations of quinolones compared to other antibiotics. Numerous studies have been conducted to estimate quinolone concentrations in bone (see Table 5.1-1).

Table 5.1-1   Bone penetration of quinolones

Antibiotic	Range of time after last dose	Range of average bone / serum or bone / plasma concentration ratios*	Method
Ofloxacin	0.5 - 12h	0.09 - 1.04[a]	HPLC (220, 306, 307), bioassay (101)
Levofloxacin	0.7 - 2h	0.36 - 1.0	HPLC (257, 320)
Ciprofloxacin	1 - 13h	0.27 - 1.2	HPLC (107, 189, 217)
Ciprofloxacin (ischemic bone)	1h	0.16 - 0.31	HPLC (175)
Ciprofloxacin (osteomyelitis)	2 - 4.5h	0.42	HPLC (107)
Fleroxacin	2 - 24h	0.26 - 1.8	HPLC (250, 327), bioassay (225)
Fleroxacin (ischemic bone)	2h	0.28	bioassay (225)

[a]:   Wittmann et al. (340) report concentration ratios of 0.17 to 0.48 related to organic bone mass only. Assuming 35% for the organic fraction, ratios were 0.06 to 0.17 for total bone mass.

*:   Each concentration ratio was based on at least 4 samples.

The average concentration ratios bone / serum reported for ciprofloxacin, ofloxacin and levofloxacin are most often between about 0.3 and 1. Concentration ratios tend to be higher at the end of the observation period

when plasma levels are lower. This would suggest a slow redistribution of drug from bone to blood.

Two recent studies with levofloxacin (257, 320) have been conducted. Rimmelé et al. (257) report average $\pm$ SD bone / plasma ratios of 1.0 $\pm$ 0.4 for cortical and 0.5 $\pm$ 0.1 for cancellous bone in 12 elderly patients undergoing hip replacement 40min to 2.0h after the infusion. Von Baum et al. (320) collected 6 cortical and 14 cancellous bone samples 1 to 2h after infusion of levofloxacin. The average concentration ratios bone / serum were about 0.36 for cortical and 0.85 for cancellous bone. Therefore, bone / serum concentration ratios were comparable in those two studies. However one study showed concentrations in cortical bone being twice as high as in cancellous bone (257) and the other study showed concentrations in cancellous bone being twice as high as in cortical bone (320).

For ciprofloxacin, not only concentration ratios but also an AUC ratio has been reported based on the naïve averaging approach. Massias et al. (217) report an AUC ratio between cortical bone and serum of 0.63 after oral doses of 500 mg twice daily at steady state in 21 patients. The AUCs were calculated by the trapezoidal method based on data from 5 different time points. Concentrations in bone were corrected for blood content. More recently, Leone et al. (189) determined concentrations in 14 patients undergoing brain tumor excision. Ciprofloxacin was infused 30min before skin incision and the average $\pm$ SD concentrations ratios bone / serum were 0.44 $\pm$ 0.29 at opening of the skull bone and 0.97 $\pm$ 1.57 at closure. These results support good average penetration of ciprofloxacin into bone, although there is a large between patient variability.

For fleroxacin an average bone / plasma concentration ratio of 1.2 was reported 2h to 24h after an oral dose of 400 mg (250, 327). Recently, Miglioli et al. (225) studied fleroxacin concentrations in 13 patients undergoing metatarsal amputation due to arterial occlusive disease about 2h after the start of a 20min infusion of 400 mg fleroxacin. Average serum concentrations were very similar to those reported previously (250, 327), but average bone /

serum concentration ratios were lower: 0.26 in non-ischemic and 0.28 in ischemic bone tissues.

5.1.9.2   Macrolides

Studies on macrolide concentrations in bone have been performed rarely and mostly before 1990, using microbiological assays. A wide range of average concentration ratios between bone and plasma has been reported for macrolides (Table 5.1-2).

Table 5.1-2   Bone penetration of macrolides, telithromycin, clindamycin, rifampicin and linezolid

Antibiotic	Range of time after last dose	Range of average bone / serum or bone / plasma concentration ratios	Method
Erythromycin	0.25 - 2h	0.18 - 0.28[a]	Bioassay (54, 281)
Roxithromycin	3 - 24h	0.4 - 1.2	Bioassay (81)
Azithromycin	12h - 6.5 days	2.5 - 6.3	Bioassay (208, 209)
Telithromycin	3.3 - 24h	1.5 - 2.6	HPLC (181)
Clindamycin	1 -1.5	0.21 - 0.40[b]	Bioassay (54, 239)
Rifampicin	2 - 12h	0.20 - 0.46[c,d]	Bioassay (62, 260)
Rifampicin (osteomyelitis)	3.5 - 4.5h	0.57	Bioassay (260)
Linezolid	0.5 - 1.5h	0.40 - 0.51	HPLC (198, 252)
Linezolid (osteomyelitis)	1h	0.23	HPLC (183)

[a]:   Detectable concentrations only in 3 of 7 cortical bone samples, whereas erythromycin was detected in all 8 cancellous bone samples (281).

[b]:   Ratios of 0.45 (75) and 0.98 (42) were reported in reviews.

[c]:   Three (3) of 18 samples were not detectable.

[d]:   A ratio of 0.17 was reported in a review (42).

Erythromycin has been recommended for treatment of streptococcal osteomyelitis (192). Low and variable concentrations in bone and concentration ratios of about 0.2 have been reported for erythromycin (54,

281) in the 1970s. In one study, concentrations in cortical bone could only be detected in 3 of the 7 tested samples (281), however recovery from cortical bone was only 19 to 50%. Therefore, it is difficult to interpret the bone penetration of erythromycin. In contrast, higher concentration ratios (bone/plasma or bone/serum) of 0.4 to 1.2 have been reported for roxithromycin (81) and flurithromycin (26). Those ratios changed over time and the results were only presented in figures.

More recently, Malizia et al. performed two studies (208, 209) with very similar results on the concentration of azithromycin in alveolar bone in 24 and 28 patients undergoing surgery for third-molar removal after administration of 500 mg once daily for three days. In the more recent study, 12h after the last dose, average $\pm$ SD concentrations were 1.61 ± 0.22 mg/kg in bone and 0.37 ± 0.05 mg/L in plasma, therefore concentrations in bone were on average about 4.4 times as high as in plasma. Concentrations ratios at the other time points were similar to those reported after 12h. Both studies report very similar results and also the BSV was low in both studies. The authors used a microbiological assay for drug analysis and prepared their calibration standards in blank alveolar bone. In summary, macrolides seem to be a very heterogeneous group concerning their PK in bone, with low penetration into bone reported for erythromycin and very high bone penetration of azithromycin as shown in Table 5.1-2.

5.1.9.3   Telithromycin

Recently, Kuehnel et al. (181) studied the penetration of telithromycin into ethmoid bone in 29 patients undergoing sinus surgery after a single oral dose. Patients were divided into groups based on sampling times at 3, 6, 9, 15, and 24h. Drug concentrations were determined by a HPLC assay with fluorescence detection after pulverization of bone under liquid nitrogen with mortar and pestle. In addition to concentration ratios (Table 5.1-2), the AUC was calculated by naïve averaging and the trapezoidal method. The average AUC was 4230 mg·h/L in plasma and 6730 mg·h/L in bone, which results in a

high average AUC ratio bone / plasma of about 1.6. However, the authors did not report, which bone density they used for conversion of bone concentrations from mg/kg to mg/L.

5.1.9.4   Clindamycin

Clindamycin is recommended for long-term oral therapy in bone infections with susceptible pathogens (192) and is often cited as an antibiotic with very good bone penetration (75, 192). Bone penetration studies have mostly been conducted in the 1970s. Average bone / serum concentration ratios of 0.21 (54) and 0.29 (42, 87) have been reported 1.5 to 2h after 300 mg clindamycin given orally or intravenously. Two other studies find average bone / serum concentration ratios of 0.45 (75, 265) and 0.40 (SD 0.30) (239) (Table 5.1-2). However Boselli et al. (42) cite a more recent study with concentration ratios between infected bone and serum of 0.98 after an intravenous dose of 70 mg/kg. Mueller et al. (230) investigated concentrations in bone from 13 patients undergoing oral or maxillofacial surgery after 600 mg clindamycin as short infusion. Concentrations in bone between 0.5h and 8h after the infusion ranged from about 0.2 mg/L to 3.4 mg/L. Average plasma levels decreased from 12.8 mg/L immediately after the infusion to 1.4 mg/L after 8h.

These different results for the bone / plasma concentration ratio of clindamycin could be due to different analytical techniques applied or could have been caused by active metabolites of clindamycin measured in bioassay (75). Although it is difficult to draw a final conclusion, the average reported bone / plasma concentration ratio of clindamycin ranges from 0.21 to 0.98.

5.1.9.5   Rifampicin

Rifampicin is used in combination with quinolones or beta-lactams for staphylococcal bone infections (75, 192). Average bone / serum concentration ratios of about 0.4 in cancellous bone and of 0.2 in cortical bone 3h after a dose of 600 mg have been reported (62) (Table 5.1-2). Bone / serum

concentration ratios of 0.17 to 0.41 for cancellous and of 0.20 and below for cortical bone were found in two other studies (42). Roth et al. (260) administered a bolus dose of 300 mg followed by a 1h infusion of 300 mg rifampicin and used a microbiological assay. The average bone / serum concentration ratios were 0.46 (range: from below quantification limit up to 1.15) at 2 to 5h after the bolus dose in non-infected bone and 0.57 (range 0.15 to 0.89) at 3.5 to 4.5h in infected bone. These studies were performed in the 1970 or 1980s and it should be noted that there was a substantial BSV.

5.1.9.6   Linezolid

Linezolid is a relatively new agent for treatment of MRSA infections and clinical experience in osteomyelitis is limited (192). Kutscha-Lissberg et al. (183) studied the concentrations in infected cancellous bone of 11 patients with implant associated infections after a 30min infusion of 600 mg linezolid. Average ± SD concentrations were 3.9 ± 2.0 mg/L in bone and 17.1 ± 5.1 mg/L in plasma. This results in an average bone / plasma ratio of about 0.23 (Table 5.1-2).

Lovering et al. (198) administered 600 mg linezolid as 20min infusion to 12 patients undergoing hip replacement. The average (95% confidence interval) serum concentrations dropped from 19.2 (15.5 - 22.8) mg/L at 30min after start of the infusion to 14.3 (11.3 - 17.2) mg/L after 50min and bone concentrations were 9.1 (7.7 - 10.6) mg/L after 30min and 6.3 (3.9 - 8.6) mg/L after 50 min. Those data suggest a rapid equilibration between serum and bone. The concentration ratios bone / serum were 0.51 (0.43 - 0.75), average (95% confidence interval) between 30 and 50min post start of infusion. The BSV of those bone / plasma concentration ratios was low compared to the results of older studies with other antibiotics.

Rana et al. (252) studied ten elderly patients undergoing knee arthroplasty who were given 600 mg linezolid orally q12h for 48h before surgery and 600 mg intravenously 1h before induction of anesthesia. Average ± SD concentrations 90min after the infusion were 8.49 ± 3.92 mg/kg in bone

and 23 ± 6.5 mg/L in serum. The concentration ratio bone / serum was 0.40 ± 0.24. All of these three studies (183, 198, 252) used HPLC with UV detection to determine drug concentrations and report the reproducibility of the assay. Recoveries of 95-110% from spiked bone samples (and other tissues) were reported (183, 198). Results from these three studies (183, 198, 252) suggest a lower penetration of linezolid into infected than into noninfected bone, that could be due to an inflammation related decrease in blood supply to the infected bone (183). Kutscha-Lissberg et al. (183) also considered a possible bias secondary to sample preparation.

5.1.9.7   Glycopeptides

Vancomycin and teicoplanin are recommended for the treatment of MRSA osteomyelitis (192). Widely varying average concentration ratios between bone and serum have been reported for both glycopeptides (Table 5.1-3). For vancomycin, average bone / serum concentration ratios of about 0.5 - 0.6 (218) and 0.3 - 0.6 (213) have been reported for sternum. In hip replacement patients average ± SD concentration ratios of 0.07 ± 0.07 were reported in cortical and 0.132 ± 0.24 in cancellous bone (129). Only 3 of 6 bone samples from osteomyelitis patients had concentrations above the quantification limit (129). These data show a substantial BSV of the bone/serum concentration ratios.

Table 5.1-3   Bone penetration of glycopeptides

Antibiotic	Range of time after last dose	Range of average bone / serum or bone / plasma concentration ratios	Method
Vancomycin	0.7 - 6h	0.05 - 0.67	HPLC (176, 218), FPIA (129, 213), or bioassay (322)
Vancomycin (osteomyelitis)	1 - 7h	0.21 - 0.38 [a]	FPIA (129)
Teicoplanin	0.5 - 3.2h	0.15 - 0.85	Bioassay (78, 237, 333)

[a]:   Concentrations not detectable in 3 of 6 samples, lower limit of detection not reported.

More recently two studies investigated concentrations in sternum of patients undergoing coronary artery bypass surgery. Vuorisalo et al. (322) report that the individual concentration ratios between bone and serum ranged from 0.02 to 0.14 in ten patients. The average concentration ratios were about 0.05 and average concentrations in sternum were about 1.0 mg/L at about 42min after start of the infusion and 1.3 mg/L at about 254min after start of the infusion.

Kitzes-Cohen et al. (176) found vancomycin concentrations in sternum of 15 patients between 8.2 and 10.9 mg/kg at 2 to 4.5h after start of the infusion. Average bone / serum concentration ratios of 0.30 to 0.60 were reported, with the ratio increasing with time. Thus, Kitzes-Cohen et al. found 8-10 times higher concentrations in sternum and much higher bone / serum concentration ratios than Vuorisalo et al., although both administered a similar dose. Vuorisalo et al. used fluorescence polarization immunoassay, did not homogenize the bone samples before extraction, and started to collect bone samples during the infusion of vancomycin, whereas Kitzes-Cohen et al. used HPLC and extraction of homogenized bone samples. Data from two previous studies (213, 218) are in agreement with those higher ratios from Kitzes-Cohen et al. (176).

For teicoplanin, the average bone / serum concentration ratio increased from about 0.15 at about 45min to 0.30 at about 80min after an intravenous dose of 10 mg/kg (237) in one study, and was 0.20 (78) at about 3h after a 5min infusion of 800 mg in another study. A higher value for the median bone / serum concentration ratio of 0.65 was found at about 30min to 3h after a 400 mg iv injection (average ratio at 3h about 0.85) (333). Recently, Lazzarini et al. (184) performed a study with 800 mg teicoplanin administered as 10min infusion to five patients with total knee replacement. Serum levels were not determined. Average teicoplanin concentrations in bone were reported between 1.72 and 2.36 mg/L at 3h to about 5h after start of the infusion. Assuming that Lazzarini et al. used a density of 1 kg/L for bone, their results are similar to the concentrations in bone reported by de Lalla et al. (78) about 3h after the infusion. These studies with teicoplanin (78, 237, 333) used

microbiological assays. In a study using a cryogenic mill and HPLC with UV detection, teicoplanin could only be detected in sternal bone of 3 out of 23 patients (limit of quantification / detection not reported) (214), despite average concentrations of 9 to 32 mg/L in serum and high concentrations in other cardiac tissues.

5.1.9.8   Penicillins and beta-lactamase inhibitors

Ampicillin in combination with sulbactam or amoxicillin with clavulanic acid are used in mixed (aerobic and anaerobic pathogens) bone infections (191, 192). An overview of the expected bone / serum concentration ratios for penicillins is shown in Table 5.1-4.

Table 5.1-4   Bone penetration of penicillins

Antibiotic / beta-lactamase inhibitor	Range of time after last dose	Range of average bone / serum or bone / plasma concentration ratios	Method
Amoxicillin	0.5 - 8h	0.03 - 0.44	HPLC (160), bioassay (132, 328)
Clavulanic acid	0.5 - 6h	0.01 - 0.09[a]	Bioassay (132, 328)
Ampicillin	0.25 - 4h	0.11 - 0.71	Bioassay (79, 324, 331)
Sulbactam	0.25 - 4h	0.17 - 0.71	Gas chromatography (79, 324, 331)
Piperacillin	1 - 1.5h	0.18 - 0.3	HPLC (44, 156)
Tazobactam	1 - 1.5h	0.22 - 0.3	HPLC (44, 156)
Flucloxacillin	0.3 - 3h	0.12 - 1.2[b]	HPLC (333), bioassay (312), method not reported (178)

[a]:   Other authors find substantially higher values.

[b]:   A ratio of 0.16 was reported in a review (180).

For ampicillin in combination with sulbactam average bone / serum concentration ratios of 0.11 to 0.20 were found 15min to 1h after the dose. For sulbactam average ratios were between 0.17 and 0.58 and were therefore higher than the values for ampicillin in both studies (324, 331).

More recently, Dehne et al. (79) found a higher penetration of both drugs. Average bone / serum concentration ratios of ampicillin were about 0.44, 0.52, 0.56 and 0.71 after 1, 2, 3, and 4h, respectively. The respective ratios for sulbactam were similar to those for ampicillin: 0.58, 0.62, 0.50, and 0.71. The high ratios compared to previous studies (324, 331), probably arise from the lower serum concentrations of ampicillin and sulbactam reported by Dehne et al. In their study, Dehne et al. performed intra-operative blood saving with washing of the drained blood before reinfusion into the patient. The authors mention that this technique may increase drug elimination (79). This might contribute to the lower serum concentrations and higher bone / serum concentration ratios reported by Dehne et al. compared to other authors. Dehne et al. (79) applied the same blood saving technique while studying the bone penetration of cefuroxime, cefotiam and cefamandole (chapter 5.1.9.9).

For amoxicillin and clavulanic acid Grimer et al. (132) report at least 10 times lower concentrations in bone than in serum about 30min after the dose. Related to total bone mass, Weismeier et al. (328) found average concentration ratios in bone / serum of about 8 to 18% during the first 4h after the dose for amoxicillin, and of 4 to 8% for clavulanic acid. When related to total bone mass, the concentrations of clavulanic acid in bone reported by Adam et al. (3) are approximately 20 to 30 times higher than the concentrations reported by Grimer et al. (132) and Weismeier et al. (328) after the same dose. However, the authors did not provide a possible explanation for this observation. More recently, Jehl et al. (160) reported average bone / serum concentration ratios of 0.09 to 0.44 between 1.5h and 8h after the last dose of amoxicillin. The time above MIC for amoxicillin was probably determined by the naïve averaging approach. For an MIC of 1 mg/L bone concentrations were above the MIC for 50% of the dosing interval with the 1g dose of amoxicillin twice daily, and for 37.5% of the dosing interval with the 500 mg dose three times daily. Bone penetration of amoxicillin / clavulanic acid will be discussed in more detail in chapter 5.3.5

For piperacillin / tazobactam two studies by different authors used the same methods for sample preparation and drug determination and report

consistent results. Incavo et al. (156) report average concentration ratios of 0.18 in cortical and 0.23 in cancellous bone for piperacillin 1h after an infusion of 3g piperacillin and 375 mg tazobactam. For tazobactam the ratios were 0.22 in cortical and 0.26 in cancellous bone. Boselli et al. (44) studied 12 patients undergoing hip replacement surgery 1.5h after start of a 30min infusion of 4g piperacillin and 0.5g tazobactam. The average bone / plasma concentration ratios were 0.2 for piperacillin and 0.3 for tazobactam in cortical bone, and 0.3 for both drugs in cancellous bone. Both studies report piperacillin concentration / tazobactam concentration ratios of about 8 in cortical bone and of 9 in cancellous bone. In summary most studies with penicillins and beta-lactamase inhibitors report average bone / serum ratios between 0.1 and 0.3.

5.1.9.9   Cephalosporins

Cephalosporins are used in the treatment of bone infections, especially as alternative to penicillins in *S. aureus* infections (192). The range of reported bone / serum concentrations ratios is shown in Table 5.1-5.

Concentrations of ceftriaxone and cefamandole in bone have recently been studied by Lovering et al. (197). Average (95% confidence interval) ceftriaxone concentration ratios between bone and blood were 0.16 (0.12 - 0.19) at 10 to 30min after the dose (0.11 at 10 min, 0.17 at 30 min) and 0.14 (0.073 - 0.21) at 8h after the dose. For cefamandole the average ratio was 0.18 (0.16 - 0.21) at 10 to 30 min. Cefamandole has an about 10 times shorter half-life than ceftriaxone (0.8h vs. 8h) (197). Cefamandole concentrations in bone were not detectable (< 0.2 mg/L) at 8h, this indicates a fast equilibrium between bone and blood. Average bone / blood concentration ratios at 10 and 20min were very similar for both drugs, despite the higher (95%) protein binding of ceftriaxone compared to cefamandole (70%). In a previous study, Martin et al. (215) found ceftriaxone concentrations in bone that were lower by a factor of 2 to 3 at 1.5h after the same dose. However, they did not report plasma levels.

Table 5.1-5   Bone penetration of cephalosporins

Antibiotic	Range of time after last dose	Range of average bone / serum or bone / plasma concentration ratios	Method
Ceftriaxone	0.2 - 8h	0.11 - 0.17	HPLC (197)
Cefuroxime	0.2 - 6.5h	0.09 - 0.55	HPLC (79, 172, 196, 255), or bioassay (188, 255)
	0.6h	0.01 - 0.12[a]	bioassay (322)
Cefuroxime (osteomyelitis)	1h	0.04 - 0.08	HPLC (172)
Cefamandole	0.2 - 4h	0.12 - 0.77	HPLC (79, 196-198), or bioassay (188)
	2 - 4h	1.6 - 2.3	HPLC (79)
Cefotiam	1 - 4h	0.27 - 0.44	HPLC (79)
Cefepime	1 - 2h	0.46 - 0.76	HPLC (48)
Ceftazidime (ischemic bone)	1 - 2h	0.04 - 0.08	HPLC (253, 254)
Ceftazidime	2h	0.54	bioassay (4)

[a]: Detectable concentrations only in 14 of 20 samples, lower limit of detection: 7.6 - 9.2 mg/kg

In another study by Lovering et al. (198), a bolus dose of 1g cefamandole was administered to 12 patients undergoing hip replacement. Average (95% confidence interval) bone / blood concentration ratios at 10, 20, and 30min after the dose were 0.25 (0.16 - 0.34), 0.25 (0.13 - 0.37), and 0.23 (0.13 - 0.32) for cefamandole and therefore comparable to the results of their previous study (197). However during the first 10 to 20min after the dose the equilibrium between blood and bone might not yet have been reached. Dehne et al. (79) found average bone / serum concentration ratios for cefamandole that were increasing from about 0.77 at 1h to about 2.3 at 4h after the dose, and were therefore much higher than the ratios reported by Lovering et al. (197, 198) at earlier time points after the dose. Most studies report average bone / serum concentration ratios for cefamandole between 0.1 and 0.4, whereas Dehne et al. report higher ratios.

From the same study, Dehne et al. (79) reported average cefuroxime bone serum / concentration ratios of about 0.30 at 1h, 0.54 at 2h, 0.55 at 3h,

and 0.38 at 4h after the end of the infusion. Vuorisalo et al. (322) could detect cefuroxime at an average of 36min after the dose in 14 of 20 sternal bone samples, and bone / serum concentration ratios were between 0.01 and 0.12. At about 4h after the infusion, cefuroxime could not be detected in any of 20 samples, however the detection limit of 7.6 to 9.2 mg/kg for the bioassay was high. For cefotiam Dehne et al. (79) report average bone / serum concentration ratios of about 0.27 at 1h, 0.30 at 2h, 0.44 at 3h, and 0.38 at 4h. The ratios are similar to those reported for cefuroxime and to many of the results for cefamandole.

Raymakers et al. (253) investigated ceftazidime concentrations in ischemic bone of 16 patients undergoing lower limb amputation. Median bone / plasma concentration ratios at 1h to 1.5h after the dose ranged from 0.04 to 0.08 in the forefoot, midfoot, and tibial bone. These results are similar to a previous study, that was conducted by the same group, and in a similar patient collective (254). Because of poor circulation in ischemic tissue, high concentration ratios would not have been expected.

Recently, Breilh et al. (48) investigated the bone concentrations of cefepime in 10 patients. At 1 to 2h after the start of the infusion, average $\pm$ SD bone / serum concentration ratios were 0.87 $\pm$ 0.37 for cortical and 1.06 $\pm$ 0.23 for cancellous bone. The ratios were calculated with bone concentrations in mg/L, and a density of 1.9 kg/L for cortical and 1.4 kg/L for cancellous bone. Therefore, concentration ratios were about 0.46 in cortical and 0.76 in cancellous bone, based on bone concentrations expressed as mg/kg total bone mass. These ratios for cefepime, especially in cancellous bone, are higher than most results reported for other beta-lactams. In summary, most studies report bone / serum concentration ratios between 0.1 and 0.5 for cephalosporins. The ratios tend to be slightly higher than for most penicillins.

5.1.9.10 Aminoglycosides

There are few reports on aminoglycoside concentrations in human bone after systemic administration and most studies were published some

decades ago. This renders interpretation of the penetration of aminoglycosides into bone difficult. For gentamicin, bone / serum concentration ratios at 1h to 12h after intramuscular administration of 1 mg/kg range between 0.057 and 0.75 (42). Smilack et al. (277) found detectable concentrations in bone only in 1 of 4 patients at 1h after an intramuscular dose of 1.7 mg/kg, and report a high limit of detection of 2.1 mg/kg dry weight of bone. For tobramycin, the average bone / serum concentration ratio is 0.13 at 0.3h (333) and 0.091 at 14.3h (42) after the dose.

Recently, Boselli et al. (43) investigated concentrations of isepamicin in bone 1 to 2h after the dose in 12 patients. They report bone / plasma concentration ratios of 0.31 in cortical and 0.28 in cancellous bone. These ratios are based on bone concentrations in mg/L assuming a density of 1.9 kg/L for cortical and 1.4 kg/L for cancellous bone. Based on bone concentrations in mg/kg, the average ratios are 0.16 for cortical and 0.20 for cancellous bone.

Gentamicin is often used in beads, bone cement etc. for local treatment or prophylaxis of bone infections. However local delivery of antibiotics to bone is beyond the scope of this overview.

5.1.10   Conclusions

In summary, most of the studies find a substantial BSV in the observed bone concentrations. There is also a considerable variability of the average bone / serum concentration ratio between different studies on the same drug, and between drugs within the same group of antibiotics. However, there are some trends for the comparison of antibiotic groups. Most studies on quinolones report high average bone / serum concentration ratios between 0.3 and about 1. Linezolid shows average bone / serum concentration ratios of 0.2 to 0.5. For macrolides and clindamycin, a large range of bone / serum concentrations has been reported. Two recent studies showed that on average azithromycin achieves higher concentrations in bone than in serum. For glycopeptides very different results have been reported with the majority of studies finding average bone / serum concentration ratios of 0.2 to 0.4.

Beta-lactams usually achieve average bone / serum concentration ratios of less than 0.5 and most studies with penicillins report ratios between 0.1 and 0.3. For cephalosporins most studies report average bone / serum concentration ratios between 0.1 and 0.5, whereas higher values have also been reported. Average bone serum concentration ratios reported for aminoglycosides are mostly between 0.05 and 0.2.

These trends among the antibiotic groups are caused by the physicochemical characteristics of the different drug groups. For the passage through the capillary walls into bone, molecular size, protein binding, lipophilicity and acid / base characteristics are probably important determinants (155). Binding to calcium in bone, as has been reported for quinolones, or binding of fosfomycin to hydroxyapatite might also influence bone concentrations of an antibiotic. Beta-lactams have been suggested to distribute mainly in the interstitial fluid space in bone (202).

There is no prospectively evaluated PKPD target for treatment of bone infections based on bone or serum concentrations. The PKPD target for treatment of bone infections should be evaluated in future clinical trials. Those studies should emphasize the validation, standardization, and reporting of the analytical assay. Serum or plasma concentrations are probably a useful surrogate measure for antibiotic effectiveness in bone, since some studies on antibiotics suggest a fast rate of equilibration between bone and serum. The PKPD targets based on serum concentrations are likely to be drug specific due to the differences in the extent of bone penetration between various antibiotics. Optimal design theory, population PK, and MCS are the methods of choice to evaluate the average rate and extent of bone penetration as well as the BSV.

Future studies are warranted to determine the influence of osteomyelitis or ischemia on antibiotic concentrations in bone. There is also very little data on the variability of bone penetration in different bone types. Ideally, optimal dosage regimens should account for the disease state and site of bone infection.

5.2   Penetration of moxifloxacin into bone evaluated by Monte Carlo simulation

5.2.1   Chemical structure of moxifloxacin

$(C_{21}H_{24}FN_3O_4$, Mol. Wt.: 401.43)
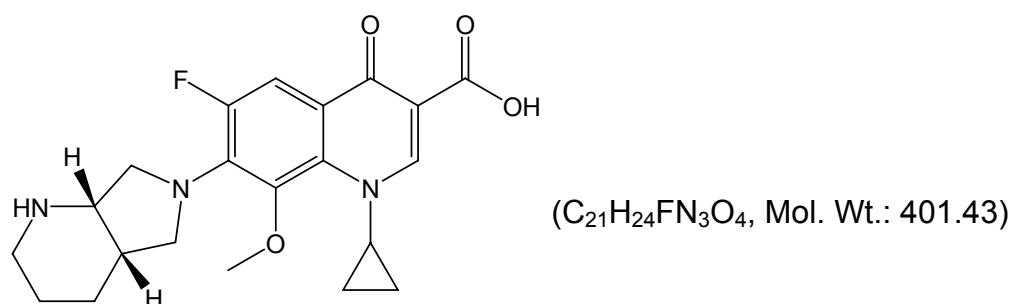
Chemical structure 5.2-1   Moxifloxacin

5.2.2   Use of quinolones in treatment and prophylaxis of bone infections

Quinolones are established in the treatment of osteomyelitis. Most clinical experience has been gained with ciprofloxacin and ofloxacin, that were shown to be efficacious in treatment of gram-negative osteomyelitis, especially if caused by Enterobacteriaceae (193). Quinolones have the advantage that they may be administered orally which facilitates a prolonged therapy as well as perioperative prophylaxis. Oral administration of quinolones, e.g. ciprofloxacin, ofloxacin and levofloxacin, has been reported effective in surgical prophylaxis after multiple (315, 345) or single dose (34, 266, 296). As *S. aureus* penetrates into bone cells (chapter 5.1.9.1), intracellular penetration of quinolones might be of advantage.

Good penetration into bone has been reported for ciprofloxacin (189, 217), ofloxacin (306, 307), levofloxacin (320), lomefloxacin (244), enoxacin (108), fleroxacin (250) and pefloxacin (82). Resistance to the older quinolones has been emerging, and they do not show sufficient microbiological activity against *S. aureus*, coagulase-negative staphylococci and streptococci (193).

Moxifloxacin is a fluoroquinolone antimicrobial that is used mostly for treatment of respiratory tract infections as well as skin and skin structure

infections. It has a wider spectrum and improved activity against gram-positive and anaerobic pathogens frequently found as causative agents in osteomyelitis (193), while retaining potency and broad spectrum coverage against gram-negative pathogens comparable to the earlier quinolones (37). Moxifloxacin has lower MICs than levofloxacin, ciprofloxacin, ofloxacin, and norfloxacin (313) for *S. aureus*, which is the most common pathogen in osteomyelitis. Moxifloxacin achieves high concentrations in many tissues and body fluids, e.g. gastrointestinal tissues (336), lung tissues and bronchial secretions (49, 55, 274, 280), sinus tissues (85, 118), subcutaneous tissues (165), skin blister fluid and saliva (231). However, bone penetration in humans has not been reported for moxifloxacin and we are not aware of any reports about PKPD modeling of quinolones in bone in humans or animals.

As described in chapter 5.1.3, reporting only bone / serum concentration ratios makes interpretation of bone penetration difficult. Modeling the full serum and bone concentration time course allows one to evaluate the penetration of antimicrobials into bone and to study the PD profile in bone. Therefore the first objective of our study was to determine moxifloxacin concentrations after oral administration in cortical and cancellous bone in a controlled study in subjects undergoing hip replacement surgery. As our second objective we intended to develop a PK model to describe the time course of moxifloxacin concentrations in bone and serum. Our third objective was to calculate the PTA for serum, cortical and cancellous bone based on PKPD targets for successful microbiological and clinical outcome.

5.2.3   Methods

Study participants: Our study comprised twenty-four patients (10 males, 14 females) who were scheduled to undergo total hip replacement. Their average $\pm$ SD weight was 76.8 ± 13.4 kg, height was 168.3 ± 9.9 cm and age was 63 ± 15 years.

Study design and drug administration: Each patient received a single oral dose of 400 mg moxifloxacin (Avalox®, BayerVital, Germany) 2 to 7h before surgery. Before surgery, 20 patients received amoxicillin / clavulanic

acid, three patients received levofloxacin, and one patient received clindamycin, as intravenous infusion. Since there were no data on the bone penetration of moxifloxacin prior to this study, those standard treatments for perioperative prophylaxis were given in parallel to moxifloxacin to assure antibacterial prophylaxis by an established treatment option.

Determination of Serum and Bone Concentrations: Serum and bone samples were obtained as described in chapter 2.3. For determination of moxifloxacin in plasma, 100µL of each sample were precipitated by adding 25µL of acetonitrile / perchloric acid containing the internal standard. After thorough mixing the samples were centrifuged and 20µL of the clear supernatant were analyzed by reversed-phase HPLC. For analysis of bone samples, an aliquot of the bone powder was shaken with 6 times the amount of buffer for 24h. After centrifugation, 100µL of the aqueous supernatant were deproteinized by addition of 25µL of acetonitrile / perchloric acid containing the internal standard. After thorough mixing and centrifugation, 20µL of the aqueous supernatant were analyzed by HPLC.

The HPLC system consisted of a LaChrom L-7100 (E. Merck, Darmstadt, Germany) pump, an autosampler (Autosampler L-7250, E. Merck, Germany), an analytical reversed phase chomatographic column, and a fluorescence detector (Jasco FP-920 Intelligent Fluoreszenz Detektor, Jasco, Gross-Umstadt, Germany). The excitation wavelength was 296nm and the emission wavelength 504nm. The mobile phase was a mixture of citric acid solution, ammonium perchlorate, and acetonitrile. Moxifloxacin and the internal standard were eluted by gradient elution after 4.4 and 3.1min, respectively. For evaluation of the calibration standards a weighted linear regression ($1/y^2$) was performed with theoretical concentrations of calibration standards and measured peak height ratios (peak height moxifloxacin / peak height internal standard).

No interferences were observed in serum and bone for moxifloxacin and the internal standard. The linearity of the moxifloxacin calibration curves was demonstrated from 0.0100 to 5.00 mg/L in serum, and from 0.009 to 4.76 mg/L in bone homogenate. The inter-day precision and accuracy of the spiked quality control standards of moxifloxacin in human serum ranged from

1.8 to 5.9% and from 95.1 to 103.8%, respectively. The inter-day precision and accuracy of the spiked quality control standards of moxifloxacin in cortical (cancellous) bone homogenate ranged from 3.7 to 9.2% (0.4 to 0.7%) and from 94.7 to 97.6% (92.6 to 101.7%), respectively.

Pharmacokinetics

PK analysis: We used a model with four disposition compartments and a first-order absorption. The predictive performance of our final model was tested via visual predictive checks and standard diagnostic plots were used.

Structural model: We had observations for moxifloxacin concentrations in serum, cortical bone, and cancellous bone. We used a two compartment disposition model for moxifloxacin in serum and in the peripheral compartment plus one peripheral compartment for each bone matrix. The differential equations for the model are as follows:

$$\frac{dX(1)}{dt} = -ka \cdot X(1)$$

Formula 5.2-1

$$\frac{dX(2)}{dt} = ka \cdot X(1) - \left[\frac{CL+CLic}{V_{Serum}} + k_{24} + k_{25}\right] \cdot X(2)$$
$$+ \frac{CLic}{V_{Peripheral}} \cdot X(3) + k_{42} \cdot X(4) + k_{52} \cdot X(5)$$

Formula 5.2-2

$$\frac{dX(3)}{dt} = \frac{CLic}{V_{Serum}} \cdot X(2) - \frac{CLic}{V_{Peripheral}} \cdot X(3)$$

Formula 5.2-3

$$\frac{dX(4)}{dt} = k_{24} \cdot X(2) - k_{42} \cdot X(4)$$

Formula 5.2-4

$$\frac{dX(5)}{dt} = k_{25} \cdot X(2) - k_{52} \cdot X(5)$$

Formula 5.2-5

Compartment 1 is the gut compartment, compartment 2 is the serum compartment and compartment 3 the peripheral compartment. Compartment 4 is the compartment for cortical bone, and compartment 5 is the compartment for cancellous bone. X(1), X(2), X(3), X(4) and X(5) denote the amounts of drug in the respective compartment. CL is the apparent total

clearance from the central compartment, ka is the absorption rate constant, CLic is the apparent intercompartmental clearance between the serum and peripheral compartment, and k_{24}, k_{42}, k_{25}, k_{52} are first order intercompartmental transfer rate constants. V_{Serum} and $V_{Peripheral}$ are the apparent volumes of distribution of the respective compartment. For all apparent clearance and apparent volume terms the extent of absorption term (1/F) is left out for simplicity.

We included scale terms for the concentrations in cortical and cancellous bone that describe the equilibrium concentration ratio between cortical bone and serum ($F_{cortical}$) and between cancellous bone and serum ($F_{cancellous}$). An $F_{cortical}$ equal to 1 means that concentrations after a continuous infusion at steady-state are the same in bone and serum, an $F_{cortical}$ smaller (greater) than 1 means that these concentrations are lower (higher) in bone than in serum.

PK modeling: We had sparse serum concentration time data between 2 and 7h post oral administration. As the moxifloxacin half-life is about 12h, these data did not allow us to estimate all PK parameters for a two compartment model. Therefore, we used MAP-Bayesian estimation based on the disposition parameters of Simon et al. (274) and derived the average clearance and its standard deviation from published studies (274, 285-287, 337). Based on those disposition parameters and their standard deviation, we estimated a typical half-life of absorption from our serum data via population PK in NONMEM V (25).

We had no prior information on the rate or extent of bone penetration of moxifloxacin. The raw data and initial modeling showed that the equilibrium between serum and bone was virtually achieved 2h after dosing, indicating that the rate of equilibration (k_{42} and k_{52}) was fast. Therefore we could not estimate k_{42} and k_{52} and fixed those values to an equilibration half-life of 15min. We assured the plausibility of this choice via visual predictive checks.

The disposition parameters of moxifloxacin as described above have been determined in absence of a bone compartment. As we used MAP-Bayesian estimation (see below), we had to keep the amount of moxifloxacin in the bone compartments minimal so that the serum PK was not affected by

the presence of the bone compartments. This can be achieved by choosing a small volume for the bone compartment or equivalently a small value for the rate constants k_{24} and k_{25}. Therefore, we chose a volume of distribution of 0.5L each for the cortical and cancellous bone compartments which is equivalent to fixing k_{24} and k_{25} to 0.022 h^{-1} in our model.

MAP-Bayesian estimation: We estimated the individual PK parameters by MAP-Bayesian estimation as implemented in ADAPT II (74). We used informative priors with prior means and standard deviations and a log-normal distribution to estimate the individual disposition parameters. In absence of prior information on the bone penetration, we used non-informative priors (uniform distribution) to estimate $F_{cortical}$ and $F_{cancellous}$ in the MAP-Bayesian step. We described the residual unidentified variability by a proportional error model for the serum and bone concentrations.

Reverse engineering method for PKPD targets: The ratio of the free (non-protein bound) area under the plasma concentration time curve and MIC (*f*AUC/MIC) has been shown to be predictive for the microbiological and clinical outcome for fluoroquinolones (67, 92, 240). However, there is no PKPD target for moxifloxacin in osteomyelitis patients in serum or for quinolones in bone. Therefore, we used a reverse engineering method (38) to propose a PKPD target for moxifloxacin in serum and bone based on studies in osteomyelitis patients.

The reverse engineering method uses the success rate from clinical studies in osteomyelitis patients, the expected AUCs after the doses given in these studies, and published MIC distributions from the relevant time period to derive the most likely target. The target which best predicts the observed clinical success rate is derived via MCS in an iterative process.

We used published data from four studies (119, 131, 150, 242) on the clinical or microbiological outcome of osteomyelitis caused by *S. aureus* in patients who obtained ciprofloxacin orally at 500 mg or 750 mg every 12h. We derived their expected AUCs based on published PK data for ciprofloxacin (12, 348) or based on the AUCs reported by the authors (242). We assumed a log-normal distribution for clearance and used a 25% protein binding for ciprofloxacin to simulate the expected *f*AUCs for 5,000 virtual subjects for

each osteomyelitis study. We combined these *f*AUCs with susceptibility data for *S. aureus* (21, 52, 59, 60, 99, 110, 137, 210, 211, 278, 279, 297, 338) from the time period of the osteomyelitis studies to derive the PKPD target in serum which predicted the observed success rate. This yielded the PKPD target for *S. aureus* infections of osteomyelitis patients in serum ($f\text{AUC}_{\text{SERUM}}$/MIC). We assumed a protein binding of 0% in bone, because there are no data on protein binding of ciprofloxacin or moxifloxacin in bone. The ratio of total concentrations in bone and serum (AUC_{BONE}/$\text{AUC}_{\text{SERUM}}$) has been reported to be 0.63 for ciprofloxacin (217). We derived the PKPD target in bone (AUC_{BONE}/MIC) based on this ratio.

__Monte Carlo simulation:__ We studied a range of MICs from 0.125 to 16 mg/L. The protein binding of moxifloxacin has been reported to range between 47% and 55% (13, 273, 285, 348). Therefore, we assumed an average protein binding of 50% for moxifloxacin in serum. We simulated the serum and bone concentration time curves for 10,000 patients after an oral moxifloxacin dose of 400 mg q24h at steady-state in absence of residual error.

5.2.4   Results

Concentrations of moxifloxacin in serum and cortical and cancellous bone are shown in Figure 5.2-1. Moxifloxacin concentrations in cortical and cancellous bone were similar to those found in serum. We had samples of femoral neck only from 11 of the 24 patients. These were not enough samples to allow differentiation between femoral head and femoral neck in the PK analysis.

Figure 5.2-1   Concentrations in serum and bone of subjects undergoing hip replacement surgery after a single oral dose of 400 mg moxifloxacin.
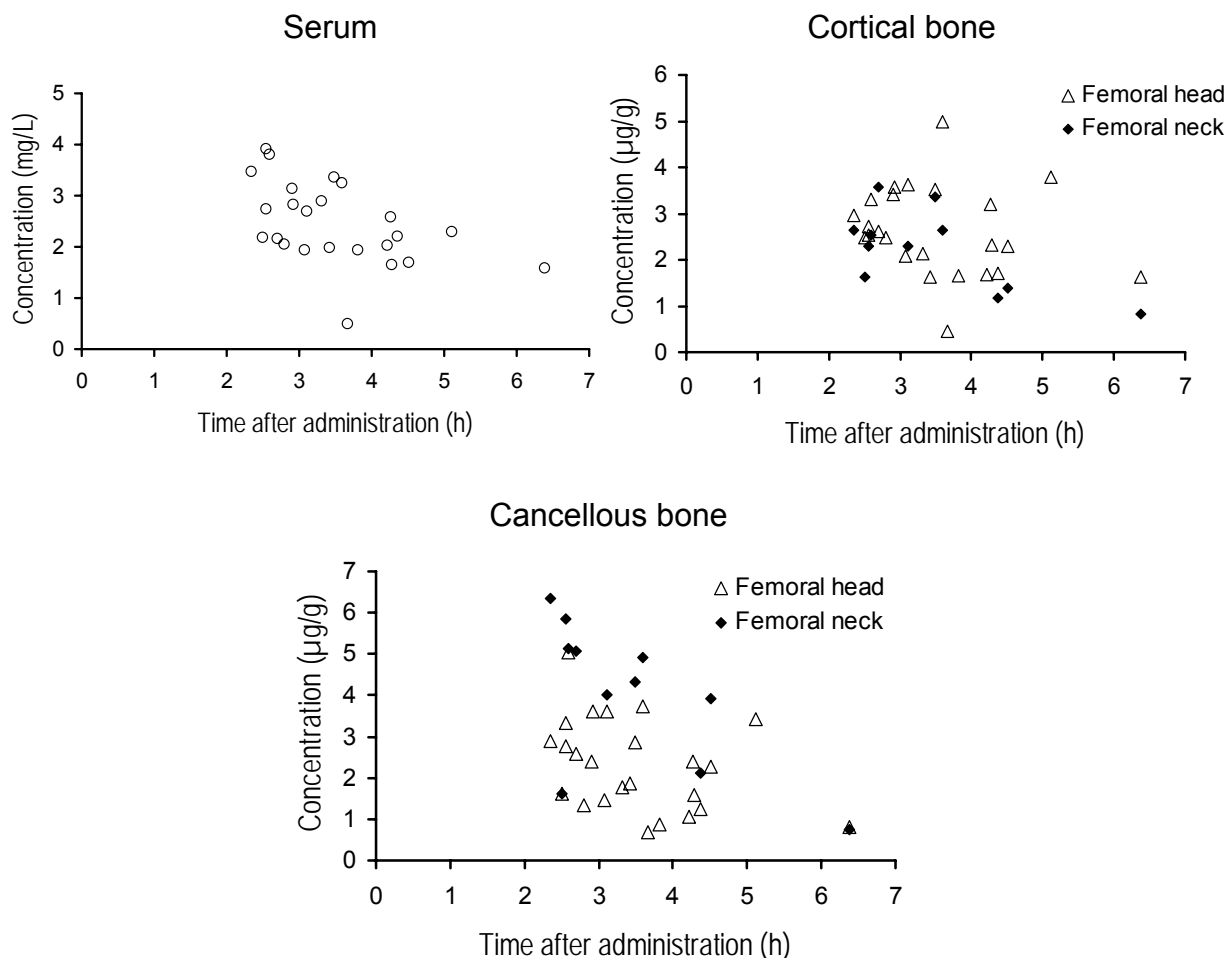
PK analysis: We estimated an absorption half-life of 26min. Table 5.2-1 shows our final parameter estimates from the MAP-Bayesian estimation.

Figure 5.2-2 shows the extent of moxifloxacin penetration into cortical and cancellous bone, and its BSV, calculated from the ratios of AUC$_{cortical}$ / AUC$_{serum}$ and AUC$_{cancellous}$ / AUC$_{serum}$ of 10,000 subjects that we simulated at steady-state. The median AUC ratio [10% - 90% percentile] was 80% [51% - 126%] for cortical bone and 78% [42% - 144%] for cancellous bone.

Table 5.2-1 Median parameter estimates for moxifloxacin (coefficient of variation)

Parameter	Unit	Median (% CV) [range]
CL	L h^{-1}	10.8 [9.85-11.5]
V$_{Serum}$	L	62.0 [58.5-65.4]
V$_{Peripheral}$	L	59.5 [48.0-71.6]
CLic	L h^{-1}	18.9 [15.3-23.2]
F$_{Cortical}$	-	0.803 (35%) [0.185-1.71]
F$_{Cancellous}$	-	0.775 (48%) [0.278-1.56]

CL is the apparent total clearance from the serum compartment. V$_{Serum}$ and V$_{Peripheral}$ are the apparent volumes of distribution of the central and peripheral compartment, and CLic is the apparent intercompartmental clearance. F$_{Cortical}$ and F$_{Cancellous}$ describe the equilibrium concentration ratio between bone and serum (see chapter 5.2.3 for details).

Figure 5.2-2 Penetration of moxifloxacin into cortical and cancellous bone, determined by the ratio of AUCs in bone to serum at steady-state
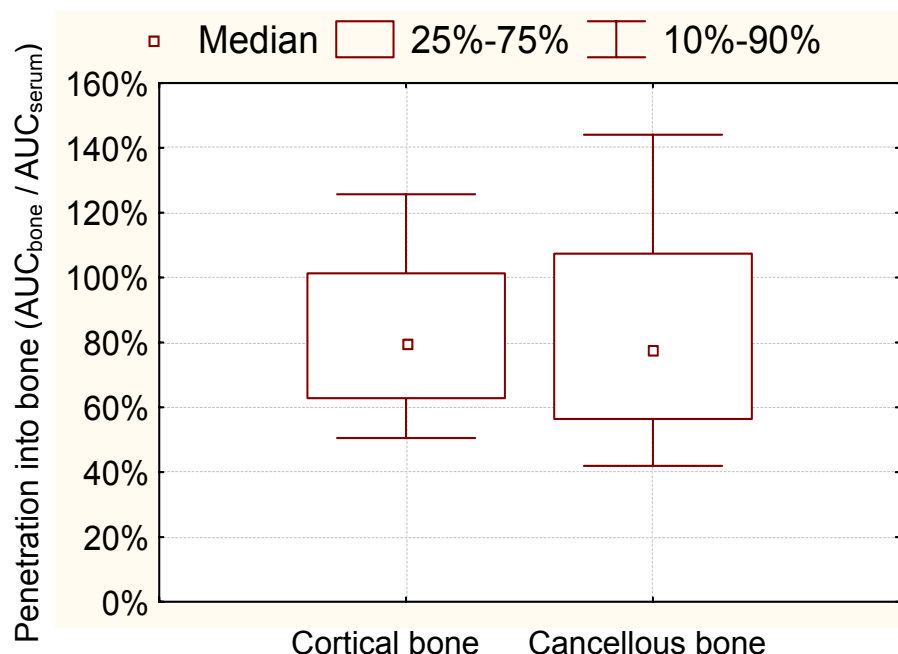
The visual predictive checks showed highly sufficient predictive performance of the final model for all three matrices (Figure 5.2-3). This qualified our model for use in the MCS.

Figure 5.2-3   Visual predictive check for serum and bone concentrations after 400 mg oral moxifloxacin

Serum

Cortical bone

Cancellous bone
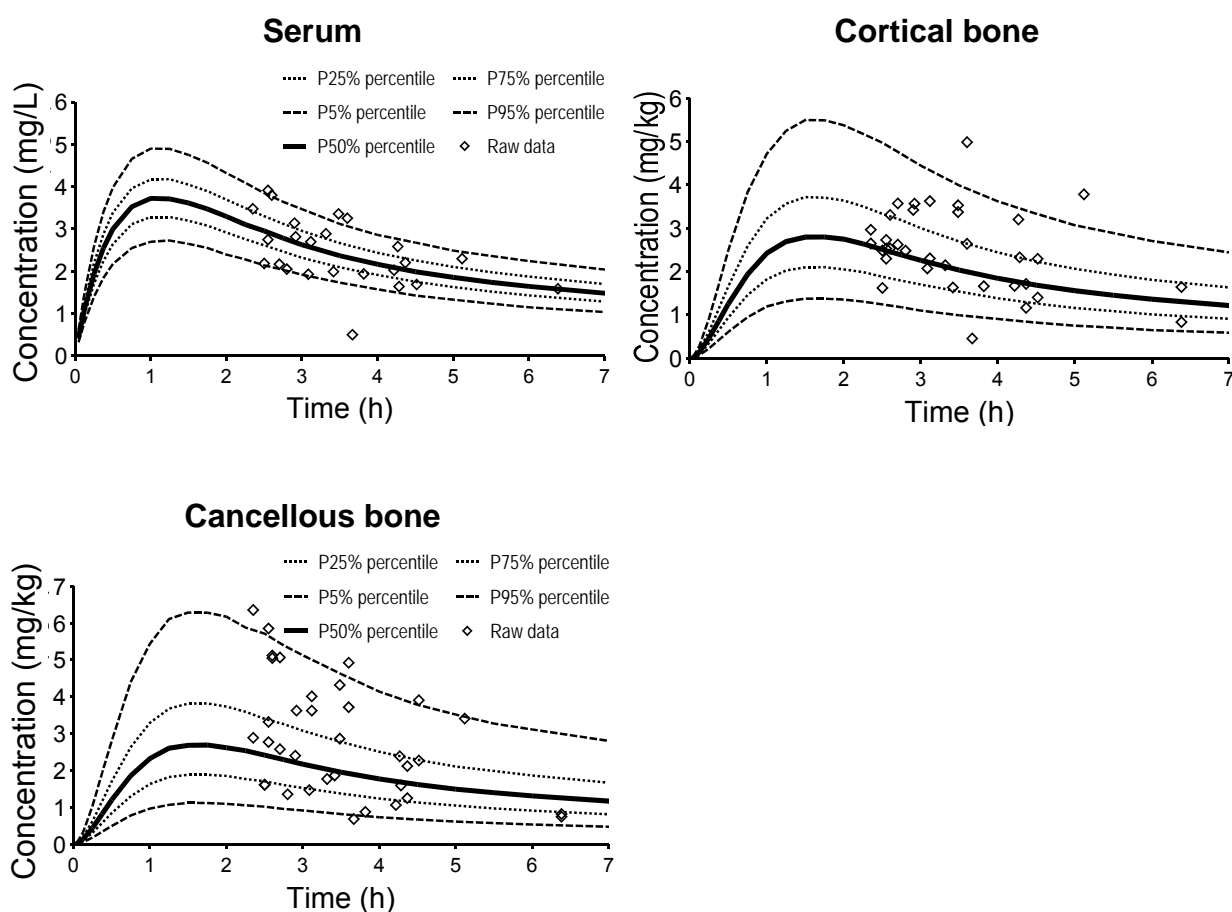
The plots show the raw data, the 90% prediction interval [5 - 95% percentile] and the interquartile range [25 - 75% percentile]. Ideally, 50% of the raw data points should fall inside the interquartile range at each time point and 90% of the raw data should fall inside the 90% prediction interval.

Reverse engineering method for PKPD targets: We used data from published clinical studies with ciprofloxacin in osteomyelitis patients and assumed a protein binding of 25% for ciprofloxacin and of 50% for moxifloxacin in serum. The resulting PKPD targets for successful clinical or microbiological outcome were $fAUC_{SERUM}/MIC \geq 15$ (119), $fAUC_{SERUM}/MIC \geq 36$ (242), $fAUC_{SERUM}/MIC \geq 43$ (150), and $fAUC_{SERUM}/MIC \geq 66$ (131). The respective targets for total bone concentrations were $AUC_{BONE}/MIC \geq 13$ (119), $AUC_{BONE}/MIC \geq 30$ (242), $AUC_{BONE}/MIC \geq 36$ (150), and $AUC_{BONE}/MIC \geq 55$ (131). As the targets calculated from the studies by Nix et al. (242) and

Hoogkamp-Korstanje et al. (150) were very similar, we used the mean from both studies, i.e. $f\text{AUC}_{\text{SERUM}}/\text{MIC} \geq 40$ and $\text{AUC}_{\text{BONE}}/\text{MIC} \geq 33$ for MCS.

  Monte Carlo simulation: The PKPD breakpoints for serum, cortical bone and cancellous bone are listed in Table 5.2-2 and the PTA versus MIC plots are shown in Figure 5.2-4. The breakpoints were similar in serum and bone. The PKPD breakpoint was about 0.375-0.5 mg/L for the median PKPD target in serum and bone.

Table 5.2-2   PKPD breakpoints for moxifloxacin in serum, cortical and cancellous bone, and various PKPD targets for $f\text{AUC/MIC}$

$f\text{AUC/MIC}$	PKPD breakpoint (mg/L)	AUC/MIC	PKPD breakpoint (mg/L)	
Target in serum	Serum*	Target in bone	Cortical bone*	Cancellous bone*
15	1	13	1	1
40	0.375	33	0.5	0.375
66	0.19	55	0.25	0.25

*: Assuming a protein binding of 50% in serum and of 0% in bone.

Figure 5.2-4   Probabilities of target attainment for serum, cortical and cancellous bone after 400 mg oral moxifloxacin

*f*AUC/MIC Serum	AUC/MIC Bone	Target calculated from
15	13	Gentry et al. (119)[1]
40	33	Nix et al. (242)[2] and Hoogkamp-Korstanje (150)[1]
66	55	Greenberg et al. (131)[1]

[1] Targets for successful clinical outcome in osteomyelitis patients
[2] Target for bacterial eradication in osteomyelitis patients
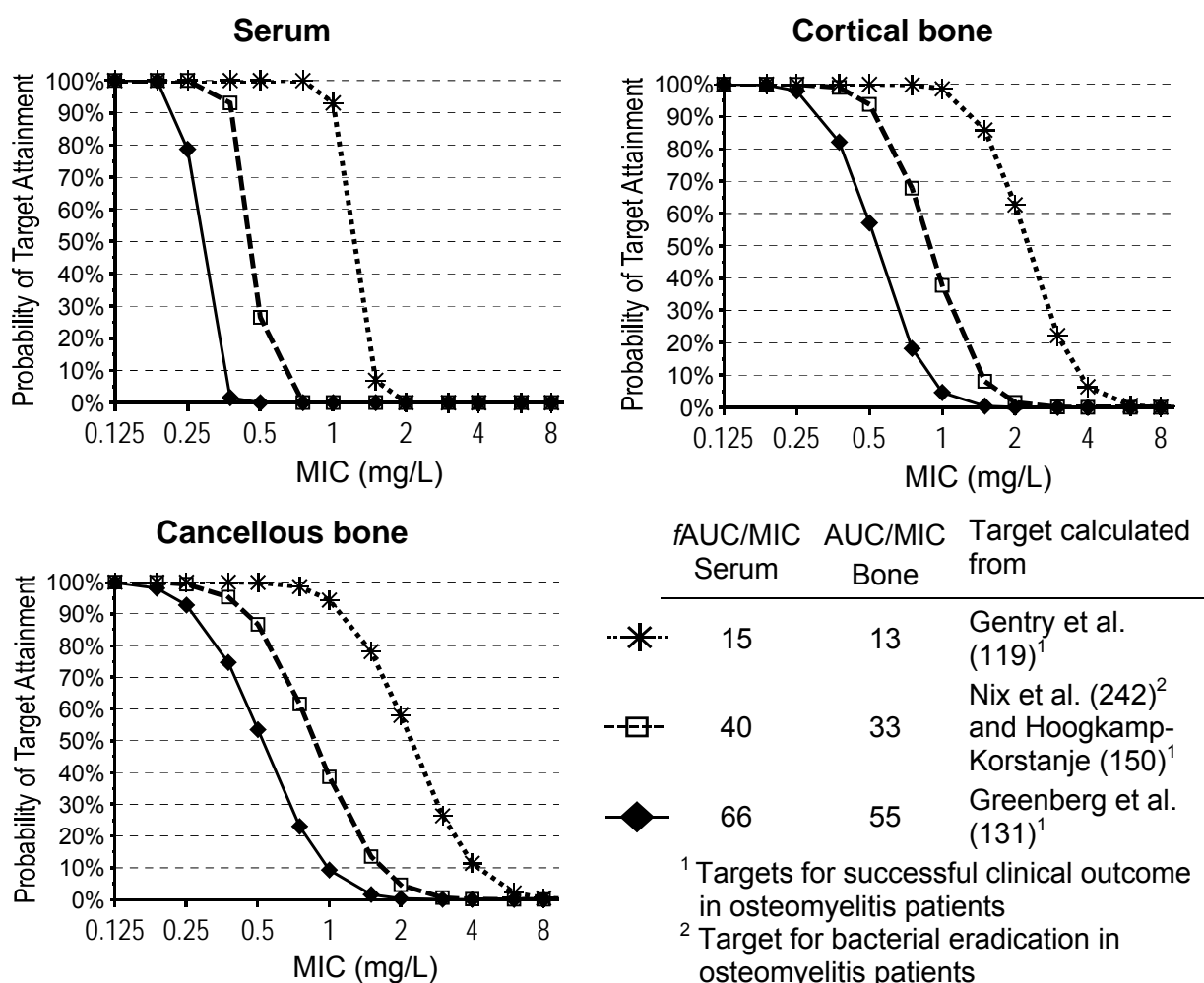
5.2.5   Discussion

Bone is not as highly vascularised as for example the lungs or skin. Therefore it is important to investigate the time course and extent of bone penetration of an antimicrobial before starting a clinical effectiveness trial (94, 313). Knowledge about how fast effective levels in bone are achieved may be critical for the timing of perioperative prophylaxis and surgery. For selecting the maintenance dose in treating bone infections, the AUC ratio (AUC in bone / AUC in serum) is the most informative measure for the extent of bone penetration.

Therefore we studied the penetration of moxifloxacin into cortical and cancellous bone in patients undergoing surgery for hip replacement and used PK modeling and MCS for data analysis. We intended to study, if moxifloxacin shows a sufficient extent of bone penetration to be used in perioperative prophylaxis or treatment of bone infections. Furthermore we intended to study the rate of bone penetration in order to determine the optimal time for initiation of surgical prophylaxis. In absence of an established PKPD target for moxifloxacin in bone infections, we used a reverse engineering method to propose a necessary $f\text{AUC}_{SERUM}$/MIC and AUC_{BONE}/MIC for clinical or microbiological success. For this method we used published MIC distributions of *S. aureus* for ciprofloxacin and data on the effectiveness of ciprofloxacin in osteomyelitis patients with *S. aureus* infection.

Our data showed high concentrations of moxifloxacin in both cortical and cancellous bone tissues in subjects undergoing hip replacement surgery (Figure 5.2-1). Moxifloxacin showed similar AUCs in bone and serum (Figure 5.2-2). Measures for the central tendency and BSV of the ratios AUC_{BONE} / AUC_{SERUM} (median penetration [10% - 90% percentile]) were 80% [51% - 126%] for cortical bone and 78% [42% - 144%] for cancellous bone. We studied the concentrations of moxifloxacin in bone and serum between 2 and 7h post the oral dose of moxifloxacin. The average concentration ratios between serum and bone showed no obvious change with time during our observation period. The raw data and initial modeling showed that the bone penetration observed in our study was faster than expected, and equilibrium between serum and bone was virtually achieved 2h after dosing. Therefore, the bone and the serum compartment were in pseudo-equilibrium during our observation period (from 2 to 7h post dose) and the bone concentrations declined in parallel (on log-scale) to the serum concentration. As absorption of moxifloxacin and bone penetration were fast, antibacterial prophylaxis should be achieved within 2h in both cortical and cancellous bone after an oral dose of moxifloxacin.

Secondary to the high extent of bone penetration for moxifloxacin, MCS showed robust ($\geq$90%) PTAs for MICs up to 0.375 mg/L in serum and in cancellous bone, and up to 0.5 mg/L in cortical bone, for the targets

fAUC$_{SERUM}$/MIC $\geq$ 40 and AUC$_{BONE}$/MIC $\geq$ 33 (Table 5.2-2). This PKPD target seems the most reasonable one, as it was the average reverse engineered target of two studies investigating clinical and microbiological outcome. In one of these two studies PK parameters were reported for several subjects and could be used for calculation of the AUCs. The resulting targets from this study (fAUC$_{SERUM}$/MIC $\geq$ 40 and AUC$_{BONE}$/MIC $\geq$ 33) fall between the targets calculated from the other two studies (Table 5.2-2).

The calculated breakpoints were similar, or even slightly higher in bone than in serum, although concentrations were slightly lower and more variable in bone than in serum. However, it should be noted that we used a protein binding of 50% for moxifloxacin in serum and assumed no protein binding in bone, because of the absence of reports on moxifloxacin (and ciprofloxacin) protein binding in bone. If 50% of moxifloxacin was bound to protein, or e.g. to Ca^{2+}, in bone, the PKPD breakpoints in bone would be half as high as shown in Table 5.2-2. Assuming a (protein) binding of 50% in bone, breakpoints would still be 0.125 mg/L (or above) in both cortical and cancellous bone for all calculated targets.

An MIC$_{90}$ of 0.125 mg/L has been reported for moxifloxacin against *S. aureus* (313). If one simplifies the PTA vs. MIC profile by assuming a PTA of 100% for all MICs $\leq$0.125 mg/L and a PTA of 0% for all MICs $\geq$0.25 mg/L, it is possible to calculate that the overall probability of target attainment will be $\geq$90% for moxifloxacin against *S. aureus* based on an MIC$_{90}$ of 0.125 mg/L. Therefore, a high ($\geq$90%) probability for successful clinical and microbiological outcome would be predicted for *S. aureus* infections up to a target AUC$_{BONE}$/MIC $\geq$ 55 and a protein binding in bone of 50%.

In conclusion, we found a good penetration of moxifloxacin into bone. Based on AUC ratios, the median penetration [10% - 90% percentile for BSV] was 80% [51% - 126%] for cortical bone and 78% [42% - 144%] for cancellous bone. We found a fast equilibrium half-life (< 60 min) between serum and cortical bone as well as between serum and cancellous bone. As the absorption of moxifloxacin was also fast, administering moxifloxacin 2h before surgery would result in effective concentrations during surgery. The

PKPD breakpoint for moxifloxacin was 0.375 mg/L in serum and cancellous bone, and 0.5 in cortical bone, based on the target $AUC_{BONE}/MIC \geq 33$ ($fAUC_{SERUM}/MIC \geq 40$) for successful microbiological outcome and assuming a protein binding of 50% for moxifloxacin in serum and 0% in bone. As the MIC_{90} of moxifloxacin is often reported to be 0.125 mg/L against *S. aureus*, moxifloxacin was predicted to have a high probability ($\geq 90\%$) for successful microbiological outcome. This provides the required basis for a larger study on the clinical effectiveness of moxifloxacin against bone infections.

5.3 Penetration of amoxicillin and clavulanic acid into bone

5.3.1 Chemical structures of amoxicillin and clavulanic acid

$(C_{16}H_{19}N_3O_5S$, Mol. Wt.: 365.4$)$
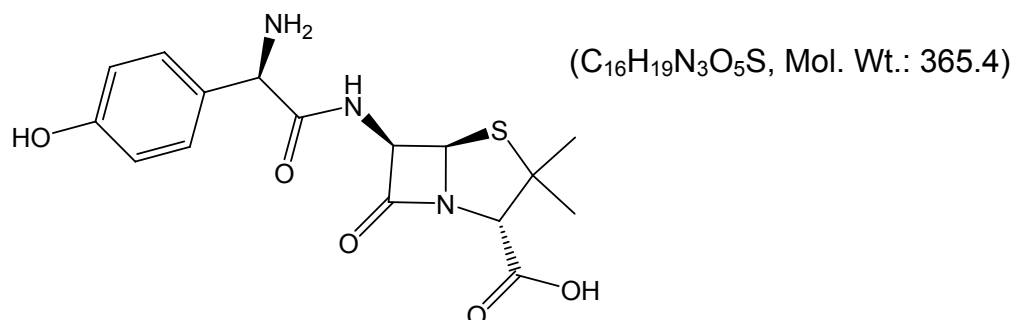
Chemical structure 5.3-1 Amoxicillin

$(C_8H_8KNO_5$, Mol. Wt.: 237.25$)$
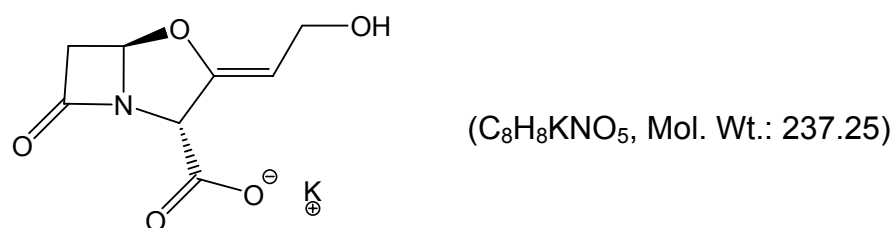
Chemical structure 5.3-2 Clavulanic acid

5.3.2 Perioperative prophylaxis in orthopedic surgery

It is standard practice to administer perioperative prophylaxis to reduce the incidence of infections after orthopedic surgery. Insertion of artificial joints is undertaken increasingly, and each year more than a million hip replacements are done worldwide (192). Insertion of prosthetic devices is particularly susceptible to infection. If a prosthesis becomes infected, it usually has to be removed and this causes long hospital stays and disabilities for the patient. Therefore, it is vitally important to use adequate surgical prophylaxis and antibiotics that achieve sufficient concentrations in bone and are highly active against frequently involved pathogens. Sufficient antibiotic concentrations in bone have to be assured for prevention of infection, even for drugs that are highly active against the commonly involved pathogens. In more than 50% of infected prostheses, *S. aureus* or coagulase-negative

staphylococci, e.g. *S. epidermidis* or *S. saprophyticus*, are the causative pathogens (192).

Amoxicillin in combination with clavulanic acid is one of the most frequently used antibiotics worldwide. It has a broad spectrum of activity against gram-positive and gram-negative pathogens and is used for treatment of respiratory tract infections, skin and skin structure infections, bone and joint infections (often in combination with other antibiotics), and for perioperative prophylaxis. Although amoxicillin / clavulanic acid shows good activity against the pathogens commonly encountered in prosthesis-related bone infections (MIC_{90}s: 1 mg/L for methicillin-susceptible *S. aureus*, 8 mg/L for *S. epidermidis*, and 0.5 mg/L for *S. saprophyticus* (141)), its PK profile in bone (except bone / serum concentration ratios) and the PKPD breakpoints in bone have not been determined. To the best of our knowledge there are no reports about PKPD models in humans or animals for beta-lactam penetration into bone. Therefore, we studied the rate and extent of penetration of amoxicillin / clavulanic acid into cortical and cancellous bone in patients undergoing surgery for hip replacement

The first objective of our study was to determine amoxicillin and clavulanic acid concentrations in cancellous and cortical bone in a controlled study in subjects undergoing hip replacement surgery. As our second objective we intended to develop a PK model to describe the time course of amoxicillin and clavulanic acid concentrations in bone as well as the exposure (AUC ratios) of these drugs in bone relative to serum. Our third objective was to calculate the probability to attain the PKPD targets for bacteriostasis and near-maximal bacterial killing (67, 89) in serum, cortical and cancellous bone. We derived the PKPD breakpoints and calculated the PTA expectation values for target attainment against *S. aureus*, *S. epidermidis*, and *S. saprophyticus* based on published MIC distributions.

5.3.3   Methods

Study design and drug administration: Twenty patients (9 males, 11 females) who were scheduled to undergo total hip replacement

participated in the study. Their average ± SD weight was 78 ± 12 kg, height was 169 ± 9 cm and age was 63 ± 16 years. Each patient received a single dose of 2000 mg amoxicillin in combination with 200 mg clavulanic acid (Augmentan®) as intravenous short-term infusion at the induction of anesthesia.

Determination of Serum and Bone Concentrations: Serum and bone samples were obtained as described in chapter 2.3. For determination of amoxicillin and clavulanic acid in plasma, 50µL of ammonium acetate buffer containing the internal standard were added to 100µL of each sample. The samples were deproteinized by addition of 300µL acetonitrile. After thorough mixing, the samples were centrifuged and 50µL of the clear supernatant were analyzed by LC-MS/MS. For analysis of bone samples, an aliquot of the bone powder was shaken with 6 times the amount of buffer for 4h. After centrifugation, 50µL of buffer containing the internal standard were added to 50µL of the aqueous supernatant. After addition of 175µL acetonitrile, the samples were thoroughly mixed and centrifuged. The clear supernatant was diluted by twice the amount of buffer.

For determination of amoxicillin, 50µL of each sample were chromatographed on a reversed-phase column (Ultracarb 5 ODS 30) and eluted by an isocratic solvent system consisting of 0.001 M ammonium acetate buffer and acetonitrile (90/10, v/v). The samples were monitored by LC-MS/MS with a SRM method as follows: Precursor → product ion for amoxicillin m/z 366 → m/z 208 and internal standard m/z 350 → m/z 160. Both analyses were in positive mode. Under these conditions amoxicillin and the internal standard were eluted after approximately 0.8 min.

For determination of clavulanic acid, 25µL of each sample were chromatographed on a reversed-phase column (Nucleosil 100 Amino) and eluted by an isocratic solvent system consisting of 0.01 M ammonium acetate buffer and acetonitrile (40/60, v/v). The samples were monitored by LC-MS/MS with a SRM method as follows: Precursor → product ion for clavulanic acid m/z 198 → m/z 108 and internal standard m/z 232 → m/z 140. Both analyses were in negative mode. Under these conditions clavulanic acid and

the internal standard were eluted after approximately 2min. The MacQuan software was used for evaluation of chromatograms. The precision and accuracy of the SQCs for amoxicillin (clavulanic acid) in serum ranged from 1.8 to 10% (0.8 to 4.8%) and from 97.3 to 107.8% (96.0 to 100.5%), respectively. The precision and accuracy of the SQCs for amoxicillin (clavulanic acid) in bone homogenate ranged from 5.8 to 8.1% (5.0 to 7.8%) and from 97.2 to 99.5% (91.7 to 100.0%), respectively.

Pharmacokinetics

Population PK analysis: We used a model with two compartments for amoxicillin and one compartment for clavulanic acid to describe the serum concentrations. We added a bone compartment to describe the bone penetration and used a time constrained zero-order input. The predictive performance of our final model was tested via visual predictive checks.

Structural model: We had observations for amoxicillin and clavulanic acid concentrations in serum, cortical bone, and cancellous bone. The differential equations for amoxicillin were as follows:

$$\frac{dX(1)}{dt} = \text{input rate} - \left[\frac{CL + CLic + CLic_{Bone}}{V_{Central}}\right] \cdot X(1)$$
$$+ \frac{CLic}{V_{Peripheral}} \cdot X(2) + \frac{CLic_{Bone}}{V_{Bone}} \cdot X(3)$$

Formula 5.3-1

$$\frac{dX(2)}{dt} = \frac{CLic}{V_{Central}} \cdot X(1) - \frac{CLic}{V_{Peripheral}} \cdot X(2)$$

Formula 5.3-2

$$\frac{dX(3)}{dt} = \frac{CLic_{Bone}}{V_{Bone}} \cdot X(1) - \frac{CLic_{Bone}}{V_{Bone}} \cdot X(3)$$

Formula 5.3-3

Compartment 1 is the central compartment. Compartment 2 is the peripheral compartment. Compartment 3 is the bone compartment. $X(1)$, $X(2)$ and $X(3)$ denote the amounts of drug in the respective compartment. CL is the total clearance from the central compartment, CLic is the intercompartmental clearance between the central and peripheral compartment, and $CLic_{Bone}$ the intercompartmental clearance between the central and the bone compartment. $V_{Central}$, $V_{Peripheral}$ and V_{Bone} are the volumes of distribution of the

respective compartment. The differential equations for clavulanic acid can be obtained from the above equations by setting CLic to zero. The raw data and initial models showed that the rates of equilibration between serum and cortical as well as between serum and cancellous bone were very similar. Therefore we used only one bone compartment.

We included scale terms for the concentrations in cortical and cancellous bone that describe the equilibrium concentration ratio between cancellous bone and serum ($F_{cancellous}$) and between cortical bone and serum ($F_{cortical}$). $F_{cortical}$ equal to 1 means that the concentrations at steady-state after a continuous infusion are the same in cortical bone and serum, $F_{cortical}$ smaller (greater) than 1 means that these concentrations are lower (higher) in cortical bone than in serum.

We had sparse serum concentration time data between 0 and 1.1h post end of infusion. Therefore, these data did not allow us to estimate all PK parameters of the population PK model. We derived the average disposition parameters for the serum concentration profiles and their variability from published studies (9, 17, 142, 152, 241, 248). As those studies were conducted in healthy volunteers, we used the amoxicillin clearance reported by Sjovall et al. (276) for elderly subjects. This was in agreement with the age-related decrease in renal function predicted by the Cockcroft and Gault formula (63) based on the clearance from the other studies. For clavulanic acid we accounted for the age-related decrease in renal function according to the Cockcroft and Gault formula.

The disposition parameters of amoxicillin and clavulanic acid from literature have been determined in absence of a bone compartment. Therefore, we had to keep the amount of amoxicillin and clavulanic acid in the bone compartment of our model minimal so that the serum PK was not affected by the presence of the bone compartment. This can be achieved by choosing a small volume V_{Bone} for the bone compartment.

Between subject variability and observation model: We estimated the BSV for $F_{cortical}$ and $F_{cancellous}$. The residual unidentified variability was described by a proportional error model for serum and bone concentrations.

Extent of drug exposure in bone: We determined the extent of drug exposure in bone for amoxicillin and clavulanic acid by simulating the AUCs in serum, cortical and cancellous bone. We simulated 10,000 virtual subjects at steady-state and calculated the individual ratios of AUC in bone / serum as well as their BSV.

Monte Carlo simulation: We used $fT_{>MIC}$ for at least 30% or 50% of the dosing interval as PKPD targets for amoxicillin. We studied a range of MICs from 0.25 to 64 mg/L and used a protein binding of 18% for amoxicillin (124). In absence of data on protein binding in bone, a protein binding of 18% in bone was assumed. We studied a 30min infusion of 2000 mg amoxicillin q4h, q6h, or q8h at steady-state and simulated 10,000 virtual subjects in absence of residual error. The PTAs and the PKPD breakpoints were derived from those simulated profiles. We calculated the PTA expectation value based on published MIC distributions. These comprised susceptibility data on MSSA, *S. epidermidis,* and *S. saprophyticus* from North America (141).

5.3.4   Results

The concentrations of amoxicillin and clavulanic acid in serum, cortical and cancellous bone are shown in Figure 5.3-1. Samples of femoral neck were available only from 8 patients. These were not enough samples to account for differences between femoral head and femoral neck in the PK model.

Figure 5.3-1   Concentrations in serum and bone of subjects undergoing hip replacement surgery after a single intravenous dose of 2000 mg amoxicillin and 200 mg clavulanic acid.
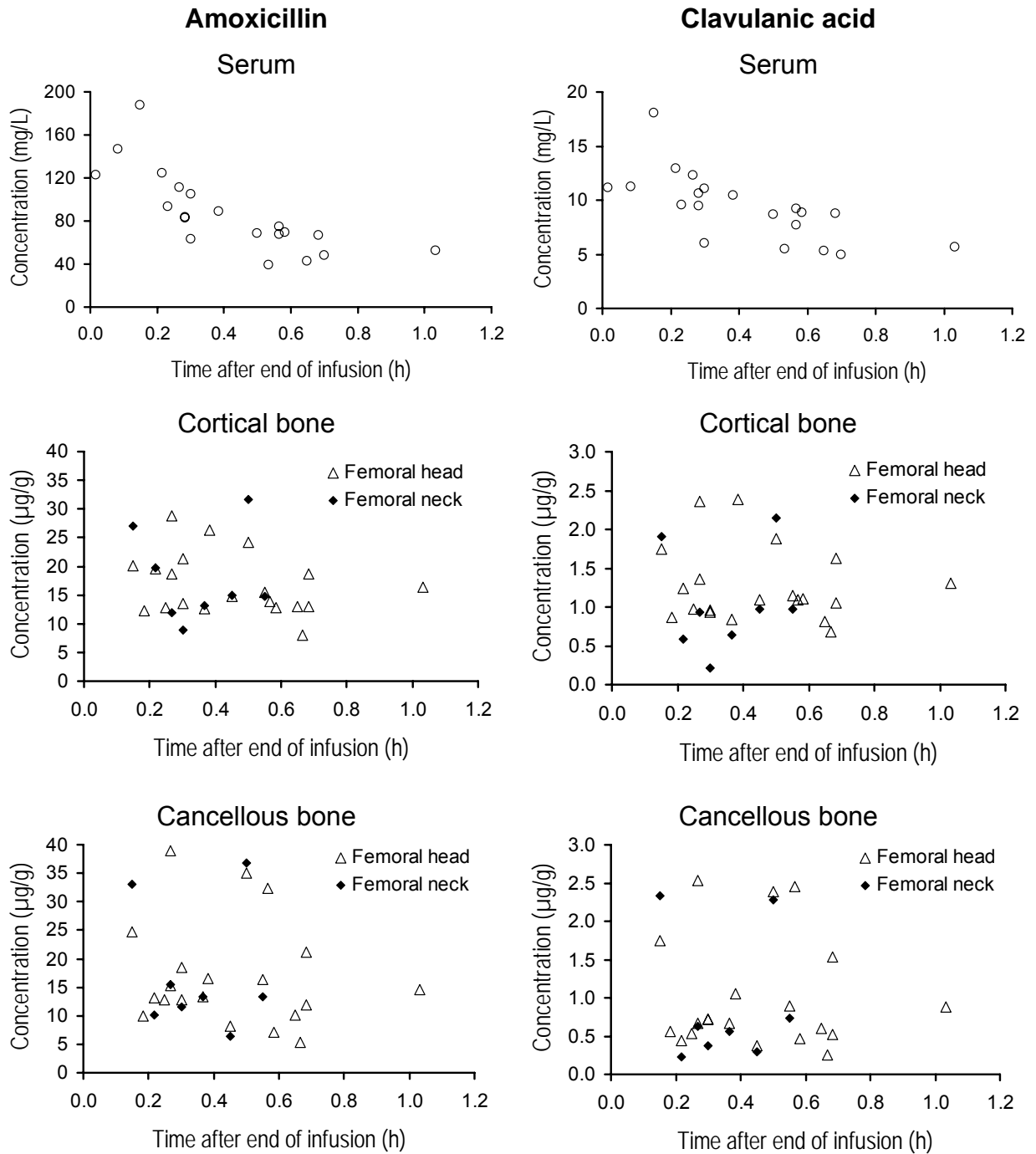
The concentrations of both drugs were lower in cortical and cancellous bone than in serum. The concentration ratios between bone and serum samples are shown in Figure 5.3-2 for amoxicillin versus clavulanic acid.

Page 195

Figure 5.3-2   Concentration ratios of amoxicillin versus clavulanic acid

Cortical bone

$y = 1.54x$
$R^2 = 0.81$

Cancellous bone

$y = 1.85x$
$R^2 = 0.90$
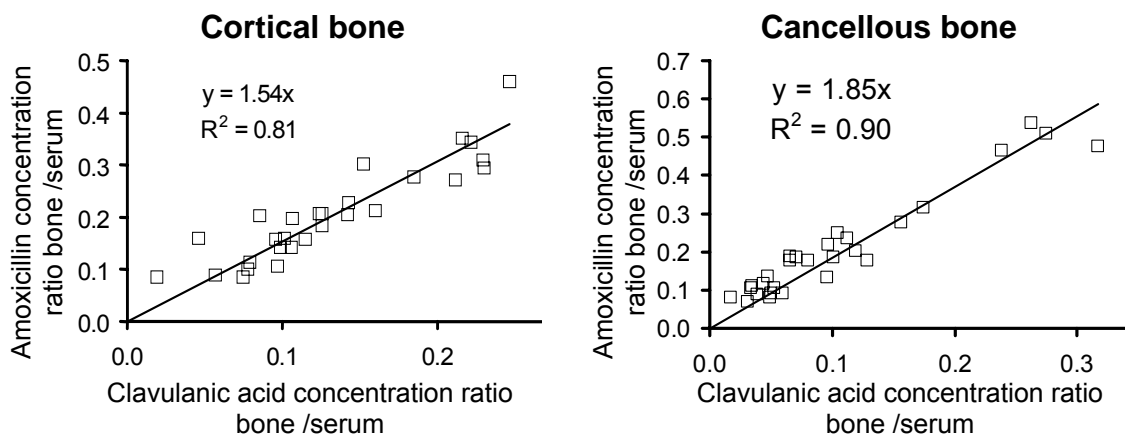
Population Pharmacokinetics: The final parameter estimates of the population PK model and their between subject coefficients of variation are shown in Table 5.3-1.

Table 5.3-1   PK parameter estimates and coefficients of variation for the between subject variability

Parameter	Unit	Estimate (%CV)	
		Amoxicillin	Clavulanic acid
CL	$L\,h^{-1}$	12.4 (19%)	11.0 (6.2%)
$V_{Central}$	L	11.3 (12%)	16.7 (25%)
$V_{Peripheral}$	L	6.17 (3.7%)	
CLic	$L\,h^{-1}$	11.1 (19%)	
$T_{1/2,Equilibration}$	min	11.8	14.0
$F_{Cortical}$		0.199 (11%)	0.156 (17%)
$F_{Cancellous}$		0.192 (39%)	0.119 (57%)

CL is the total clearance from the central compartment. $V_{Central}$ is the volume of distribution of the central compartment and $V_{Peripheral}$ the volume of distribution of the peripheral compartment. CLic is the intercompartmental clearance between the central and the peripheral compartment. $T_{1/2,Equilibration}$ is the half-life of equilibration between serum and bone. $F_{Cortical}$ and $F_{Cancellous}$ describe the equilibrium concentration ratio between bone and serum (see chapter 5.3.3 for details).

Figure 5.3-3 shows the extent of amoxicillin and clavulanic acid penetration into cortical and cancellous bone, and its BSV, calculated from the ratios of $AUC_{cortical}$ / AUC_{serum} and $AUC_{cancellous}$ / AUC_{serum} at steady-state for 10,000 virtual subjects. The median AUC ratio of amoxicillin [10% - 90% percentile for the BSV] was 20% [16% - 25%] for cortical bone and 18% [11% - 29%] for cancellous bone. The median AUC ratio of clavulanic acid [10% - 90% percentile for the BSV] was 15% [11% - 21%] for cortical bone and 10% [5.1% - 21%] for cancellous bone. Therefore, for both drugs the AUC ratio for cancellous bone was more variable and (slightly) lower than for cortical bone. The AUC ratios were lower for clavulanic acid than for amoxicillin.

Figure 5.3-3   AUC ratios between bone and serum at steady-state. The plots show the median, interquartile range, and 10-90% percentiles.
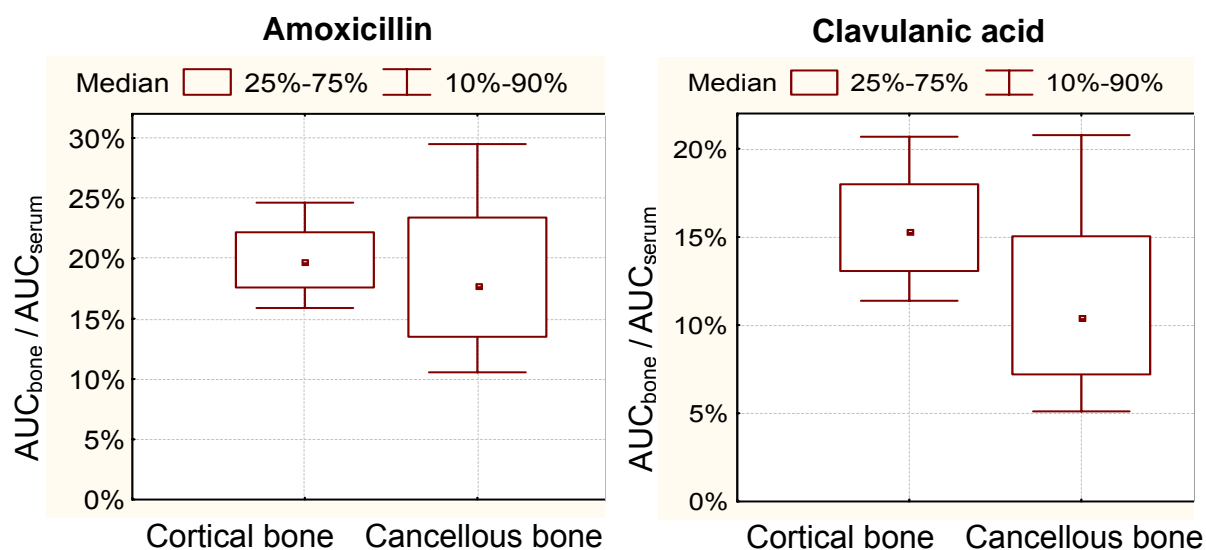
The rate of equilibration between serum and bone was fast for both drugs. The estimate for the equilibration half-life was about 12min for amoxicillin and 14min for clavulanic acid. The visual predictive checks showed a highly sufficient predictive performance of the final model for both drugs (Figure 5.3-4). This qualified our model for use in the MCS.

Figure 5.3-4   Visual predictive check after 2000 mg amoxicillin and 200 mg clavulanic acid (30min iv infusion)
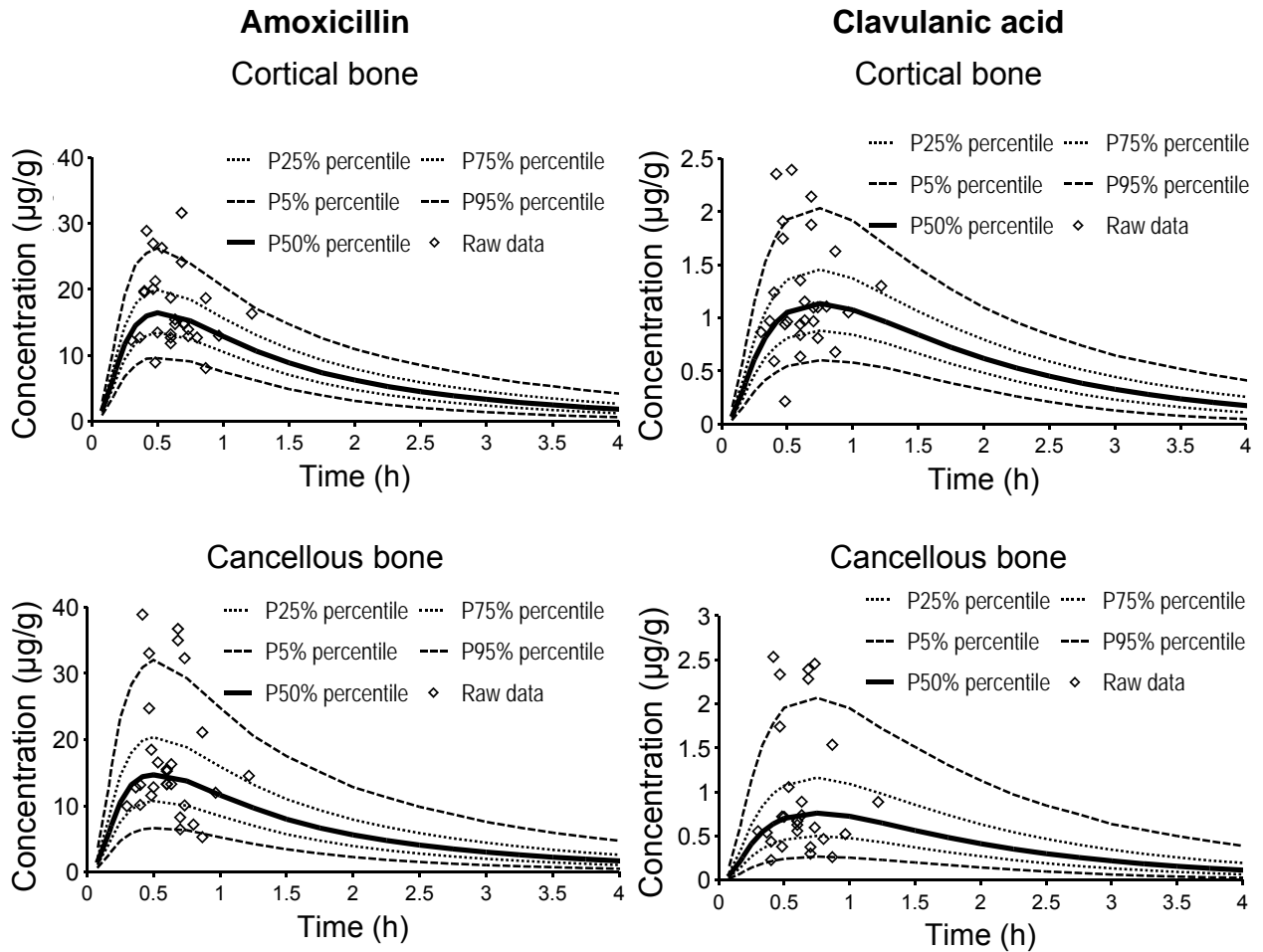
See chapter 2.6.5 and Figure 5.2-3 for explanation of the plots.

Monte Carlo simulation of amoxicillin's PKPD: The PTA versus MIC profiles are shown in Figure 5.3-5, and the PKPD breakpoints for serum, cortical bone and cancellous bone are listed in Table 5.3-2.

Figure 5.3-5

─△─ Cancellous bone

─⊟─ Cortical bone

─◆─ Serum

Probabilities of target attainment for serum, cortical and cancellous bone after 2000 mg amoxicillin (and 200 mg clavulanic acid) as 30min infusion at steady-state.

Target $fT_{>MIC} \geq 30\%$
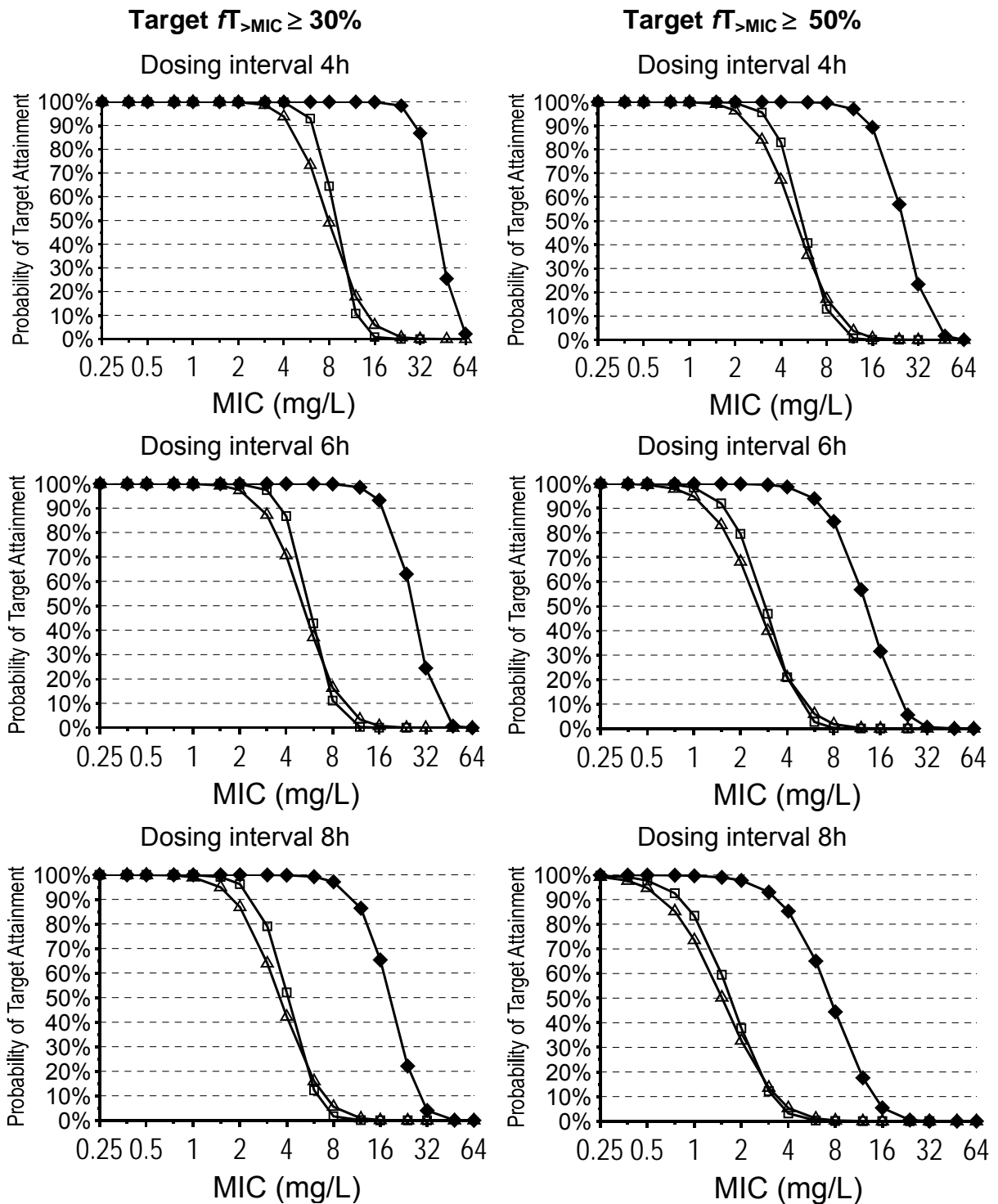
Target $fT_{>MIC} \geq 50\%$

Table 5.3-2   PKPD breakpoints for amoxicillin in serum, cortical and cancellous bone for 30min infusions of 2000 mg amoxicillin and 200 mg clavulanic acid q4h, q6h, or q8h at steady-state.

Target $f\text{T}_{>\text{MIC}}$	Dosing interval	PKPD breakpoint		
		Serum (mg/L)	Cortical bone (µg/g)	Cancellous bone (µg/g)
30%	4h	24	6	4
30%	6h	16	3	2
30%	8h	8	2	1.5
50%	4h	12	3	2
50%	6h	6	1.5	1
50%	8h	3	0.75	0.5

The breakpoints were about 4 times higher in serum than in cortical bone, and about 6 times higher in serum than in cancellous bone. The PTA expectation values for the MIC distributions of three different pathogens are shown in Table 5.3-3. With dosing intervals of 4h or 6h, PTA expectation values above 90% were achieved against MSSA and *S. saprophyticus* in serum, cortical and cancellous bone, based on the target $f\text{T}_{>\text{MIC}} \geq 50\%$ for near-maximal killing. For *S. epidermidis*, a dosing interval of 4h was required to reach PTA expectation values above 80% in bone.

5.3.5   Discussion

There is a wide variability of the reported bone concentrations for amoxicillin and clavulanic acid in literature. One possible reason could be that the determination of concentrations in bone is methodologically more complex than in serum. Another reason might be that most bone penetration studies in the past used microbiological assays. In the study described here a highly standardized LC-MS/MS method was used. More specifically, we used pulverization under liquid nitrogen by a cryogenic mill, as a very efficient method for sample preparation that allows reproducible extraction of amoxicillin and clavulanic acid from the resulting bone powder. A rapid and

efficient extraction of an unstable drug like clavulanic acid may be critical for studying its bone penetration. The degree of extraction was tested over time to ensure reproducible results. Amoxicillin and clavulanic acid remained stable during the 4h extraction period.

Table 5.3-3   Comparison of the PTA expectation values for target attainment against MSSA, *S. epidermidis*, and *S. saprophyticus* (141) for amoxicillin (30min infusion of 2000 mg amoxicillin and 200 mg clavulanic acid at steady-state).

Target fT$_{>MIC}$	Dosing interval	MSSA (n=196 isolates)	S. epidermidis (n=119)	S. saprophyticus (n=75)
		Serum		
30%	4h	99.5%	99.7%	100%
30%	6h	97.2%	98.0%	100%
30%	8h	96.4%	96.8%	100%
		Cortical bone		
30%	4h	95.7%	93.4%	99.5%
30%	6h	95.3%	87.7%	98.8%
30%	8h	94.8%	80.9%	98.7%
		Cancellous bone		
30%	4h	95.6%	91.5%	99.3%
30%	6h	95.1%	85.1%	98.9%
30%	8h	94.2%	77.9%	98.7%
		Serum		
50%	4h	97.2%	97.9%	100%
50%	6h	96.0%	95.1%	99.8%
50%	8h	95.3%	89.4%	99.2%
		Cortical bone		
50%	4h	95.3%	87.2%	98.9%
50%	6h	93.6%	72.9%	98.6%
50%	8h	86.5%	60.3%	96.1%
		Cancellous bone		
50%	4h	95.1%	84.4%	98.9%
50%	6h	92.0%	70.4%	98.1%
50%	8h	81.8%	57.7%	93.2%

Some authors studied the bone penetration of amoxicillin and clavulanic acid. Grimer et al. (132) report average concentrations of 3.6 mg/L amoxicillin and 0.54 mg/L clavulanic acid in bone about 30min after intravenous injection of 1000 mg amoxicillin and 200 mg clavulanic acid q6h at steady-state (on day 2). They found at least 10 times lower concentrations in bone than in serum, and amoxicillin and clavulanic acid did not accumulate after multiple administration (132). Weismeier et al. (328) administered 2000 mg amoxicillin and 200 mg clavulanic acid by intravenous infusion. They determined the concentration in the organic bone mass which accounted for about 30 to 40% of total bone mass in their samples. They found slightly higher concentrations in cortical than in cancellous bone. Related to total bone, their average amoxicillin concentrations were about 8 mg/kg during the first 2h, and about 2.5 mg/kg between 2 and 4h after the dose, average clavulanic acid concentrations were about 0.7 to 0.8 mg/kg during the first 2h, and about 0.3 mg/kg between 2 and 4h after the dose. Average concentration ratios in total bone / serum were about 8 to 14% during the first 2h, and 15 to 18% between 2 and 4h after the dose for amoxicillin, and 4 to 8% during the first 2h, and 6 to 7% between 2 and 4h after the dose for clavulanic acid (328) related to total bone mass.

More recently, Jehl et al. (160) investigated concentrations of amoxicillin and clavulanic acid in 63 patients after multiple oral administration of amoxicillin / clavulanic acid (1g / 125 mg twice daily or 500 mg / 125 mg three times daily). Between 1.5h and 8h after the last dose, bone / serum concentration ratios of amoxicillin ranged between 0.09 and 0.44. Jehl et al. (160) determined the time above MIC for amoxicillin, probably by using the naïve averaging approach. For an MIC of 1 mg/L bone concentrations were above the MIC for 50% of the dosing interval with the 1g dose of amoxicillin twice daily, and for 37.5% of the dosing interval with the 500 mg dose three times daily. However, this approach neglects the BSV and therefore does not allow to determine a PKPD breakpoint.

Adam et al. (3) find 9.8 mg/kg clavulanic acid in cortical bone and 15 mg/kg in cancellous bone, between 0.5 and 1h after the end of a 20min infusion of 200 mg clavulanic acid. Grimer et al (132), Weismeier et al. (328),

and Adam et al. (3) used microbiological assays for determination of drug concentrations. Dose-normalized amoxicillin and clavulanic acid concentrations in bone found by Grimer et al. (132) and Weismeier et al. (328) are approximately 2 to 3 times lower than the concentrations in our study, whereas Adam et al. (3) report approximately 10 times higher concentrations of clavulanic acid compared to our study (Figure 5.3-1). This pronounced (20 to 30-fold) difference for clavulanic acid underlines the need for standardized methods for sample preparation, drug analysis and PK analysis.

We found lower concentrations for amoxicillin and clavulanic acid in both cortical and cancellous bone compared to serum. Similar concentrations were found in femoral head and femoral neck (Figure 5.3-1). As we had only concentrations in femoral neck for eight patients, our final model did not differentiate between femoral head and femoral neck. Concentrations of amoxicillin and clavulanic acid showed a high correlation in cortical (r=0.90, from raw data) as well as in cancellous bone (r=0.95 from raw data, see also Figure 5.3-2). This suggests that both drugs were stable, and sample preparation and drug analysis were precise and reproducible.

Our concentrations in cortical and cancellous bone were also correlated for both drugs (r=0.76 for amoxicillin, r=0.75 for clavulanic acid). This correlation was in agreement with the results from Weismeier et al. (328) and indicated that the rate of equilibrium between cortical bone and serum was probably similar to that between cancellous bone and serum. When we estimated different equilibration half-lives for these two processes, we obtained very similar estimates for both half-lives. Consequently, we assumed both equilibration half-lives to be the same in our final model. Although bone is not one of the most highly vascularised tissues, we observed short equilibration half-lives between bone and serum of about 12min for amoxicillin and of 14min for clavulanic acid (Table 5.3-1 and Figure 5.3-4). Therefore, the peak concentration in bone will be reached within less than 45min post end of a 30min infusion for most subjects. As the concentrations are decreasing in serum and bone after the end of a short-term infusion, these fast equilibration half-lives would suggest from a PK point of view that the surgery should start within the first 30min post end of a 30min infusion. However, clinical

effectiveness studies of amoxicillin/clavulanic acid are warranted to support this suggestion and the PKPD target for surgical prophylaxis needs to be determined.

The AUC in bone was lower than in serum for both drugs. We found median (90% prediction interval for the BSV) ratios for AUC(bone) / AUC(serum) of 20% [16% - 25%] for cortical bone and 18% [11% - 29%] for cancellous bone for amoxicillin and of 15% [11% - 21%] for cortical bone and 10% [5.1% - 21%] for cancellous bone for clavulanic acid. Therefore, the AUCs of amoxicillin in bone were on average about 5 to 6 times lower than in serum and the AUCs of clavulanic acid in bone were on average about 6 to 10 times lower than in serum. For both drugs the AUC ratio for cancellous bone was (slightly) lower than for cortical bone. This is in agreement to the data from Weismeier et al. (328). The BSV of bone penetration was substantially larger for cancellous bone than for cortical bone (see also variability for $F_{Cortical}$ and $F_{Cancellous}$ in Table 5.3-1) for both drugs.

We used our final population PK model to calculate the PTA vs. MIC profiles and the PKPD breakpoints for amoxicillin in bone and serum for three different dosing intervals. For a 4h dosing interval, amoxicillin achieved robust (≥90%) PTAs in serum for MICs ≤24 mg/L for the bacteriostasis target ($fT_{>MIC}$ ≥ 30%) and for MICs ≤12 mg/L for the near-maximal killing target ($fT_{>MIC}$ ≥ 50%). The corresponding PKPD breakpoints in cortical and cancellous bone for amoxicillin were 4-6 mg/L for the bacteriostasis target and 2-3 mg/L for the near-maximal killing target (Table 5.3-2).

In order to put these PTAs into clinical perspective, we calculated the PTA expectation values based on published MIC distributions for MSSA, *S. epidermidis*, and *S. saprophyticus* which are frequently involved in prosthesis related bone infections. Amoxicillin achieved excellent (>90%) PTA expectation values against MSSA and *S. saprophyticus* for both targets in bone and in serum for 30min infusions of 2000 mg / 200 mg amoxicillin / clavulanic acid q4h and q6h (Table 5.3-3). As the *S. epidermidis* isolates were less susceptible to amoxicillin / clavulanic acid, the PTA expectation values were slightly lower for this pathogen. If 2000 mg / 200 mg amoxicillin /

clavulanic acid were dosed q4h, the PTA expectation values were above or equal to 90% for the bacteriostasis target and above 80% for the near-maximal killing target for *S. epidermidis*. The susceptibility patterns of each local hospital should be used to decide, whether amoxicillin / clavulanic acid will be a promising choice for treatment of bone infections.

In conclusion, we found ratios for AUC(bone) / AUC(serum) of 20% [16% - 25%] for cortical bone and 18% [11% - 29%] for cancellous bone for amoxicillin and of 15% [11% - 21%] for cortical bone and 10% [5.1% - 21%] for cancellous bone for clavulanic acid (median [90% prediction interval for the BSV]). Equilibration between serum and bone was rapid with a half-life of about 12min for amoxicillin and 14min for clavulanic acid. From a PK point of view, this suggests that the surgery should start within the first 30min post end of a 30min infusion. Assuming a 4h dosing interval, amoxicillin achieved robust ($\geq$90%) PTAs for MICs $\leq$12 mg/L in serum and 2-3 mg/L in cortical and cancellous bone for the near-maximal killing target ($fT_{>MIC} \geq 50\%$). Amoxicillin achieved excellent (>90%) PTA expectation values against MSSA and *S. saprophyticus* for both targets in bone and in serum for 30min infusions of 2000 mg / 200 mg amoxicillin / clavulanic acid q4h and q6h. Slightly lower PTA expectation values were found for *S. epidermidis*. Clinical studies are warranted to evaluate these results for amoxicillin / clavulanic acid in treatment and surgical prophylaxis.

5.4 Critical view on assessment of bone penetration studies and future perspectives

5.4.1 Advantages of population pharmacokinetics and Monte Carlo simulations for bone penetration studies

Modeling the full serum and bone concentration time course is required to describe the rate and extent of drug penetration into bone and to study the PD profile in bone. For experimental reasons, only sparse concentration data can be obtained in bone penetration studies (usually one bone sample per patient). Therefore population PK modeling is needed to analyze these sparse datasets. By the STS approach it is mathematically not possible to model sparse data. The naïve averaging approach (chapter 5.1.3) has severe methodological shortcomings, as it ignores the BSV. Population PK modeling considers the full time course of penetration and allows one to calculate the extent of penetration by the ratio of AUCs in tissue and serum. As the concentration ratios between tissue and serum change over time, an AUC ratio is a better measure for the extent of penetration than concentration ratios. Comparing concentration ratios between studies is difficult due to the different sampling times and different dosage regimens. A comparison between studies is much more useful, if AUC ratios are reported. To obtain reliable estimates for these ratios, population PK analysis is a powerful approach.

Especially for sites of infections that may not be in a rapid equilibrium with the blood stream, it is important to predict the probability of successful outcome based on concentrations at the site of infection. Serum concentrations might not be such a good surrogate marker in this case. Based on a population PK model, MCS may be used to estimate PTAs for the desired PD endpoint (e.g. successful microbiological outcome) in bone as well as in serum. Evaluation of a PKPD target in bone would probably allow one to obtain more reliable predictions for outcome of bone infections, than by use of

a PKPD target established in serum. However our bone penetration studies showed that the equilibration between bone and serum had a half-life of < 30min for amoxicillin, clavulanic acid, and moxifloxacin.

Appropriate PKPD targets in bone may be derived in studies where both, the time course of the bone concentration profiles and the treatment outcome, are determined, e.g. in osteomyelitis patients. Based on such a validated target in osteomyelitis patients, optimal dosage regimens for treatment of these patients with bone infections can be derived. Future studies will have to show if a PKPD target in bone better predicts the outcome than a PKPD target in serum.

5.4.2   Strengths and limitations of our bone penetration studies

Quantification of a drug in bone requires more extensive procedures than in serum. Therefore the use of a standardized and validated analytical method is very important to obtain reliable estimates of antimicrobial bone penetration. In our studies pulverization of the bone samples under liquid nitrogen by a cryogenic mill was used to ensure efficient and reproducible extraction of the study drugs. The degree of extraction over time was monitored and the stability of the study drugs during the extraction was tested. Moxifloxacin, amoxicillin and clavulanic acid remained stable during the extraction period. For studying the bone penetration of an unstable drug like clavulanic acid, a rapid and efficient extraction is probably critical. Contrary to many studies in literature, our spiked quality controls were prepared with bone tissue. We assured that those bone tissue samples were free of the study drug.

A highly precise and reproducible analytical method (including sample preparation) needs special attention for datasets which contain only one sample per patient for experimental reasons. The total variability of the observed bone concentrations is determined by two components: 1) between subject variability and 2) residual unexplained variability (primarily) due to analytical imprecision (besides other factors). Those two types of variability

cannot be separated mathematically, if there is only one sample per patient for the bone matrix.

There are two extreme cases: a) If there was no (or only negligible) analytical imprecision, all the observed variability would represent BSV. b) If the assay or sample preparation was very imprecise and if BSV was relatively small, almost all of the observed variability in bone concentrations would be due to analytical error. In real life, the results fall between those two extremes and the data analyst has to pre-specify a realistic estimate for the analytical precision in bone. It is possible to suggest a value and justify the chosen pre-specified value for the residual variability e.g. via visual predictive checks, but there is no proof for such a choice to be optimal.

If one is only interested in the average bone concentrations, a precise analytical assay is important, but not vital. However, if one wishes to apply Monte Carlo techniques and explicitly accounts for the BSV in those simulations, obtaining a realistic (unbiased) estimate for the BSV is vitally important.

As described above, a population PK model estimates the BSV of bone penetration and accounts for the full time course of penetration. Thus, population PK allows one to calculate the extent and time course of tissue penetration. Unlike the naïve averaging approach, population PK and MCS consider both the average antibiotic penetration into bone as well as its BSV. Therefore, we used population PK and MCS to determine the variability of bone penetration and to predict the PTAs and PTA expectation values for the desired targets in serum and bone. The PTA expectation value is especially helpful, since it can be used to predict the probability of successful treatment in a local hospital. We are not aware of any reports about PKPD modeling of quinolones or beta-lactams in bone in humans or animals.

One limitation of our study is that we had only sparse serum and bone concentration time data between 2 and 7h post oral administration for moxifloxacin and between 0 and 1.1h post end of infusion for amoxicillin / clavulanic acid. We did not apply optimal sampling time theory to assign sampling times or sampling time windows for our bone penetration studies. Our bone penetration datasets did not allow us to estimate the PK parameters

of a full population PK model. Consequently, we used MAP-Bayesian estimation of the individual PK parameters by including prior information from literature for moxifloxacin. In the case of very sparse data, MAP-Bayesian estimation is a powerful method to estimate the individual PK parameters. For amoxicillin / clavulanic acid we derived the average disposition parameters and their variability from published studies and used these in our population PK model.

5.4.3   Application of optimal sampling times

Generally, in patients undergoing joint replacement, only one bone sample can be obtained per subject, which yields very sparse bone penetration data. If not all samples are collected within a narrow time window, but are spread throughout the whole concentration time course, usually more information can be gained about the distribution into and about the redistribution out of the bone tissue.

It is important to take those precious bone samples at the most informative time points. Informative refers to the ability to estimate the rate and extent of bone penetration most precisely. Optimal sampling time theory has been introduced in PK more than two decades ago by D'Argenio (73). In bone penetration studies, one wishes to estimate the rate and extent of bone penetration as well as their between patient variability, i.e. the full range of observed bone penetration time curves.

While the optimal sampling time algorithm introduced by D'Argenio originally aimed at providing optimal sampling times for one individual patient, this theory has been extended to optimal sampling times for a population of patients. Optimal sampling times for a population aim at estimating the parameters of a population PK model for bone penetration most precisely (58, 94-96, 128, 130, 222, 238, 256, 300). Thus, the best estimates for the average rate and extent of penetration as well as their variability should be achieved. Optimal sampling times for a population of patients usually comprise optimal sampling time windows. Those time windows could e.g. state that from eight patients the bone sample has to be taken between 10

and 30min post end of infusion, from eight patients between 1 and 2h, and from eight patients between 5 and 7h post end of infusion. A detailed description of optimal sampling time is beyond the scope of this thesis. However, it should be pointed out that the application of this theory may greatly improve the precision of the results and conclusions that are drawn from such studies.

5.4.4   Importance of clinical trial design for future studies

As outlined above, clinical trial design may be very valuable especially for studies where only sparse data can be collected. Optimal trial design allows one to choose optimal sampling time windows, so that the optimal information can be gained from a limited number of samples. Ideally, optimal design theory should be applied while planning a clinical study. Its application may reveal that the number of patients originally planned is not sufficient to draw the desired conclusions with an adequate precision. This underlines that population PK is not only an option for data evaluation after conclusion of the analytical part of a study, rather than that data collection, bio-analysis, and data analysis are often very amalgamated.

Optimal trial design aims at estimating the population PK parameters with at least a pre-specified precision. This yields more reliable predictions for the PTA in subsequent PD simulations. Application of clinical trial design with optimal sampling time windows may also allow one to study less patients and might therefore be advantageous also for ethical reasons.

6 Strengths, weaknesses, and alternative approaches

6.1 Assessment of dose linearity and saturable elimination

6.1.1 Alternative approaches

The presence of linear PK is often investigated by use of a crossover study with ascending dose levels. The area under the plasma concentration time curve (AUC) is usually plotted against the administered dose. Alternatively, the dose normalized AUC is compared at various dose levels. Such a simulated data example is shown in Figure 6.1-1.

Figure 6.1-1   Average ± SD AUCs of a simulated data example for assessment of dose linearity
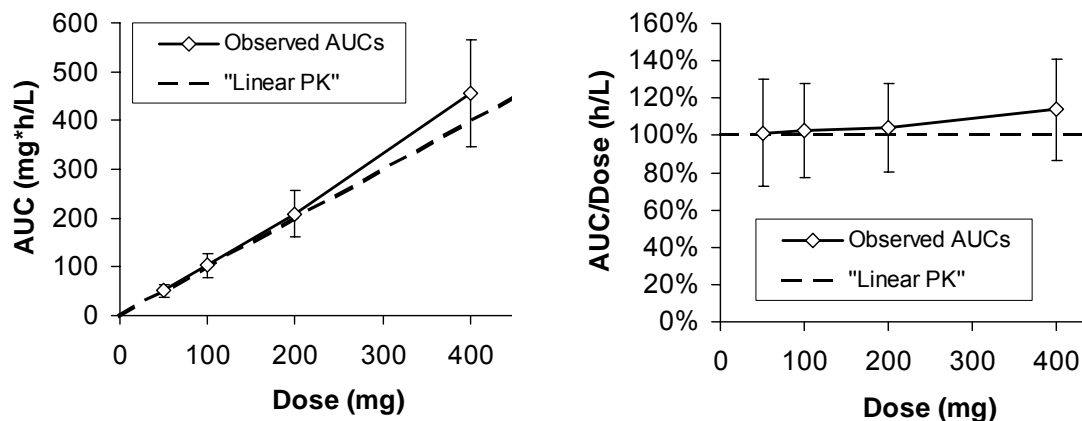
The AUCs shown in Figure 6.1-1 are most often calculated by NCA and could also be calculated by the STS approach. This simulation example suggests a slightly more than proportional increase of AUC with dose. The AUC vs. dose data are sometimes fitted by a power model by use of the following equation:

$$AUC = a \cdot Dose^{b} \hspace{3cm} \text{Formula 6.1-1}$$

This equation converges to a simple linear relationship between AUC and dose, if the exponent "b" is 1.0. Conversely, if "b" is significantly different from 1.0, the nonlinearity is concluded to be statistically significant.

At this point, there are several possibly important questions:

1.) Is the deviation from dose linearity statistically significant?

2.) What is the extent of saturation at the studied dose levels?

3.) Is the nonlinearity only observed in some patients (e.g. patients with "special" demographic characteristics)?

4.) Is the deviation from dose linearity clinically significant?

5.) What are possible mechanisms of the nonlinearity?

6.) Which extent of saturation would be expected at doses that are higher or lower than the studied doses (extrapolation)?

There are three different data analytical methods which are commonly applied to answer some or all of those questions:

a) Assessment of PK parameters by NCA and comparison of AUCs by ANOVA statistics to test for statistical significance between dose levels. Additionally, equivalence statistics are often applied to assess the extent of nonlinearity.

b) Assessment of PK parameters by NCA and use of the power model (as shown above) to describe the AUC vs. dose relationship.

c) Population PK analysis of the plasma concentration time raw data.

Those three methods differ in their ability to answer the above mentioned questions and are compared in Table 6.1-1. As shown in this table, population PK in combination with MCS is the most powerful approach to study linear vs. nonlinear PK. The only drawback of this method is the time it takes to prepare the raw data and the computation time to run the analysis. Probably the most important advantage of population PK analysis compared to the other two methods is the ability of population PK to predict the clinical significance by use of a PKPD model and MCS.

Table 6.1-1   Comparison of three approaches to assess the importance
of nonlinear PK

	Method 1 **NCA + ANOVA statistics**	**Method 2** **NCA + power model**	**Method 3** **Population PK analysis**
Statistical significance	applicable, by ANOVA statistics	applicable	applicable
Extent of saturation at the studied dose levels	applicable, by equivalence statistics	partly applicable	applicable
Method accounts for between subject variability	yes	no (for standard power model)	yes
Saturation in special patient groups (demographic model)	may be inefficient and difficult to implement	cannot be assessed	most appropriate method
Clinical significance	cannot easily be assessed	cannot easily be assessed	assessable by Monte Carlo simulations
Possible mechanism	very difficult to assess, inefficient	cannot be assessed	can be directly estimated, most powerful method
Extent of saturation at higher or lower dose levels (extrapolation)	extrapolation lacks scientific basis	extrapolation lacks scientific basis	extrapolation has a pharmacological basis
Applicable for sparse concentration time raw data	not by standard methods	not by standard methods	yes
Time for data preparation	<1h	<1h	several hours to days, may be <1h by use of software
Time for data analysis	<1h	<1h	hours to days, can be weeks (depending on complexity of problem)
Visualization of results	good for ANOVA statistics	not as good as NCA+ANOVA	ideal

6.1.2 Strengths and weaknesses of our dose linearity assessment

Strengths: We used NCA in combination with ANOVA statistics (method 1, Table 6.1-1) and population PK (method 3) to analyze the flucloxacillin and piperacillin dose linearity studies. The comparison of PK parameters at two dose levels by ANOVA directly assesses the statistical significance of the nonlinearity in PK (Table 3.2-1 and Table 3.3-1). The equivalence statistics (also shown in those two tables) provided a measure for the extent of nonlinearity at the studied dose levels.

We used population PK analysis and MCS as a powerful technique to suggest the sites and possible mechanisms of the saturable elimination of piperacillin. Additionally, we studied the possible clinical significance of the saturable elimination of piperacillin. We assessed the influence of saturable elimination for various dosage regimens at daily piperacillin doses between 6 and 18g (per 70kg body weight). To the best of our knowledge, this is the first analysis of data from a crossover study for piperacillin by population PK. We had frequent plasma and urine samples at both dose levels and we could show that this supported the estimation of the saturable renal elimination pathway. Our data were analyzed by validated HPLC methods which are often superior to bioassays.

Weaknesses: There are some weaknesses of our flucloxacillin and piperacillin studies: 1) The sample size of n=10 healthy volunteers was rather small. Therefore, it was not feasible to study the influence of covariates (e.g. demographic characteristics) on the PK. 2) Our studies were in healthy volunteers and not in ill patients. Studying healthy volunteers is probably advantageous to assess e.g. the mechanisms of renal elimination, because the BSV in healthy volunteers is often substantially lower than in patients (see chapter 1.5). However, the PK data used in a MCS should ideally arise from the patient population of interest and not from healthy volunteers. Therefore, the PTAs predicted by our simulations are probably conservative estimates for ill patients. Although those limitations exist, their influence on our conclusions on the dose linearity is probably limited to small.

6.2   Pharmacokinetic drug-drug interaction studies

6.2.1   Alternative approaches

We assessed the extent of the PK drug-drug interactions by NCA in combination with ANOVA statistics and tested for significance and equivalence (Table 4.2-2, Table 4.3-2, and Table 4.4-2). This method adequately quantifies the extent of the drug-drug interation at the studied dose levels and for the studied dosage regimens.

Additionally, we used the STS approach to construct a mechanistic population PK model. This approach is inferior to directly estimating a population PK model (e.g. with NONMEM). However, there is a substantial difference in computation time between the STS method and population PK for analysis of drug-drug interaction studies. While even our most complex models took less than 2h on a laptop PC with the STS method in WinNonlin, estimating a population PK model would require several days to weeks on the fastest available personal computer at this time. For model development and comparison, estimation of at least 10 to 20 of those population PK models would have been required. Therefore, use of population PK for our drug-drug interaction studies was not feasible.

Studies on a mechanistic model for the drug-drug interaction *in vivo* are rare in the PK literature and the STS approach is commonly applied for mechanistic models. The presence or absence of an interacting drug can be treated as a covariate within a population PK analysis. This approach is often chosen in population PK analyses of clinical trials in patients who received other medication. Those clinical trials usually do not aim at studying the mechanism of drug-drug interactions. This approach can quantify the extent of interaction at the studied dose levels, but, in contrary to a mechanistic model, it is usually not possible to draw conclusions about the mechanism and site of the drug-drug interaction. As we were interested in the mechanism of the PK drug-drug interaction, we did not select this approach.

6.2.2   Strengths and weaknesses of our drug-drug interaction
studies

Strengths: The use of STS to construct a population PK model allowed us to study a large number of mechanistic interaction models. We were especially able to study various combinations of sites and mechanisms of interaction. We could show that our population PK models constructed by the STS approach had adequate predictive performance (Figure 4.2-2 and Figure 4.4-4) which supported our selected approach and conclusions.

We studied the full time course of interaction with our interaction models (Table 4.2-3, Table 4.3-3, and Table 4.4-3) and tried to gain the maximum possible information from our data. Studying the full time course of interaction by a mechanistic model is superior to NCA, because NCA ignores the time course of interaction. Therefore, the use of NCA to draw conclusions about the mechanism of interaction is an inefficient and to some extent "wasteful" use of data and resources.

The strengths of the STS approach became especially apparent for the analysis of the ciprofloxacin metabolite data. We were interested in a possible effect of probenecid on the formation and elimination of the metabolite. We could develop a full mechanistic model which explained the full time course of the ciprofloxacin and metabolite data in plasma and urine with or without probenecid. This would not have been possible by NCA.

We used our PK parameter estimates from the STS approach to construct population PK models and to assess the clinical significance of the drug-drug interactions for clinically relevant dosage regimens for gemifloxacin (Figure 4.5-1 to Figure 4.5-3). Those simulations were helpful to balance the possible clinical benefit with the increased risk for toxicity when gemifloxacin and probenecid would be co-administered.

Weaknesses: The sample size in our interaction studies was small (less than 20 subjects per study), although we had data from crossover studies which allowed us to make intra-individual comparisons.

One limination of our interaction studies with probenecid is that the sampling times were not optimized to characterize the PK of probenecid.

Therefore, the uncertainty of our PK parameters for probenecid is probably larger than the uncertainty for the PK parameters of the antibiotics in those studies. However, the aim of the PK model for probenecid in these studies was to adequately describe the probenecid concentrations, as they were included in the interaction models, and not to estimate the PK parameters of probenecid most accurately. We could show that our PK models adequately described and predicted the concentrations of probenecid.

We had to make several assumptions for the analysis of the ciprofloxacin-probenecid dataset which were beyond the standard assumptions. Although we could not prove those assumptions to be correct, our results suggested that those were adequate and the best available option. (see chapter 4.3.4)

6.3　　　Bone penetration of antibiotics

Alternative approaches for the assessment of bone penetrations have been described in detail in chapter 5.1. The strengths and weaknesses of our bone penetration studies are summarized in brief here.

Strengths: The main strengths of our bone penetration studies were the highly standardized analysis of the bone samples and the data analysis by population PK and MCS. From a data analytical perspective, there was no viable alternative to population PK for our extremely sparse bone penetration datasets.

Weaknesses: As a common weakness of almost all bone penetration studies, the sample size of our bone penetration studies was small. As described in chapter 5.4, the sampling times of the bone samples were not optimized to estimate the population PK parameters most precisely. As discussed above, there is no prospectively determined and validated PKPD target for bone infections. Therefore, the results of our MCS for bone should be interpreted conservatively. Although those limitations exist, we could outline a perspective for the design and analysis of future bone penetration studies. Future studies about the effect of disease state on the rate and extent of bone penetration will be very valuable. Optimal clinical trial design is

probably very important for those trials, not only for ethical reasons. Additionally, studies are required on the PKPD target for bone infections.

7   Summary

There are numerous areas of application for which PKPD models are a valuable tool. We studied dose linearity, bone penetration and drug-drug interactions of antibiotics by PKPD modeling.

Knowledge about possible saturation of elimination pathways at therapeutic concentrations is important for studying the probability of successful treatment of dosage regimens via MCS at various doses, other modes of administration, or both. We studied the dose linearity of flucloxacillin and piperacillin. For data analysis of the dose linearity studies, population PK modeling and MCS was used. Population PK has been reported to detect saturable elimination at lower doses, and to estimate BSV more precisely than the STS approach. The variability in PK and the expected variability in PD are combined in a MCS to predict the probability of successful treatment.

Flucloxacillin showed no saturation of elimination at the studied doses of 500 mg and 1000 mg. Comparison of various dosage regimens showed, that only one third of the daily dose is needed with prolonged or continuous infusion to achieve the same probability of successful treatment as short-term infusions at the full dose. For serious infections with sensitive staphylococci that are treated with intravenous flucloxacillin, prolonged infusion and continuous infusion are an appealing treatment option.

Contrary to flucloxacillin, renal elimination and to a lesser extent also nonrenal elimination of piperacillin were saturable at therapeutic concentrations. Renal clearance decreased by 24% (p = 0.02) after a dose of 3000 mg piperacillin compared to the 1500 mg dose. A model without saturable elimination predicted PTA expectation values that were 6 to 11% lower for high dose short-term infusions and 2 to 5% higher for low dose continuous infusions, compared to models with saturable elimination. These differences depend on the MIC distributions of the local hospital. However, more accurate estimates for the PTA expectation value can be obtained by including an existent saturable elimination pathway into the PK model.

Developing a mechanistic model of an interaction allows one to predict the extent of the interaction for other doses of drug and inhibitor. We studied

the interactions between gemifloxacin and probenecid, between ciprofloxacin, its metabolite M1 and probenecid, and between flucloxacillin and piperacillin. Mechanistic models for drug-drug interactions were developed by the STS approach. This approach directly accounts for the concentration dependence of an interaction and describes the full time course of an interaction.

Probenecid significantly inhibited the renal elimination of gemifloxacin, ciprofloxacin and ciprofloxacin's metabolite M1, and slightly decreased nonrenal clearance of gemifloxacin. Piperacillin significantly decreased renal and nonrenal clearance of flucloxacillin, but hardly vice versa. For all three interactions competitive inhibition of a capacity-limited renal elimination pathway was identified as the most likely mechanism. As those drugs are all actively secreted in the renal tubules, competitive interaction is physiologically reasonable. Probenecid had a lower affinity to the renal transporter than gemifloxacin, ciprofloxacin and M1. Due to its substantially higher concentrations, probenecid inhibited the elimination of the quinolones. The affinity of piperacillin for the renal transporter was 13 times higher compared to flucloxacillin. Piperacillin PK was only slightly affected by flucloxacillin. PK interactions with piperacillin are likely to occur also with other betalactam combinations. PK interactions may be useful to improve the PD profile of an antibiotic, however possibly increased risks for side effects (e.g. risk of rash for gemifloxacin and probenecid) have to be considered.

Bone infections are difficult to treat. To ensure appropriate surgical prophylaxis and antimicrobial treatment, knowledge about the rate and extent of antibiotic bone penetration is valuable. Very different methods for sample preparation, drug analysis, data analysis and reporting have been applied in literature. The reported bone / serum concentration ratios differ widely between studies, even for the same drug. Average concentration ratios are usually between 0.1 and 0.4 for betalactams and glycopeptides, between 0.3 and 1.2 for quinolones, macrolides and linezolid, and even higher for azithromycin. Standardization of methods is critical to be able to compare the results from different studies. Population PK modeling and MCS should be employed to predict penetration into bone and to investigate the PKPD characteristics of antibiotics in bone.

The bone penetration of moxifloxacin, amoxicillin and clavulanic acid was studied in patients undergoing hip replacement surgery. The bone penetration studies were evaluated by population PK, MAP-Bayesian estimation and MCS. For evaluation of the PD profile of an antibiotic by MCS, a population PK model is the best method, as it directly considers between subject variability.

Moxifloxacin showed a high penetration into bone with a median AUC ratio bone / serum of 80% for cortical and 78% for cancellous bone, while amoxicillin and clavulanic acid had an about 5-10 times lower median AUC in bone than in serum. All three studied antibiotics showed a fast equilibrium between serum and bone with an average equilibration half-life of less than about 30min. Amoxicillin achieved PTA expectation values of $\geq$95% in bone and serum against *S. aureus* (methicillin-susceptible) and *S. saprophyticus*, two pathogens commonly encountered in bone infections. Moxifloxacin showed favorable PTAs compared to the MIC_{90} of *S. aureus*.

Future clinical trials are warranted to assess the effectiveness of amoxicillin / clavulanic acid and moxifloxacin in bone infections and surgical prophylaxis, and to evaluate possible PKPD targets in bone or serum for these infections.

Overall, modeling and simulation techniques were applied to various aspects of clinical studies for antibiotics within this thesis. The advantages of population PK and MCS compared to standard NCA have been highlighted based on practical problems. Probably one of the most important advantages of population PK and MCS is their ability to incorporate additional pharmacological data (e.g. PKPD targets) into the analysis. This greatly supports assessment of the clinical relevance and emphasizes the power of population PK and MCS to analyse data and visualize the results while accounting for the true between patient variability. Such techniques should be applied more frequently in the future to support drug development and therapy at various stages.

8 Zusammenfassung

Es gibt viele Anwendungsgebiete für die PKPD-Modelle wertvoll sind. In der vorliegenden Arbeit wurden Studien zu Dosislinearität, Knochenpenetration und Arzneistoffinteraktionen von Antibiotika mit Hilfe von PKPD-Modellen ausgewertet.

Um die Wahrscheinlichkeit einer erfolgreichen Therapie durch Dosierungsregime mit verschiedenen Dosen, Verabreichungsmethoden oder beidem zu studieren, ist es nötig, Kenntnisse über möglicherweise vorhandene, bei therapeutischen Konzentrationen sättigbare Eliminations-wege zu haben. Flucloxacillin und Piperacillin wurden auf ihre Dosislinearität untersucht. Zur Datenanalyse der Dosislinearitätsstudien wurden PopulationsPK-Modelle und MCS verwendet. Mit Hilfe von PopulationsPK kann eine sättigbare Elimination schon bei geringeren Dosen erkannt werden, und die Variabilität zwischen den Probanden kann genauer abgeschätzt werden als mit der STS-Methode. In einer MCS wird die Variabilität in der PK mit der erwarteten Variabilität in der PD kombiniert, um die Wahrscheinlichkeit einer erfolgreichen Behandlung vorherzusagen.

Flucloxacillin zeigte bei 500 mg und 1000 mg keine Sättigung der Elimination. Ein Vergleich verschiedener Dosierungsregime zeigte, dass bei mehrstündiger oder kontinuierlicher Infusion im Vergleich zur Kurzzeitinfusion nur ein Drittel der Dosis benötigt wird, um die gleiche Wahrscheinlichkeit für eine erfolgreiche Behandlung zu erreichen. Für die Behandlung von schweren Infektionen durch empfindliche Staphylokokken ist mehrstündige oder kontinuierliche Infusion eine attraktive Möglichkeit.

Im Gegensatz zu Flucloxacillin war die renale, und in einem geringeren Ausmaß auch die nicht-renale Elimination von Piperacillin bei therapeutischen Dosen sättigbar. Die renale Clearance war nach der 3000 mg Dosis um 24% (p = 0.02) verringert im Vergleich zur 1500 mg Dosis. Ein Modell ohne sättigbare Elimination sagte für hochdosierte Kurzzeitinfusionen 6 bis 11% niedrigere, und für niedrig dosierte kontinuierliche Infusion 2 bis 5% höhere Erwartungswerte für die Erfolgswahrscheinlichkeit voraus, als Modelle mit sättigbarer Elimination. Diese Unterschiede hängen von den minimalen

Hemmkonzentrationen der Pathogene im jeweiligen Krankenhaus ab. Durch die Berücksichtigung eines vorhandenen sättigbaren Eliminationsweges im Modell kann der Erwartungswert für die Erfolgswahrscheinlichkeit genauer abgeschätzt werden.

Die Entwicklung eines mechanistischen Interaktionsmodells ermöglicht es, das Ausmaß einer Interaktion für andere als die hier eingesetzten Dosen von Arzneistoff und Inhibitor vorherzusagen. In der vorliegenden Arbeit wurden die Interaktionen zwischen Gemifloxacin und Probenecid, sowie zwischen Ciprofloxacin, dessen Metaboliten M1 und Probenecid, und zwischen Flucloxacillin und Piperacillin untersucht. Die mechanistischen Interaktionsmodelle wurden mit Hilfe der STS-Methode entwickelt. Diese Methode bezieht die Konzentrationsabhängigkeit einer Interaktion direkt mit ein und beschreibt den vollständigen zeitlichen Verlauf der Interaktion.

Probenecid hemmte die renale Elimination von Gemifloxacin, Ciprofloxacin und M1 signifikant und verringerte leicht die nicht-renale Clearance von Gemifloxacin. Piperacillin verminderte die renale und nicht-renale Clearance von Flucloxacillin signifikant. Für alle drei Interaktionen wurde eine kompetitive Inhibition eines sättigbaren renalen Eliminationsweges als wahrscheinlichster Mechanismus identifiziert. Da alle untersuchten Arzneistoffe aktiver renaler Sekretion unterliegen, ist eine kompetitive Interaktion auch physiologisch sinnvoll. Die Affinität von Probenecid zum renalen Transporter war niedriger als diejenige von Gemifloxacin, Ciprofloxacin und M1. Trotzdem wurde die Elimination der Chinolone durch Probenecid gehemmt, da Probenecid wesentlich höhere Konzentrationen erreichte. Die Affinität von Piperacillin zum renalen Transporter war 13 Mal höher als diejenige von Flucloxacillin. Die PK von Piperacillin wurde durch Flucloxacillin nur leicht beeinflusst. Es ist wahrscheinlich, dass Piperacillin auch mit anderen Betalaktamen PK-Interaktionen eingeht. PK-Interaktionen können zur Verbesserung des PD-Profils eines Antibiotikums genutzt werden, allerdings muss dabei auch das möglicherweise erhöhte Nebenwirkungsrisiko (z.B. Hautausschlag bei Probenecid und Gemifloxacin) bedacht werden.

Knocheninfektionen sind schwierig zu behandeln. Zur Gewährleistung einer geeigneten chirurgischen Prophylaxe und antibiotischen Therapie sind

Kenntnisse über Geschwindigkeit und Ausmaß der Knochenpenetration von Antibiotika sehr wertvoll. In publizierten Studien wurden sehr unterschiedliche Methoden der Probenvorbereitung, Arzneistoffanalyse, Datenauswertung und Berichterstattung verwendet. Die berichteten Konzentrationsquotienten zwischen Knochen und Serum unterscheiden sich stark zwischen den Studien, sogar innerhalb eines Arzneistoffes. Bei Betalaktamen und Glykopeptiden liegen die mittleren Konzentrationsquotienten meist zwischen 0.1 und 0.4, bei Chinolonen, Makroliden und Linezolid zwischen 0.3 und 1.2, und bei Azithromycin noch höher. Eine Standardisierung der Methoden ist sehr wichtig, um einen Vergleich der Ergebnisse verschiedener Studien zu ermöglichen. PopulationsPK-Modelle und MCS sollten angewandt werden, um die Knochenpenetration vorherzusagen und PKPD-Eigenschaften von Antibiotika zu untersuchen.

Die Knochenpenetration von Moxifloxacin, Amoxicillin und Clavulansäure wurde an Patienten mit Hüftersatzoperationen untersucht. Die Knochenpenetrationsstudien wurden mit PopulationsPK, Bayes-Methoden und MCS ausgewertet. Für die Untersuchung der PD-Eigenschaften eines Antibiotikums durch MCS ist ein PopulationsPK-Modell die beste Methode, da es die Variabilität zwischen den Probanden direkt berücksichtigt.

Moxifloxacin zeigte eine hohe Penetration in den Knochen mit einem AUC-Quotienten von 0.8 (Median) zwischen Knochen und Serum. Die AUC von Amoxicillin und Clavulansäure im Knochen war dagegen im Median ca. 5-10 mal niedriger als im Serum. Alle drei untersuchten Antibiotika zeigten eine schnelle Gleichgewichtseinstellung zwischen Serum und Knochen (mittlere Halbwertszeit der Äquilibrierung kleiner als ca. 30min). Sowohl im Serum als auch im Knochen erreichte Amoxicillin Erwartungswerte von $\geq 95\%$ für die Erfolgswahrscheinlichkeit gegen *S. aureus* (methicillin-empfindlich) und *S. saprophyticus*, zwei häufige Auslöser von Knocheninfektionen. Moxifloxacin zeigte vorteilhafte Erfolgswahrscheinlichkeiten im Vergleich mit der MHK_{90} von *S. aureus*. Zukünftige klinische Studien werden benötigt, um die Wirksamkeit von Amoxicillin / Clavulansäure und Moxifloxacin in der Therapie und Prophylaxe von Knocheninfektionen zu untersuchen, und mögliche PKPD-Zielwerte für diese Infektionen in Knochen oder Serum zu evaluieren.

Diese Arbeit zeigt verschiedene Aspekte für Anwendungen von Modellierung und Simulationen am Bespiel ausgewählter Antibiotika. Die Vorteile von PopulationsPK und MCS im Vergleich zu Standard NCA wurden an praktischen Beispielen aufgezeigt. Einer der wahrscheinlich wichtigsten Vorteile von PopulationsPK und MCS ist deren Fähigkeit, zusätzliche pharmakologische Daten (z.B. PKPD-Zielwerte) in die Analyse mit einzubeziehen. Dies unterstützt die Abschätzung der klinischen Relevanz sehr und betont die Vorteile von PopulationsPK und MCS bei der Datenanalyse und Visualisierung von Ergebnissen, während gleichzeitig die wahre Variabilität zwischen Patienten berücksichtigt wird. Diese Technik sollte in der Zukunft häufiger angewendet werden, um die Entwicklung neuer Substanzen und die Arzneistofftherapie an verschiedensten Stellen zu unterstützen.

9   List of abbreviations

Ae	amount excreted unchanged in urine (expressed as fraction of administered dose)
AIC	Akaike information criterion
ANOVA	analysis of variance
APCI	atmospheric pressure chemical ionization
AUC	area under the curve
AUC_{0-last}	AUC from time of administration up to the last quantifiable concentration
$AUC_{0-\infty}$	AUC from time of administration up to time infinity
AUMC	area under the first moment concentration time curve
BSAC	British Society for Antimicrobial Chemotherapy
BSV	between subject variability
C_{last}	last quantifiable concentration
CIP	ciprofloxacin
$CL_{F,M1}$	formation clearance of the metabolite M1
CLic	intercompartmental clearance
$CLic_{deep}$	intercompartmental clearance between the central and the deep peripheral compartment
$CLic_{shallow}$	intercompartmental clearance between the central and the shallow peripheral compartment
CL_R	renal clearance
CL_{NR}	nonrenal clearance
CLSI	Clinical and Laboratory Standards Institute (formerly NCCLS)
CL_T	total body clearance
Cmax	maximum observed plasma concentration
CV	coefficient of variation
DIN	Deutsches Institut für Normung
E. coli	*Escherichia coli*
EARSS	European Antimicrobial Resistance Surveillance System
ECCMID	European Congress of Clinical Microbiology and Infectious Diseases
ESBL	extended-spectrum beta-lactamase
ESI	electrospray ionization
*f*AUC/MIC	ratio of the free area under the concentration time curve over 24h to the MIC

$F_{cancellous}$	describes the equilibrium concentration ratio between cancellous bone and serum
$F_{cortical}$	describes the equilibrium concentration ratio between cortical bone and serum
FDA	US Food and Drug Administration
$fT_{>MIC}$	time that the non-protein bound plasma concentration remains above the MIC of a pathogen
f_u	non-protein bound fraction of drug in plasma
GEM	gemifloxacin
GFR	glomerular filtration rate
HPLC	high performance liquid chromatography
ICAAC	Interscience Conference on Antimicrobial Agents and Chemotherapy
iv	intravenous
K. pneumoniae	*Klebsiella pneumoniae*
Ka	absorption rate constant
Ki	noncompetitive inhibition constant
Kic	competitive inhibition constant
Kiu	uncompetitive inhibition constant
K_m	Michaelis Menten constant, drug concentration associated with a half maximal rate of the mixed order process
$K_{mF,M1}$	Michaelis Menten constant of the mixed order formation of the metabolite M1
LC-MS/MS	liquid chromatography with tandem mass spectrometry
ln	natural logarithm
log	logarithm
M1	2-aminoethylamino-metabolite of ciprofloxacin
MAP	maximum *a posteriori* probability
MCS	Monte Carlo simulation
MIC	minimum inhibitory concentration
Mol. Wt.	molecular weight
MRSA	methicillin-resistant *Staphylococcus aureus*
MRT	mean residence time
MSSA	methicillin-susceptible *Staphylococcus aureus*
m/z	mass to charge ratio
NCA	non-compartmental analysis
NCCLS	National Committee for Clinical Laboratory Standards (now CLSI)
NONMEM	nonlinear mixed effects modeling

OAT	organic anion transporter
P10	10% percentile
P90	90% percentile
P. aeruginosa	*Pseudomonas aeruginosa*
PD	pharmacodynamics or pharmacodynamic
PK	pharmacokinetics or pharmacokinetic
PKPD	pharmacokinetics-pharmacodynamics
PRO	probenecid
PTA	probability of target attainment
q	quaque, every
q4h	every 4 hours
q8h	every 8 hours
S. aureus	*Staphylococcus aureus*
S. epidermidis	*Staphylococcus epidermidis*
S. pneumoniae	*Streptococcus pneumoniae*
S. saprophyticus	*Staphylococcus saprophyticus*
SD	standard deviation
SENTRY	a global antimicrobial surveillance program
SQC	spiked quality control
SRM	selected reaction monitoring
STS	standard-two-stage
$T_{1/2}$	half-life
$T_{1/2,Equilibration}$	half-life of equilibration between serum and bone
TCI	target concentration intervention
TDM	therapeutic drug monitoring
TI	transporter-inhibitor complex
Tlag	absorption lag-time
Tmax	time to peak concentration
TS	transporter-substrate complex
TSI	transporter-substrate-inhibitor complex
US	United States
UV	ultraviolet
V1	volume of distribution for the central compartment
V2	volume of distribution for the shallow peripheral compartment
V3	volume of distribution for the deep peripheral compartment

Vmax	maximum rate of a mixed order process
$Vmax_{F,M1}$	maximum rate of the mixed order formation of the metabolite M1
Vss	volume of distribution at steady-state
WRSS	weighted residual sum of squares
λ_z	terminal slope of the time vs. logarithmic concentration curve, λ_z is defined as the absolute value of this slope and therefore positive

10 References

1. 2005. British National Formulary 49. British Medical Association and Royal Pharmaceutical Society of Great Britain.

2. 2001. Guidance for Industry: Statistical Approaches to Establishing Bioequivalence. Center for Drug Evaluation and Research (CDER). U.S. Department of Health and Human Services. Food and Drug Administration.

3. **Adam, D., H. D. Heilmann, and K. Weismeier.** 1987. Concentrations of ticarcillin and clavulanic acid in human bone after prophylactic administration of 5.2 g of timentin. Antimicrob Agents Chemother **31:**935-9.

4. **Adam, D., B. Reichart, and K. J. Williams.** 1983. Penetration of ceftazidime into human tissue in patients undergoing cardiac surgery. J Antimicrob Chemother **12 Suppl A:**269-73.

5. **Adam, D., K. Weismeier, F. Sorgel, and J. Zurcher.** 1989. [Enoxacin concentration in bone tissue]. Infection **17 Suppl 1:**S25-6.

6. **Ahmed, S., S. Meghji, R. J. Williams, B. Henderson, J. H. Brock, and S. P. Nair.** 2001. Staphylococcus aureus fibronectin binding proteins are essential for internalization by osteoblasts but do not account for differences in intracellular levels of bacteria. Infect Immun **69:**2872-7.

7. **Allen, A., Bird, N., Dixon, R., Hickmott, F., Pay, V., Smith, A., Stahl, M.** 2001. Effect of Cimetidine on the Pharmacokinetics of Oral Gemifloxacin in Healthy Volunteers. Clin Drug Invest **21:**519-526.

8. **Allen, A., E. Bygate, S. Oliver, M. Johnson, C. Ward, A. J. Cheon, Y. S. Choo, and I. C. Kim.** 2000. Pharmacokinetics and tolerability of gemifloxacin (SB-265805) after administration of single oral doses to healthy volunteers. Antimicrob Agents Chemother **44:**1604-8.

9. **Allen, G. D., P. E. Coates, and B. E. Davies.** 1988. On the absorption of clavulanic acid. Biopharm Drug Dispos **9:**127-36.

10. **Ambrose, P. G., S. M. Bhavnani, and R. N. Jones.** 2003. Pharmacokinetics-pharmacodynamics of cefepime and piperacillin-tazobactam against Escherichia coli and Klebsiella pneumoniae strains producing extended-spectrum beta-lactamases: report from the ARREST program. Antimicrob Agents Chemother **47:**1643-6.

11. **Ambrose, P. G., D. M. Grasela, T. H. Grasela, J. Passarell, H. B. Mayer, and P. F. Pierce.** 2001. Pharmacodynamics of fluoroquinolones against Streptococcus pneumoniae in patients with community-acquired respiratory tract infections. Antimicrob Agents Chemother **45:**2793-7.

12. **Aminimanizani, A., P. Beringer, and R. Jelliffe.** 2001. Comparative pharmacokinetics and pharmacodynamics of the newer fluoroquinolone antibacterials. Clin Pharmacokinet **40:**169-87.

13. **Andersson, M. I., and A. P. MacGowan.** 2003. Development of the quinolones. J Antimicrob Chemother **51 Suppl 1:**1-11.

14. **Anonymous.** 1998. E-Test Product information AB BIODISK.

15. **Anonymous.** FACTIVE Investigator Brochure. Fourth edition. 16 January 1999.

16. **Anonymous.** Revised 5 April 1999. Piperacillin sodium and tazobactam sodium (Zosyn) product information. Lederle Laboratories, Pearl River, N.Y.

17. **Arancibia, A., J. Guttmann, G. Gonzalez, and C. Gonzalez.** 1980. Absorption and disposition kinetics of amoxicillin in normal human subjects. Antimicrob Agents Chemother **17:**199-202.

18. **Bailer, A. J.** 1988. Testing for the equality of area under the curves when using destructive measurement techniques. J Pharmacokinet Biopharm **16:**303-9.

19. **Barriere, S. L.** 1986. Therapeutic considerations in using combinations of newer beta-lactam antibiotics. Clin Pharm **5:**24-33.

20. **Barriere, S. L., D. H. Catlin, P. L. Orlando, A. Noe, and R. W. Frost.** 1990. Alteration in the pharmacokinetic disposition of ciprofloxacin by simultaneous administration of azlocillin. Antimicrob Agents Chemother **34:**823-6.

21. **Barry, A. L., R. N. Jones, C. Thornsberry, L. W. Ayers, E. H. Gerlach, and H. M. Sommers.** 1984. Antibacterial activities of ciprofloxacin, norfloxacin, oxolinic acid, cinoxacin, and nalidixic acid. Antimicrob Agents Chemother **25:**633-7.

22. **Barza, M., and L. Weinstein.** 1976. Pharmacokinetics of the penicillins in man. Clin Pharmacokinet **1:**297-308.

23. **Batra, V. K., J. A. Morrison, K. C. Lasseter, and V. A. Joy.** 1979. Piperacillin kinetics. Clin Pharmacol Ther **26:**41-53.

24. **Bauernfeind, A., and D. H. Wittmann.** 1982. Presented at the International Symposium: Fosfomycin - ein neuartiges Antibiotikum, Salzburg.

25. **Beal, S. L., A. J. Boeckmann, L. B. Sheiner, and NONMEM Project Group.** 1999. NONMEM Users Guides, Version 5 ed. University of California at San Francisco, San Francisco.

26. **Benoni, G., L. Cuzzolin, R. Leone, U. Consolo, G. Ferronato, C. Bertrand, V. Puchetti, and M. E. Fracasso.** 1988. Pharmacokinetics and human tissue penetration of flurithromycin. Antimicrob Agents Chemother **32:**1875-8.

27. **Bergan, T.** 1981. Overview of acylureidopenicillin pharmacokinetics. Scand J Infect Dis Suppl **29:**33-48.

28. **Bergan, T.** 1978. Penicillins. Antibiot Chemother **25:**1-122.

29. **Bergan, T.** 1978. Pharmacokinetics of mezlocillin in healthy volunteers. Antimicrob Agents Chemother **14:**801-6.

30. **Bergan, T., A. Engeset, W. Olszewski, N. Ostby, and R. Solberg.** 1986. Extravascular penetration of highly protein-bound flucloxacillin. Antimicrob Agents Chemother **30:**729-32.

31. **Bergan, T., and J. D. Williams.** 1982. Dose dependence of piperacillin pharmacokinetics. Chemotherapy **28:**153-9.

32. **Bergeron, M. G., J. L. Brusch, M. Barza, and L. Weinstein.** 1976. Bactericidal activity and pharmacology of flucloxacillin. Am J Med Sci **271:**13-20.

33. **Bhavnani, S. M., J. A. Passarell, J. S. Owen, J. S. Loutit, S. B. Porter, and P. G. Ambrose.** 2006. Pharmacokinetic-Pharmacodynamic Relationships Describing the Efficacy of Oritavancin in Patients with Staphylococcus aureus Bacteremia. Antimicrob Agents Chemother **50:**994-1000.

34. **Bijl, W., and R. A. Janknegt.** 1993. Single-dose versus 3-day prophylaxis with ciprofloxacin in transurethral surgery. A clinical trial. Urol Int **51:**73-8.

35. **Bilello, J. A., P. A. Bilello, K. Stellrecht, J. Leonard, D. W. Norbeck, D. J. Kempf, T. Robins, and G. L. Drusano.** 1996. Human serum alpha 1 acid glycoprotein reduces uptake, intracellular concentration, and antiviral activity of A-80987, an inhibitor of the human immunodeficiency virus type 1 protease. Antimicrob Agents Chemother **40:**1491-7.

36. **Birkett, D. J.** 1998. Pharmacokinetics Made Easy. The McGraw-Hill Companies, Inc.

37. **Blondeau, J. M.** 1999. A review of the comparative in-vitro activities of 12 antimicrobial agents, with a focus on five new respiratory quinolones'. J Antimicrob Chemother **43 Suppl B:**1-11.

38. **Blumer, J. L., M. D. Reed, E. L. Kaplan, and G. L. Drusano.** 2005. Explaining the poor bacteriologic eradication rate of single-dose ceftriaxone in group a streptococcal tonsillopharyngitis: a reverse engineering solution using pharmacodynamic modeling. Pediatrics **116:**927-32.

39. **Bonate, P. L.** 1998. Coverage and precision of confidence intervals for area under the curve using parametric and non-parametric methods in a toxicokinetic experimental design. Pharm Res **15:**405-10.

40. **Bonten, M. J., S. Slaughter, A. W. Ambergen, M. K. Hayden, J. van Voorhis, C. Nathan, and R. A. Weinstein.** 1998. The role of "colonization pressure" in the spread of vancomycin-resistant enterococci: an important infection control variable. Arch Intern Med **158:**1127-32.

41. **Booth, B. P., and J. V. Gobburu.** 2003. Considerations in analyzing single-trough concentrations using mixed-effects modeling. J Clin Pharmacol **43:**1307-15.

42. **Boselli, E., and B. Allaouchiche.** 1999. [Diffusion in bone tissue of antibiotics]. Presse Med **28:**2265-76.

43. **Boselli, E., D. Breilh, J. C. Bel, R. Debon, M. C. Saux, D. Chassard, and B. Allaouchiche.** 2002. Diffusion of isepamicin into cancellous and cortical bone tissue. J Chemother **14:**361-5.

44. **Boselli, E., D. Breilh, L. Biot, J. C. Bel, M. C. Saux, and B. Allaouchiche.** 2001. Penetration of Piperacillin/Tazobactam into Cancellous and Cortical Bone Tissue. Current Therapeutic Research **62:**538-545.

45. **Bottcher, S., H. von Baum, T. Hoppe-Tichy, C. Benz, and H. G. Sonntag.** 2001. An HPLC assay and a microbiological assay to determine levofloxacin in soft tissue, bone, bile and serum. J Pharm Biomed Anal **25:**197-203.

46. **Bradford, P. A.** 2005. Presented at the 45th Interscience Conference on Antimicrobial Agents and Chemotherapy (ICAAC), Washington, D.C., USA.

47. **Bradley, J. S., M. N. Dudley, and G. L. Drusano.** 2003. Predicting efficacy of antiinfectives with pharmacodynamics and Monte Carlo simulation. Pediatr Infect Dis J **22:**982-92; quiz 993-5.

48. **Breilh, D., E. Boselli, J. C. Bel, D. Chassard, M. C. Saux, and B. Allaouchiche.** 2003. Diffusion of cefepime into cancellous and cortical bone tissue. J Chemother **15:**134-8.

49. **Breilh, D., J. Jougon, S. Djabarouti, J. B. Gordien, F. Xuereb, J. F. Velly, P. Arvis, V. Landreau, and M. C. Saux.** 2003. Diffusion of oral and intravenous 400 mg once-daily moxifloxacin into lung tissue at pharmacokinetic steady-state. J Chemother **15:**558-62.

50. **Bulitta, J., M. Kinzig-Schippers, U. Holzgrabe, F. Sörgel, and N. H. G. Holford.** 2005. Replicate Design to Study the Population Pharmacokinetics (PopPK) of Piperacillin (PIP). Description of Saturable Elimination (EL) and Application to the Design of Optimal Dosage Regimens, Interscience Conference on Antimicrobial Agents and Chemotherapy, Washington, DC, USA.

51. **Burckhardt, B. C., and G. Burckhardt.** 2003. Transport of organic anions across the basolateral membrane of proximal tubule cells. Rev Physiol Biochem Pharmacol **146:**95-158.

52. **Bustamante, C. I., G. L. Drusano, R. C. Wharton, and J. C. Wade.** 1987. Synergism of the combinations of imipenem plus ciprofloxacin and imipenem plus amikacin against Pseudomonas aeruginosa and other bacterial pathogens. Antimicrob Agents Chemother **31:**632-4.

53. **Butler, D.** 2005. Wartime tactic doubles power of scarce bird-flu drug. Nature **438:**6.

54. **Bystedt, H., D. A. A, K. Dornbusch, and C. E. Nord.** 1978. Concentrations of azidocillin, erythromycin, doxycycline and clindamycin in human mandibular bone. Int J Oral Surg **7:**442-9.

55. **Capitano, B., H. M. Mattoes, E. Shore, A. O'Brien, S. Braman, C. Sutherland, and D. P. Nicolau.** 2004. Steady-state intrapulmonary concentrations of moxifloxacin, levofloxacin, and azithromycin in older adults. Chest **125:**965-73.

56. **Cawello, W.** 1998. Parameter zur modellunabhängigen Pharmakokinetik - Standardisierung von Planung, Auswertung und Berichterstattung. Shaker, Aachen, Germany.

57. **Chen, Y. H., C. F. Peng, P. L. Lu, J. J. Tsai, and T. P. Chen.** 2004. In vitro activities of antibiotic combinations against clincal isolates of Pseudomonas aeruginosa. Kaohsiung J Med Sci **20:**261-7.

58. **Chenel, M., K. Ogungbenro, V. Duval, C. Laveille, R. Jochemsen, and L. Aarons.** 2005. Optimal blood sampling time windows for parameter estimation using a population approach: design of a phase II clinical trial. J Pharmacokinet Pharmacodyn **32:**737-56.

59. **Chin, N. X., D. C. Brittain, and H. C. Neu.** 1986. In vitro activity of Ro 23-6240, a new fluorinated 4-quinolone. Antimicrob Agents Chemother **29:**675-80.

60. **Chin, N. X., and H. C. Neu.** 1984. Ciprofloxacin, a quinolone carboxylic acid compound active against aerobic and anaerobic bacteria. Antimicrob Agents Chemother **25:**319-26.

61. **Clinckers, R., I. Smolders, A. Meurs, G. Ebinger, and Y. Michotte.** 2005. Quantitative in vivo microdialysis study on the influence of multidrug transporters on the blood-brain barrier passage of oxcarbazepine: concomitant use of hippocampal monoamines as pharmacodynamic markers for the anticonvulsant activity. J Pharmacol Exp Ther.

62. **Cluzel, R. A., R. Lopitaux, J. Sirot, and S. Rampon.** 1984. Rifampicin in the treatment of osteoarticular infections due to staphylococci. J Antimicrob Chemother **13 Suppl C:**23-9.

63. **Cockcroft, D. W., and M. H. Gault.** 1976. Prediction of creatinine clearance from serum creatinine. Nephron **16:**31-41.

64. **Cormican, M. G., and R. N. Jones.** 1997. Antimicrobial activity and spectrum of LB20304, a novel fluoronaphthyridone. Antimicrob Agents Chemother **41:**204-11.

65. **Cosgrove, S. E., Y. Qi, K. S. Kaye, S. Harbarth, A. W. Karchmer, and Y. Carmeli.** 2005. The impact of methicillin resistance in Staphylococcus aureus bacteremia on patient outcomes: mortality, length of stay, and hospital charges. Infect Control Hosp Epidemiol **26:**166-74.

66. **Cotran, R. S., V. Kumar, T. Collins, and S. L. Robbins.** 1994. Robbins Pathological Basis of Disease, Philadelphia.

67. **Craig, W. A.** 1998. Pharmacokinetic/pharmacodynamic parameters: rationale for antibacterial dosing of mice and men. Clin Infect Dis **26:**1-10; quiz 11-2.

68. **Craig, W. A., and D. Andes.** 1996. Pharmacokinetics and pharmacodynamics of antibiotics in otitis media. Pediatr Infect Dis J **15:**255-9.

69. **Craig, W. A., and S. C. Ebert.** 1992. Continuous infusion of beta-lactam antibiotics. Antimicrob Agents Chemother **36:**2577-83.

70. **Cremieux, A. C., A. S. Mghir, R. Bleton, M. Manteau, N. Belmatoug, L. Massias, L. Garry, N. Sales, B. Maziere, and C. Carbon.** 1996. Efficacy of sparfloxacin and autoradiographic diffusion pattern of [14C]Sparfloxacin in experimental Staphylococcus aureus joint prosthesis infection. Antimicrob Agents Chemother **40:**2111-6.

71. **Cummins, C. L., C. Y. Wu, and L. Z. Benet.** 2002. Sex-related differences in the clearance of cytochrome P450 3A4 substrates may be caused by P-glycoprotein. Clin Pharmacol Ther **72:**474-89.

72. **D'Argenio, D. Z.** 1990. Incorporating prior parameter uncertainty in the design of sampling schedules for pharmacokinetic parameter estimation experiments. Math Biosci **99:**105-18.

73. **D'Argenio, D. Z.** 1981. Optimal sampling times for pharmacokinetic experiments. J Pharmacokinet Biopharm **9:**739-56.

74. **D'Argenio, D. Z., and A. Schumitzky.** 1997. ADAPTII User's Guide: Pharmacokinetic/Pharmacodynamic Systems Analysis Software. Biomedical Simulations Resource, Los Angeles.

75.   **Darley, E. S., and A. P. MacGowan.** 2004. Antibiotic treatment of gram-positive bone and joint infections. J Antimicrob Chemother **53:**928-35.

76.   **de Abajo, F. J., D. Montero, M. Madurga, and L. A. Garcia Rodriguez.** 2004. Acute and clinically relevant drug-induced liver injury: a population based case-control study. Br J Clin Pharmacol **58:**71-80.

77.   **De Jongh, C. A., J. H. Joshi, B. W. Thompson, K. A. Newman, R. S. Finley, M. R. Moody, P. C. Salvatore, J. H. Tenney, G. L. Drusano, and S. C. Schimpff.** 1986. A double beta-lactam combination versus an aminoglycoside-containing regimen as empiric antibiotic therapy for febrile granulocytopenic cancer patients. Am J Med **80:**101-11.

78.   **de Lalla, F., A. Novelli, G. Pellizzer, F. Milocchi, R. Viola, A. Rigon, C. Stecca, V. Dal Pizzol, S. Fallani, and P. Periti.** 1993. Regional and systemic prophylaxis with teicoplanin in monolateral and bilateral total knee replacement procedures: study of pharmacokinetics and tissue penetration. Antimicrob Agents Chemother **37:**2693-8.

79.   **Dehne, M. G., J. Muhling, A. Sablotzki, H. Nopens, and G. Hempelmann.** 2001. Pharmacokinetics of antibiotic prophylaxis in major orthopedic surgery and blood-saving techniques. Orthopedics **24:**665-9.

80.   **del Piano, M., R. Nicosia, R. Sessa, G. Grippaudo, R. Lolli, and B. Monaco.** 1988. Study on tissue concentrations of antibiotics: bacampicillin in gingiva and maxillary bones. Chemotherapy **34:**13-7.

81.   **Del Tacca, M., R. Danesi, N. Bernardini, M. Ducci, I. Zolfino, S. Senesi, E. Panattoni, M. Gabriele, M. Marcucci, A. Lazzarini, and et al.** 1990. Roxithromycin penetration into gingiva and alveolar bone of odontoiatric patients. Chemotherapy **36:**332-6.

82.   **Dellamonica, P., E. Bernard, H. Etesse, and R. Garraffo.** 1986. The diffusion of pefloxacin into bone and the treatment of osteomyelitis. J Antimicrob Chemother **17 Suppl B:**93-102.

83.   **Derendorf, H., T. Gramatté, and H. G. Schäfer.** 2002. Pharmakokinetik. Einführung in die Theorie und Relevanz für die Arzneimitteltherapie, 2nd ed. Wissenschaftliche Verlagsgesellschaft mbH, Stuttgart.

84.   **DiMasi, J. A., R. W. Hansen, and H. G. Grabowski.** 2003. The price of innovation: new estimates of drug development costs. J Health Econ **22:**151-85.

85.   **Dinis, P. B., M. C. Monteiro, M. L. Martins, N. Silva, and J. G. Morais.** 2004. Sinus tissue concentration of moxifloxacin after a single oral dose. Ann Otol Rhinol Laryngol **113:**142-6.

86.   **Djabarouti, S., E. Boselli, B. Allaouchiche, B. Ba, A. T. Nguyen, J. B. Gordien, J. M. Bernadou, M. C. Saux, and D. Breilh.** 2004. Determination of levofloxacin in plasma, bronchoalveolar lavage and bone tissues by high-performance liquid chromatography with ultraviolet detection using a fully automated extraction method. J Chromatogr B Analyt Technol Biomed Life Sci **799:**165-72.

87. **Dornbusch, K., A. Carlstrom, H. Hugo, and A. Lidstrom.** 1977. Antibacterial activity of clindamycin and lincomycin in human bone. J Antimicrob Chemother **3:**153-60.

88. **Dounis, E., S. Tsourvakas, L. Kalivas, and H. Giamacellou.** 1995. Effect of time interval on tissue concentrations of cephalosporins after tourniquet inflation. Highest levels achieved by administration 20 minutes before inflation. Acta Orthop Scand **66:**158-60.

89. **Drusano, G. L.** 2004. Antimicrobial pharmacodynamics: critical interactions of 'bug and drug'. Nat Rev Microbiol **2:**289-300.

90. **Drusano, G. L.** 2003. Prevention of resistance: a goal for dose selection for antimicrobial agents. Clin Infect Dis **36:**S42-50.

91. **Drusano, G. L., A. Forrest, D. Fiore, F. Auger, and E. S. Caplan.** 1984. Effect of saturable clearance during high-dose mezlocillin therapy. Antimicrob Agents Chemother **26:**686-8.

92. **Drusano, G. L., S. L. Preston, C. Fowler, M. Corrado, B. Weisinger, and J. Kahn.** 2004. Relationship between fluoroquinolone area under the curve: minimum inhibitory concentration ratio and the probability of eradication of the infecting pathogen, in patients with nosocomial pneumonia. J Infect Dis **189:**1590-7.

93. **Drusano, G. L., S. L. Preston, C. Hardalo, R. Hare, C. Banfield, D. Andes, O. Vesga, and W. A. Craig.** 2001. Use of preclinical data for selection of a phase II/III dose for evernimicin and identification of a preclinical MIC breakpoint. Antimicrob Agents Chemother **45:**13-22.

94. **Drusano, G. L., S. L. Preston, M. Van Guilder, D. North, M. Gombert, M. Oefelein, L. Boccumini, B. Weisinger, M. Corrado, and J. Kahn.** 2000. A population pharmacokinetic analysis of the penetration of the prostate by levofloxacin. Antimicrob Agents Chemother **44:**2046-51.

95. **Duffull, S., T. Waterhouse, and J. Eccleston.** 2005. Some considerations on the design of population pharmacokinetic studies. J Pharmacokinet Pharmacodyn **32:**441-57.

96. **Duffull, S. B., F. Mentre, and L. Aarons.** 2001. Optimal design of a population pharmacodynamic experiment for ivabradine. Pharm Res **18:**83-9.

97. **Duffull, S. B., S. Retout, and F. Mentre.** 2002. The use of simulated annealing for finding optimal population designs. Comput Methods Programs Biomed **69:**25-35.

98. **Eagle, H., R. Fleischman, and M. Levy.** 1953. "Continuous" vs. "discontinuous" therapy with penicillin; the effect of the interval between injections on therapeutic efficacy. N Engl J Med **248:**481-8.

99. **Eliopoulos, G. M., A. Gardella, and R. C. Moellering, Jr.** 1984. In vitro activity of ciprofloxacin, a new carboxyquinoline antimicrobial agent. Antimicrob Agents Chemother **25:**331-5.

100. **Emanuelsson, B. M., B. Beermann, and L. K. Paalzow.** 1987. Non-linear elimination and protein binding of probenecid. Eur J Clin Pharmacol **32:**395-401.

101. **Etesse-Carsenti, H., F. Giaume, A. Barbarin, C. Argenson, V. Mondain, M. F. Masseyeff, E. Bernard, and P. Dellamonica.** 1990. Presented at the Third Symposium on New Quinolones, Vancouver.

102. **Fauroux, C. M., and S. Freeman.** 1999. Inhibitors of inositol monophosphatase. J Enzyme Inhib **14:**97-108.

103. **Fischman, A. J., J. W. Babich, A. A. Bonab, N. M. Alpert, J. Vincent, R. J. Callahan, J. A. Correia, and R. H. Rubin.** 1998. Pharmacokinetics of [18F]trovafloxacin in healthy human subjects studied with positron emission tomography. Antimicrob Agents Chemother **42:**2048-54.

104. **Fischman, A. J., E. Livni, J. Babich, N. M. Alpert, Y. Y. Liu, E. Thom, R. Cleeland, B. L. Prosser, J. A. Correia, H. W. Strauss, and et al.** 1993. Pharmacokinetics of [18F]fleroxacin in healthy human subjects studied by using positron emission tomography. Antimicrob Agents Chemother **37:**2144-52.

105. **Fish, D. N., and A. T. Chow.** 1997. The clinical pharmacokinetics of levofloxacin. Clin Pharmacokinet **32:**101-19.

106. **Flaherty, J. F., S. L. Barriere, J. Mordenti, and J. G. Gambertoglio.** 1987. Effect of dose on pharmacokinetics and serum bactericidal activity of mezlocillin. Antimicrob Agents Chemother **31:**895-8.

107. **Fong, I. W., W. H. Ledbetter, A. C. Vandenbroucke, M. Simbul, and V. Rahm.** 1986. Ciprofloxacin concentrations in bone and muscle after oral dosing. Antimicrob Agents Chemother **29:**405-8.

108. **Fong, I. W., B. R. Rittenhouse, M. Simbul, and A. C. Vandenbroucke.** 1988. Bone penetration of enoxacin in patients with and without osteomyelitis. Antimicrob Agents Chemother **32:**834-7.

109. **Forrest, A., S. Chodosh, M. A. Amantea, D. A. Collins, and J. J. Schentag.** 1997. Pharmacokinetics and pharmacodynamics of oral grepafloxacin in patients with acute bacterial exacerbations of chronic bronchitis. J Antimicrob Chemother **40 Suppl A:**45-57.

110. **Foster, J. K., J. R. Lentino, R. Strodtman, and C. DiVincenzo.** 1986. Comparison of in vitro activity of quinolone antibiotics and vancomycin against gentamicin- and methicillin-resistant Staphylococcus aureus by time-kill kinetic studies. Antimicrob Agents Chemother **30:**823-7.

111. **Fracasso, M. E., V. Consolo, G. Ferronato, R. Leone, L. Cuzzolin, and G. Benoni.** 1989. Aztreonam penetration of bone and soft tissue, after i.v. infusion and bolus injection. J Antimicrob Chemother **23:**465-7.

112. **Fraschini, F., F. Scaglione, M. Falchi, P. Manzoni, S. D'Orsi, S. Badile, and M. Pignanelli.** 1989. Miokamycin penetration into oral cavity tissues and crevicular fluid. Int J Clin Pharmacol Res **9:**293-6.

113. **Gabrielsson, J., and D. Weiner.** 2001. Pharmacokinetic and Pharmacodynamic Data Analysis, Concepts and Applications, 3rd ed. Swedish Pharmaceutical Press, Stockholm, Sweden.

114. **Gaitonde, M., Mendes, P., House, E. S. A., Lehr, K.H.** 1995. The Effects of Cimetidine and Probenecid on the Pharmacokinetics of Levofloxacin, Interscience Conference on Antimicrobial Agents and Chemotherapy, San Francisco.

115. **Gambertoglio, J. G., S. L. Barriere, E. T. Lin, and J. E. Conte, Jr.** 1983. Amdinocillin pharmacokinetics. Simultaneous administration with cephalothin and cerebrospinal fluid penetration. Am J Med **75:**54-9.

116. **Garton, A. M., R. P. Rennie, J. Gilpin, M. Marrelli, and S. D. Shafran.** 1997. Comparison of dose doubling with probenecid for sustaining serum cefuroxime levels. J Antimicrob Chemother **40:**903-6.

117. **Gee, T., J. M. Andrews, J. P. Ashby, G. Marshall, and R. Wise.** 2001. Pharmacokinetics and tissue penetration of gemifloxacin following a single oral dose. J Antimicrob Chemother **47:**431-4.

118. **Gehanno, P., S. Darantiere, C. Dubreuil, J. C. Chobaut, S. Bobin, J. C. Pages, G. Renou, F. Bobin, P. Arvis, and H. Stass.** 2002. A prospective, multicentre study of moxifloxacin concentrations in the sinus mucosa tissue of patients undergoing elective surgery of the sinus. J Antimicrob Chemother **49:**821-6.

119. **Gentry, L. O., and G. G. Rodriguez.** 1990. Oral ciprofloxacin compared with parenteral antibiotics in the treatment of osteomyelitis. Antimicrob Agents Chemother **34:**40-3.

120. **Gibaldi, M., and D. Perrier.** 1982. Pharmacokinetics. Marcel Dekker, Inc., New York, USA.

121. **Gisclon, L. G., R. A. Boyd, R. L. Williams, and K. M. Giacomini.** 1989. The effect of probenecid on the renal elimination of cimetidine. Clin Pharmacol Ther **45:**444-52.

122. **Glantz, S. A.** 1996. Primer of Biostatistics, fourth ed. McGraw-Hill.

123. **GlaxoSmithKline.** 2005. Flucloxacillin product information (Floxapen), Uxbridge, Middlesex, UK.

124. **Goodman Gilman, A.** 1996. Goodman & Gilman's: The pharmacological basis of therapeutics, 9th ed. McGraw-Hill, New York.

125. **Gould, I. M.** 1999. A review of the role of antibiotic policies in the control of antibiotic resistance. J Antimicrob Chemother **43:**459-65.

126. **Gradl, W., and D. Adam.** 1985. Apalcillinpharmakokinetik in verschiedenen Geweben einschließlich des Knochens bei Patienten mit Totalendoprothese-Operation. FAC Fortschritte der antimikrobiellen und antineoplastischen Chemotherapie **4-7:**1729-1736.

127. **Gradl, W., and D. Adam.** 1988. Gewebekonzentrationen von Mezlocillin und Oxacillin bei Hüftprothesen-Implantationen. ZAC Zeitschrift für antimikrobielle antineoplastische Chemotherapie **6:**107-112.

128. **Graham, G., I. Gueorguieva, and K. Dickens.** 2005. A program for the optimum design of pharmacokinetic, pharmacodynamic, drug metabolism and drug-drug interaction models. Comput Methods Programs Biomed **78:**237-49.

129. **Graziani, A. L., L. A. Lawson, G. A. Gibson, M. A. Steinberg, and R. R. MacGregor.** 1988. Vancomycin concentrations in infected and noninfected human bone. Antimicrob Agents Chemother **32:**1320-2.

130. **Green, B., and S. B. Duffull.** 2003. Prospective evaluation of a D-optimal designed population pharmacokinetic study. J Pharmacokinet Pharmacodyn **30:**145-61.

131. **Greenberg, R. N., D. J. Kennedy, P. M. Reilly, K. L. Luppen, W. J. Weinandt, M. R. Bollinger, F. Aguirre, F. Kodesch, and A. M. Saeed.** 1987. Treatment of bone, joint, and soft-tissue infections with oral ciprofloxacin. Antimicrob Agents Chemother **31:**151-5.

132. **Grimer, R. J., M. R. Karpinski, J. M. Andrews, and R. Wise.** 1986. Penetration of amoxycillin and clavulanic acid into bone. Chemotherapy **32:**185-91.

133. **Gumbo, T., A. Louie, M. R. Deziel, L. M. Parsons, M. Salfinger, and G. L. Drusano.** 2004. Selection of a moxifloxacin dose that suppresses drug resistance in Mycobacterium tuberculosis, by use of an in vitro pharmacodynamic infection model and mathematical modeling. J Infect Dis **190:**1642-51.

134. **Guyton, A. C., and J. E. Hall.** 1996. Textbook of Medical Physiology, 9 ed. Saunders.

135. **Haag, R., R. Hölzlberger, E. Rienhoff, F. Bartels, and A. Meissner.** 1989. Experimentelle Untersuchungen und Überlegungen zur Verteilung und zur verzögerten Freisetzung von Fosfomycin aus Knochengewebe. ZAC Zeitschrift für antimikrobielle antineoplastische Chemotherapie **7:**3-10.

136. **Hande, K., M. Messenger, J. Wagner, M. Krozely, and S. Kaul.** 1999. Inter- and intrapatient variability in etoposide kinetics with oral and intravenous drug administration. Clin Cancer Res **5:**2742-7.

137. **Hardy, D. J., R. N. Swanson, D. M. Hensey, N. R. Ramer, R. R. Bower, C. W. Hanson, D. T. Chu, and P. B. Fernandes.** 1987. Comparative antibacterial activities of temafloxacin hydrochloride (A-62254) and two reference fluoroquinolones. Antimicrob Agents Chemother **31:**1768-74.

138. **Hashimoto, Y., J. Ozaki, T. Koue, A. Odani, M. Yasuhara, and R. Hori.** 1994. Simulation for the analysis of distorted pharmacodynamic data. Pharm Res **11:**545-8.

139. **Hayashi, T., Y. Watanabe, K. Kumano, R. Kitayama, T. Yasuda, I. Saikawa, K. Totsuka, T. Kumada, and K. Shimizu.** 1986. Pharmacokinetic studies on the concomitant administration of piperacillin and cefazolin, and piperacillin and cefoperazone in rabbits. J Antibiot (Tokyo) **39:**699-712.

140. **Hill, G., T. Cihlar, C. Oo, E. S. Ho, K. Prior, H. Wiltshire, J. Barrett, B. Liu, and P. Ward.** 2002. The anti-influenza drug oseltamivir exhibits low potential to induce pharmacokinetic drug interactions via renal secretion-correlation of in vivo and in vitro studies. Drug Metab Dispos **30:**13-9.

141. **Hoban, D. J., S. K. Bouchillon, J. L. Johnson, G. G. Zhanel, D. L. Butler, K. A. Saunders, L. A. Miller, and J. A. Poupard.** 2003. Comparative in vitro potency of amoxycillin-clavulanic acid and four oral agents against recent North American clinical isolates from a global surveillance study. Int J Antimicrob Agents **21:**425-33.

142. **Hoffken, G., H. Tetzel, P. Koeppe, and H. Lode.** 1985. Pharmacokinetics and serum bactericidal activity of ticarcillin and clavulanic acid. J Antimicrob Chemother **16:**763-71.

143. **Holder, D. J., F. Hsuan, R. Dixit, and K. Soper.** 1999. A method for estimating and testing area under the curve in serial sacrifice, batch, and complete data designs. J Biopharm Stat **9:**451-64.

144. **Holford, N., P. Black, R. Couch, J. Kennedy, and R. Briant.** 1993. Theophylline target concentration in severe airways obstruction - 10 or

20 mg/L? A randomised concentration-controlled trial. Clin Pharmacokinet **25:**495-505.

145. **Holford, N. H.** 1987. Clinical pharmacokinetics of ethanol. Clin Pharmacokinet **13:**273-92.

146. **Holford, N. H.** 2001. Target concentration intervention: beyond Y2K. Br J Clin Pharmacol **52 Suppl 1:**55S-59S.

147. **Holford, N. H., and L. B. Sheiner.** 1982. Kinetics of pharmacologic response. Pharmacol Ther **16:**143-66.

148. **Holford, N. H., and L. B. Sheiner.** 1981. Understanding the dose-effect relationship: clinical application of pharmacokinetic-pharmacodynamic models. Clin Pharmacokinet **6:**429-53.

149. **Holford, N. H. G.** 2003. Pharmacokinetics & Pharmacodynamics: Rational Dosing & the Time Course of Drug Action. *In* B. G. Katzung (ed.), Basic & Clinical Pharmacology, ninth ed. McGraw-Hill.

150. **Hoogkamp-Korstanje, J. A.** 1987. Treatment of chronic postsurgical osteomyelitis with ciprofloxacin. Pharm Weekbl Sci **9 Suppl:**S90-2.

151. **Hope, W. W., P. A. Warn, A. Sharp, P. Reed, B. Keevil, A. Louie, D. W. Denning, and G. L. Drusano.** 2005. Surface response modeling to examine the combination of amphotericin B deoxycholate and 5-fluorocytosine for treatment of invasive candidiasis. J Infect Dis **192:**673-80.

152. **Horber, F. F., F. J. Frey, C. Descoeudres, A. T. Murray, and F. C. Reubi.** 1986. Differential effect of impaired renal function on the kinetics of clavulanic acid and amoxicillin. Antimicrob Agents Chemother **29:**614-9.

153. **Howden, B. P., and M. J. Richards.** 2001. The efficacy of continuous infusion flucloxacillin in home therapy for serious staphylococcal infections and cellulitis. J Antimicrob Chemother **48:**311-4.

154. **Hudson, M. C., W. K. Ramp, N. C. Nicholson, A. S. Williams, and M. T. Nousiainen.** 1995. Internalization of Staphylococcus aureus by cultured osteoblasts. Microb Pathog **19:**409-19.

155. **Hughes, S. P., and F. M. Anderson.** 1985. Penetration of antibiotics into bone. J Antimicrob Chemother **15:**517-9.

156. **Incavo, S. J., P. J. Ronchetti, J. H. Choi, H. Wu, M. Kinzig, and F. Sorgel.** 1994. Penetration of piperacillin-tazobactam into cancellous and cortical bone tissues. Antimicrob Agents Chemother **38:**905-7.

157. **Jacquez, J. A.** 1996. Parameter identifiability is required in pooled data methods. J Pharmacokinet Biopharm **24:**301-5.

158. **Jaehde, U., F. Sorgel, A. Reiter, G. Sigl, K. G. Naber, and W. Schunack.** 1995. Effect of probenecid on the distribution and elimination of ciprofloxacin in humans. Clin Pharmacol Ther **58:**532-41.

159. **Jariyawat, S., T. Sekine, M. Takeda, N. Apiwattanakul, Y. Kanai, S. Sophasan, and H. Endou.** 1999. The interaction and transport of beta-lactam antibiotics with the cloned rat renal organic anion transporter 1. J Pharmacol Exp Ther **290:**672-7.

160. **Jehl, F., J. M. Klossek, R. Peynegre, E. Serrano, L. Castillo, S. Bobin, D. Desprez, C. Renault, V. Neel, E. Rouffiac, and C. Borie.** 2002. [Sinusal penetration of amoxicillin-clavulanic acid. Formulation 1

g./125 mg., twice daily versus formulation 500 mg./125 mg., three times daily]. Presse Med **31:**1596-603.

161. **Jevon, M., C. Guo, B. Ma, N. Mordan, S. P. Nair, M. Harris, B. Henderson, G. Bentley, and S. Meghji.** 1999. Mechanisms of internalization of Staphylococcus aureus by cultured human osteoblasts. Infect Immun **67:**2677-81.

162. **Jones, P. D., R. L. Henry, J. Stuart, and L. Francis.** 1998. Suspected infection in children with cancer. J Qual Clin Pract **18:**275-84.

163. **Jonsson, E. N., J. R. Wade, and M. O. Karlsson.** 2000. Nonlinearity detection: advantages of nonlinear mixed-effects modeling. AAPS PharmSci **2:**E32.

164. **Joukhadar, C., and M. Muller.** 2005. Microdialysis: current applications in clinical pharmacokinetic studies and its potential role in the future. Clin Pharmacokinet **44:**895-913.

165. **Joukhadar, C., H. Stass, U. Muller-Zellenberg, E. Lackner, F. Kovar, E. Minar, and M. Muller.** 2003. Penetration of moxifloxacin into healthy and inflamed subcutaneous adipose tissues in humans. Antimicrob Agents Chemother **47:**3099-103.

166. **Jumbe, N., A. Louie, R. Leary, W. Liu, M. R. Deziel, V. H. Tam, R. Bachhawat, C. Freeman, J. B. Kahn, K. Bush, M. N. Dudley, M. H. Miller, and G. L. Drusano.** 2003. Application of a mathematical model to prevent in vivo amplification of antibiotic-resistant bacterial populations during therapy. J Clin Invest **112:**275-85.

167. **Jungbluth, G. L., and W. J. Jusko.** 1989. Dose-dependent pharmacokinetics of mezlocillin in rats. Antimicrob Agents Chemother **33:**839-43.

168. **Kamali, F.** 1993. The effect of probenecid on paracetamol metabolism and pharmacokinetics. Eur J Clin Pharmacol **45:**551-3.

169. **Kamali, F., and M. D. Rawlins.** 1992. Influence of probenecid and paracetamol (acetaminophen) on zidovudine glucuronidation in human liver in vitro. Biopharm Drug Dispos **13:**403-9.

170. **Kampf, D., K. Borner, M. Moller, and M. Kessel.** 1984. Kinetic interactions between azlocillin, cefotaxime, and cefotaxime metabolites in normal and impaired renal function. Clin Pharmacol Ther **35:**214-20.

171. **Kaukonen, J. P., P. Tuomainen, J. Makijarvi, R. Mokka, and P. T. Mannisto.** 1995. Intravenous cefuroxime prophylaxis. Tissue levels after one 3-gram dose in 40 cases of hip fracture. Acta Orthop Scand **66:**14-6.

172. **Ketterl, R., and W. Wittwer.** 1993. [Possibilities for the use of the basic cephalosporin cefuroxime in bone surgery. Tissue levels, effectiveness and tolerance]. Infection **21 Suppl 1:**S21-7.

173. **Kim, K. A., S. O. Oh, P. W. Park, and J. Y. Park.** 2005. Effect of probenecid on the pharmacokinetics of carbamazepine in healthy subjects. Eur J Clin Pharmacol.

174. **Kim, M. J., J. S. Bertino, Jr., T. A. Erb, P. L. Jenkins, and A. N. Nafziger.** 2004. Application of Bayes theorem to aminoglycoside-associated nephrotoxicity: comparison of extended-interval dosing, individualized pharmacokinetic monitoring, and multiple-daily dosing. J Clin Pharmacol **44:**696-707.

175. **Kitzes-Cohen, R., M. Erde, E. Sharvit, A. Gilboa, A. Laor, and I. Shweppy.** 1990. Presented at the Third Symposium on New Quinolones, Vancouver.

176. **Kitzes-Cohen, R., D. Farin, G. Piva, S. Ivry, R. Sharony, R. Amar, and G. Uretzky.** 2000. Pharmacokinetics of vancomycin administered as prophylaxis before cardiac surgery. Ther Drug Monit **22:**661-7.

177. **Klaren, P. H., A. N. Giesberts, J. Chapman, S. J. White, C. J. Taylor, P. T. Hardcastle, and J. Hardcastle.** 2000. Effect of loperamide on Na+/D-glucose cotransporter activity in mouse small intestine. J Pharm Pharmacol **52:**679-86.

178. **Kondell, P. A., C. E. Nord, and A. Nordenram.** 1982. Concentrations of cloxacillin, dicloxacillin and flucloxacillin in dental alveolar serum and mandibular bone. Int J Oral Surg **11:**40-3.

179. **Kosmidis, J., C. Stathakis, K. Mantopoulos, T. Pouriezi, B. Papathanassiou, and G. K. Daikos.** 1980. Clinical pharmacology of cefotaxime including penetration into bile, sputum, bone and cerebrospinal fluid. J Antimicrob Chemother **6 Suppl A:**147-51.

180. **Kropec, A., and F. D. Daschner.** 1991. Penetration into tissues of various drugs active against gram-positive bacteria. J Antimicrob Chemother **27 Suppl B:**9-15.

181. **Kuehnel, T. S., C. Schurr, K. Lotter, and F. Kees.** 2005. Penetration of telithromycin into the nasal mucosa and ethmoid bone of patients undergoing rhinosurgery for chronic sinusitis. J Antimicrob Chemother **55:**591-4.

182. **Kuti, J. L., C. H. Nightingale, R. Quintiliani, and D. P. Nicolau.** 2002. Pharmacodynamic profiling of continuously infused piperacillin/tazobactam against Pseudomonas aeruginosa using Monte Carlo analysis. Diagn Microbiol Infect Dis **44:**51-7.

183. **Kutscha-Lissberg, F., U. Hebler, G. Muhr, and M. Koller.** 2003. Linezolid penetration into bone and joint tissues infected with methicillin-resistant staphylococci. Antimicrob Agents Chemother **47:**3964-6.

184. **Lazzarini, L., A. Novelli, N. Marzano, L. Timillero, S. Fallani, R. Viola, and F. de Lalla.** 2003. Regional and systemic prophylaxis with teicoplanin in total knee arthroplasty: a tissue penetration study. J Arthroplasty **18:**342-6.

185. **Leder, K., J. D. Turnidge, T. M. Korman, and M. L. Grayson.** 1999. The clinical efficacy of continuous-infusion flucloxacillin in serious staphylococcal sepsis. J Antimicrob Chemother **43:**113-8.

186. **Lee, W., and R. B. Kim.** 2004. Transporters and renal drug elimination. Annu Rev Pharmacol Toxicol **44:**137-66.

187. **Leigh, D. A.** 1989. Determination of serum and bone concentrations of cephradine and cefuroxime by HPLC in patients undergoing hip and knee joint replacement surgery. J Antimicrob Chemother **23:**877-83.

188. **Leigh, D. A., J. Marriner, D. Nisbet, H. D. Powell, J. C. Church, and K. Wise.** 1982. Bone concentrations of cefuroxime and cefamandole in the femoral head in 96 patients undergoing total hip replacement surgery. J Antimicrob Chemother **9:**303-11.

189. **Leone, M., E. Sampol-Manos, D. Santelli, S. Grabowski, B. Alliez, A. Durand, B. Lacarelle, and C. Martin.** 2002. Brain tissue penetration of ciprofloxacin following a single intravenous dose. J Antimicrob Chemother **50:**607-9.

190. **Lesko, L.** 2003, posting date. Proposal for end-of-phase 2A (EOP2A) meetings, FDA Advisory Committee for Pharmaceutical Science, Clinical Pharmacology Subcommittee. [Online.]

191. **Lew, D. P., and F. A. Waldvogel.** 1997. Osteomyelitis. N Engl J Med **336:**999-1007.

192. **Lew, D. P., and F. A. Waldvogel.** 2004. Osteomyelitis. Lancet **364:**369-79.

193. **Lew, D. P., and F. A. Waldvogel.** 1999. Use of quinolones in osteomyelitis and infected orthopaedic prosthesis. Drugs **58 Suppl 2:**85-91.

194. **Lodise, T. P., Jr., B. Lomaestro, K. A. Rodvold, L. H. Danziger, and G. L. Drusano.** 2004. Pharmacodynamic profiling of piperacillin in the presence of tazobactam in patients through the use of population pharmacokinetic models and Monte Carlo simulation. Antimicrob Agents Chemother **48:**4718-24.

195. **Lomaestro, B. M., and G. L. Drusano.** 2005. Pharmacodynamic evaluation of extending the administration time of meropenem using a Monte Carlo simulation. Antimicrob Agents Chemother **49:**461-3.

196. **Lovering, A. M., J. Perez, K. E. Bowker, D. S. Reeves, A. P. MacGowan, and G. Bannister.** 1997. A comparison of the penetration of cefuroxime and cephamandole into bone, fat and haematoma fluid in patients undergoing total hip replacement. J Antimicrob Chemother **40:**99-104.

197. **Lovering, A. M., T. R. Walsh, G. C. Bannister, and A. P. MacGowan.** 2001. The penetration of ceftriaxone and cefamandole into bone, fat and haematoma and relevance of serum protein binding to their penetration into bone. J Antimicrob Chemother **47:**483-6.

198. **Lovering, A. M., J. Zhang, G. C. Bannister, B. J. Lankester, J. H. Brown, G. Narendra, and A. P. MacGowan.** 2002. Penetration of linezolid into bone, fat, muscle and haematoma of patients undergoing routine hip replacement. J Antimicrob Chemother **50:**73-7.

199. **Lowe, M. N., and H. M. Lamb.** 2000. Gemifloxacin. Drugs **59:**1137-47; discussion 1148.

200. **Lubrich, B., and D. van Calker.** 1999. Inhibition of the high affinity myo-inositol transport system: a common mechanism of action of antibipolar drugs? Neuropsychopharmacology **21:**519-29.

201. **Ludden, T. M.** 1991. Nonlinear pharmacokinetics: clinical Implications. Clin Pharmacokinet **20:**429-46.

202. **Lunke, R. J., R. H. Fitzgerald, Jr., and J. A. Washington, 2nd.** 1981. Pharmacokinetics of cefamandole in osseous tissue. Antimicrob Agents Chemother **19:**851-8.

203. **Lynn, B.** 2002. Recent work on parenteral penicillins. Journal of Hospital Pharmacy **29:**183-194.

204. **Mager, H., and G. Goller.** 1995. Analysis of pseudo-profiles in organ pharmacokinetics and toxicokinetics. Stat Med **14:**1009-24.

205.	**Mager, H., and G. Goller.** 1998. Resampling methods in sparse sampling situations in preclinical pharmacokinetic studies. J Pharm Sci **87:**372-8.

206.	**Mahmood, S., T. Revesz, and C. Mpofu.** 1996. Febrile episodes in children with cancer in the United Arab Emirates. Pediatr Hematol Oncol **13:**135-42.

207.	**Makiyama, T., and T. Asai.** 1988. Study on transfer of cefotaxime into bone tissue. Drugs **35 Suppl 2:**88-92.

208.	**Malizia, T., G. Batoni, E. Ghelardi, F. Baschiera, F. Graziani, C. Blandizzi, M. Gabriele, M. Campa, M. Del Tacca, and S. Senesi.** 2001. Interaction between piroxicam and azithromycin during distribution to human periodontal tissues. J Periodontol **72:**1151-6.

209.	**Malizia, T., M. R. Tejada, E. Ghelardi, S. Senesi, M. Gabriele, M. R. Giuca, C. Blandizzi, R. Danesi, M. Campa, and M. Del Tacca.** 1997. Periodontal tissue disposition of azithromycin. J Periodontol **68:**1206-9.

210.	**Mandell, W., and H. C. Neu.** 1986. In vitro activity of CI-934, a new quinolone, compared with that of other quinolones and other antimicrobial agents. Antimicrob Agents Chemother **29:**852-7.

211.	**Manek, N., J. M. Andrews, and R. Wise.** 1986. In vitro activity of Ro 23-6240, a new difluoroquinolone derivative, compared with that of other antimicrobial agents. Antimicrob Agents Chemother **30:**330-2.

212.	**Mangione, A., F. D. Boudinot, R. M. Schultz, and W. J. Jusko.** 1982. Dose-dependent pharmacokinetics of mezlocillin in relation to renal impairment. Antimicrob Agents Chemother **21:**428-35.

213.	**Martin, C., M. Alaya, M. N. Mallet, X. Viviand, K. Ennabli, R. Said, and P. De Micco.** 1994. Penetration of vancomycin into mediastinal and cardiac tissues in humans. Antimicrob Agents Chemother **38:**396-9.

214.	**Martin, C., P. Bourget, M. Alaya, A. Sertin, C. Atlani, K. Ennabli, and R. Said.** 1997. Teicoplanin in cardiac surgery: intraoperative pharmacokinetics and concentrations in cardiac and mediastinal tissues. Antimicrob Agents Chemother **41:**1150-5.

215.	**Martin, C., X. Viviand, M. Alaya, F. Lokiec, K. Ennabli, R. Said, and M. Pecking.** 1996. Penetration of ceftriaxone (1 or 2 grams intravenously) into mediastinal and cardiac tissues in humans. Antimicrob Agents Chemother **40:**812-5.

216.	**Masereeuw, R., and F. G. Russel.** 2001. Mechanisms and clinical implications of renal drug excretion. Drug Metab Rev **33:**299-351.

217.	**Massias, L., P. Buffe, B. Cohen, Y. Cudennec, P. Gehanno, O. Sterkers, and R. Farinotti.** 1994. Study of the distribution of oral ciprofloxacin into the mucosa of the middle ear and the cortical bone of the mastoid process. Chemotherapy **40 Suppl 1:**3-7.

218.	**Massias, L., C. Dubois, P. de Lentdecker, O. Brodaty, M. Fischler, and R. Farinotti.** 1992. Penetration of vancomycin in uninfected sternal bone. Antimicrob Agents Chemother **36:**2539-41.

219.	**Meier, P. J., U. Eckhardt, A. Schroeder, B. Hagenbuch, and B. Stieger.** 1997. Substrate specificity of sinusoidal bile acid and organic anion uptake systems in rat and human liver. Hepatology **26:**1667-77.

220. **Meissner, A., K. Borner, and P. Koeppe.** 1990. Concentrations of ofloxacin in human bone and in cartilage. J Antimicrob Chemother **26 Suppl D:**69-74.
221. **Meissner, A., R. Haag, and R. Rahmanzadeh.** 1989. Adjuvant fosfomycin medication in chronic osteomyelitis. Infection **17:**146-51.
222. **Mentre, F., C. Dubruc, and J. P. Thenot.** 2001. Population pharmacokinetic analysis and optimization of the experimental design for mizolastine solution in children. J Pharmacokinet Pharmacodyn **28:**299-319.
223. **Merrikin, D. J., J. Briant, and G. N. Rolinson.** 1983. Effect of protein binding on antibiotic activity in vivo. J Antimicrob Chemother **11:**233-8.
224. **Meyer, B., S. Ahmed el Gendy, G. Delle Karth, G. J. Locker, G. Heinz, W. Jaeger, and F. Thalhammer.** 2003. How to calculate clearance of highly protein-bound drugs during continuous venovenous hemofiltration demonstrated with flucloxacillin. Kidney Blood Press Res **26:**135-40.
225. **Miglioli, P. A., R. Kafka, H. Bonatti, G. Fraedrich, F. Allerberger, and U. Schoeffel.** 2001. Fleroxacin uptake in ischaemic limb tissue. Acta Microbiol Immunol Hung **48:**11-5.
226. **Mizuno, N., T. Niwa, Y. Yotsumoto, and Y. Sugiyama.** 2003. Impact of drug transporter studies on drug discovery and development. Pharmacol Rev **55:**425-61.
227. **Morganroth, J., G. H. Talbot, M. B. Dorr, R. D. Johnson, W. Geary, and D. Magner.** 1999. Effect of single ascending, supratherapeutic doses of sparfloxacin on cardiac repolarization (QTc interval). Clin Ther **21:**818-28.
228. **Mouton, J. W., M. N. Dudley, O. Cars, H. Derendorf, and G. L. Drusano.** 2005. Standardization of pharmacokinetic/pharmacodynamic (PK/PD) terminology for anti-infective drugs: an update. J Antimicrob Chemother.
229. **Mouton, J. W., H. P. Endtz, J. G. den Hollander, N. van den Braak, and H. A. Verbrugh.** 1997. In-vitro activity of quinupristin/dalfopristin compared with other widely used antibiotics against strains isolated from patients with endocarditis. J Antimicrob Chemother **39 Suppl A:**75-80.
230. **Mueller, S. C., K. O. Henkel, J. Neumann, E. M. Hehl, K. K. Gundlach, and B. Drewelow.** 1999. Perioperative antibiotic prophylaxis in maxillofacial surgery: penetration of clindamycin into various tissues. J Craniomaxillofac Surg **27:**172-6.
231. **Muller, M., H. Stass, M. Brunner, J. G. Moller, E. Lackner, and H. G. Eichler.** 1999. Penetration of moxifloxacin into peripheral compartments in humans. Antimicrob Agents Chemother **43:**2345-9.
232. **Mutschler, E., G. Thews, and P. Vaupel.** 1999. Anatomie, Physiologie, Pathophysiologie des Menschen, 5 ed. Wissenschafliche Verlagsgesellschaft mbH Stuttgart.
233. **Nakashima, M., T. Uematsu, K. Kosuge, H. Kusajima, T. Ooie, Y. Masuda, R. Ishida, and H. Uchida.** 1995. Single- and multiple-dose pharmacokinetics of AM-1155, a new 6-fluoro-8-methoxy quinolone, in humans. Antimicrob Agents Chemother **39:**2635-40.

234. **Nauta, E. H., and H. Mattie.** 1976. Dicloxacillin and cloxacillin: pharmacokinetics in healthy and hemodialysis subjects. Clin Pharmacol Ther **20:**98-108.

235. **Nedelman, J. R., and E. Gibiansky.** 1996. The variance of a better AUC estimator for sparse, destructive sampling in toxicokinetics. J Pharm Sci **85:**884-6.

236. **Nedelman, J. R., E. Gibiansky, and D. T. Lau.** 1995. Applying Bailer's method for AUC confidence intervals to sparse sampling. Pharm Res **12:**124-8.

237. **Nehrer, S., F. Thalhammer, E. Schwameis, S. Breyer, and R. Kotz.** 1998. Teicoplanin in the prevention of infection in total hip replacement. Arch Orthop Trauma Surg **118:**32-6.

238. **Nestorov, I., G. Graham, S. Duffull, L. Aarons, E. Fuseau, and P. Coates.** 2001. Modeling and stimulation for clinical trial design involving a categorical response: a phase II case study with naratriptan. Pharm Res **18:**1210-9.

239. **Nicholas, P., B. R. Meyers, R. N. Levy, and S. Z. Hirschman.** 1975. Concentration of clindamycin in human bone. Antimicrob Agents Chemother **8:**220-1.

240. **Nicolau, D. P.** 2003. Optimizing outcomes with antimicrobial therapy through pharmacodynamic profiling. J Infect Chemother **9:**292-6.

241. **Nilsson-Ehle, I., H. Fellner, S. A. Hedstrom, P. Nilsson-Ehle, and J. Sjovall.** 1985. Pharmacokinetics of clavulanic acid, given in combination with amoxycillin, in volunteers. J Antimicrob Chemother **16:**491-8.

242. **Nix, D. E., T. J. Cumbo, P. Kuritzky, J. M. DeVito, and J. J. Schentag.** 1987. Oral ciprofloxacin in the treatment of serious soft tissue and bone infections. Efficacy, safety, and pharmacokinetics. Am J Med **82:**146-53.

243. **Nungu, K. S., S. Larsson, L. Wallinder, and S. Holm.** 1995. Bone and wound fluid concentrations of cephalosporins. Oral cefadroxil and parenteral cefuroxime compared in 52 patients with a trochanteric fracture. Acta Orthop Scand **66:**161-5.

244. **On, A., C. H. Nightingale, R. Quintiliani, K. R. Sweeney, H. S. Pasternak, and E. G. Maderazo.** 1992. Lomefloxacin concentrations in bone after a single oral dose. Am J Med **92:**15S-17S.

245. **Pai, S. M., J. R. Nedelman, G. Hajian, E. Gibiansky, and V. K. Batra.** 1996. Performance of Bailer's method for AUC confidence intervals from sparse non-normally distributed drug concentrations in toxicokinetic studies. Pharm Res **13:**1280-2.

246. **Petitjean, O., M. Tod, and K. Louchahi.** 1995. Influence of methodological aspects on tissue drug concentration estimation. J Pharm Biomed Anal **13:**817-22.

247. **Piegorsch, W. W., and A. J. Bailer.** 1989. Optimal design allocations for estimating area under curves for studies employing destructive sampling. J Pharmacokinet Biopharm **17:**493-507.

248. **Piotrovskij, V. K., G. Paintaud, G. Alvan, and T. Trnovec.** 1994. Modeling of the saturable time-constrained amoxicillin absorption in humans. Pharm Res **11:**1346-51.

249. **Plaue, R., O. Müller, K. Fabricius, and B. Oellers.** 1980. Untersuchungen über die Diffusionsrate von Fosfomycin in verschiedene menschliche Gewebe. Therapiewoche **30:**8329-8333.

250. **Portmann, R., and E. Weidekamm.** 1992. Penetration of fleroxacin into human and animal tissues. Chemotherapy **38:**145-9.

251. **Preston, S. L., G. L. Drusano, A. L. Berman, C. L. Fowler, A. T. Chow, B. Dornseif, V. Reichl, J. Natarajan, and M. Corrado.** 1998. Pharmacodynamics of levofloxacin: a new paradigm for early clinical trials. Jama **279:**125-9.

252. **Rana, B., I. Butcher, P. Grigoris, C. Murnaghan, R. A. Seaton, and C. M. Tobin.** 2002. Linezolid penetration into osteo-articular tissues. J Antimicrob Chemother **50:**747-50.

253. **Raymakers, J. T., A. J. Houben, J. J. van der Heyden, J. H. Tordoir, P. J. Kitslaar, and N. C. Schaper.** 2001. The effect of diabetes and severe ischaemia on the penetration of ceftazidime into tissues of the limb. Diabet Med **18:**229-34.

254. **Raymakers, J. T., N. C. Schaper, J. J. van der Heyden, J. H. Tordoir, and P. J. Kitslaar.** 1998. Penetration of ceftazidime into bone from severely ischaemic limbs. J Antimicrob Chemother **42:**543-5.

255. **Renneberg, J., O. M. Christensen, N. O. Thomsen, and C. Torholm.** 1993. Cefuroxime concentrations in serum, joint fluid and bone in elderly patients undergoing arthroplasty after administration of cefuroxime axetil. J Antimicrob Chemother **32:**751-5.

256. **Retout, S., F. Mentre, and R. Bruno.** 2002. Fisher information matrix for non-linear mixed-effects models: evaluation and application for optimal design of enoxaparin population pharmacokinetics. Stat Med **21:**2623-39.

257. **Rimmele, T., E. Boselli, D. Breilh, S. Djabarouti, J. C. Bel, R. Guyot, M. C. Saux, and B. Allaouchiche.** 2004. Diffusion of levofloxacin into bone and synovial tissues. J Antimicrob Chemother **53:**533-5.

258. **Roder, B. L., N. Frimodt-Moller, F. Espersen, and S. N. Rasmussen.** 1995. Dicloxacillin and flucloxacillin: pharmacokinetics, protein binding and serum bactericidal titers in healthy subjects after oral administration. Infection **23:**107-12.

259. **Rodondi, L. C., J. F. Flaherty, P. Schoenfeld, S. L. Barriere, and J. G. Gambertoglio.** 1989. Influence of coadministration on the pharmacokinetics of mezlocillin and cefotaxime in healthy volunteers and in patients with renal failure. Clin Pharmacol Ther **45:**527-34.

260. **Roth, B.** 1984. Penetration of parenterally administered rifampicin into bone tissue. Chemotherapy **30:**358-65.

261. **Rougier, F., D. Claude, M. Maurin, A. Sedoglavic, M. Ducher, S. Corvaisier, R. Jelliffe, and P. Maire.** 2003. Aminoglycoside nephrotoxicity: modeling, simulation, and control. Antimicrob Agents Chemother **47:**1010-6.

262. **Rowland, M., and T. N. Tozer.** 1995. Clinical Pharmacokinetics: concepts and applications. Lippincott Williams & Wilkins, Philadelphia, PA, USA.

263. **Russmann, S., J. A. Kaye, S. S. Jick, and H. Jick.** 2005. Risk of cholestatic liver disease associated with flucloxacillin and flucloxacillin

prescribing habits in the UK: cohort study using data from the UK General Practice Research Database. Br J Clin Pharmacol **60:**76-82.

264. **Scaglione, F., G. De Martini, L. Peretto, R. Ghezzi, M. Baratelli, M. M. Arcidiacono, and F. Fraschini.** 1997. Pharmacokinetic study of cefodizime and ceftriaxone in sera and bones of patients undergoing hip arthroplasty. Antimicrob Agents Chemother **41:**2292-4.

265. **Schurman, D. J., B. L. Johnson, Jr., G. Finerman, and H. C. Amstutz.** 1975. Antibiotic bone penetration. Concentrations of methicillin and clindamycin phosphate in human bone taken during total hip replacement. Clin Orthop Relat Res:142-6.

266. **Schwarz, M., R. Isenmann, J. Thomsen, W. Gaus, and H. G. Beger.** 2001. Efficacy of oral ofloxacin for single-dose perioperative prophylaxis in general surgery--a controlled randomized clinical study. Langenbecks Arch Surg **386:**397-401.

267. **Sheiner, L. B.** 1997. Learning versus confirming in clinical drug development. Clin Pharmacol Ther **61:**275-91.

268. **Sheiner, L. B.** 1984. The population approach to pharmacokinetic data analysis: rationale and standard data analysis methods. Drug Metab Rev **15:**153-71.

269. **Shiba, K., A. Saito, J. Shimada, S. Hori, M. Kaji, T. Miyahara, H. Kusajima, S. Kaneko, S. Saito, T. Ooie, and et al.** 1990. Renal handling of fleroxacin in rabbits, dogs, and humans. Antimicrob Agents Chemother **34:**58-64.

270. **Shimada, J., T. Nogita, and Y. Ishibashi.** 1993. Clinical pharmacokinetics of sparfloxacin. Clin Pharmacokinet **25:**358-69.

271. **Shimada, J., T. Yamaji, Y. Ueda, H. Uchida, H. Kusajima, and T. Irikura.** 1983. Mechanism of renal excretion of AM-715, a new quinolonecarboxylic acid derivative, in rabbits, dogs, and humans. Antimicrob Agents Chemother **23:**1-7.

272. **Shitara, Y., H. Sato, and Y. Sugiyama.** 2005. Evaluation of drug-drug interaction in the hepatobiliary and renal transport of drugs. Annu Rev Pharmacol Toxicol **45:**689-723.

273. **Siefert, H. M., A. Domdey-Bette, K. Henninger, F. Hucke, C. Kohlsdorfer, and H. H. Stass.** 1999. Pharmacokinetics of the 8-methoxyquinolone, moxifloxacin: a comparison in humans and other mammalian species. J Antimicrob Chemother **43 Suppl B:**69-76.

274. **Simon, N., E. Sampol, J. Albanese, C. Martin, P. Arvis, S. Urien, B. Lacarelle, and B. Bruguerolle.** 2003. Population pharmacokinetics of moxifloxacin in plasma and bronchial secretions in patients with severe bronchopneumonia. Clin Pharmacol Ther **74:**353-63.

275. **Sirot, J., R. Lopitaux, C. Dumont, S. Rampon, and R. Cluzel.** 1983. [Diffusion of fosfomycin into bone tissue in man]. Pathol Biol (Paris) **31:**522-4.

276. **Sjovall, J., G. Alvan, and B. Huitfeldt.** 1986. Intra- and inter-individual variation in pharmacokinetics of intravenously infused amoxycillin and ampicillin to elderly volunteers. Br J Clin Pharmacol **21:**171-81.

277. **Smilack, J. D., W. H. Flittie, and T. W. Williams, Jr.** 1976. Bone concentrations of antimicrobial agents after parenteral administration. Antimicrob Agents Chemother **9:**169-71.

278. **Smith, S. M.** 1986. In vitro comparison of A-56619, A-56620, amifloxacin, ciprofloxacin, enoxacin, norfloxacin, and ofloxacin against methicillin-resistant Staphylococcus aureus. Antimicrob Agents Chemother **29:**325-6.

279. **Smith, S. M., and R. H. Eng.** 1985. Activity of ciprofloxacin against methicillin-resistant Staphylococcus aureus. Antimicrob Agents Chemother **27:**688-91.

280. **Soman, A., D. Honeybourne, J. Andrews, G. Jevons, and R. Wise.** 1999. Concentrations of moxifloxacin in serum and pulmonary compartments following a single 400 mg oral dose in patients undergoing fibre-optic bronchoscopy. J Antimicrob Chemother **44:**835-8.

281. **Sorensen, T. S., H. Colding, E. Schroeder, and V. T. Rosdahl.** 1978. The penetration of cefazolin, erythromycin and methicillin into human bone tissue. Acta Orthop Scand **49:**549-53.

282. **Sorgel, F., J. Bulitta, and M. Kinzig-Schippers.** 2001. [How well do gyrase inhibitors work? The pharmacokinetics of quinolones]. Pharm Unserer Zeit **30:**418-27.

283. **Sorgel, F., and M. Kinzig.** 1993. The chemistry, pharmacokinetics and tissue distribution of piperacillin/tazobactam. J Antimicrob Chemother **31 Suppl A:**39-60.

284. **Sorgel, F., and M. Kinzig.** 1994. Pharmacokinetic characteristics of piperacillin/tazobactam. Intensive Care Med **20 Suppl 3:**S14-20.

285. **Stass, H., A. Dalhoff, D. Kubitza, and U. Schuhly.** 1998. Pharmacokinetics, safety, and tolerability of ascending single doses of moxifloxacin, a new 8-methoxy quinolone, administered to healthy subjects. Antimicrob Agents Chemother **42:**2060-5.

286. **Stass, H., and D. Kubitza.** 1999. Pharmacokinetics and elimination of moxifloxacin after oral and intravenous administration in man. J Antimicrob Chemother **43 Suppl B:**83-90.

287. **Stass, H., D. Kubitza, A. Halabi, and H. Delesen.** 2002. Pharmacokinetics of moxifloxacin, a novel 8-methoxy-quinolone, in patients with renal dysfunction. Br J Clin Pharmacol **53:**232-7.

288. **Stass, H., and R. Sachse.** 2001. Effect of probenecid on the kinetics of a single oral 400mg dose of moxifloxacin in healthy male volunteers. Clin Pharmacokinet **40 Suppl 1:**71-6.

289. **Steer, J. A., R. P. Papini, A. P. Wilson, D. A. McGrouther, and N. Parkhouse.** 1997. Teicoplanin versus flucloxacillin in the treatment of infection following burns. J Antimicrob Chemother **39:**383-92.

290. **Stein, G. E.** 1991. Drug interactions with fluoroquinolones. Am J Med **91:**81S-86S.

291. **Steinhauer, S.** 2002. Erhebung pharmakokinetischer Daten von Cisaprid, SC-72393, Haloperidol, Linezolid, Methotrexat und Ketoprofen nach Methodenentwicklung und Validierung durch LC-MS/MS Detektion. Ph.D. thesis, University of Würzburg.

292. **Stepensky, D., L. Kleinberg, and A. Hoffman.** 2003. Bone as an effect compartment: models for uptake and release of drugs. Clin Pharmacokinet **42:**863-81.

293. **Stolle, L. B., M. Arpi, P. Holmberg-Jorgensen, P. Riegels-Nielsen, and J. Keller.** 2004. Application of microdialysis to cancellous bone tissue for measurement of gentamicin levels. J Antimicrob Chemother **54:**263-5.

294. **Stolle, L. B., M. Arpi, P. H. Jorgensen, P. Riegels-Nielsen, and J. Keller.** 2003. In situ gentamicin concentrations in cortical bone: an experimental study using microdialysis in bone. Acta Orthop Scand **74:**611-6.

295. **Stolle, L. B., N. Plock, C. Joukhadar, M. Arpi, K. J. Emmertsen, C. Buerger, P. Riegels-Nielsen, and C. Kloft.** 2005. Presented at the 45th Interscience Conference on Antimicrobial Agents and Chemotherapy, Washington, DC, USA, December 16 - 19, 2005.

296. **Stranne, J., G. Aus, C. Hansson, P. Lodding, E. Pileblad, and J. Hugosson.** 2004. Single-dose orally administered quinolone appears to be sufficient antibiotic prophylaxis for radical retropubic prostatectomy. Scand J Urol Nephrol **38:**143-7.

297. **Stratton, C. W., C. Liu, and L. S. Weeks.** 1987. Activity of LY146032 compared with that of methicillin, cefazolin, cefamandole, cefuroxime, ciprofloxacin, and vancomycin against staphylococci as determined by kill-kinetic studies. Antimicrob Agents Chemother **31:**1210-5.

298. **Styers, D., D. J. Sheehan, P. Hogan, and D. F. Sahm.** 2006. Laboratory-Based Surveillance of Current Antimicrobial Patterns and Trends Among Staphylococcus aureus: 2005 Status in the United States. Ann Clin Microbiol Antimicrob **5:**2.

299. **Tam, V. H., P. S. McKinnon, R. L. Akins, M. J. Rybak, and G. L. Drusano.** 2002. Pharmacodynamics of cefepime in patients with Gram-negative infections. J Antimicrob Chemother **50:**425-8.

300. **Tam, V. H., S. L. Preston, and G. L. Drusano.** 2003. Optimal sampling schedule design for populations of patients. Antimicrob Agents Chemother **47:**2888-91.

301. **Teorell, T.** 1937. Kinetics of distribution of substances administered to the body. I: The extravascular modes of administration. Arch Intern Pharmacodyn **57:**205-225.

302. **Teorell, T.** 1937. Kinetics of distribution of substances administered to the body. II: The intravascular mode of administration. Arch Intern Pharmacodyn **57:**226-240.

303. **Thibonnier, M., N. H. Holford, R. A. Upton, C. D. Blume, and R. L. Williams.** 1984. Pharmacokinetic-pharmacodynamic analysis of unbound disopyramide directly measured in serial plasma samples in man. J Pharmacokinet Biopharm **12:**559-73.

304. **Tjandramaga, T. B., A. Mullie, R. Verbesselt, P. J. De Schepper, and L. Verbist.** 1978. Piperacillin: human pharmacokinetics after intravenous and intramuscular administration. Antimicrob Agents Chemother **14:**829-37.

305. **Tod, M., F. Mentre, Y. Merle, and A. Mallet.** 1998. Robust optimal design for the estimation of hyperparameters in population pharmacokinetics. J Pharmacokinet Biopharm **26:**689-716.

306. **Tolsdorff, P.** 1993. Penetration of ofloxacin into nasal tissues. Infection **21:**66-70.

307. **Tolsdorff, P.** 1993. Tissue and serum concentrations of ofloxacin in the ear region following a single daily oral dose of 400 mg. Infection **21:**63-5.
308. **Touw, D. J.** 1998. Clinical pharmacokinetics of antimicrobial drugs in cystic fibrosis. Pharm World Sci **20:**149-60.
309. **Tse, F. L., and J. R. Nedelman.** 1996. Serial versus sparse sampling in toxicokinetic studies. Pharm Res **13:**1105-8.
310. **Ullrich, K. J., G. Rumrich, C. David, and G. Fritzsch.** 1993. Bisubstrates: substances that interact with both, renal contraluminal organic anion and organic cation transport systems. II. Zwitterionic substrates: dipeptides, cephalosporins, quinolone-carboxylate gyrase inhibitors and phosphamide thiazine carboxylates; nonionizable substrates: steroid hormones and cyclophosphamides. Pflugers Arch **425:**300-12.
311. **Undevia, S. D., G. Gomez-Abuin, and M. J. Ratain.** 2005. Pharmacokinetic variability of anticancer agents. Nat Rev Cancer **5:**447-58.
312. **Unsworth, P. F., F. W. Heatley, and I. Phillips.** 1978. Flucloxacillin in bone. J Clin Pathol **31:**705-11.
313. **Van Bambeke, F., J. M. Michot, J. Van Eldere, and P. M. Tulkens.** 2005. Quinolones in 2005: an update. Clin Microbiol Infect **11:**256-80.
314. **van de Sande-Bruinsma, N.** 2006. Presented at the 16th European Congress of Clinical Microbiology and Infectious Diseases (ECCMID), Nice, France.
315. **van de Wetering, M. D., M. A. de Witte, L. C. Kremer, M. Offringa, R. J. Scholten, and H. N. Caron.** 2005. Efficacy of oral prophylactic antibiotics in neutropenic afebrile oncology patients: a systematic review of randomised controlled trials. Eur J Cancer **41:**1372-82.
316. **van Dyck, C. H.** 2004. Understanding the latest advances in pharmacologic interventions for Alzheimer's disease. CNS Spectr **9:**24-8.
317. **Vinks, A. A., J. G. Den Hollander, S. E. Overbeek, R. W. Jelliffe, and J. W. Mouton.** 2003. Population pharmacokinetic analysis of nonlinear behavior of piperacillin during intermittent or continuous infusion in patients with cystic fibrosis. Antimicrob Agents Chemother **47:**541-7.
318. **Vlasses, P. H., A. M. Holbrook, J. J. Schrogie, J. D. Rogers, R. K. Ferguson, and W. B. Abrams.** 1980. Effect of orally administered probenecid on the pharmacokinetics of cefoxitin. Antimicrob Agents Chemother **17:**847-55.
319. **Vogelman, B., S. Gudmundsson, J. Leggett, J. Turnidge, S. Ebert, and W. A. Craig.** 1988. Correlation of antimicrobial pharmacokinetic parameters with therapeutic efficacy in an animal model. J Infect Dis **158:**831-47.
320. **von Baum, H., S. Bottcher, R. Abel, H. J. Gerner, and H. G. Sonntag.** 2001. Tissue and serum concentrations of levofloxacin in orthopaedic patients. Int J Antimicrob Agents **18:**335-40.

321. **Vree, T. B., E. W. Van Ewijk-Beneken Kolmer, E. W. Wuis, and Y. A. Hekster.** 1992. Capacity-limited renal glucuronidation of probenecid by humans. A pilot Vmax-finding study. Pharm Weekbl Sci **14:**325-31.

322. **Vuorisalo, S., R. Pokela, J. Satta, and H. Syrjala.** 2000. Internal Mammary Artery Harvesting and Antibiotic Concentrations in Sternal Bone During Coronary Artery Bypass. Int J Angiol **9:**78-81.

323. **Walker, R., and C. Edwards.** 2000. Clinical Pharmacy and Therapeutics, second ed. Churchill Livingstone.

324. **Warnke, J. P., A. Wildfeuer, G. Eibel, G. Pfaff, and A. Klammer.** 1998. Pharmacokinetics of ampicillin/sulbactam in patients undergoing spinal microneurosurgical procedures. Int J Clin Pharmacol Ther **36:**253-7.

325. **Waterhouse, T. H., S. Redmann, S. B. Duffull, and J. A. Eccleston.** 2005. Optimal Design for Model Discrimination and Parameter Estimation for Itraconazole Population Pharmacokinetics in Cystic Fibrosis Patients. J Pharmacokinet Pharmacodyn.

326. **Waters** 2006, posting date. HPLC primer. [Online.]

327. **Weidekamm, E., and R. Portmann.** 1993. Penetration of fleroxacin into body tissues and fluids. Am J Med **94:**75S-80S.

328. **Weismeier, K., D. Adam, H. D. Heilmann, and P. Koeppe.** 1989. Penetration of amoxycillin/clavulanate into human bone. J Antimicrob Chemother **24 Suppl B:**93-100.

329. **West, J. B. (ed.).** 1985. Best & Taylor's Physiological Basis of Medical Practice, 10 ed. Williams & Wilkins, Baltimore, MD.

330. **Wijnands, W. J., T. B. Vree, A. M. Baars, and C. L. van Herwaarden.** 1988. Pharmacokinetics of enoxacin and its penetration into bronchial secretions and lung tissue. J Antimicrob Chemother **21 Suppl B:**67-77.

331. **Wildfeuer, A., J. Mallwitz, H. Gotthardt, E. Hille, H. Gruber, G. Dahmen, G. Pfaff, and C. Gobel.** 1997. Pharmacokinetics of ampicillin, sulbactam and cefotiam in patients undergoing orthopedic surgery. Infection **25:**258-62.

332. **Wildfeuer, A., V. Muller, M. Springsklee, and H. G. Sonntag.** 1991. Pharmacokinetics of ampicillin and sulbactam in patients undergoing heart surgery. Antimicrob Agents Chemother **35:**1772-6.

333. **Wilson, A. P., B. Taylor, T. Treasure, R. N. Gruneberg, K. Patton, D. Felmingham, and M. F. Sturridge.** 1988. Antibiotic prophylaxis in cardiac surgery: serum and tissue levels of teicoplanin, flucloxacillin and tobramycin. J Antimicrob Chemother **21:**201-12.

334. **Wilson, K. J., and J. T. Mader.** 1984. Concentrations of vancomycin in bone and serum of normal rabbits and those with osteomyelitis. Antimicrob Agents Chemother **25:**140-1.

335. **Winston, D. J., W. G. Ho, R. E. Champlin, R. P. Gale, and R. W. Busuttil.** 1986. Ureidopenicillins, aztreonam, and thienamycin: efficacy as single-drug therapy of severe infections and potential as components of combined therapy. J Antimicrob Chemother **17 Suppl A:**55-66.

336. **Wirtz, M., J. Kleeff, S. Swoboda, I. Halaceli, H. K. Geiss, T. Hoppe-Tichy, M. W. Buchler, and H. Friess.** 2004. Moxifloxacin penetration into human gastrointestinal tissues. J Antimicrob Chemother **53:**875-7.

337. **Wise, R., J. M. Andrews, G. Marshall, and G. Hartman.** 1999. Pharmacokinetics and inflammatory-fluid penetration of moxifloxacin following oral or intravenous administration. Antimicrob Agents Chemother **43:**1508-10.

338. **Wise, R., C. Cross, and J. M. Andrews.** 1984. In vitro activity of CGP 31523A, a broad-spectrum cephalosporin, in comparison with those of other agents. Antimicrob Agents Chemother **26:**876-80.

339. **Wittmann, D. H.** 1980. Chemotherapeutic Principles of Difficult-to-Treat Infections in Surgery: II. Bone and Joint Infections. Infection **8:**330-333.

340. **Wittmann, D. H., and E. Kotthaus.** 1986. Further methodological improvement in antibiotic bone concentration measurements: penetration of ofloxacin into bone and cartilage. Infection **14 Suppl 4:**S270-3.

341. **Wright, P. M., and D. M. Fisher.** 1998. Can bioavailability of low-variance drugs be estimated with an unpaired, sparse sampling design? Clin Pharmacol Ther **63:**437-43.

342. **Wyeth.** 2005. Piperacillin / tazobactam product information (Tazocin), Maidenhead, Berks, UK.

343. **Wyeth** 2006, posting date. Tygacil receives positive opinion from European Regulatory Authority. [Online.]

344. **Wysocki, S.** 1976. Gewebespiegel verschiedener Antibiotika beim Menschen. Infection **4:**S115-S119.

345. **Yoda, T., E. Sakai, K. Harada, M. Mori, I. Sakamoto, and S. Enomoto.** 2000. A randomized prospective study of oral versus intravenous antibiotic prophylaxis against postoperative infection after sagittal split ramus osteotomy of the mandible. Chemotherapy **46:**438-44.

346. **Yoo, B. K., D. M. Triller, C. S. Yong, and T. P. Lodise.** 2004. Gemifloxacin: a new fluoroquinolone approved for treatment of respiratory infections. Ann Pharmacother **38:**1226-35.

347. **Zeitlinger, M., M. Muller, and C. Joukhadar.** 2005. Lung microdialysis--a powerful tool for the determination of exogenous and endogenous compounds in the lower respiratory tract (mini-review). Aaps J **7:**E600-8.

348. **Zhanel, G. G., K. Ennis, L. Vercaigne, A. Walkty, A. S. Gin, J. Embil, H. Smith, and D. J. Hoban.** 2002. A critical review of the fluoroquinolones: focus on respiratory infections. Drugs **62:**13-59.

Curriculum Vitae

Name   Cornelia Barbara Landersdorfer
Date of birth   June 22, 1977
Place of birth   Landshut, Germany
Nationality   German
Marital status: Unmarried

Studies:

July 2005 to January 2006	Internship in population pharmacokinetic data analysis and simulations at the Ordway Research Institute, Albany, NY, USA, supervisor: Professor Dr George Drusano
February 2005 to May 2005	Internship in modeling and simulations of pharmacokinetic and pharmacodynamic data at the University of Queensland, Brisbane, Australia, supervisor: Dr Carl Kirkpatrick
Since August 2002	Ph.D. student at the Institute for Biomedical and Pharmaceutical Research (IBMP) in Nürnberg-Heroldsberg, Germany, supervisor: Professor Dr Fritz Sörgel, and the Department of Pharmaceutical Chemistry, University of Würzburg, Germany, supervisor: Professor Dr Ulrike Holzgrabe
July 2002	Registration as a pharmacist
November 2001 to April 2002	Pre-registration training at a retail pharmacy, Munich, Germany
April to October 2001	Pre-registration training at Charing Cross Hospital, London, UK
August to October 1999	Practical training at the Centro de Investigación Biomedico del Occidente, Guadalajara, Mexico
1996 - 2001	Studies in pharmacy at the University of Regensburg, Germany
1987 - 1996	Gymnasium Seligenthal, Landshut, Bavaria, Germany
1983 - 1987	Primary School, Eching, Bavaria, Germany